Functional analysis of the nitrate/potassium transporter NPF7.3/NRT1.5 in *Arabidopsis thaliana*

Inaugural-Dissertation

to obtain the academic degree

Doctor rerum naturalium (Dr. rer. nat.)

submitted to the Department of Biology, Chemistry and Pharmacy

of Freie Universität Berlin

by

Yue Zheng

November 2018

Die vorliegende Arbeit wurde in der Zeit von Oktober 2011 bis September 2017 unter der Leitung von Prof. Dr. Reinhard Kunze am Institut für Biologie - Angewandte Genetik angefertigt.

1. Gutachter: Prof. Dr. Reinhard Kunze
   Freie Universität Berlin
   Institut für Biologie – Angewandte Genetik

2. Gutachter: Prof. Dr. Thomas Schmülling
   Freie Universität Berlin
   Institut für Biologie – Angewandte Genetik

   Disputation am 07.03.2019

Contents

List of Figures ..... **V**
List of Tables ..... **VII**
Abbreviations ..... **VIII**
1 Introduction **1**
1.1 Nitrate is the main nitrogen source available to plants 1
1.2 Nitrate transport mediated by nitrate transporters 2
1.2.1 Nitrate uptake by roots 5
1.2.2 Nitrate root-to-shoot translocation 7
1.2.2.1 NPF7.3/NRT1.5 is the main nitrate transporter for nitrate xylem loading 8
1.2.2.2 NPF7.2/NRT1.8 is responsible for nitrate unloading from xylem . 10
1.2.2.3 Ethylene and jasmonic acid signaling pathway converge to regulate *NRT1.5* and *NRT1.8* 10
1.2.3 Nitrate distribution in aerial tissues 11
1.3 Other substrates of *Arabidopsis* NPF proteins 12
1.4 Nitrate serves as a signal molecule 13
1.5 Potassium uptake and translocation in *Arabidopsis* 14
1.5.1 Potassium acquisition from soil 15
1.5.2 SKOR is responsible for potassium root-to-shoot translocation 17
1.5.3 NRT1.5 affects potassium root-to-shoot translocation at limited nitrate supply 18
1.6 The intersection of nitrate and potassium transport 19
1.6.1 Co-regulation of transporters at the molecular level 20
1.6.2 CIPK23: a common regulator for nitrate and potassium transport 21
1.6.3 Protein-protein interaction between nitrate and potassium transporters. 22
1.7 The influence of nitrate and potassium on root plasticity of *Arabidopsis* 22
1.8 Aim of the present study 24
2 Materials and Methods **26**
2.1 Materials 26
2.1.1 Chemicals 26
2.1.2 Enzymes and Kits 26
2.1.3 Ladders 27
2.1.4 Oligonucleotides 27
2.1.5 Plasmids 30
2.1.6 Bacteria and yeast strains 33
2.1.7 Plant material 33
2.1.8 Database and Software 34
2.1.9 Sequencing 35
2.1.10 Medium and selection 35
2.1.10.1 Medium for cultivating bacteria 35
2.1.10.2 Medium for cultivating *S. cerevisiae* 35
2.1.10.3 Medium for cultivating *Arabidopsis thaliana* 36

2.2 Methods 37
2.2.1 Transformation into bacteria, yeast and *Arabidopsis* 37
2.2.1.1 *Escherichia coli* transformation 37
2.2.1.2 *Agrobacterium tumefaciens* electroporation 38
2.2.1.3 *Saccharomyces cerevisiae* transformation and culture 38
2.2.1.4 *Arabidopsis thaliana* transformation 38
2.2.2 Cultivation of *Arabidopsis thaliana* plants 39
2.2.2.1 Sterilization of seeds 39
2.2.2.2 Cultivation of *Arabidopsis* seedlings on plates 39
2.2.2.3 Cultivation of *Arabidopsis* seedlings with liquid medium 39
2.2.2.4 Cultivation of *Arabidopsis* on soil 40
2.2.3 Analysis of *Arabidopsis* root architecture traits 40
2.2.4 Crossing of *Arabidopsis* plants 40
2.2.5 Transient expression in *Nicotiana benthamiana* 41
2.2.6 Live-cell imaging using confocal laser scanning microscopy (CLSM) 41
2.2.7 Molecular biological methods 42
2.2.7.1 Cloning of constructs 42
2.2.7.1.1 Cloning of constructs for yeast complementation 42
2.2.7.1.2 Cloning of *35Sp::NRT1.5* construct 42
2.2.7.1.3 Gateway® cloning of the pBiFC-2in1 constructs 43
2.2.7.1.4 Gateway® cloning to generate the split-ubiquitin prey constructs 43
2.2.7.1.5 Cloning of pDOE-08 constructs 43
2.2.7.2 Genomic DNA isolation 44
2.2.7.3 RNA extraction 44
2.2.7.4 cDNA synthesis 45
2.2.7.5 Quantitative real time PCR 45
2.2.8 Total C and N concentration measurement 46
2.2.9 Elemental analysis 46
2.2.10 Cooperation 46
3 Results 48
3.1 Phenotypical analysis of *nrt1.5* knockout mutants 48
3.1.1 Comparable root growth of *nrt1.5* mutants as wild type at various nitrate concentrations 48
3.1.2 Impaired lateral root development of *nrt1.5* mutants under potassium deficit 49
3.1.3 Restoration of lateral root growth in *nrt1.5* complementation lines 52
3.1.4 Auxin and cytokinin related gene were not deregulated in *nrt1.5-5* roots at limited K^+ supply 54
3.1.5 *35Sp::NRT1.5* lines phenocopied *nrt1.5* at low K^+ availability 56
3.1.6 The *nrt1.5-5* and 35Sp::*NRT1.5* lines had higher K accumulation in roots 58
3.1.7 Root growth retardation in *nrt1.5* mutants by brassinazole treatment 60
3.1.8 Smaller shoot size *of nrt1.5* mutants by Jasmonic acid treatment 61

3.2 Functional analysis of NRT1.5 62
3.2.1 Potassium import assay of NRT1.5 in *Saccharomyces cerevisiae* 63
3.2.2 Ammonium uptake assay of NRT1.5 in *Saccharomyces cerevisiae* 64
3.2.3 Potassium export assay of NRT1.5 in *Saccharomyces cerevisiae* 67
3.2.4 The expression of *NRT1.5* renders *Saccharomyces cerevisiae* cells the susceptibility to toxic cationic compounds 68
3.2.5 The *NRT1.5* level in *Arabidopsis* seedlings corelates with the sensitivity to hygromycin B 69
3.3 Functional analysis of NRT1.8 in *Saccharomyces cerevisiae* 72
3.3.1 Potassium uptake and export assay of NRT1.8 in *Saccharomyces cerevisiae* 72
3.3.2 The expression of NRT1.8 renders *Saccharomyces cerevisiae* cells more sensitive to cationic compounds 73
3.4 The interplay of NRT1.5 and SKOR in potassium root-to-shoot transfer 74
3.4.1 Generation of the *nrt1.5-5/skor-2* double mutant 75
3.4.2 The leaf chlorosis phenotype of *nrt1.5* is caused by low potassium concentration 77
3.4.3 NRT1.5 affects shoot potassium accumulation at limited nitrate supply 79
3.4.4 SKOR contributes to root-to-shoot transfer of potassium at high nitrate supply 79
3.4.5 The induction of *SKOR* expression by high nitrate supply 81
3.4.6 Ion homeostasis-associated genes deregulated in *nrt1.5-5* were not altered in *skor-2* 82
3.4.7 The *nrt1.5-5/skor-2* double mutant accumulated more sodium, sulfur and phosphorus at low nitrate supply 85
3.4.8 The *skor* mutants showed no root phenotype at K^+ deprivation……...86
3.5 Identification of interacting partners of NRT1.5 88
3.5.1 Verification of NRT1.5-interacting partners by Bimolecular Fluorescence Complementation (BiFC) 88
3.5.2 NRT1.5 interacts with CIPK23-CBL1/CBL9 complex in *Saccharomyces cerevisiae* 92
3.6 Phenotypical studies of double mutant lack NRT1.5 and its interacting partner 93
3.6.1 Identification of *slah3*, *nrt1.8* and *aha2* knockout mutants 93
3.6.2 Phenotypical analysis of the *nrt1.5-5/nrt1.8* double mutant 95
3.6.3 Phenotypical analysis of the *nrt1.5-5/slah3* double mutant 97
3.6.4 Phenotypical analysis of the *nrt1.5-5/aha2* double mutant 101
3.7 Potassium reduction in shoots of *35Sp::NRT1.5* at low nitrate supply 106
3.8 Expression profiles of nitrate- and potassium- transporters upon hormone treatment 109
3.8.1 Genes involved in the uptake of nitrate and potassium 109
3.8.2 Genes involved in root-to-shoot transfer of nitrate and potassium 110
4 Discussion 113

4.1 Expression of *NRT1.5* in roots influences the lateral root growth at potassium deprivation....113
4.2 NRT1.5 showed no potassium transport activity in yeast....116
4.3 Expression of *NRT1.5* increases the plasma membrane polarization....117
4.4 Job Sharing between NRT1.5 and SKOR in nitrate- dependent potassium translocation....120
4.5 NRT1.5 affects potassium root-to-shoot transfer independent on SKOR....123
4.6 Interaction complex NRT1.5-SLAH1-SLAH3?....123
4.7 Could AHA2 and NRT1.5 activate each other?....125
4.8 NRT1.5 is regulated by CIPK23-CBL1/CBL9 complex....129
4.9 Overexpression studies of *NRT1.5* in *Arabidopsis*....129
4.10 Phytohormones regulate nitrate and potassium transporters....131
5 Summary....134
6 Zusammenfassung....136
7 References....138
8 Publications....155
9 Acknowledgements....156
10 Appendix....157

List of Figures

Figure 1	Diagrammatic representation of apoplastic and symplastic ion transport across higher plant roots	5
Figure 2	Localization and function of the *Arabidopsis* nitrate transporters from the NPF and the NRT2 family	8
Figure 3	Schematic model of the crosstalk between K^+ and NO_3^- signaling responses to K^+ and NO_3^- deficiencies in *Arabidopsis*	21
Figure 4	Nitrate supply does not lead to visible root phenotypes of *nrt1.5* mutants.	49
Figure 5	Potassium deficiency affects root development of *nrt1.5* mutant seedlings	50
Figure 6	Reduced lateral root density in *nrt1.5-5* by K^+ starvation is independent of NO_3^- supply	51
Figure 7	The impairment of lateral root and lateral root primordia density of *nrt1.5-5* by K^+ starvation	52
Figure 8	The root development of *CAB2p::NRT1.5* lines under K^+ deprivation	53
Figure 9	The K^+ deficiency dependent root phenotype of *nrt1.5* is complemented by root specific *NRT1.5* expression	54
Figure 10	Expression level of auxin and cytokinin related genes in roots of *nrt1.5-5* at K^+ starvation condition by qRT-PCR	55
Figure 11	Expression of *NRT1.5* in Col-0 and *35Sp::NRT1.5* lines and their growth at K^+ deficiency conditions	57
Figure 12	Brassinosteroid biosynthesis inhibitor brassinazole resulted in a stronger root retardation in *nrt1.5* seedlings	61
Figure 13	*Arabidopsis nrt1.5* mutant seedlings are more sensitive to jasmonic acid treatment	62
Figure 14	Potassium uptake capacity analysis of NRT1.5 *in Saccharomyces cerevisiae*	64
Figure 15	Ammonium uptake capacity analysis of NRT1.5 in *Saccharomyces cerevisiae*	66
Figure 16	Potassium export capacity analysis of NRT1.5 in *Saccharomyces cerevisiae*	67
Figure 17	Cationic compound sensitivity test of *Saccharomyces cerevisiae* cells expressing *NRT1.5*	69
Figure 18	Growth of different plant lines in response to hygromycin B and high concentration of K^+ treatment	71
Figure 19	Potassium transport capacity analysis of NRT1.8 in *Saccharomyces cerevisiae*	73
Figure 20	Cationic drug sensitivity test of *Saccharomyces cerevisiae* cells expressing *NRT1.8*	74
Figure 21	Identification and confirmation of the absence of full-length transcripts of *NRT1.5* and *SKOR* in the double mutant *nrt1.5-5/skor-2*	76
Figure 22	Correlation of the rosette phenotype with the K, Ca and Mg elemental composition in Col-0, *nrt1.5-5*, *skor-2* and *nrt1.5-5/skor-2* plants	78
Figure 23	Rosette phenotype and K, Ca and Mg concentrations in Col-0, *nrt1.5-5*, *skor-2* and *nrt1.5-5/skor-2* plants at 20/1/1 and 10/10/1 N/K/P [mM] supply	80
Figure 24	Expression of *NRT1.5* and *SKOR* under different fertilization regimes	82
Figure 25	Expression of nitrate and potassium homeostasis-associated genes in roots of *nrt1.5-5*, *skor-2* and *nrt1.5-5/skor-2* under various fertilization regimes	84
Figure 26	Concentrations of sodium, phosphorus and sulfur in rosettes of Col-0, *skor-2*,	86

nrt1.5-5 and the double mutant

Figure 27 Potassium deficiency does not cause visible phenotype of *skor* mutants 87

Figure 28 The root development of *skor-2* and *nrt1.5-5/skor-2* mutant under potassium deficiency 87

Figure 29 Verification of interacting partners of NRT1.5 by BiFC assay (pBiFC-2in1) in leaf epidermis cells of *Nicotiana benthamiana* 89

Figure 30 Verification of interacting partners of NRT1.5 by BiFC assay (pDOE-08) in leaf epidermis cells of *Nicotiana benthamiana* 91

Figure 31 The Interaction between NRT1.5 and CIPK23 with the help of CBLs in heterologous *Saccharomyces cerevisiae* system 93

Figure 32 Scheme of T-DNA insertion lines and identification of homozygous knockout mutants 94

Figure 33 Rosette morphology of Col-0, *nrt1.5-5*, *nrt1.8* and *nrt1.5-5/nrt1.8* plants in response to varying N/K/P supply 96

Figure 34 Rosette morphology and the total N concentration of Col-0, *nrt1.5-5*, *slah3* and *nrt1.5-5/slah3* plants in response to varying N/K/P supply 98

Figure 35 Elemental concentrations in the rosettes of Col-0, *nrt1.5-5*, *slah3* and *nrt1.5-5/slah3* plants 100

Figure 36 Root morphology of Col-0, *nrt1.5-5*, *aha2* and the the *nrt1.5/aha2* double mutant in response to hygromycin B treatment 102

Figure 37 Rosette morphology of Col-0, *nrt1.5-5*, *aha2* and *nrt1.5-5/aha2* plants in response to varying N/K/P supply 103

Figure 38 Potassium concentration and fresh weight of the rosettes of Col-0, *nrt1.5-5*, *aha2* and *nrt1.5-5/aha2* plants under various N/K regimes 104

Figure 39 Expression of *AHA2* in roots of Col-0 and *nrt1.5-5* under various N/K regimes 105

Figure 40 Rosette phenotype of Col-0, *nrt1.5-5* and *35Sp::NRT1.5* plants under varying N/K supply 107

Figure 41 Potassium, calcium, magnesium and sodium concentration in the rosettes of Col-0, *nrt1.5-5*, *35Sp::NRT1.5* plants 108

Figure 42 Expression profiles of nitrate and potassium transporters in roots by phytohormone treatment 111

List of Tables

Table 1	Summary of characterized *Arabidopsis thaliana* nitrate transporters and their substrates	4
Table 2	Oligonucleotides used for qRT-PCR	27
Table 3	Oligonucleotides used for conventional and Gateway cloning	28
Table 4	Oligonucleotides used for genotyping PCR and RT-PCR to check the transcript in T-DNA insertion lines.	30
Table 5	Plasmids acquired commercially or obtained from other studies	31
Table 6	Plasmids newly constructed in this work	32
Table 7	Bacteria and yeast strains used in this work	33
Table 8	*Arabidopsis* thaliana lines used and generated in this work	34
Table 9	Database and software applicated in this work	34
Table 10	Antibiotic stock solution for selecting recombinant bacteria.	35
Table 11	Selective yeast media used in this work	36
Table 12	Phytohormone stock solution used in this work	37
Table 13	Elemental analysis in Col-0, *nrt1.5-5* and three *35Sp::NRT1.5* lines growing vertically on plates with 10 μM K^+	59
Table S1	The detail description of existing plasmids	157
Table S2	Nutrient composition of the soil used in this study	158
Table S3	The composition of various N/K/P fertilization solutions	159

Abbreviations

ABA	abscisic acid
ABRC	*Arabidopsis* Biological Resource Center
AGI	*Arabidopsis* genome initiative.
BAP	6-Benzylaminopurine
BiFC	bimolecular fluorescence complementation
BR	brassinosteroid
BZ	brassinazole
C	carbon
CAB2	chlorophyll A/B-Binding Protein 2
CaMV	cauliflower mosaic virus
CBL	Calcineurin B-Like
CDS	coding DNA sequence
CIPK	CBL Interacting Protein Kinase
CK	cytokinin
CLC	Chloride Channels
CLSM	confocal laser scanning microscopy
Col-0	*Arabidopis thaliana* ecotype Columbia-0
DAS	days after sowing
DPI	days post infiltration
DW	dry weight
EBR	24-epibrassinloide
ET	ethylene
FC	fold change
FW	fresh weight
GA3	gibberellin A3
GUS	β-glucuronidase
HATS	high-affinity transport system
HN	high nitrate
HygB	hygromycin B
IAA	indole-3-acetic acid
ICP-OES	Inductively Coupled Plasma Optical Emission Spectrometry
IPTG	Isopropyl β-D-1-thiogalactopyranoside
JA	jasmonic acid
JA-Ile	jasmonoyl-isoleucine
LATS	low-affinity transport system
LB	lysogeny broth
LN	low nitrate
LR	lateral root
LRP	lateral root primordium
MeJA	methyl jasmonate

Mep	methylamine and ammonium permeases
MES	2-(N-morpholino)ethanesulfonic acid
MS	Murashige-Skoog
N	nitrogen
NPF	nitrate Transporter 1 (NRT1)/Peptide transporter Family
NRT1/PTR	NRT1/PTR Nitrate Transporter 1/Peptide Transporter
NRT2	Nitrate Transporter 2
OD	optical density
PEG	polyethylene glycol
PHO1	PHOSPHATE1
PR	primary root
qRT-PCR	quantitative real time PCR
ROS	reactive oxygen species
RT-PCR	reverse transcription PCR
SA	salicylic acid
SD	standard deviation
SINAR	Stress-Initiated Nitrate Allocation to Roots
SLAC1/SLAH	Slow-type Anion Channel-Associated 1/Homologs
T-DNA	Transfer-DNA
TEA	tetraethylammonium
TMA	tetramethylammonium
w/v	weight/volume
X-gal	5-bromo-4-chloro-3-indolyl-β-D-galactopyranoside
YNB	yeast nitrogen base
YPAD	yeast extract-peptone-dextrose + adenine medium
3-AT	3-amino-1,2,4-triazole
4MTB	4-methylthiobutyl glucosinolate
8MTO	8-methylthiooctyl glucosinolate

1 Introduction

1.1 Nitrate is the main nitrogen source available to plants

Nitrogen (N), quantitatively the most abundant macroelement for all living organisms, is involved in the building of nucleotides, amino acids, proteins, chlorophyll, phytohormones, phospholipids and secondary metabolites. In plants, N constitutes up to 5% of dry matter (Chen *et al.* 2012; Marschner 2012) and approximately 16% of total protein mass (Frink *et al.* 1999). N availability affects carbon (C) allocation (Scheible *et al.* 1997), leaf growth (Ma *et al.* 1997; Vos *et al.* 2005), root branching (Walch-Liu *et al.* 2006), flowering time (Ma *et al.* 1997), seed development and yield (Wetherell and Dougall 1976).

N is present in soil solutions in the form of organic and inorganic N. Organic N including soluble proteins, peptides, urea and amino acids constitutes more than 98% of the total N (Dechorgnat *et al.* 2011). Even though various studies have indicated that plants are capable of absorbing organic N such as amino acids from soil (Falkengren-Grerup *et al.* 2000; Thornton and Robinson 2005; Jamtgard *et al.* 2008), most of organic N is not directly available to plants.

With the assistance of soil microorganisms, organic N can be converted to inorganic forms such as ammonium (NH_4^+) and nitrate (NO_3^-) (Crawford and Glass 1998) which are main sources of N absorbed by plant roots. Compared with NH_4^+, NO_3^- is more mobile and can reach plant roots more quickly (Miller and Cramer 2005). In regular agricultural soils, concentration of NO_3^- (1-5 mM) is generally much higher than that of NH_4^+ (20-200 µM) (Owen and Jones 2001). Thus, in agricultural systems, NO_3^- is the major N source that plants can take up directly.

1.2 Nitrate transport mediated by nitrate transporters

Since NO_3^- is the major N source that plants can take advantage of, highly efficient transport of NO_3^- into and between different compartments of plants is of great importance for plant growth. NO_3^- uptake from soil and subsequent translocation into various tissues rely on the function of nitrate transporters. Affected by soil properties like pH, microbial activity and moisture, NO_3^- concentration varies dramatically in different soil types (Robinson *et al.* 1994) by up to four orders of magnitude (Crawford and Glass 1998). To better cope with the big fluctuation in NO_3^- availability, plants have evolved two classes of nitrate transport systems, so-called High Affinity Transport System (HATS) and Low Affinity Transport System (LATS), respectively. HATS operates at low external NO_3^- concentrations (K_M in μM range), whereas LATS works predominantly when NO_3^- concentration is in mM range (Sun *et al.* 2014).

So far, 27 genes encoding nitrate transporters have been characterized from *Arabidopsis thaliana* (Table 1). They belong to four gene groups: (1) the Nitrate Transporter 1 (NRT1)/Peptide transporter Family (NPF) (Leran *et al.* 2014), (2) the Nitrate Transporter 2 (NRT2) family, (3) Chloride Channels (CLC) and (4) Slow-type Anion Channel-Associated 1/Homologues (SLAC1/SLAHs).

The NRT1 family is the biggest nitrate transporter family which consists of 53 members in *Arabidopsis*. NRT1 proteins are predicted to have short N- and C- terminal ends and 12 transmembrane domains, and the first six transmembrane domains are separated from the second six by a long loop (Varshney and Koebner 2006). Except NRT1.1 which has dual affinity through the phosphorylation of an intracellular threonine Thr 101 (Liu and Tsay 2003), all other characterized nitrate transporters from this family are LATS transporters.

The NRT2 family is a subclade of the major facilitator superfamily (MFS) of transporters and it has seven members in *Arabidopsis*. All characterized NRT2 members belong to HATS and NO_3^- is their only substrate. Except NRT2.7, all other *Arabidopsis* NRT2 members are predominantly expressed in roots (Okamoto *et al.* 2003) and require an

additional small protein Nitrate Assimilation Related protein (NAR2.1, also known as NRT3.1) (Okamoto *et al.* 2006; Kotur *et al.* 2012) to fulfill the HATS function for nitrate transport. NRT2 and NAR2.1 probably form a tetramer through an unknown mechanism (Yong *et al.* 2010).

The *Arabidopsis* CLC family contains seven members (a-g). Up to now, only CLCa has been demonstrated as a major protein that affects NO_3^- storage in vacuoles (Monachello *et al.* 2009). NO_3^- transport function of CLCb was demonstrated in *Xenopus laevis* oocytes, however, it is still unclear whether it is indeed involved in nitrate transport *in planta* (von der Fecht-Bartenbach *et al.* 2010). The anion transport mechanism and selectivity of the other five CLC members have not been characterized yet (Barbier-Brygoo *et al.* 2011).

The *Arabidopsis* SLAC1/SLAHs family has five members, which are SLAC1, the first identified guard cell S-type anion channel, and its four homologues SLAH1 to SLAH4. The five members demonstrated distinct tissue-specific expression patterns (Negi *et al.* 2008). *SLAC1* is exclusively expressed in guard cells. *SLAH1* and *SLAH4* are mainly expressed in the root vascular system. *SLAH2* is expressed in lateral root primordia and tap root tips. *SLAH3* is expressed in the whole plant tissues including guard cells (Negi *et al.* 2008; Geiger *et al.* 2011; Zheng *et al.* 2015). SLAC1 and SLAH3 are permeable for both chloride (Cl^-) and NO_3^- (Negi *et al.* 2008). SLAH3 is deemed as a NO_3^- efflux channel because it exhibits about 20-fold stronger selectivity for NO_3^- over Cl^- (Geiger *et al.* 2011). Recently, Cubero-Font *et al.* (2016) showed *SLAH1* is co-expressed with *SLAH3* in xylem-pole pericycle cells. SLAH1 itself is a silent anion channel subunit, however, SLAH1 could specifically activate SLAH3 and modifies the Cl^- conductance of SLAH3 in both oocyte and guard cell protoplasts independent of NO_3^- and phosphorylation. By this means that Cl^- root-to-shoot transfer was decreased in *slah1* knockout mutant. Different from SLAC1, SLAH1 and SLAH3, SLAH2 is a NO_3^- specific channel impermeable for Cl^- (Maierhofer *et al.* 2014).

Table 1. Summary of characterized *Arabidopsis thaliana* nitrate transporters and their substrates.

Adapted from Corratgé-Faillie and Lacombe (2017). AGI: *Arabidopsis* Genome Initiative.

Gene	Gene family	AGI	Substrates	References
NPF6.3/NRT1.1	NPF	At1G12110	NO_3^-	(Tsay *et al.* 1993)
			IAA	(Krouk *et al.* 2010)
NPF4.6/NRT1.2	NPF	At1G69850	NO_3^-	(Huang *et al.* 1999)
			ABA	(Kanno *et al.* 2012; Chiba *et al.* 2015)
NPF6.2/NRT1.4	NPF	At2G26690	NO_3^-	(Chiu *et al.* 2004)
NPF7.3/NRT1.5	NPF	At1G32450	NO_3^-	(Lin *et al.* 2008)
			K^+	(Li *et al.* 2017)
NPF2.12/NRT1.6	NPF	At1G27080	NO_3^-	(Almagro *et al.* 2008)
			$GA_{1/3}$	(Chiba *et al.* 2015)
NPF2.13/NRT1.7	NPF	At1G69870	NO_3^-	(Fan *et al.* 2009)
			4MTB	(Nour-Eldin *et al.* 2012)
			$GA_{1/3/4}$, JA-Ile	(Chiba *et al.* 2015)
NPF7.2/NRT1.8	NPF	At4G21680	NO_3^-	(Li *et al.* 2010)
			K^+	(Li *et al.* 2017)
NPF2.9/NRT1.9	NPF	At1G18880	NO_3^-	(Wang and Tsay 2011)
			4MTB	(Nour-Eldin *et al.* 2012)
NPF2.11/GTR2	NPF	At5G62680	NO_3^-, 4MTB	(Nour-Eldin *et al.* 2012)
			4MTB, 8MTO	(Andersen *et al.* 2013)
			GA_3	(Tal *et al.* 2016)
NPF2.10/GTR1	NPF	At3G47960	NO_3^-, 4MTB	(Nour-Eldin *et al.* 2012)
			4MTB, 8MTO	(Andersen *et al.* 2013)
			4MTB	(Saito *et al.* 2015)
			$GA_{1/3/4}$, JA-Ile	(Chiba *et al.* 2015)
			GA_3, JA-Ile	(Saito *et al.* 2015)
NPF1.2/NRT1.11	NPF	At1G52190	NO_3^-	(Hsu and Tsay 2013)
			$GA_{1/3/4}$, JA-Ile	(Chiba *et al.* 2015)
			GA_3	(Kanno *et al.* 2016)
NPF1.1/NRT1.12	NPF	At3G16180	NO_3^-	(Hsu and Tsay 2013)
			ABA, $GA_{1/3/4}$, JA-Ile	(Chiba *et al.* 2015)
NPF3.1/Nitr	NPF	At1G68570	NO_3^-, NO_2	(Pike *et al.* 2014)
			ABA, $GA_{1/3/4/8/20}$	(Tal *et al.* 2016)
			$GA_{1/3}$, JA-Ile	(Chiba *et al.* 2015)
			$GA_{1/3/4/8/19}$	(David *et al.* 2016)
NPF2.7/NAXT1	NPF	At3G45650	NO_3^-	(Segonzac *et al.* 2007)
			$GA_{1/3/4}$, JA-Ile	(Chiba *et al.* 2015)
NPF5.5	NPF	At2G38100	NO_3^-	(Leran *et al.* 2015)

NPF5.10	NPF	At1G22540	NO_3^-	(Leran *et al.* 2015)
NPF2.3	NPF	At3G45680	NO_3^-	(Taochy *et al.* 2015)
			$GA_{1/3/4}$	(Chiba *et al.* 2015)
NRT2.1	NRT2	At1G08090	NO_3^-	(Filleur *et al.* 2001)
NRT2.2	NRT2	At1G08100	NO_3^-	(Cerezo *et al.* 2001)
NRT2.4	NRT2	At5G60770	NO_3^-	(Kiba *et al.* 2012)
NRT2.5	NRT2	At1G12940	NO_3^-	(Lezhneva *et al.* 2014)
NRT2.7	NRT2	At5G14570	NO_3^-	(Chopin *et al.* 2007)
CLCa	CLC	At5G40890	NO_3^-	(Monachello *et al.* 2009)
CLCb	CLC	At3G27170	NO_3^-	(von der Fecht-Bartenbach *et al.* 2010)
SLAC1	SLAC1/SLAH	At1G12480	NO_3^-, Cl^-	(Negi *et al.* 2008)
SLAH2	SLAC1/SLAH	At4G27970	NO_3^-	(Maierhofer *et al.* 2014)
SLAH3	SLAC1/SLAH	At5G24030	NO_3^-, Cl^-	(Negi *et al.* 2008)

1.2.1 Nitrate uptake by roots

Plants take up NO_3^- from soil solution. The *Arabidopsis* root is composed of different cell layers including epidermis, cortex, endodermis, pericycle and stele (Dolan *et al.* 1993). Nitrate transport from soil to endodermis can be accomplished by two pathways: apoplast pathway and symplast pathway (Figure 1).

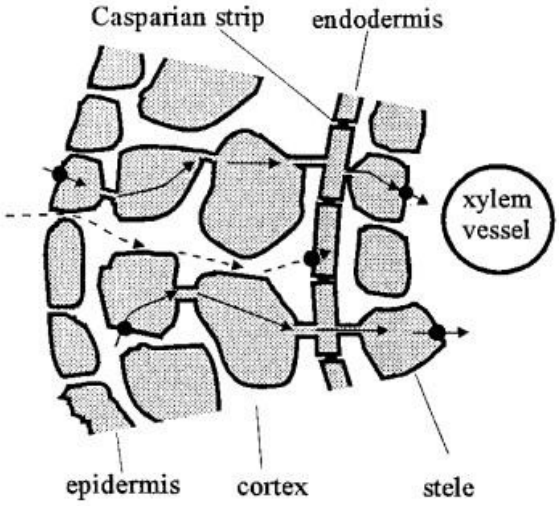

Figure 1. Diagrammatic representation of apoplastic and symplastic ion transport across higher plant roots.

The apoplastic pathway (dashed arrows) conducts ion movement through the cell wall matrix as far as the outer cell walls of the endodermis, since the Casparian strip blocks movement of ions to the stele. Consequently, ions are taken up into the symplasm (shaded area) at the plasma membranes of the epidermis or cortex or the outer face of the endodermis. Symplastic

movement of ion (solid arrows) to the stellar symplasm occurs via the plasmodesmata. Release of the ions into the stellar apoplasts (and ultimately the xylem vessels) occurs across the plasma membrane of the stellar cells (Roberts and Snowman 2000).

By apoplastic transport in the intracellular space, driven by diffusion or mass flow, NO_3^- can enter the root as deep as to the endodermis (Marschner 2012). For symplastic transport, NO_3^- must transit different cell layers (epidermis, cortex or endodermis) before being loaded into pericycle cells. In this process, specific nitrate transporters located at the plasma membrane of root cells are involved (Parker and Newstead 2014). To date, in *Arabidopsis*, two NPF transporters (AtNPF6.3/NRT1.1, AtNPF4.6/NRT1.2) and three NRT2 transporters (AtNRT2.1, AtNRT2.2 and AtNRT2.4) have been functionally identified as key players in NO_3^- uptake (Krapp *et al.* 2014) (Figure 2).

NPF6.3/NRT1.1 (hereafter NRT1.1) is the first characterized nitrate transporter from *Arabidopsis* (Tsay *et al.* 1993). *NRT1.1* is NO_3^- inducible and is primarily expressed in epidermis cells close to root tips as well as in cortex and endodermis, but not in the central cylinder, which suggests it is directly involved in NO_3^- uptake (Huang *et al.* 1996). Indeed, an *in vivo* study demonstrated that NO_3^- uptake in *nrt1.1* knockout mutant plants was significantly reduced compared to wild type (Huang *et al.* 1996). NRT1.1 is the only dual affinity nitrate transporter among 53 NRT1 members. Under low NO_3^- concentrations, Calcineurin B-like interacting protein kinase 23 (CIPK23) phosphorylates threonine 101 (T101), which converts NRT1.1 to a high affinity nitrate transporter (Liu and Tsay 2003). Therefore, in addition to nitrate transport function, NRT1.1 also works as a NO_3^- sensor. This mechanism will beneficial for plants when NO_3^- availability in soil is fluctuating. A recent crystal structure study further showed that dephosphorylation/phosphorylation of T101 is critical for the formation/decoupling of NRT1.1 homodimer (Sun *et al.* 2014). The key residue histidine 356 was shown to play an important role in NO_3^- binding to NRT1.1 (Parker and Newstead 2014).

AtNPF4.6/NRT1.2 has surprisingly low similarity (36% amino acid identical) with NRT1.1, which can be attributed to the long loop connecting the sixth and seventh transmembrane domains (Huang *et al.* 1999). It is expressed in root hair and epidermal

cells of root tip and mature root regions, which is consistent with its role in nitrate uptake. In contrast to *NRT1.1*, the expression of *AtNPF4.6*/*NRT1.2* is not induced by NO_3^- and is constant during different root developmental stages. Antisense *NPF4.6/NRT1.2* transgenic plants exhibited reduced nitrate uptake activities (Huang *et al.* 1999).

NRT2.1 is the best characterized member of the *Arabidopsis* NRT2 family (Orsel *et al.* 2002). It is expressed in epidermis, cortex and endodermis of mature roots, but not in young root parts (Nazoa *et al.* 2003). In addition, its expression is induced by low NO_3^- concentration and is repressed by amino acids (Nazoa *et al.* 2003). *nrt2.1* T-DNA knock out mutant plants were impaired in high affinity nitrate uptake, whereas the low affinity uptake activity was not affected (Filleur *et al.* 2001). Compared to *AtNRT2.1*, expression of *AtNRT2.2* is substantially lower in roots (Zhuo *et al.* 1999; Orsel *et al.* 2002). Disruption of both *AtNRT2.1* and *AtNRT2.2* reduced nitrate uptake and shoot NO_3^- level of mutant plants grown under N deprivation (Orsel *et al.* 2004). *AtNRT2.4* is expressed in epidermis of lateral roots and its expression is also induced by N starvation (Kiba *et al.* 2012). Interestingly, AtNRT2.4 also has a role in maintaining shoot NO_3^- level under N starvation (Kiba *et al.* 2012). AtNRT3.1 (NAR2.1) itself could not transport NO_3^- directly, but it was indispensable for NO_3^- transport function of AtNRT2.1 through directly interacting with AtNRT2.1 on the plasma membrane (Yong *et al.* 2010).

1.2.2 Nitrate root-to-shoot translocation

To reach the foliar chloroplasts where the NO_3^- assimilation preferentially occurs, after absorption by roots, NO_3^- must be loaded into xylem vessels of the vascular stele before being transferred towards the aerial parts of plants. Root xylem loading is a key control point for delivering nutrients to the shoot (Glass *et al.* 2001; Herdel *et al.* 2001). Suberin on endodermal cells acts as a barrier to block NO_3^- across endodermis (Baxter *et al.* 2009). Therefore, transporters and channel proteins are involved in rectifying the outward transport of NO_3^- into the xylem (Figure 2).

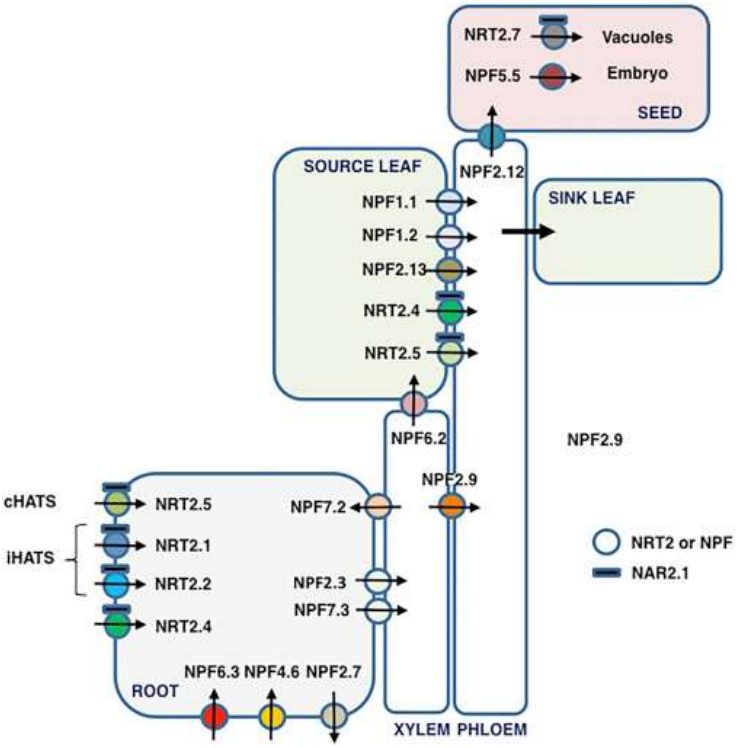

Figure 2. Localization and function of the *Arabidopsis* nitrate transporters from the NPF and the NRT2 family.

The functions depicted are: root uptake (influx/efflux), loading/unloading of the xylem, loading/unloading of the phloem, accumulation in seed vacuoles, and transport into the embryo. At the cellular level, all proteins are localized at the plasma membrane, except NRT2.7 localized at the tonoplast. Except for NRT2.7, all NRT2 proteins are assumed to interact with NAR2.1 to be functional. cHATS, constitutive high-affinity transport system; iHATS, inducible high-affinity transport system (O'Brien *et al.* 2016).

1.2.2.1 NPF7.3/NRT1.5 is the main nitrate transporter for nitrate xylem loading

To date, NPF7.3/NRT1.5 (hereafter NRT1.5) is the most pivotal nitrate transporter involved in NO_3^- xylem loading in *Arabidopsis* (Figure 2). Lin *et al.* (2008) found that NRT1.5 is located to the plasma membrane and is mainly expressed in root pericycle cells adjacent to xylem. Electrophysiological studies demonstrated that NRT1.5 can transport NO_3^- in *Xenopus* oocyte cells, both inwardly and outwardly, depending on the pH value. The nitrate export activity of NRT1.5 in oocytes was mediated by a proton-coupled mechanism. The shoot-to-root ratio of NO_3^- was decreased in *nrt1.5* plants

compared to wild-type plants, suggesting NRT1.5 is responsible for the root-to-shoot long distance transport of nitrate. However, the nitrate transport from roots to shoots is not completely abolished in *nrt1.5* mutants, indicating more proteins are involved in the nitrate xylem loading process. Interestingly, Lin *et al.* (2008) also observed a nitrate-dependent reduction in K^+ root-to-shoot transport in *nrt1.5* mutants. Since the nitrate export by NRT1.5 was not coupled with K^+, they hypothesized that there exists a regulatory loop to maintain the balance of NO_3^- and K^+ xylem loading.

Recently, NPF2.3, a member of the nitrate excretion transporter (NAXT) subgroup within the NPF family, was also suggested to contribute to root-to-shoot transfer of NO_3^-, but only under salt stress condition (Figure 2). *NPF2.3* is expressed in root pericycle cells and localized to plasma membrane. Expression of *NPF2.3* in oocyte cells failed to demonstrate NO_3^- transport activity, but bacteria-expressed *NPF2.3* protein exhibited nitrate transport activity in soybean proteoliposomes (Taochy *et al.* 2015). Unlike *NRT1.5* whose expression was strongly repressed by salt stress, expression of *NPF2.3* was barely altered by salt stress. Disruption of *NPF2.3* in knock out mutants generated no phenotype under control conditions, however, mutants showed lower shoot NO_3^- content and decreased tolerance under salt stress conditions (Taochy *et al.* 2015). Interestingly, similar to what has been observed in *nrt1.5* mutants, K^+ translocation was also decreased in *npf2.3* mutant (Taochy *et al.* 2015). This observation supports the hypothesis that there is a strong interaction between the secretion of K^+ and NO_3^- into the xylem sap.

Recently, it has been observed that NRT1.1 and AtNPF6.2/NRT1.4 were also capable of mediating bidirectional transport of NO_3^- in *Xenopus* oocytes (Leran *et al.* 2013). Nitrate supplied to roots was more slowly transferred to shoots in *nrt1.1* mutants (Leran *et al.* 2013). These observations indicated that NRT1.1 and AtNPF6.2/NRT1.4 might also contribute to NO_3^- root-to-shoot transfer process. However, this speculation needs to be further verified.

In addition, SLAH2 and SLAH3 from SLAC/SLAH family have been suggested to be putatively involved in the NO_3^- root-to-shoot transport. Especially SLAH2, which is

localized in the root stele and is a nitrate specific channel, may contribute to specific NO_3^- xylem loading (Hedrich and Geiger 2017).

1.2.2.2 NPF7.2/NRT1.8 is responsible for nitrate unloading from xylem

Among 53 *Arabidopsis* NRT1 members, AtNPF7.2/NRT1.8 (hereafter NRT1.8) shares the highest similarity with NRT1.5 (Li *et al.* 2010; Leran *et al.* 2014). Opposite to the NO_3^- xylem loading function of NRT1.5, NRT1.8 plays a role in removal of NO_3^- from xylem sap to parenchyma cells (Figure 2). In accordance with its function, *NRT1.8* is mainly expressed at vascular tissues including parenchyma cells abutting xylem vessels (Li *et al.* 2010). Interestingly, it was shown that *NRT1.5* and *NRT1.8* were oppositely regulated by stresses (Li *et al.* 2010).

Another nitrate transporter that negatively affects NO_3^- root-to-shoot transport is *AtNPF2.9/NRT1.9*, which is expressed in the companion cells of root phloem. It facilitates loading of NO_3^- into the root phloem to enhance the downward transport of NO_3^- in roots. Root-to-shoot transport of NO_3^- was therefore enhanced in *nrt1.9* mutants under high NO_3^- supply (Wang and Tsay 2011).

1.2.2.3 Ethylene and jasmonic acid signaling pathway converge to regulate *NRT1.5* and *NRT1.8*

Under normal growth conditions, most NO_3^- is supposed to undergo long distance transport from root to shoot for NO_3^- assimilation in chloroplasts. However, under adverse growth conditions such as heavy metal and low light, Stress-Initiated Nitrate Allocation to Roots (SINAR) is induced, which might be a common response to stresses (Gojon and Gaymard 2010; Li *et al.* 2010). By this means, retaining of NO_3^- to roots benefits plants to cope with stresses. It has been shown that SINAR is mediated by NRT1.5 and NRT1.8. The *nrt1.8-1* mutant showed a NO_3^--dependent cadmium (Cd^{2+}) sensitive phenotype, and NO_3^- proportion allocated to roots was

decreased in the *nrt1.8-1* mutant compared to the wild type (Li *et al.* 2010). Opposite to that of *NRT1.8*, transcription of *NRT1.5* was repressed by various stresses such as salt, drought and Cd^{2+} in roots. Remarkably, *nrt1.5* knockout mutants are more resistant to these stresses, which is possibly attributed to more retained NO_3^- in mutant plants' roots under stress conditions (Chen *et al.* 2012).

The signaling pathways of the plant hormones ethylene (ET) and jasmonic acid (JA) control the balance between plant growth and stress tolerance (Achard *et al.* 2003; Yang *et al.* 2012). Recently, Zhang *et al*. (2014) demonstrated that the *NRT1.8* promoter region could bind ethylene responsive factors (ERF) including OCTADECANOID-RESPONSIVE *ARABIDOPSIS* AP2/ERF59, while ETHYLENE INSENSITIVE3 (EIN3) binds to *NRT1.5* promoter (Zhang *et al.* 2014). Through a series of physiological studies, they revealed that ET and JA signaling pathways converge at EIN3/EIN3-Like 1 (EIL1) to regulate the downstream communication between SINAR and the environment through controlling the expression of *NRT1.5* and *NRT1.8* (Zhang *et al.* 2014).

1.2.3 Nitrate distribution in aerial tissues

Transport and remobilization of NO_3^- throughout the plant is of great importance for plant growth and the improvement of nitrogen use efficiency (NUE). NUE is defined as utilization of available N in different forms in order to maximize grain yield (Gupta *et al.* 2012). AtNPF6.2/NRT1.4 plays a role in regulating NO_3^- distribution in leaves (Figure 2). It is primarily expressed in the leaf petioles and mid-rib (Chiu *et al.* 2004). In *nrt1.4* mutant, NO_3^- content of the petiole is reduced but leaves are wider compared to wild type (Chiu *et al.* 2004), indicating that AtNPF6.2/NRT1.4 can affect leaf development through influencing NO_3^- content. NO_3^- also influences seed development, even though NO_3^- is not the main N form in seeds (Alboresi *et al.* 2005). AtNPF2.12/NRT1.6, which only shows expression in the vascular bundles of the siliques and the funiculi, plays a role in translocating NO_3^- to developing seeds (Almagro *et al.* 2008). Therefore, mature seeds of *nrt1.6* mutant accumulated less NO_3^-, and the seed abortion rate was

increased (Almagro *et al.* 2008). In addition to AtNPF2.12/NRT1.6, NRT2.7, located at the tonoplast, is also involved in NO_3^- accumulation in seeds through importing NO_3^- into the vacuole (Chopin *et al.* 2007). Efficient remobilization of NO_3^- from sink to source tissues is vital for improving NUE. AtNPF2.13/NRT1.7, NRT2.4, AtNPF1.1/NRT12 and AtNPF1.2/NRT11 participate in this process via phloem loading (Krapp *et al.* 2014) (Figure 2). AtNPF2.13/NRT1.7 is involved in remobilizing NO_3^- from older to younger growing leaves through loading NO_3^- into minor veins (Fan *et al.* 2009). Expression of AtNPF2.13/NRT1.7 is induced by N starvation and *nrt1.7* mutants showed growth retardation under low N supply (Fan *et al.* 2009). The *nrt2.4* mutant also showed decreased NO_3^- concentration in the phloem sap under N starvation (Kiba *et al.* 2012). However, the interplay of those two nitrate transporters in NO_3^- remobilization has not been investigated (Krapp *et al.* 2014). In the *nrt1.11/nrt1.12* double mutant, less NO_3^- was transferred via phloem to the youngest tissues, instead, more NO_3^- accumulated in the mature and larger expanded leaves (Hsu and Tsay 2013), suggesting these two members are important for redistributing root-derived NO_3^- to sink tissues.

1.3 Other substrates of *Arabidopsis* NPF proteins

Apart from nitrate transport function, recently, more and more nitrate transporters are reported to be able to transport other substrates including phytohormones and secondary metabolites (Table 1).

Auxin transport function of *Arabidopsis* NRT1.1 in a NO_3^--dependent manner was investigated by Krouk *et al.* (2010). When external NO_3^- concentration is low (< 1 mM), rather than transporting NO_3^-, NRT1.1 mainly favors the basipetal transport of auxin in lateral roots (LRs), thus preventing the accumulation of auxin at the LR tip, which explains the “more LR” phenotype of *nrt1.1* mutants under low NO_3^- supply. Yet, when at least 1 mM NO_3^- was present, auxin transport function was suppressed and thus *nrt1.1* behaved like the wild type (Krouk *et al.* 2010). Through using a modified yeast two-hybrid (Y2H) system, Kanno *et al.* (2012) identified four members of the NPF

family (NPF4.1/AIT3, NPF4.2/AIT4, NPF4.5/AIT2 and NPF4.6/NRT1.2/AIT1) as abscisic acid (ABA) importer candidates. Interestingly, besides ABA, NPF4.1/AIT3 could also transport gibberellin (GA; GA_3) (Kanno *et al.* 2012). The ABA import function of NPF4.6/NRT1.2/AIT1 was confirmed by phenotypical analysis of *nrt1.2* mutants and overexpression lines (Kanno *et al.* 2012). Different from NRT1.1, ABA transport activity of NPF4.6/NRT1.2/AIT1 is not inhibited by high amount of NO_3^- (Kanno *et al.* 2013).

Recently, Chiba *et al.* (2015) screened 45 NPF members for their GA and jasmonoyl-isoleucine (JA-Ile) transport function by using modified Y2H systems. They found ten of them can transport ABA, 18 of them transport GA_1, 15 of them transport GA_3 and 13 of them can transport JA-Ile in yeast (Table 1). However, *in vivo* hormone transport functions of these NPF members still need to be further confirmed. Very recently, the *in vivo* GA transport function of NPF3.1/Nitr was reported. Tal *et al.* (2016) showed that NPF3.1/Nitr is expressed in the root endodermis and its expression is repressed by GA. NPF3.1/Nitr could efficiently transport fluorescently labeled GAs across cell membranes *in vivo*.

In addition to phytohormones, several NPF members are capable of transporting the secondary metabolite gluocosinolate. For instance, NPF2.10/GTR1 and NPF2.11/GTR2 are characterized as high-affinity glucosinolate specific transporters which contribute to glucosinolate accumulation in seeds, through controlling glucosinolate loading from apoplasm into phloem (Nour-Eldin *et al.* 2012).

1.4 Nitrate serves as a signal molecule

In addition to being an essential nutrient, NO_3^- also functions as a signal molecule controlling leaf development (Rahayu *et al.* 2005), regulating root architecture (Zhang and Forde 2000) and breaking seed dormancy (Alboresi *et al.* 2005). Moreover, NO_3^- also coordinates the expression of up to 1000 genes including genes encoding nitrate transporters and nitrate assimilation related enzymes rapidly (within minutes), which is called primary nitrate response (Wang *et al.* 2000). In contrast to the well characterized molecuar mechanism of nitrate transport, the signaling components in nitrate

responses are pooly understood. No global nitrate-responsive promoter elements have been identified so far, which might be attributed to the fact that nitrate responsive cascades comprise a large number of molecular players and are in cross-talk with other signaling cascades (Krapp *et al.* 2014).

Transcription factors are expected to be key molecular players in the primary nitrate response. The Nodule Inception-Like Protein 7 (NLP7) belong to the RWP-RK transcription factor family, has been reported to be involved in NO_3^- starvation responses through binding to 851 genes in *Arabidopsis* (Marchive *et al.* 2013). The NLP7 is delocalized from the nucleus to the cytosol under N starvation condition, however, resupply of NO_3^- leads to its rapid nuclear accumulation by an unknown mechanism (Marchive *et al.* 2013). Two Calcineurin B-like (CBL)-interacting protein kinase (CIPK), CIPK8 and CIPK23 are involved in the primary nitrate response. CIPK8, rapidly induced by nitrate, has been demonstrated as a positive regulator of primary nitrate responsive genes (Hu *et al.* 2009). Unlike CIPK8, CIPK23 negatively regulates this process. Independent of its nitrate uptake function, NRT1.1 also works as a nitrate sensor. In response to low nitrate concentrations, NRT1.1 is phosphorylated by CIPK23 at residue T101, which then reduces the primary nitrate response (Ho *et al.* 2009). Recently, the role of calcium as a second messenger in nitrate signaling pathway has been explored. Riveras *et al.* (2015) monitored *in vivo* cytoplasmic Ca^{2+} accumulation after NO_3^- treatments, which is necessary for regulating expression of some primary response genes. They proposed a model of nitrate signaling: NO_3^- is sensed by NRT1.1 and activates the phospholipase C which triggers an increase in cytoplasmic Ca^{2+} level. By this means that expression of nitrate responsive genes is activated (Riveras *et al.* 2015).

1.5 Potassium uptake and translocation in *Arabidopsis*

Potassium ion (K^+), the most abundant cation in the cytosol, plays crucial roles in plant growth and development. It is involved in regulating enzyme activity, stabilizing protein synthesis as well as neutralizing negative charges. Apart from that, through influencing

cation-anion balance and osmoregulation, K^+ also affects pH homeostasis, membrane potential, xylem and phloem transport as well as cellular turgor (Maathuis 2009; Sharma *et al.* 2013). K^+ is the most abundant counterion for NO_3^- in long-distance transport in the xylem and for storage in vacuoles (Marschner 2012). Cation deficit caused by K^+ deficiency limits NO_3^- transport in the xylem, thereby forcing plants to transport amino acids as substitute (Forster and Jeschke 1993).

In plants, K can constitute 2-10% of dry weight (Leigh and Jones 1984). The typical K concentration in regular soil is 0.1-1 mM (Maathuis 2009), which is about three to four orders of magnitude lower than within plants (100 mM). Electrical gradient and proton motive force established by H^+-ATPase provides energy for plants to transport K^+ throughout the plant via low and high-affinity transport systems. Channel proteins from three families: Shaker, TPK (tandem-pore K^+) and Kir (K^+ inward rectifier), and transporters from HAK/KUP/KT (High-Affinity K^+/K^+ UPtake/K^+ Transporter), HKT (High-Affinity Potassium Transporter), NHX (Na^+/H^+ antiporter) and CHX (cation:proton antiporters) families are responsible for K^+ transport in plants.

1.5.1 Potassium acquisition from soil

AKT1 (*Arabidopsis* K^+ Transporter 1) and HAK5 (High Affinity K^+ Transporter 5) are two main proteins responsible for K^+ uptake by roots. AKT1 is predominant in this process when external K^+ concentrations ($[K_+]_{ext}$) are between sub-millimolar and millimolar ranges (Rubio *et al.* 2010; Nieves-Cordones *et al.* 2014), whereas HAK5 is more important when $[K_+]_{ext}$ is lower than 10 µM (Rubio *et al.* 2010). When $[K_+]_{ext}$ is in the range of 10-200 µM, both of them contribute to the K^+ uptake (Ragel *et al.* 2015).

In agreement with its K^+ uptake function, *AKT1* is preferentially expressed in root epidermis, cortex and endodermis (Lagarde *et al.* 1996). The *akt1* mutant plants grew indistinguishably from the wild-type plants under K^+ sufficient conditions, but their growth was significantly impaired on the low K^+ medium in the presence of ammonium (Hirsch *et al.* 1998). Expression of *AKT1* is not regulated by low K^+ at the transcriptional level (Lagarde *et al.* 1996), however, several studies revealed its post-transcriptional

regulation. Under low K^+ conditions, AKT1 is phosphorylated and activated by CIPK23 with the help of Calcineurin B-like protein (CBL) CBL1 and CBL9 (Li *et al.* 2006; Xu *et al.* 2006). In addition to CIPK23-CBL1/CBL9 complex, AKT1 is also activated by multiple CIPKs (CIPK6 and CIPK16) together with multiple CBLs (CBL2, CBL3 and CBL5), and the ankyrin repeat domain of AKT1 is responsible for the interaction with CIPKs (Lee *et al.* 2007). Opposite to the activation effect by the CIPK-CBL network, AKT1 activity is strongly inhibited by the PP2C protein AIP1 (AKT1 interacting PP2C 1) through physical interaction, which suggests that CIPK kinase and PP2C could modify AKT1 activity through phosphorylation and dephosphorylation (Lee *et al.* 2007). Recently, one CIPKs-independent regulatory mechanism of AKT1 has been reported. It was shown that CBL10 can directly interact with AKT1, and may compete with CIPK23 for the binding to AKT1, therefore, AKT1 activity was impaired by CBL10 (Ren *et al.* 2013). Moreover, under low K^+ conditions, AKT1 was also negatively regulated by KC1, the shaker K^+-channel α-subunit. KC1 itself did not have any K^+ transport activity, however, through the formation of heteromeric K^+ channels, it inhibited the AKT1-mediated inward K^+ transport (Wang *et al.* 2010). Through KC1 serving as a bridge, AKT1, KC1 and membrane vesicle trafficking protein (SNARE) SYP121 can form a heterotrimeric complex and enhance the gating of AKT1 channel (Honsbein *et al.* 2009).

Transcriptional regulation of *HAK5* has been intensively studied. Under ample K^+ supply, *HAK5* was expressed weakly only in the root vasculature. However, upon K^+ deprivation treatment, it was strongly induced at the transcriptional level and was expressed in root epidermis and stele of the main root (Armengaud *et al.* 2004; Shin and Schachtman 2004; Gierth *et al.* 2005). Induction of *HAK5* by low K^+ was attributed to the hyperpolarized membrane potential and subsequent increase in ethylene and reactive oxygen species (ROS) production (Shin and Schachtman 2004; Nieves-Cordones *et al.* 2008; Jung *et al.* 2009; Kim *et al.* 2010), but this induction effect was inhibited by the presence of ammonium ($NH4^+$) (Qi *et al.* 2008). *HAK5* expression was also strongly depressed by salinity stress (Nieves-Cordones *et al.* 2010). Several

transcription factors regulating the *HAK5* expression have been identified (Hong *et al.* 2013), and also the post-transcriptional regulation of HAK5 has been reported in the recent study of Ragel *et al.* (2015). Similar to AKT1, HAK5 can also be activated by the CIPK-CBL complex. More specifically, CIPK23 and CBLs including CBL1, CBL8, CBL9 and CBL10 are involved in the activation of HAK5 function in *Saccharomyces cerevisiae* (Ragel *et al.* 2015).

Very recently, KUP7 was characterized as another crucial protein contributing to the K^+ uptake in *Arabidopsis*. *KUP7* is strongly expressed in roots and it is localized at the plasma membrane. Expression of *KUP7* is able to complement the K^+ uptake deficiency of yeast mutant R5421. *kup7* plants exhibit a low K^+ sensitive phenotype. Phosphorylation on S80, S719 and S721 is critical for maintaining K^+ uptake function of KUP7 (Han *et al.* 2016).

In addition to AKT1, HAK5 and KUP7, when external K^+ is sufficiently high, it was suggested that unknown mechanisms and non-selective cation channels (NSCCs) might also contribute to unspecific K^+ uptake in plants (Nieves-Cordones *et al.* 2014).

1.5.2 SKOR is responsible for potassium root-to-shoot translocation

After taken up by roots, K^+ is translocated into xylem vessels for long distance transport to the shoots. SKOR (Stelar K^+ Outward Rectifier), a voltage-dependent channel protein belonging to the *Arabidopsis* Shaker channel family, is the major K^+ channel protein contributing to this process. *SKOR* was mainly expressed in root pericycle cells and in parenchymal cells surrouding the xylem vessels, and its transcription was strongly inhibited by hormone ABA (Gaymard *et al.* 1998). *Xenopus* oocytes injected with *SKOR* cRNA demonstrated K^+ permeability. T-DNA knockout mutant *skor1* had no alteration in root K content, but exhibited an approximate 50% decrease in shoot K content which was likely resulted from the reduced root-to-shoot translocation rate of K^+ via xylem. The reduced K content in leaves was compensated with the accumulation of calcium (Ca) (Gaymard *et al.* 1998).

The gating of SKOR has been intensively studied since two decades. SKOR activity is

sensitive to pH. The decrease of internal and external pH in *Xenopus* oocytes strongly impaired the SKOR current (Lacombe *et al.* 2000). In contrast, hydrogen peroxide (H_2O_2) treatment led to an increase in the SKOR outward currents and a decrease in its half activation time (Garcia-Mata *et al.* 2010). The opening or closure of SKOR channel was also modulated by $[K^+]_{ext.}$ Under high $[K^+]_{ext}$, the Pore (P) domain of SKOR was occupied with K^+, which caused the conformational change of the C terminus of two S6 subunits, therefore, the SKOR channel was closed and more energy input was required for the opening of the channel (Johansson *et al.* 2006). Moreover, SKOR was activated by the increase in intracellular K^+ ($[K^+]_i$), which was a voltage-independent process. The C-terminal cytoplasmic domain of SKOR is important for this internal K^+ sensing (Liu *et al.* 2006).

Besides SKOR, the recently characterized KUP7 may be also involved in root-to-shoot translocation of K^+. Under low K^+ availability, *kup7* mutant plants demonstrated significantly lower shoot/root K ratio and lower K content in xylem sap compared to wild-type control. No significant difference was observed when K^+ supply was sufficient (Han *et al.* 2016). These findings indicated that KUP7 may contribute to K^+ xylem loading under low K^+ growth conditions.

Apart from SKOR and KUP7, other K^+ unspecific transporters and channels like AtCCC (Cation Chloride Cotransporter) and NORC (Non-selective Outwardly Rectifying Current) are also suggested to facilitate K^+ efflux into xylem sap (Colmenero-Flores *et al.* 2007; Zepeda-Jazo *et al.* 2008).

1.5.3 NRT1.5 affects potassium root-to-shoot translocation at limited nitrate supply

Before the nitrate transport funcion of NRT1.5 was characterized by Lin *et al.* (2008), the early study in our group has found that NRT1.5 is one of the NRT1 members which is highly upregulated during the leaf senescence (van der Graaff *et al.* 2006). This expression pattern of *NRT1.5* prompted us to investigate its function and the role in leaf senescence. Our subsequent studies found an early leaf senescence phenotype

of *nrt1.5* mutant plants, which occured after bolting when growing on low fertilized soil. The more detailed phenotypical analysis showed that *nrt1.5* mutants had a pleiotropic reduction in rosette fresh weight, anthocyanins, seed yield, seed weight and seed oil content compared to wild-type plants growing on low fertilized soil (Drechsler *et al.* 2015). Interestingly, the development of those pleiotropic symptoms of *nrt1.5* mutants were diminished or even abolished when 10 mM KNO_3 was supplied. Even though NRT1.5 has been reported to be involved in NO_3^- xylem loading, neither NO_3^- nor total N content in *nrt1.5* plants was significantly differed from the levels in wild-type plants. This finding suggested that the low K conccentration might account for the early senescence phenotype of *nrt1.5* plants. Moreover, Chen *et al.* (2012) did not observe the similar leaf senescence phenotype when growing *nrt1.5* plants in hydroponic culture with high NO_3^- concentration (4-12.5 mM), which implies the early leaf senescence phenotype of *nrt1.5* plants observed in our study might also depend on the low NO_3^- availability.

To access to the root material, *nrt1.5* mutants and wild-type plants were cultivated in hydroponic solutions with low NO_3^- concentration (0.1 mM). Both NO_3^- and total N content in rosette leaves were even higher in *nrt1.5* than in the wild-type plants, which is consistent with the previous result from soil experiments. K concentration in roots of *nrt1.5* and wild type was comparable. Strikingly, the K concentrations in aerial parts of *nrt1.5*, including rosette leaves and infloresence stems, were significantly reduced compared to the wild-type level (Drechsler *et al.* 2015). These results suggested that the K^+ translocation from root to shoot was blocked in *nrt1.5* at NO_3^- deprivation.

In addition to our study, a recent study by Meng *et al.* (2016) also reported the similar observations of *nrt1.5* mutants. They concluded that NRT1.5 can prevent the leaf senesence provoked by low NO_3^- availability through modulating foliar K^+ level.

1.6 The intersection of nitrate and potassium transport

Physiological studies since the 1960s have described a close relationship between NO_3^- and K^+ in respect of their uptake, translocation and recycling. It was often

observed that the acquisition and xylem translocation of NO_3^- and K^+ are commonly positively correlated, which might be attributed to the improved charge balance (Rufty *et al.* 1981; Siebrecht and Tischner 1999; Zhang *et al.* 2010). K^+ can also activate nitrate assimilation enzymes (Balkos *et al.* 2010), therefore enhancing crop yields (Zhang *et al.* 2010). The internal translocation and cycling of both ions can be well explained by the 'Dijkshoorn-Benzioni model'. NO_3^- is transported from root to shoot in xylem, accompanied with K^+ as a counterion. In shoot, NO_3^- is reduced and assimilated into amino acids in the form of organic acids like malate. Then, organic acids are further transferred to root via phloem with K^+ as a counterion. In root, organic acids are decarboxylated and release negative charged HCO_3^-.

1.6.1 Co-regulation of transporters at the molecular level

Except physiological studies, however, to date, little is known about the crosstalk of NO_3^- and K^+ at the molecular level. ROS elevation is observed in plant roots by NO_3^- and K^+ deficiency treatment, indicating that ROS serve as a common signal component in NO_3^- and K^+ signaling pathways (Shin *et al.* 2005). Recently, gene expression studies indicate a close relationship between nitrate and potassium transport at the transcriptional level. On the one hand, K^+ deficiency not only positively regulates the expression of potassium transporter genes like *HAK5*, but also inhibits the transcription of nitrate transporters involved in nitrate uptake (*NRT2.1*) and nitrate translocation (*NRT1.5*) (Figure 3), even though after K^+ resupply their transcription was quickly recovered (Armengaud *et al.* 2004; Lin *et al.* 2008). On the other hand, NO_3^- availability also regulates the expression of potassium transporters/channels. For instance, *SKOR* transcription was significantly downregulated by NO_3^- deprivation (Menz *et al.* 2016), and *HAK5* was strongly induced by NO_3^- (Wang *et al.* 2001). Based on the observation that the root-to-shoot translocation of K^+ was reduced in *nrt1.5* mutants (Lin *et al.* 2008), it was speculated that K^+ root-to-shoot translocation conducted by SKOR may be dependent on the nitrate transport activity of NRT1.5 (Wang and Wu 2013). Interestingly, the knockout mutant of recently identified nitrate exporter *NPF2.3* also

showed decreased K^+ root-to-shoot translocation (Taochy *et al.* 2015). This observation corroborates that the root-to-shoot K^+ transport is influenced by the root-to-shoot transport of its counterion NO_3^-.

1.6.2 CIPK23: a common regulator for nitrate and potassium transport

Recently, CIPK23, which is regulated by CBL1 and CBL9 under both NO_3^- and K^+ deficiencies, was identified as one important node in controlling uptake of both NO_3^- and K^+. At low NO_3^- concentrations, once activated by CBL9, CIPK23 phosphorylates nitrate transporter NRT1.1 at Thr101 to convert its nitrate uptake mode from low affinity to high affinity (Ho *et al.* 2009). Similarly, low K^+ stress also leads to the activation of CIPK23 by CBL proteins. As a consequence, the two potassium inward transporters AKT1 and HAK5 are activated via phosphorylation (Xu *et al.* 2006; Ragel *et al.* 2015), which will eventually benefit plants to taking up more K^+ under K^+ deficiency.

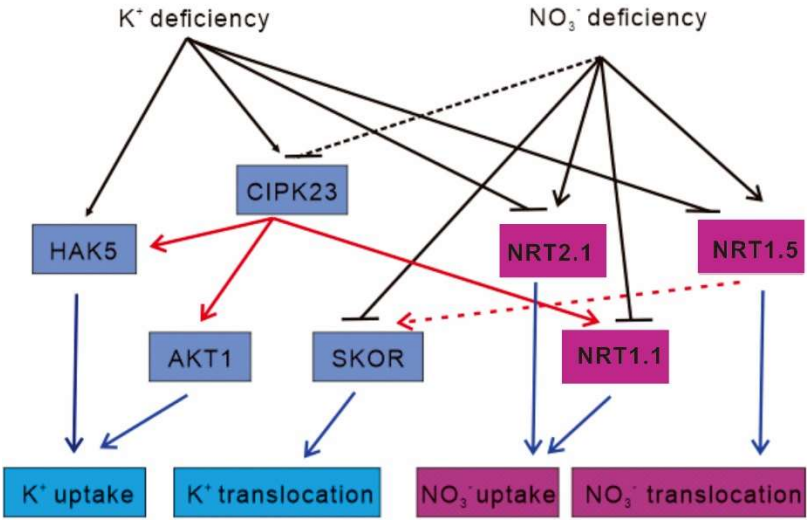

Figure 3. Schematic model of the crosstalk between K^+ and NO_3^- signaling responses to K^+ and NO_3^- deficiencies in *Arabidopsis*.

K^+ deficiency enhances *HAK5* and *CIPK23* transcription but reduces *NRT2.1* and *NRT1.5* transcription. NO_3^- deficiency induces *NRT2.1* and *NRT1.5* transcription but downregulates *NRT1.1* and SKOR expression. The increased CIPK23 regulates activities of AKT1, HAK5 and NRT1.1 by phosphorylation, which coordinately modulates K^+ uptake and NO_3^- uptake. NRT1.5-mediated NO_3^- translocation may also affects the root-to-shoot K^+ translocation conducted by

SKOR. Modified from (Wang and Wu 2013).

1.6.3 Protein-protein interaction between nitrate and potassium transporters

Interestingly, recent studies showed that members of the SLAC1/SLAH family can influence the activity of Shaker channels through their physical protein-protein interaction. SLAC1 and its homologue SLAH3 which have NO_3^- permeability, can negatively affect inward K^+ rectifying channel proteins KAT1 (K^+ channel in *Arabidopsis thaliana* 1) through the direct protein-protein interaction, which then impairs light-induced K^+ import and consequently prevents stomatal opening under light in *Arabidopsis*. This inhibition effect of KAT1 by SLAC1 and SLAH3 is a different mechanism than the inhibition of KAT1 by KC1 (Zhang *et al.* 2016). In addition to KAT1, SLAH1, SLAH2 and SLAH4 are also able to interact with AKT2 (*Arabidopsis* potassium transporter 2) which mediates both K^+ influx and efflux activity, but only the AKT2-mediated K^+ influx is inhibited by the interaction with SLAHs. In addition, all four SLAHs can significantly reduce the KAT2 (K^+ channel in *Arabidopsis thaliana* 2) mediated inward K^+ channel currents. These observations indicated that the protein-protein interaction between inward K^+ rectifiers from Shaker channel and S-type anion channels could be a general molecular mechanism to coordinate the movement of anions and K^+ in plants (Yao *et al.* 2017).

1.7 The influence of nitrate and potassium on root plasticity of *Arabidopsis*

It is well known that besides plant hormones, nutrient availability also has a profound impact on root system architecture (RSA) of plants by influencing parameters including number, length, angle and diameter of roots (Malamy 2005). The influence of NO_3^- on RSA has been intensively studied with respect to both uniformly supplied NO_3^- or locally concentrated NO_3^- supply. In the former experiments, *Arabidopsis* plants were grown with a range of uniformly supplied NO_3^- concentrations to examine their RSA. In

the latter experiments, *Arabidopsis* plants were first grown on agar plates with low NO_3^- to produce NO_3^--starved plants. The plants were then transferred to agar plates divided into three segments. The upper and lower segment contained low NO_3^- level, while the middle segment contained high NO_3^- concentration (Zhang and Forde, 1998; Linkohr *et al.* 2002). Alternatively, agar plates were simply separated into two segments with either low or high NO_3^- supply (Remans *et al.* 2006).

High concentration of NO_3^- (>10 mM) applied uniformly to whole plants had little effect on primary root (PR) elongation, whereas it repressed lateral root (LR) development at the specific stage when LRs just emerged from the PR and before maturation. The suppression is due to an effect on LR elongation rather than on initiation (Zhang and Forde, 1998). This repression is systemic and is caused by NO_3^- itself rather than its metabolites (Zhang *et al.* 1999). Signora *et al.* (2001) found that ABA is involved in mediating this systemic inhibitory effect of LR elongation by high NO_3^-(Signora *et al.* 2001).The similar inhibitory effect of high NO_3^- on LR growth was also found by Linkohr *et al.* (2002). They observed that LR density remained unchanged while LR elongation was suppressed by uniformly high NO_3^- supply. In addition, Linkohr *et al.* (2002) found PR of *Arabidopsis* plants was shorter with increasing NO_3^- supply.

In contrast to uniform NO_3^- supply, locally concentrated NO_3^- supply had no influence on PR length of *Arabidopsis* plants (Zhang and Forde 1998; Linkohr *et al.* 2002). Similar observations were also reported in other organisms like barley and maize (Drew *et al.* 1973; Granato and Raper 1989). The increase in LR density was induced by locally high NO_3^- supply (Linkohr *et al.* 2002). Moreover, LR elongation within NO_3^--rich patch (the segment of agar plates with locally high-NO_3^- concentration) was induced, whereas the growth of LR outside the NO_3^--rich patches was suppressed (Drew *et al.* 1973; Granato and Raper 1989; Sattelmacher *et al.* 1993; Zhang and Forde 1998; Linkohr *et al.* 2002). This stimulatory effect was triggered by the function of NO_3^- as a signal rather than by its nutritional properties (Zhang and Forde 1998). The ANR1 MADS-box transcription factor is involved in this localized NO_3^- stimulation effect because *anr1* knockdown mutant failed to colonize in NO_3^--rich zones (Zhang

and Forde 1998). Based on observations that *nrt1.1* mutant plants have a similar phenotype like *anr1* and *ANR1* expression is reduced in *nrt1.1* mutants, it was suggested that *NRT1.1* is located upstream of *ANR1* in the local stimulation pathway (Remans *et al.* 2006). Moreover, so far it is not clear whether auxin is involved in this stimulation effect. Zhang *et al.* (1999) observed that the stimulation effect of NO_3^- on LR proliferation was abolished in *arx4* (Auxin resistant 4) mutant, suggesting an overlap between auxin and nitrate response pathways (Zhang *et al.* 1999). In contrast, Linkohr *et al.* (2002) observed the wild-type responses of *axr4* mutant inside and outside NO_3^--rich patches.

Armengaud *et al.* (2004) observed that K^+ deficiency reduced LR length. Shin and Schachtman (2004) observed that low K^+ supply decreased LR length and LR numbers rather than affecting PR length. However, Gruber *et al.* (2013) found that K^+ deficit mainly affected total root length by decreasing PR length and the 1° (first-order) lateral roots length, but the 1° LR density remained unchanged. In agreement with this observation, the PR length of *athak5* knockout mutant plants was significantly decreased compared to wild-type control under K^+ deficient growth conditions (Qi *et al.* 2008). Inhibition of LR growth in K^+ starved plants may be due to the elevated ethylene level, even though genes related to ethylene metabolism and signaling were not activated during this development response (Armengaud *et al.* 2004). Moreover, it has been observed that K^+ availability affected root gravitropic behavior and auxin distribution within root tip (Vicente-Agullo *et al.* 2004), indicating that auxin might also be involved in regulation of RSA by low K^+ availability.

1.8 Aim of the present study

In our previous study, it has been demonstrated that the transcription level of *NRT1.5* was strongly upregulated during the leaf senescence (van der Graaff *et al.* 2006), which prompted us to presume that the impairment in *NRT1.5* would change the senescence development pattern of *nrt1.5* mutant plants. Indeed, subsequent studies of our group (Drechsler *et al.* 2015) and Meng *et al.* (2016) discovered an early leaf

chlorosis phenotype of *nrt1.5* mutants only under low NO_3^- availability, which turned out to be provoked by the low K level in rosette leaves of *nrt1.5.* However, as a nitrate transporter, how does NRT1.5 affect K^+ root-to-shoot translocation, is still poorly understood. The main aim of the present work is to elucidate the role of NRT1.5 in potassium transport process, either through its potassium transport function or through influencing other potassium transport proteins.

Since *NRT1.5* is mainly expressed in root pericycle cells, to explore the role of NRT1.5 in the root morphological adaptions to NO_3^- and K^+ availability, the root phenotype of *nrt1.5* mutants will be examined under various NO_3^- and K^+ supplies on plates. Moreover, to investigate the role of NRT1.5 in potassium transport, on the one hand, the potassium transport function of NRT1.5 will be examined in *Saccharomyces cerevisiae* mutant cells which are deficient in either K^+ uptake or export function, respectively. On the other hand, the *in vivo* protein-protein interaction between NRT1.5 and its interacting partners will be investigated in tobacco by using bimolecular fluorescence complementation (BiFC) methods. Subsequently, to analyze the physiological meaning of the protein-protein interactions, the double mutants of NRT1.5 and prospective interacting partners will be generated by crossing and used for phenotypical analysis under various nutrient supplies. Plant material will be harvested for elemental analysis by Inductively Coupled Plasma Optical Emission Spectrometry (ICP-OES) to examine the composition of K and other elements. In the last, qRT-PCR will be employed to analyze the expression pattern of several important nitrate and potassium transporter genes including *NRT1.5* in response to hormone treatments. These results will shed a light on understanding how ion transport processes are controlled by phytohormones, which might act as the subsequent signals of nutrient deficiency.

2 Materials and Methods

2.1 Materials

2.1.1 Chemicals

The chemicals used in this study were purchased from the companies Carl Roth (Karlsruhe, Germany), Duchefa (Haarlem, Netherlands), Formedium (Hunstanton, United Kingdom), Merck (Darmstadt, Germany), Serva (Heidelberg, Germany) and Sigma-Aldrich (Taufkirchen, Germany).

Without special indications, deionized (dH_2O) or double deionized water (ddH_2O) (Milli-Q Water System, Merck Millipore, Billerica, USA) was used for solutions and reaction preparation. The solutions and medium were autoclaved at 121°C (1.2 bar) for 15 min or filter (Sarstedt, Nümbrecht, Germany, pore diameter 0.2 µm) sterilized. Customary solutions and buffers in molecular biology have been described in Molecular cloning (3rd edition) (Sambrook and Russell 2001).

2.1.2 Enzymes and Kits

All restriction enzymes used in this study were purchased from company Thermo Fisher Scientific (Waltham, USA) or New England Biolabs (Frankfurt am Main, Germany).

Without special indications, self-made *Taq* DNA polymerase was applied to all regular PCR reactions. Preparation of self-made *Taq* DNA polymerase is according to Desai and Pfaffle (1995). Phusion Hot Start II High-Fidelity DNA Polymerase (Thermo Fisher Scientific, Waltham, USA) and Q5 High-Fidelity DNA Polymerase (New England Biolabs, Frankfurt am Main, Germany) were applied for the high-proof amplification of DNA for cloning purpose.

All commercial kits used in this study were listed as follow:

- *NucleoSpin® Gel and PCR Clean-up* (MACHEREY-NAGEL, Düren, Germany)

- *Power SYBR® Green PCR Master Mix* (Thermo Fisher Scientific, Waltham, USA)

2.1.3 Ladders

λ-PstI-DNA-Marker, GeneRuler 1 kb DNA Ladder (Thermo Fisher Scientific, Waltham, USA) and 2-Log DNA ladder (New England Biolabs, Frankfurt am Main, Germany) were used for estimating the sizes of DNA fragment on agarose gel.

2.1.4 Oligonucleotides

All oligonucleotides were synthesized by Thermo Fisher Scientific (Waltham, USA) or Eurogentec Deutschland GmbH (Köln, Germany). Oligonucleotides for qRT-PCR are listed in Table 2. Oligonucleotides for cloning are listed in Table 3. Oligonucleotides for genotyping PCR and RT-PCR are listed in Table 4.

Table 2. Oligonucleotides used for qRT-PCR.

Without special indications, the sequences of the qRT-PCR oligonucleotides were generated by the Quantprime software (Arvidsson *et al.* 2008). The amplicon lengths were between 60-262 bp. fw and rv represent forward and reverse primers, respectively.

Gene name	Gene ID	Forward and reverse sequence (5'-3')
AtNRT1.5	At1g32450	fw: TGCTGGCATCGTCATTCTTCTG rv: AGCACCAAGTTCACTCCAACTCC
AtNRT1.8	At4g21680	fw: AGCAAGTTTCGTTGCAGGGTTG rv: ACTCCACAACCACTTGGTTCAAGC
AtNRT1.1	At1g12110	fw: GCCACACACTGAACAATTCCGTTC rv: ATTCGAGGTAACTCCCGCTTCC
AtSKOR	At3g02850	fw: AGCTGGAGGTGACCCGAATAAG rv: TCTAGAGGCTGCAAGATGCAAAGG
AtHAK5	At3g02850	fw: GGCAGGCTGCGTACCTAACTAAAC rv: TGTTGGCCAGTATAACGGATCAGG
AtCIPK9	At1g01440	fw: GGAAGAAACCGCAAAGCCATTAGG rv: ATGGCGCCACTTCAAACACCTC
AtSLAH1	At1g62280	fw: ATCTTCATGTCCCTGGTCTGTAGG rv: AGAACCGACCGGATCTTTCACC
AtSLAH3	At5g24030	fw: CCATGCCTGTGGACCGTTACTATG rv: ACGATCTCTTCTTGAGGCCGTAGG
AtARF7	At1g19050	fw: TCAAGGTCACAGTGAGCAAGTCG rv: TGTGGAGCATGCATATGAGCTTGG
AtARF8	At5g37020	fw: AGGGTCACAGTGAACAGGTAGC

		rv: TGGTGGTAGGCTTGGGTAATTGG
AtARF19	At1g19220	fw: ACAGCTCGAAGATCCGCTAACC
		rv: TGCACGCAGTTCACAAACTCTTC
AtLBD29	At3g58190	fw: ACTGGAAGTTCTGGGACGGTTC
		rv: ATGCCTGAGGAGGTTTCGTTGTG
AtPIN1	At1g73590	fw: GGCATGGCTATGTTCAGTCTTGGG
		rv: ACGGCAGGTCCAACGACAAATC
AtPIN2	AT5g57090	fw: TCACGACAACCTCGCTACTAAAGC
		rv: TGCCCATGTAAGGTGACTTTCCC
AtPIN5	AT5g16530	fw: ATGGCCATCGGCTCTATTGTCC
		rv: AGCAGCCTGAATGATGGCTACG
AtARR5	AT3g48100	fw: AGTTCGGTTGGATTTGAGGATCTG
		rv: TCCAGTCATCCCAGGCATAGAG
AtARR7	AT1g19050	fw: AGGTCATGAGGATGGAGATTCCC
		rv: ATCGACGGCAAGAACATGCAAC
AtARR10	AT4g31920	fw: TGATGGCTTCTGATGCTGGTTCC
		rv: TCAGATTGGCTCTGTTCCTGTGTC
AtMYB77	AT3g50060	fw: AGGAGTTACATGGCGGAAATGCAG
		rv: TGCCGCCGGATTCGTATAAACC
AtIAA4	AT5g43700	fw: GTTGGTGATGTTCCTTGGGAGATG
		rv: GGTTTGTTAAAGACCACCACAACC
AtSAUR41	AT1g11803	fw: TCCGCTCAAGAATACGGTTACGC
		rv: AAACACGATGACGTGGCAAGGG
AtSAUR	AT1g16510	fw: TTTCGAGAGCGAGTCAAGGTTTG
		rv: GGTATCTTCAGGACAAGGAATCGC

Table 3. Oligonucleotides used for conventional cloning and Gateway® cloning.

Restriction enzyme sites and Gateway® attachment sites attB1, attB2 and attB3 (highlighted and italic nucleotides) were integrated into the forward (fw) and reverse (rv) oligonucleotide sequences for amplification of coding DNA sequence (CDS).

Gene ID	Amplification	Forward and reverse sequence (5'-3')
Oligonucleotides for cloning of yeast complementation constructs		
At3G02850	*SKOR* CDS (SpeI/BamHI)	fw: G***ACTAGT***ATGGGAGGTAGTAGCGGCGG
		rv: CG***GGATCC***TTATGTTTCAACAGCCAAATAC
At1G32450	*NRT1.5* CDS (BamHI/HindIII)	fw: CG***GGATCC***ATGTCTTGCCTAGAGATTTATA
		rv: CCC***AAGCTT***TTAGACTTTAGAATCCTTCTC
At5G46240	*KAT1* CDS (BamHI/HindIII)	fw: CG***GGATCC***ATGTCGATCTCTTGGACTCG
		rv: CCC***AAGCTT***GCTCTATAAATGAAGTCGAG
At4G21680	*NRT1.8* CDS (BamHI/HindIII)	fw: CG***GGATCC***ATGGATCAAAAAGTTAGACAG
		rv: CCC***AAGCTT***TCAGACTTCCTCCTCTTC
At1G30270	*CIPK23* CDS (SpeI)	fw: CCG***ACTAGT***ATGGCTTCTCGAACAACGC
		rv: CCG***ACTAGT***TTATGTCGACTGTTTTGCA

At1G01140	*CIPK9* CDS (SpeI/BamHI)	fw: CCG***ACTAGT***ATGGGTTGTTTCCATTCCAC
		rv: CG***GGATCC***TCACGTCGCAATCTCGT
At4G17615	*CBL 1*CDS (SpeI/BamHI)	fw: CCG***ACTAGT***ATGGGCTGCTTCCACTCAAAG
		rv: CG***GGATCC***TCATGTGGCAATCTCATCGA
At4G26570	*CBL3* CDS SpeI/BamHI)	fw: CCG***ACTAGT***ATGTCGCAGTGCATAGACG
		rv: CG***GGATCC***TCAGGTATCTTCCACCTGC
At5G47100	*CBL9* CDS (SpeI/BamHI)	fw: CCG***ACTAGT***ATGGGTTGTTTCCATTCCAC
		rv: CG***GGATCC***TCACGTCGCAATCTCGT
At4G13420	*HAK5* CDS (SpeI/BamHI)	fw: CCG***ACTAGT***ATGGATGGTGAGGAACATCA
		rv: CG***GGATCC***TTATAACTCATAGGTCATGCC
Oligonucleotides for cloning of *35Sp::NRT1.5* construct		
At1G32450	*NRT1.5* CDS (BamHI/PstI)	fw: CG***GGATCC***ATGTCTTGCCTAGAGATTTATAAC
		rv: AA***CTGCAG***TTAGACTTTAGAATCCTTCTC
Oligonucleotides for cloning of pDOE08 system		
At1G32450	*NRT1.5* CDS (BamHI/SpeI)	fw: CG***GGATCC***ATGTCTTGCCTAGAGATTTA
		rv: GG***ACTAGT***TTAGACTTTAGAATCCTTCTC
At1G62280	*SLAH1* CDS (RsrII/PmlI)	fw: ATG***CGGTCC***GAAATTCCGAGGCAAGA
		rv: CG***CACGTG***CTAGTTTTGGTTAGTCGCAT
At5G24030	*SLAH3* CDS (RsrII/PmlI)	fw: ATG***CGGTCC***GAGGAGAAACCAAACTATGTG
		rv: CG***CACGTG***TTATGATGAATCACTCTCTTG
At5G62680	*NRT1.10* CDS (RsrII/PmlI)	fw: ATG***CGGTCC***GAGAGAAAGCCTCTTGA
		rv: CG***CACGTG***TCAGGCAACGTTCTTGTCTTG
At4G30190	*AHA2* CDS (RsrII/PmlI)	fw: ATG***CGGTCC***AATCGAGTCTCGAAGATATCAAG
		rv: CG***CACGTG***CTACACAGTGTAGTGACTG
Oligonucleotides for Gateway® cloning		
At1G30270	attB1-CIPK23-fw	fw: ***GGGGACAAGTTTGTACAAAAAAGCAGGCTTG*** ATGGCTTCTCGAACAACGC
	attB2-CIPK23-rv (with stop codon)	rv: ***GGGGACCACTTTGTACAAGAAAGCTGGGTT*** TTATGTGCACGACTGTTTT
At4G17615	attB1-CBL1-fw	fw: ***GGGGACAAGTTTGTACAAAAAAGCAGGCTTG*** ATGGGCTGCTTCCACTCAAAG
	attB2-CBL1-rv (with stop codon)	rv: ***GGGGACCACTTTGTACAAGAAAGCTGGGTT*** TCATGTGGCAATCTCATCGA
At5G47100	attB1-CBL9-fw	fw: ***GGGGACAAGTTTGTACAAAAAAGCAGGCTTG*** ATGGGTTGTTTCCATTCCAC
	attB2-CBL9-rv (with stop codon)	rv: ***GGGGACCACTTTGTACAAGAAAGCTGGGTT*** TCACGTCGCAATCTCGTCC
Oligonucleotides for cloning of pBiFC-2in1 system		
At4G30190	attB2-AHA2-rv (with stop codon)	rv: ***GGGGACCACTTTGTACAAGAAAGCTGGGTT*** CTACACAGTGTAGTGACTGGGAG

Table 4. Oligonucleotides used for genotyping PCR and RT-PCR to check the transcript in T-DNA insertion lines.

Primers sequences for genotyping PCR to identify mutants were obtained from T-DNA primer Design (http://signal.salk.edu/tdnaprimers.2.html)

Primer name	Sequence (5'-3')
GAPC	fw: CACTTGAAGGGTGGTGCCAAG
	rv: CCTGTTGTCGCCAACGAAGTC
LB_Gabi	CCATTTGGACGTGAATGTAGACAC
LBb1.3	ATTTTGCCGATTTCGGAAC
LP_nrt1.8	GATGTGCACCATGAAGAGTTG
RP_nrt1.8	TGTTGGAACTGTGGAATCAAC
LP_slah1	TCAGCAAATATGCACCATGAC
RP_slah1	CGATATGAATTTCTTGCCTCG
LP_nrt1.9	AAAACTGATGGAAAAACATGAGG
RP_nrt1.9	ACGAGTTATGCTGTGAATGGG
LP_slah3	AAAGCGGTAATGGTGATGATG
RP_slah3	GGTCGGTAGCCTTTGGTAGAG
LP_aha2	TGACAAAACCGGGACACTAAC
RP_aha2	ATCACCACCTTTGCAATGAAC
LP_nrt1.5-5	CTCGAAGATTGCGTTTTTCAG
RP_nrt1.5-5	CCCGATGAGTGAGTATTGTGG
LP_skor2	TATGAACCGAAACAAACTCGG
RP_skor2	ACACGATCATTCCCATTCTTG
LP_skor3	CCCATATCTCACTGGTTCACC
RP_skor3	CCAAACTTCAGCGAAACAGAG
NRT1.8-RTPCR	fw: GTTCGTTGTGCAAGGAGCAG
	rv: AAACCACGAAATCAGCAGCG
SLAH3-RTPCR	fw: GGCACCAAACCGGAATAACC
	rv: CTCGTTGGTCGGTAGCCTTT
SKOR-RTPCR	fw: CTCTCTTTCGCGGATGCTCA
	rv: GTCACCTCCAGCTCGAATCA
NRT1.5-RTPCR	fw: GGTCGCTGCAACGAAGAAATC
	rv: CAAAGCGACGCTAAGGATGTC

2.1.5 Plasmids

Plasmids acquired commercially or obtained from other studies are listed in Table 5, and plasmids newly constructed in this work are listed in Table 6.

Table 5. Plasmids acquired commercially or obtained from other studies.

Listed are the plasmids which were purchased from commercial companies or obtained from other studies. Respective selection markers in bacteria (B), plants (P) and yeasts (Y) were abbreviated as following: $Spec^R$ - spectinomycin resistance; Kan^R - kanamycin resistance; Amp^R - ampicillin resistance, Cam^R - chloramphenicol resistance; Leu^A - Leucine auxotrophic marker; Trp^A - tryptophan auxotrophic marker; Ura^A - uracil auxotrophic marker. The detail description of each plasmid is listed in Table S1.

Plasmid name	Selective marker	Reference
pPTKan3	$Spec^R$ (B), Kan^R (P)	Guillaume Pilot (Virginia Tech Blacksburg, USA)
p425	Amp^R (B), Ura^A (Y)	Mumberg *et al.*, 1995
p426	Amp^R (B), Leu^A (Y)	Mumberg *et al.*, 1995
pDONR^{TM}222	Kan^R (B)	Thermo Fisher Scientific (Waltham, MA, USA)
pDONR221_p3-p2	Kan^R (B)	Thermo Fisher Scientific (Waltham, MA, USA)
pDONR221_p3-p2_SLAH1 mit Stopp	Kan^R (B)	Navina Drechsler (Freie Universität Berlin, DE)
pDONR221_p3-p2_SLAH3 mit Stopp	Kan^R (B)	Navina Drechsler (Freie Universität Berlin, DE)
pDONR221_p3-p2_CBL3 mit Stopp	Kan^R (B)	Navina Drechsler (Freie Universität Berlin, DE)
pDONR221_p1-p4_NRT1.5 mit Stopp	Kan^R (B)	Navina Drechsler (Freie Universität Berlin, DE)
pBT3-N_AtNRT1.5	Kan^R (B), Leu^A (Y)	Navina Drechsler (Freie Universität Berlin, DE)
pBiFC-2in1-NN	$Spec^R$ (B), Kan^R(B)	Grefen and Blatt, 2012
pDOE-08	Kan^R (B)	Gookin and Assmann, 2014
pNubI-X-HA	Amp^R (B), Trp^A (Y)	ABRC stock(1) #CD3-1737
pNubG-X-HA	Amp^R (B), Trp^A (Y)	ABRC stock(1) #CD3-1739
pNubG-AtDMP2	Amp^R (B), Trp^A (Y)	Alexis Kasaras (Freie Universität Berlin, DE)
pNubG-AtDMP7	Amp^R (B), Trp^A (Y)	Alexis Kasaras (Freie Universität Berlin, DE)
pNubG-KAT1	Amp^R (B), Trp^A (Y)	Alexis Kasaras (Freie Universität Berlin, DE)
pAG426GPD-ccdb/p14156	Amp^R (B), Cam^R (B), Ura^A (Y)	Susan Lindquist; Addgene(2) plasmid #14156

(1) http://abrc.osu.edu/; (2) http://www.addgene.org/

Table 6. Plasmids newly constructed in this work.

Plasmid name	Description	Selective marker
Plasmids generated for BiFC and split-ubiquitin study		
pDONR221_p3-p2_AHA2 mit Stopp	Gateway® donor vector with *AtAHA2* full length coding sequence	Kan^R (B)
pDONR222_CIPK23	Gateway® donor vector with *AtCIPK23* full length coding sequence	Kan^R (B)
pDONR222_CBL1	Gateway® donor vector with *AtCBL1* full length coding sequence	Kan^R (B)
pDONR222_CBL9	Gateway® donor vector with *AtCBL9* full length coding sequence	Kan^R (B)
pBiFC-2in1-NN_NRT1.5/-	pBiFC-2in1: nYFP fused to N- terminus of HA tag and cYFP fused to N- terminus of NRT1.5	SpecR (B)
pBiFC-2in1-NN_NRT1.5/SLAH1	pBiFC-2in1: nYFP fused to N-terminus of SLAH1 and cYFP fused to N- terminus of NRT1.5	$Spec^R$ (B)
pBiFC-2in1-NN_NRT1.5/SLAH3	pBiFC-2in1: nYFP fused to N terminus of SLAH3 and cYFP fused to N-terminus of NRT1.5	$Spec^R$ (B)
pBiFC-2in1-NN_NRT1.5/AHA2	pBiFC-2in1: nYFP fused to N-terminus of AHA2 and cYFP fused to N-terminus of NRT1.5	$Spec^R$ (B)
pDOE-08-NRT1.5	NmVen210 fused to N-terminus of NRT1.5 and unfused CVen210	Kan^R (B)
pDOE-08-NRT1.5/SLAH1	NmVen210 fused to N- terminus of NRT1.5 and CVen210 fused to N- terminus of SLAH1	Kan^R (B)
pDOE-08-NRT1.5/NRT1.10	NmVen210 fused to N- terminus of NRT1.5 and CVen210 fused to N-terminus of NRT1.10	Kan^R (B)
p14156-CBL1	yeast expression vector with *CBL1* CDS	Amp^R (B), Cam^R (B), Ura^A (Y)
p14156-CBL9	yeast expression vector with *CBL9* CDS	Amp^R (B), Cam^R (B), Ura^A (Y)
pNubG-CIPK23	yeast expression vector with NubG-CIPK23-HA fusion construct	Amp^R (B), Trp^A (Y)
Plasmids for gain of function study in *Arabidopsis*		
pYZ1204	pPTbar+ (NptII cassette of pPTKan3 was replaced with nos-Bar cassette)	$Spec^R$ (B), $Basta^R$ (P)
p35Sp::NRT1.5	express *NRT1.5* under the control of *35S* promoter in PYZ1204	$Spec^R$ (B), $Basta^R$ (P)
Plasmids for functional study in yeast		
pYZ10	express *NRT1.5* under the control of *TEF* promoter in yeast expression vector p426	Amp^R (B), Ura^A (Y)

pYZ11	express *SKOR* under the control of *TEF* promoter in yeast expression vector p425	Amp^R (B), Leu^A (Y)
pYZ13	express *KAT1* under the control of *TEF* promoter in yeast expression vector p426	Amp^R (B), Ura^A (Y)
p426-NRT1.8	express *NRT1.8* under the control of *TEF* promoter in yeast expression vector p426	Amp^R (B), Ura^A (Y)

2.1.6 Bacteria and yeast strains

Escherichia coli, *Agrobacterium tumefaciens* and *Saccharomyces cerevisiae* strains used in this work are listed in Table 7.

Table 7. Bacteria and yeast strains used in this work.

Strain	Genotype	Reference
Escherichia coli		
DH10B™	*F- mcrA Δ(mrr-hsdRMS-mcrBC) Φ80lacZΔM15 ΔlacX74 recA1 endA1 araD139 Δ(ara,leu)7697 galU galK rpsl nupG λ-*	Thermo Fisher Scientific, Waltham, USA
Agrobacterium tumefaciens		
GV3101::pMP90	Rifampicin and Gentamycin resistant	Koncz and Schell 1986
Saccharmyces cerevisiae		
BY4741	*MATa his3Δ leu2Δ met15Δ ura3Δ*	Euroscarf, Frankfurt am Main, Germany
BYT45	BY4741 *nha1Δ::loxP ena1-5Δ::kanMX*	Borovikova *et al*., 2014
BYT12	BY4741 *trk1Δ::loxP trk2Δ::loxP*	Petrezselyova *et al*., 2010
31019b	*MATa ura3 mep1Δ mep2Δ::LEU2 mep3Δ:: KanMX2*	Marini *et al*., 1997
23344c	*MATa ura3*	Grenson, M. unpublished data
THY-AP4	*MATa ura3 leu2 his3 trp1 ade2 lexA::lacZ lexA::HIS3 lexA::ADE2*	Obrdlik *et al*., 2004

2.1.7 Plant material

In this work, *Arabidopsis* wild type control is the ecotype Columbia-0 (Col-0). The T-DNA insertion lines used as well as the generated overexpression lines are listed in Table 8. All single T-DNA insertion lines used in this work were obtained from the *Arabidopsis* Biological Resource Center. Double mutants were generated through crossing two homozygous single T-DNA insertion mutants.

Table 8. *Arabidopsis thaliana* lines used and generated in this work.

***Arabidopsis thaliana* lines**	**Description and reference**
Col-0	wild type
nrt1.5-4	*NRT1.5* knockout line, SALK_063393 (Li *et al.*, 2010)
nrt1.5-5	*NRT1.5* knockout line, GABI_347B03 (Drechsler *et al.*, 2015)
skor-2	*SKOR* knockout line, GABI_391G12 (Drechsler *et al.*, 2015)
skor-3	*SKOR* knockout line, SALK_097435 (Drechsler *et al.*, 2015)
slah3	*SLAH3* knockout line, GABI_317G03
nrt1.8	*NRT1.8* knockout line, GABI_756D01
aha2	*AHA2* knockout line, GABI_219D04
CAB2p:NRT1.5	shoot complementation line of *nrt1.5-5* (Drechsler, Dissertation 2016)
PHO1p:NRT1.5	root complementation line of *nrt1.5-5* (Drechsler *et al.*, 2015)
nrt1.5-5/skor-2	the double mutant of *nrt1.5-5* and *skor-2* (generated in this work)
nrt1.5-5/slah3	the double mutant of *nrt1.5-5* and *slah3* (generated in this work)
nrt1.5-5/nrt1.8	the double mutant of *nrt1.5-5* and *nrt1.8* (generated in this work)
nrt1.5-5/aha2	the double mutant of *nrt1.5-5* and *aha2* (generated in this work)
35Sp::NRT1.5	*NRT1.5* overexpression lines under the control of *CaMV 35S* promoter in Col-0 background (generated in this work)

2.1.8 Database and Software

All the database and software used in this work are listed in Table 9.

Table 9. Database and software applicated in this work.

Name	**Application**	**Reference**
ABRC	Order *Arabidopsis* T-DNA insertion lines	http://abrc.osu.edu/
AB 7500 Software v2.0.6	qPCR analysis	Thermo Fisher Scientific (Waltham, MA, USA)
CorelDRAW 2014	Creation of figures and tables	Corel corporation (Ottawa, Canada)
eFP Browser	Gene expression study	Winter *et al.*, 2007
Excel	Calculation and creation of diagram	Microsoft corporation (Redmond, USA)
NCBI	PubMed, BLAST, Primer design	Geer *et al.*, 2010
ImageJ 1.40	Primary root measurement	http://rsb.info.nih.gov/ij/
Leica LAS AF	Microscope imaging	Leica Microsystems (Wetzlar, Germany)
Quantprime	Design of qPCR primers	Arvidsson *et al.*, 2008
TAIR	Information of *Arabidopsis* gene sequence	Berardini *et al.*, 2015
Vector NTI 9.0	Gene sequence analysis and contig assemble	Thermo Fisher Scientific (Waltham, MA, USA)

2.1.9 Sequencing

DNA sequencing was done by GATC Biotech (Konstanz, Germany) or LGC Genomics (Berlin, Germany).

2.1.10 Medium and selection

2.1.10.1 Medium for cultivating bacteria

For the standard growth of *E. coli* and *A. tumefaciens*, LB medium (70 g/l, pH 7.0) (Roth, Karlsruhe, Germany) was used. To produce solid medium, 1.5% agar was added before autoclave. To select the recombinant bacteria, the media were supplemented with the corresponding antibiotic stock solutions (Table 10) after autoclave. For the blue-white selection, 60 µl X-gal solution (40 µg/ml) and 30 µl IPTG solution (0.1 M) were spread on top of the solid LB plates contained Spectinomycin. *E. coli* was generally grown at 37°C and *A. tumefaciens* at 28°C.

Table 10. Antibiotic stock solution for selecting recombinant bacteria.

Antibiotic (Chemical)	Stock solution (1000x)	Dissolved in
Ampicillin	100 mg/ml	H_2O
Kanamycin	50 mg/ml	H_2O
Spectinomycin	75 mg/ml	H_2O
Gentamycin	25 mg/ml	H_2O
Rifampicin	50 mg/ml	DMSO
Phosphinothricin	15 mg/ml	H_2O

2.1.10.2 Medium for cultivating *Saccharomyces cerevisiae*

The general cultivation of *S. cerevisiae* was carried out with YPAD liquid or solid medium (50 g/l of YPAD Broth and 70 g/l of YPAD agar) (Formedium, Hunstanton, United Kingdom) at 30°C. For the selection of recombinant yeast cells, the Synthetic Defined (SD) minimal media supplemented with 2% glucose and without indicated auxotrophic amino acids were used (Table 11). To support the growth of BYT12 mutant (Petrezselyova *et al.* 2010), 100 mM KCl was added to YPAD medium or SD medium.

In the split-ubiquitin assay, to inhibit the autoactivation, 3-amino-1,2,4-triazole (3-AT, competitive inhibitor of the *HIS3* gene product) was additionally added to the SD medium in various concentrations. The pH of media was adjusted with NaOH to 5.9-6.0. To make solid medium, 2% Agar (Roth, Karlsruhe, Germany) was added before autoclave.

Table 11. Selective yeast media used in this work.

Yeast medium	Composition
SD minimal medium	6.9 g/l Yeast Nitrogen Base with $(NH_4)_2SO_4$, without amino acids [(1)]; 20 g/l glucose
YNB -Ura	SD minimal medium; 0.77 g/l CSM Drop Out (-Ura) [(2)]
YNB -Ura, -Leu	SD minimal medium; 0.67 g/l CSM Drop Out (-Ura, -Leu) [(2)]
SD- Leu, -Trp	SD minimal medium; 0.64 g/l CSM Drop Out (-Leu, -Trp) [(2)]
SD- Leu, -Trp, -Ura	SD minimal medium; 0.57 g/l CSM Drop Out (-Ade, -His, -Leu, -Trp, -Ura, -Met) [(2)] ; 20 mg/l Adeninsulfat; 20 mg/l L-Histidine; 20 mg/l L-methionin
SD- Leu, -Trp, -His, -Ade	SD minimal medium; 0.59 g/l CSM Drop Out (-Ade, -His, -Leu, -Trp, -Met) [(2)] ; 20 mg/l L-methionin
SD- Leu, -Trp, -His, -Ade, -Ura	SD minimal medium; 0.57 g/l CSM Drop Out (-Ade, -His, -Leu, -Trp, -Ura, -Met) [(2)] ; 20 mg/l L-methionin

(1) Yeast Nitrogen Base without amino acids (Formedium, Hunstanton, GB)
(2) Complete Supplement Mixture Drop Out (Formedium, Hunstanton, GB)

2.1.10.3 Medium for cultivating *Arabidopsis thaliana*

For gemination of *Arabidopsis* seeds, 1/2 MS (Murashige-Skoog) medium containing 1% (w/v) sucrose and 0.3% (w/v) Gelrite (pH 5.8) was used.

For observation of root growth by various hormone treatment, seedlings were vertically growing on 1/2 MS medium containing 1% (w/v) sucrose and 0.6% (w/v) Gelrite (pH 5.8) supplemented with corresponding phytohormone stock solutions (Table 12).

For gene expression profile study by hormone treatment, liquid 1/2 MS medium containing 1% (w/v) sucrose supplemented with corresponding phytohormone stock solutions was used (Table 12).

For growth test under various NO_3^- and K^+ concentrations, seedlings were transferred to modified 1/2 MS plates (0.6% [w/v] agarose, 1.5 mM $CaCl_2$, 1 mM $MgSO_4$, 0.5 mM

NaH_2PO_4, 0.05 mM H_3BO_3, 0.05 mM $MnSO_4$, 0.05 mM FeNaEDTA, 15.0 µM $ZnSO_4$, 2.5 µM KI, 0.5 µM Na_2MoO_4, 0.05 µM $CuSO_4$, 0.05 µM $CoCl_2$, 1/2 MS vitamins, 0.5 g/l MES, 1% [w/v] sucrose, pH 5.8). K^+ and NO_3^- were added to the indicated concentrations with KCl and $Ca(NO_3)_2$, respectively.

Table 12. Phytohormone stock solution used in this work.

Phytohormone	Stock solution (1000x)	Dissolved in
Brassinazole	2 mM	DMSO
Brassinolide	1 mM	DMSO
Jasmonic acid	50 mM	EtOH
Methyl jasmonate	50 mM	EtOH
Abscisic acid	10 mM	EtOH
Salicylic acid	500 mM	EtOH
6-Benzylaminopurine	1 mM	EtOH
Indole-3-acetic acid	5 mM	EtOH
Gibberellic acid	10 mM	DMSO

2.2 Methods

2.2.1 Transformation into bacteria, yeast and *Arabidopsis*

2.2.1.1 *Escherichia coli* transformation

50 µl aliquots of *E. coli* chemical competent cells were thawed on ice, followed by mixing with 5 µl ligation product or required amount of target DNA mixture. After 20 to 30 min incubation on ice, cells were heat shocked at 42°C for 45-90 s in water bath and immediately chilled on ice for 2 min. 450 µl LB was added then cell were incubated at 37°C for 1 hour by shaking at 220 rpm. 200 µl cell culture was plated on LB plates with corresponding antibiotics (Table 10), and the plates were inversely incubated at 37°C overnight.

2.2.1.2 *Agrobacterium tumefaciens* electroporation

A. tumefaciens competent cells were taken out from - 80°C freezer and thawed on ice. 100-200 ng plasmid DNA was mixed with 50 µl competent cells and incubated on ice for 10 min. The mixture was then transferred to a pre-chilled cuvette followed by electroporation at 2.2 kV for 5 ms. After that, the cells were immediately transferred into a new Eppi containing 950 µl LB medium and then cultured at 28°C for 2 h at a speed of 220 rpm. 20-30 µl culture was plated on LB plates within required antibiotics (Table 10) and incubated at 30°C for 2 days.

2.2.1.3 Saccharomyces cerevisiae transformation and culture

One *S. cerevisiae* single colony was inoculated in 10 ml YPAD medium and was cultured overnight by shaking at 30°C, 220 rpm. After OD_{600} measurement, the second cell culture was made in 50 ml fresh YPAD medium to OD_{600} to 0.2, followed by culturing to final OD_{600} to 0.8 by shaking at 30°C, 220 rpm. Cell culture was centrifuged at 3000 g for 5 min at room temperature. Cell pellet was resuspended in 25 ml sterile deionized H_2O. Centrifugation step was repeated at 3000 g for 5 min at room temperature. Supernatant was removed, and pellet was resuspended in 400 µl 0.1 M LiAc. For transformation, 240 µl 50% PEG4000, 36 µl 1 M LiAc, 50 µl ssDNA (1 µg/µl) and 500-1000 ng plasmid (in 25 µl sterile H_2O) were added into 50 µl competent cells, followed by vortex. Competent cells were then incubated at 30°C for 30 min and another 20 min at 42°C. Cells were centrifuged 30 s at 3300 g. Pellet was resuspended in 600 µl sterile H_2O. 50-150 µl cells were plated on agar selective medium and followed by an incubation at 30°C for 2 to 4 days.

2.2.1.4 *Arabidopsis thaliana* transformation

Arabidopsis plants were transformed with constructs described above by the floral-dip-method (Clough and Bent 1998).

Two hundred ml recombinant *A. tumefaciens* overnight culture was centrifuged at 4000 rpm at room temperature. The pellet was resuspended in freshly prepared infiltration

medium (1/2 MS with 44 nM 6-Benzylaminopurine, 0.005% Silwet L-77 [v/v], and 5% sucrose [w/v], pH 5.8). Three to four single plants or a big pot with approximately 20 plants were dipped in medium with *A. tumefaciens* for about 5 s. Infiltrated plants were placed in dark overnight and then were put back to light condition in greenhouse and grew further for seed harvesting.

2.2.2 Cultivation of *Arabidopsis thaliana* plants

2.2.2.1 Sterilization of seeds

A. thaliana seeds were surface sterilized with 70% (v/v) ethanol for 2 min, followed by 10% NaClO (v/v) and 1% (w/v) SDS for 3 min, and then washed 3 times in autoclaved double deionized water for 3 min. 0.1% (w/v) agarose solution was added into seeds, and seeds were plated on solid medium. Plates were sealed with Parafilm and seeds were stratified in darkness at 4 to 8°C for two days, followed by transferred to a climate chamber or light room. Standard long-day growth conditions were 16-h/8-h light-dark cycle, 21°C/18°C day-night cycle, and 120 mmol m^{-2} s^{-1} (Weigel and Glazebrook 2002).

2.2.2.2 Cultivation of *Arabidopsis* seedlings on plates

For phenotypical analysis on plates, 5 DAS (days after sowing) *Arabidopsis* seedlings with comparable size were transferred on growth medium containing either indicated hormones, antibiotics or various nutrition supplies, and grew vertically on plates in the growth chamber under the long-day condition for 6-7 days further.

2.2.2.3 Cultivation of *Arabidopsis* seedlings with liquid medium

To get access to both root and shoot material for gene expression study after hormone treatment, ten *Arabidopsis* Col-0 seedlings were cultured in 50 ml flask with 15 ml 1/2 MS liquid medium as one biological replicate. The flasks were sealed with aluminum foil and placed on a shaker in the climate chamber (light intensity 120 µmol m^{-2} s^{-1}, relative humidity 55-70%) under 12-h/12-h light-dark cycle and 21°C/18°C day-night temperature cycles. The liquid medium of shaking cultures was renewed after 6 days

and seedlings were grown for further 2 to 3 days. Phytohormone stock solutions were added to liquid medium for 24 h. Then the root and shoot material of the seedlings were harvested separately and frozen in liquid N_2.

2.2.2.4 Cultivation of *Arabidopsis* on soil

For propagation of *Arabidopsis*, a 1:1 mixture of commercial type P soil and unfertilized type 0 soil was used (the nutrient compositions of both soil types were listed in Table S2).

For growing *Arabidopsis* on soil with various N/K regimes, seeds were sowed on commercial type P soil. 10-15 DAS seedlings with comparable size were singled out on unfertilized type 0 soil. 500 ml various modified 1/2 MS nutrient solutions (Table S3) were supplemented firstly once per week, and then twice per week in the late growth stage of plants. Plants were cultivated in a growth chamber under long-day conditions with a light intensity of 120 mmol m^{-2} s^{-1} and a relative humidity of 55% to 70%.

2.2.3 Analysis of *Arabidopsis* root architecture traits

Primary root length was measured on digital images of the plates using ImageJ 1.40 software (http://rsb.info.nih.gov/ij/). The number of emerged lateral roots was counted using a binocular. The number of lateral root primordia was determined using a Zeiss Axioskop microscope. LRP density was shown as numbers of LRPs per centimeter primary root and LR density was shown as numbers of emerged LRs per centimeter primary root.

2.2.4 Crossing of *Arabidopsis* plants

The crossing operation was carried out by using a Zeiss binocular. Immature anthers were released from buds just before flowering. Mature stamen from male plants were pollinated with pistils from female plants. Crossed plants were then grown in the greenhouse under long-day conditions until seeds were harvested.

2.2.5 Transient expression in *Nicotiana benthamiana*

For the transient expression of proteins in *N. benthamiana*, glycerol stocks of GV3101::pMP90 agrobacteria transformed with the respective plasmid constructs were streaked on the LB plates with appropriate antibiotics and incubate at 28°C for 2 days. Then, several colonies of agrobacteria from plates were inoculated in 5 ml liquid LB medium with appropriate antibiotics and grown in a shaker at 28°C, 220 rpm overnight. To prevent the onset of post-transcriptional gene silencing, the construct of interest was coexpressed with a plasmid which carries the coding sequence of p19 protein from tomato bushy stunt virus (Voinnet *et al.* 2003). The agrobacteria with p19 construct were cultured as above mentioned.

Two ml overnight culture were harvested by centrifugation at 4000 rpm for 5 min at room temperature. Pellet was washed at least one time with infiltration buffer (50 mM MES [pH 5.7], 10 mM $MgCl_2$, 100 µM Acetosyringone, 0.5% [w/v] glucose). Cells were 10-fold diluted with infiltration buffer for OD_{600} measurement. Subsequently, cells were diluted with infiltration buffer to a final OD_{600} of 0.05 for construct of interest and for p19 cells as well. After the incubation for one to two hours at room temperature, the cell mixture of construct of interest and p19 were infiltrated into *N. benthamiana* leaves with syringe.

2.2.6 Live-cell imaging using confocal laser scanning microscopy (CLSM)

Constructs with cloned genes were introduced into tobacco abaxial epidermis cells by *A. tumefaciens*-mediated transformation. BiFC assays were performed at three days post infiltration (dpi) by CLSM. CLSM was performed on a Leica TCS-SP5 AOBS confocal laser scanning microscope equipped with water immersion objectives. Simultaneous excitation of YFP and mRFP in rBiFC assays was performed using the 514 nm line of the argon laser and the 561 nm line of the diode-pumped solid-state laser, respectively. YFP and mRFP emissions were recorded using the bandwidths 520

nm-545 nm and 585 nm-655 nm, respectively. Post-acquisition image processing and fluorescence quantification was performed using the Leica LAS AF software.

2.2.7 Molecular biological methods

Methods of general molecular biological experiments followed the instructions in Molecular cloning (3rd edition) (Sambrook and Russell 2001).

2.2.7.1 Cloning of constructs

All PCR amplifications described in this work were performed by using either the Phusion® High-Fidelity DNA Polymerase or the Q5® High-Fidelity DNA Polymerase according to the manufacturer's instructions (NEB, Ipswich, USA). The NucleoSpin® gel and PCR clean-up kit (Macherey-Nagel, Düren, Germany) was used for the purification and extraction of DNA from agarose gels. All cloned sequences were verified by sequencing.

2.2.7.1.1 Cloning of constructs for yeast complementation

The full-length CDS of *NRT1.5*, *SKOR*, *KAT1* and *NRT1.8* gene was amplified with the oligonucleotides listed in Table 3. To amplify *NRT1.5* and *SKOR*, *Arabidopsis* root cDNA was used as PCR template. To amplify *KAT1* and *NRT1.8*, leaf cDNA was used as PCR template. The amplified gene products were then successively ligated into the yeast expression vector p426TEF or p425TEF via the restriction sites mentioned in Table 3.

2.2.7.1.2 Cloning of *35Sp::NRT1.5* construct

The NptII cassette of binary vector pPTKan3 was replaced with nos-Bar cassette to generate pPTbar+. The full-length CDS of the *NRT1.5* gene was amplified with the oligonucleotides listed in Table 3. The amplification product was ligated to the cauliflower mosaic virus (CAMV) *35S* promoter of pPTbar+ via the BamHI and PstI sites.

2.2.7.1.3 Gateway® cloning of the pBiFC-2in1 constructs

All potential NRT1.5 interacting candidates were amplified and cloned into the Gateway® vector pDONR221 p3-p2 via BP reaction. For this purpose, the corresponding Gateway® attachment sites attB3/attB2 were integrated into the oligonucleotides used for the PCR amplifications (Table 3). Then pDONR221 p1-p4-NRT1.5 (constructed by Dr. N. Drechsler) and pDONR221 p3-p2 contains interacting candidates were cloned into destination vector pBiFC-2in1-NN by LR reaction.

2.2.7.1.4 Gateway® cloning to generate the split-ubiquitin prey constructs

All potential NRT1.5 interacting candidates were amplified as full-length CDS constructs with the stop codon and cloned into the Gateway® Entry Clone pDONR222 via a BP reaction. For this purpose, the corresponding Gateway® attachment sites attB1 and attB2 were integrated into the oligonucleotides used for the PCR reactions (Table 3). N-terminal NubG-CIPK23 fusion were then generated by an LR reaction between the generated entry clones and the Gateway®-compatible yeast expression vector pNubG-X-HA. CBL1 and CBL9 were cloned into yeast expression vector p14156 by an LR reaction.

2.2.7.1.5 Cloning of pDOE-08 constructs

The full-length CDS of *NRT1.5* was amplified with the oligonucleotides listed in Table 3 and ligated into the empty pDOE-08 vector through ligation of BamHI and SpeI restriction enzyme sites to generate construct pDOE-08-NRT1.5. Afterwards, the full-length CDS of *SLAH1*, *SLAH3*, *NRT1.10* and *AHA2* genes was amplified with the oligonucleotides listed in Table 3. The amplified CDS of each gene were digested with RsrII and PmlI, and pDOE-08-NRT1.5 was digested with RsrII and SandI. The amplified gene products of interacting partners were then successively ligated into the pDOE-08-NRT1.5 vector.

2.2.7.2 Genomic DNA isolation

Genomic DNA of *Arabidopsis* was extracted by CTAB protocol (Murray and Thompson 1980).

Arabidopsis materials were ground into fine powder with liquid N_2 by a ball mill (Retsch MM 400). 600 µl pre-warmed (65°C) Buffer B (100 mM Tris-Cl pH 8.0, 1.4 M NaCl, 20 mM EDTA, and 2% [w/v] CTAB) was added into Eppi with ground material and mixed by vortex, followed by an incubation at 65°C for 20 min. Eppis were inverted every 5 min and were centrifuged at room temperature for 5 min at 13500 rpm. Clear supernatant was transferred to a new Eppi. One volume chloroform:isoamyl alcohol (24:1) was added and mixed well by inverting, followed by centrifuging at 13500 rpm for 5 min. The upper phase was then transferred into a new Eppi and the chloroform:isoamyl alcohol extraction step was repeated. One volume Buffer C (50 mM Tris-Cl pH 8.0, 10 mM EDTA, and 1% [w/v] CTAB) and one volume isopropanol was added to the supernatant and mixed, followed by incubating at room temperature for 10 min. Precipitated DNA was obtained by centrifuging at 12000 rpm for 5 min. Pellet was resuspended in 400 µl STE (10 mM Tris-Cl pH 8.0, 100 mM NaCl, 1 mM EDTA, 20 µg/ml RNase A) and incubated at 65°C for 5 min. 600 µl ethanol was added, followed by centrifuging at 13500 rpm for 10 min at room temperature to precipitate DNA. The pellet is then washed twice with 70% ethanol, air dried and resolved in 30 µl TE (10 mM Tris-Cl pH 8.0, 1 mM EDTA).

2.2.7.3 RNA extraction

Total RNA of *Arabidopsis* materials was isolated by using either the TRISure™ reagent (Bioline GmbH, Berlin, Germany) extraction protocol or by using Hot-Phenol method (Verwoerd *et al.* 1989).

Hot-Phenol protocol:

Arabidopsis materials were collected in 1.5 ml Eppi and frozen in liquid N_2. Materials were ground into fine powder by a ball mill (Retsch MM400). 1 ml pre-warmed (80°C) Phenol solution was added to the Eppi, thawed at room temperature, and then

vortexed for 30 s to homogenize material. 500 µl chloroform:isoamyl alcohol (24:1) was added, vortexed for 30 s, and then centrifuged for 40 min at 4000 rpm. Upper phases were transferred into new Eppi and kept on ice from now on. 1 volume 4 M LiCl was added and well mixed by shaking. Samples were kept at - 20°C overnight. On the next day, the samples were thawed at room temperature. Eppis were mixed by inverting, and then centrifuged for 20 min 16000 g at 4°C. The pellet was dissolved in 450 µl DEPC-treated ddH_2O. 1/10 volume 3 M NaOAc (pH 5.2) and 2 volume pre-cold 100% ethanol were added and were well mixed and incubated at -80°C for 30-60 min. Followed by a centrifugation for 20 min at 16000 g at 4°C, pellet was washed with 80% pre-cold ethanol. After air drying, the pellet was dissolved in 30 µl DEPC-treated ddH_2O.

TRISure reagent protocol:

Protocol of TRISure^{TM} reagent was described in the product sheet (BIO-38032).

Concentrations and purity of RNAs were analyzed by using Nanodrop ND-1000 spectrophotometer (Thermo Fisher Scientific, Waltham, USA).

2.2.7.4 cDNA synthesis

2 µg DNase I (Thermo Fisher Scientific, Waltham, USA) digested (37°C for 1 h) total RNA from each sample was used for cDNA synthesis. 1µl SuperScript® III Reverse Transcriptase (Thermo Fisher Scientific, Waltham, USA) or RevertAid Reverse Transcriptase (Thermo Fisher Scientific, Waltham, USA) was used in 20 µl cDNA synthesis reaction. To examine whether cDNA has genomic DNA contamination, primers span the intron of *glyceraldehyde-3-phosphate dehydrogenase C subunit 1* (*GAPC*) (Table 4) were used to carry on a standard PCR.

2.2.7.5 Quantitative real time PCR

Applied Biosystems® 7500 Fast Real-Time PCR System (Thermo Fisher Scientific, Waltham, USA) was used for qRT-PCR. Each 5 µl reaction contained 2.5 µl Applied Biosystems® Power SYBR® Green PCR Mastermix (Thermo Fisher Scientific, Waltham, USA), 0.5 µl cDNA, and 2 µl forward and reverse primers mix (0.5 µM each).

The qRT-PCR procedure is as follows: 95°C for 10 min; 95°C 15 s → 60°C 60 s (40 cycles); melting curve analysis. All qRT-PCR assays were performed with three biological replicates and two technical replicates. Data analysis was performed using the Applied Biosystems® SDS 2.2.1 software (Thermo Fisher Scientific, Waltham, USA). The expression values of the individual genes were normalized to the CT value of the reference gene *UBIQUITIN10* (At4g05320). All qRT-PCR oligonucleotides used are listed in Table 2.

2.2.8 Total C and N concentration measurement

The total C and total N analysis was performed using the Euro EA3000 Single Elemental Analyzer (EuroVector, Redavalle, Italy) according to the manufacturer's instructions. 1.5 to 2.5 mg of homogenized and dried plant material (48 h at 80°C.) were used for each measurement. Data analysis was carried out using the EuroVector Callidus 5.1 software.

2.2.9 Elemental analysis

The dried plant material was weighed into polytetrafluorethylene digestion tubes. After adding HNO_3, the plant material was digested under pressure using a microwave digester (ultraCLAVE 4, MLS GmbH, Leutkirch, Germany). ICP-OES analyzes were done by using the iCAP 6500 Dual OES Spectrometer (Thermo Fisher Scientific, Waltham, USA). The certified Standard Reference Material 1515 Apple Leaves (National Institute of Standards and Technology, Gaithersburg, USA) was used as the quality control.

2.2.10 Cooperation

The ICP-OES measurements was carried out in cooperation with Prof. Dr. N. von Wirén at the Leibniz Institute of Plant Genetics and Crop Plant Research in Gatersleben.

The C/N analyses were carried out by Sabine Artelt und Gabriele Erzigkeit (FU Berlin,

Institute of Biology, Ecology of Plants).

The constructs $pNub_G$-DMP2, $pNub_G$-DMP7, $pNub_G$-KAT1 and $pNub_G$-StSUT1 used as controls in split-ubiquitin study were generated by Dr. A. Kasaras (Kasaras, Dissertation 2012). Plasmid pBT3-N_AtNRT1.5 for split-ubiquitin study, and constructs pDONR221_P1P4_NRT1.5, pDONR221_P3P2_SLAH1 and pDONR221_P3P2_SLAH1 for BiFC study were generated by Dr. N. Drechsler (Drechsler, Dissertation 2016 and unpublished data).

3 Results

3.1 Phenotypical analysis of *nrt1.5* knockout mutants

Part of the subsequent results reported in 3.1.1, 3.1.2 and 3.1.3 has been published in the publication: Zheng, Y., Drechsler, N., Rausch, C. and Kunze, R. (2016). The *Arabidopsis* nitrate transporter NPF7.3/NRT1.5 is involved in lateral root development under potassium deprivation. Plant Signaling & Behavior 11(5).

3.1.1 Comparable root growth of *nrt1.5* mutants as wild type at various nitrate concentrations

Our group reported the pleiotropic shoot phenotype and early leaf senescence symptoms of *nrt1.5* mutants caused by K deficiency in rosettes (see section 1.5.3). However, the *NRT1.5* gene is mainly expressed in the root pericycle cells (Lin *et al.* 2008). Therefore, it was tempting to investigate whether *nrt1.5* mutants also exhibit an altered root development in response to various nitrate or potassium concentrations. To test how NO_3^- amount affects root development, wild type Col-0 and two T-DNA insertion knockout mutants *nrt1.5-4* and *nrt1.5-5* were grown vertically on petri dishes with various NO_3^- concentrations (constant 1 mM K^+ supply). At 0 mM NO_3^-, all plant lines demonstrated impaired shoot growth, decreased chlorophyll biosynthesis and the accumulation of anthocyanins (Figure 4A). When external NO_3^- concentration was elevated to 2 mM, shoot growth of all lines was restored, however, no morphological abnormalities in root development of *nrt1.5* mutants were observed. Compared to Col-0, *nrt1.5* mutants gained slightly less shoot and root fresh weight under various NO_3^- concentrations from 0.2 to 2 mM (Figure 4B). However, when either 0 mM or 1 mM NO_3^- was supplied, neither primary root (PR) length nor lateral root (LR) density was altered in *nrt1.5* plantlets in comparison to Col-0, except the reduced PR length of *nrt1.5-5* at 0 mM NO_3^- (Figure 4C). The results showed that different NO_3^- concentrations cannot cause the root morphological changes of *nrt1.5* mutants.

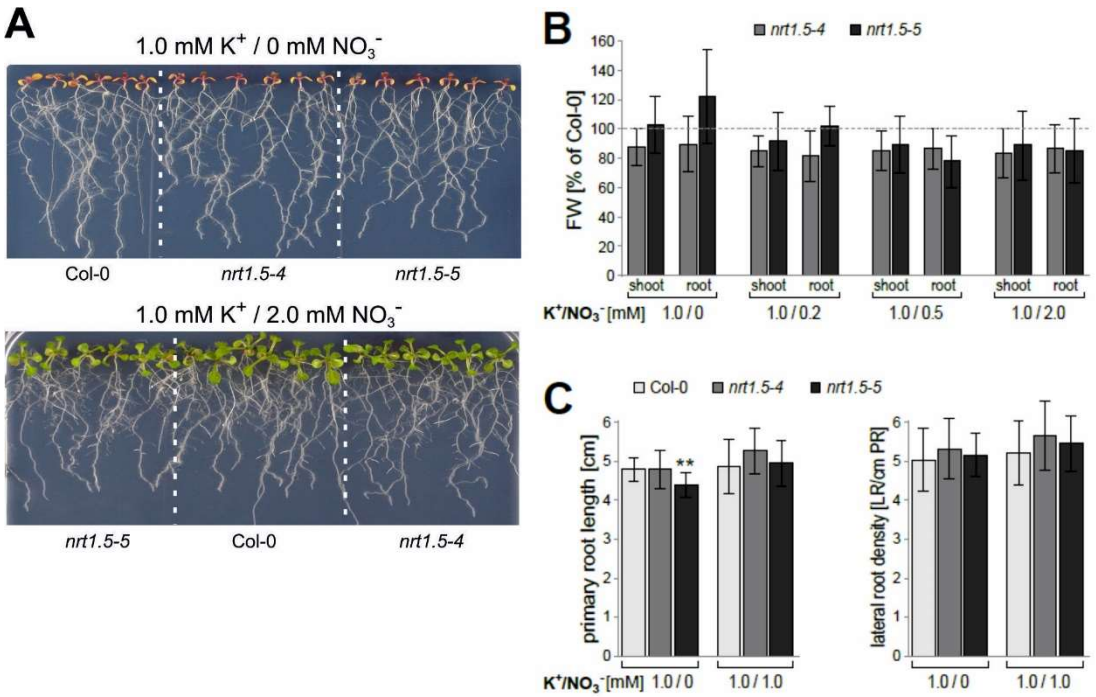

Figure 4. Nitrate supply does not lead to visible root phenotypes of *nrt1.5* mutants.

(A) Nitrate-dependent phenotype of wild type Col-0 and *nrt1.5* mutant seedlings. Col-0 and the two knockout lines *nrt1.5-4* and *nrt1.5-5* were grown on plates containing 0 mM or 2.0 mM NO_3^- (constant 1.0 mM K^+). **(B)** Shoot and root fresh weight of *nrt1.5* seedlings grown on plates containing increasing concentrations of NO_3^- from 0 to 2 mM (constant 1.0 mM K^+). Four seedlings were pooled as one biological replicate. Results are displayed relative to the FW of Col-0 (means ± SD; n ≥ 8). **(C)** Primary root length and lateral root density (means ± SD; n ≥ 30) of seedlings grown on plates containing 0 mM or 1 m NO_3^- (constant 1.0 mM K^+). ** indicates a statistically significant difference (Student's *t*-test) between mutants and Col-0 with $P < 0.01$. Representative results from one out of three independent experiments are shown.

3.1.2 Impaired lateral root development of *nrt1.5* mutants under potassium deficit

To investigate whether K^+ supply has an influence on root phenotype development of *nrt1.5* mutants, Col-0, *nrt1.5-4* and *nrt1.5-5* were grown vertically on plates with various K^+ concentrations (constant 1 mM NO_3^- supply). Compared to 2 mM K^+ supply, all plant lines gained less lateral root numbers and smaller rosettes at 0 mM K^+ supply (Figure 5A). When the K^+ concentration was decreased below 1 mM, the fresh weight of roots and shoots of *nrt1.5* mutants was only 50% and 60% relative to Col-0, respectively. At 2 mM K^+, the reduction of shoot and root FW relative to Col-0 were diminished in *nrt1.5*

mutants (Figure 5B). Notably, the root architecture of *nrt1.5* mutants was conspicuously altered under K^+ deficiency in comparison to wild type. The primary roots were slightly but still significantly shorter, and the lateral root density of *nrt1.5* mutants was significantly reduced to approximately 60% of Col-0 (Figure 5C). When 2 mM K^+ was provided, the root growth of *nrt1.5* mutants restored as Col-0 (Figure 5A).

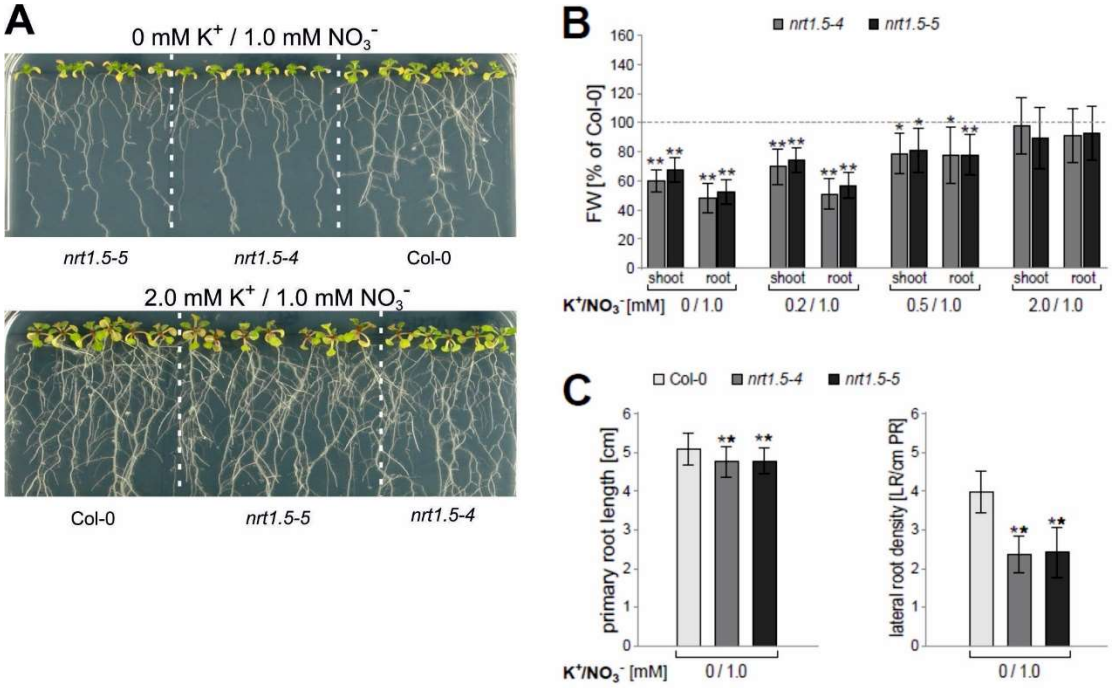

Figure 5. Potassium deficiency affects root development of *nrt1.5* mutant seedlings.

(A) Potassium-dependent phenotype of wild type Col-0 and *nrt1.5* mutant seedlings. Col-0 and two knockout lines *nrt1.5-4* and *nrt1.5-5* were grown on plates containing 0 mM or 2 mM K^+ (constant 1 mM NO_3^-). **(B)** Shoot and root FW of *nrt1.5* seedlings grown on plates containing increasing concentrations of K^+ from 0 to 2 mM (constant 1 mM NO_3^-). Three seedlings were pooled as one biological replicate. Results are displayed relative to the Col-0 FW (means ± SD; n = 12). **(C)** Primary root length and lateral root density (means ± SD; n ≥ 30) of seedlings grown on plates containing 0 mM and 1 mM K^+ (constant 1 mM NO_3^-). * and ** indicate statistically significant differences (Student's *t*-test) between mutants and Col-0 with $P < 0.05$ and $P < 0.01$, respectively. Representative results from one out of three independent experiments are shown.

To further investigate whether the inhibition of LR growth in *nrt1.5* mutants is dependent on the presence of NO_3^-, 1 mM ammonium, instead of 1 mM NO_3^-, was supplied. When ammonium was used as the sole N source, LR density of *nrt1.5-4* and *nrt1.5-5* was still significantly reduced than that of Col-0 (Figure 6A), suggesting NO_3^-

is not needed for the development of the root phenotype of *nrt1.5* mutants. At high NO_3^- concentration (5 mM), *nrt1.5* mutants also demonstrated the same reduced LR density phenotype (Figure 6B). Therefore, the reduced LR density phenotype of *nrt1.5* mutants was only caused by the low K^+ availability and was independent of the NO_3^- amount.

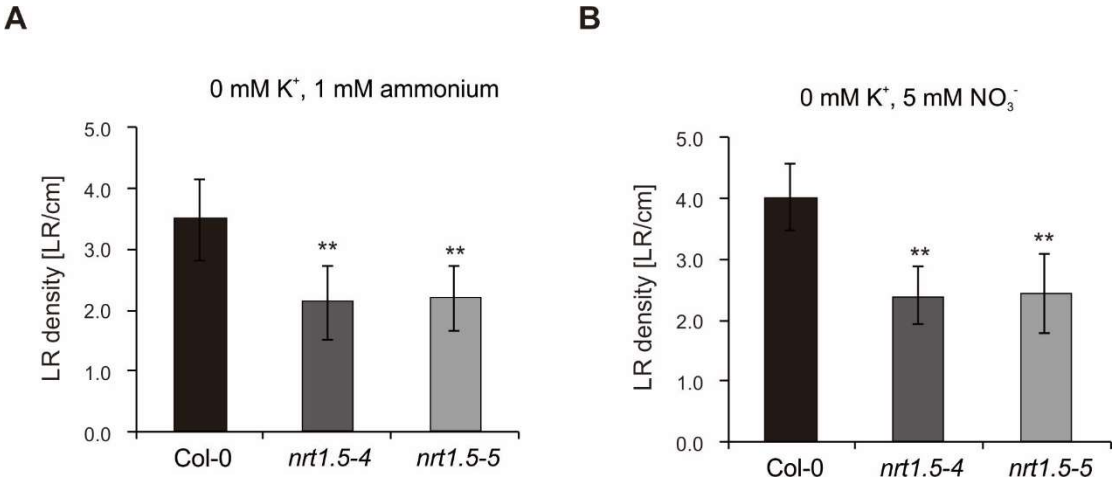

Figure 6. Reduced lateral root density in *nrt1.5* mutants by K^+ starvation is independent of NO_3^- supply.

(A) Lateral root density was reduced in *nrt1.5* mutants on NO_3^--free medium. LR density of Col-0 and two knockout mutant lines *nrt1.5-4* and *nrt1.5-5* grown on plates containing 1 mM ammonium and 0 mM K^+ were measured (means ± SD, n ≥ 30). **(B)** Lateral root density was reduced in *nrt1.5* mutants on medium with high NO_3^- concentration. LR density of Col-0 and two knockout mutant lines *nrt1.5-4* and *nrt1.5-5* grown on plates containing 5 mM NO_3^- and 0 mM K^+ were measured (means ± SD, n ≥ 30). ** indicate statistically significant differences (Student's *t*-test) between *nrt1.5* mutants and Col-0 with $P < 0.01$.

Either impairment of lateral root primordia (LRP) initiation or elongation can cause the reduced LR density. To identify the block in which step is responsible for the reduced LR density phenotype in *nrt1.5* mutants, LRP density was examined for Col-0 and *nrt1.5-5* growing on medium with 0 mM K^+ and 1.0 mM NO_3^-. LR density of *nrt1.5-5* was significantly reduced at this growth condition (Figure 7A). However, LRP density of *nrt1.5-5* was not decreased, instead, it was rather significantly higher than that of Col-0 (Figure 7B). These results indicate the reduced LR density in *nrt1.5* mutants can be attributed to the handicap in LRP elongation instead of LRP initiation.

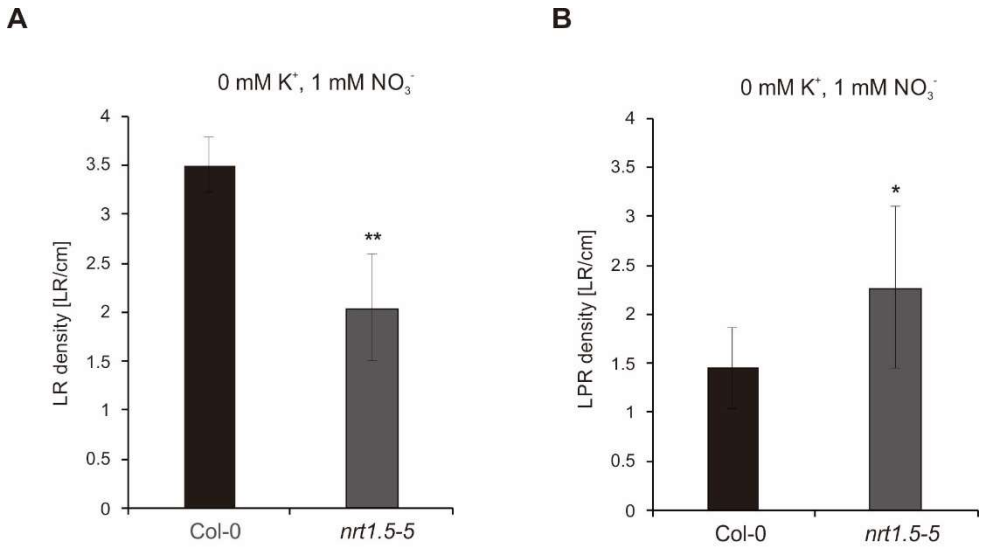

Figure 7. The impairment of lateral root density and lateral root primordia density of *nrt1.5-5* by K^+ starvation.

(A) Lateral root density of Col-0 and *nrt1.5-5* (means ± SD, n ≥ 12). **(B)** Lateral root primordia density of Col-0 and *nrt1.5-5* (means ± SD, n ≥ 12). Seedlings of *nrt1.5-5* and Col-0 grown seven days vertically on plates containing 1.0 mM NO_3^- and 0 mM K^+ were used for analysis. * and ** indicate statistically significant differences (Student's *t*-test) between *nrt1.5-5* and Col-0 with $P < 0.05$ and $P < 0.01$, respectively.

3.1.3 Restoration of lateral root growth in *nrt1.5* complementation lines

Expressing *NRT1.5* driven by the shoot specific *CAB2* (*Chlorophyll A/B-binding protein 2*) promoter in *nrt1.5-5* background led to the overexpression of *NRT1.5* in shoots, whereas *NRT1.5* was still absent in roots (Drechsler, Dissertation 2016). It has been reported that the shoot-derived signal, for example shoot nitrate accumulation, may affect root growth (Sheible *et al.* 2002). Therefore, *CAB2p::NRT1.5* (*in nrt1.5-5*) lines which have higher *NRT1.5* expression in shoots were also included in this study. At K^+ deprivation conditions, all three independent *CAB2p::NRT1.5* (*in nrt1.5-5*) lines demonstrated the similar inhibited LR growth phenotype like *nrt1.5-5* seedlings (Figure 8), indicating the expression of *NRT1.5* in shoots do not influence the development of the LR phenotype in *nrt1.5* mutants.

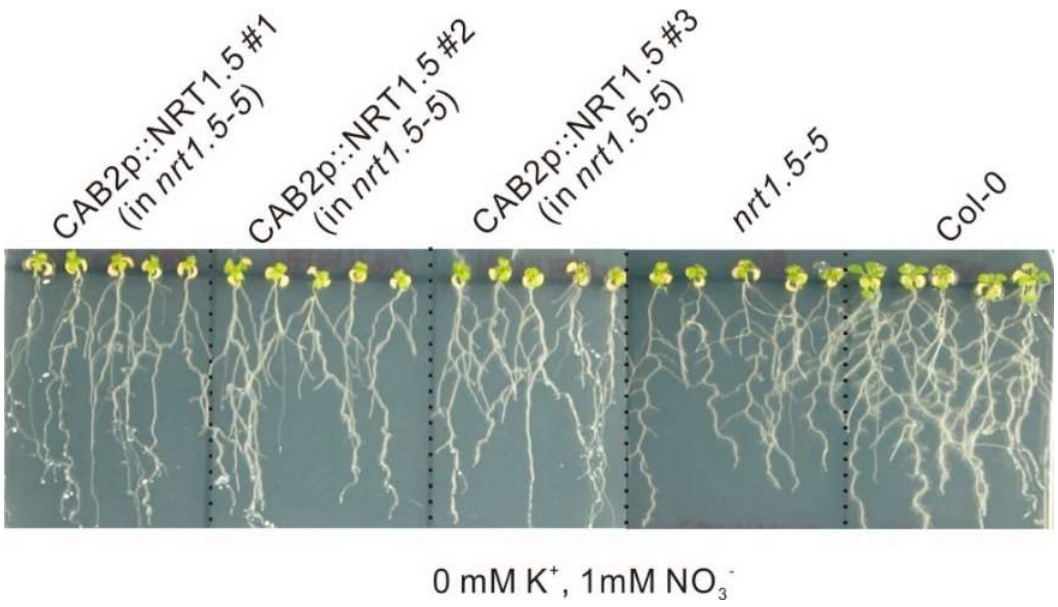

Figure 8. The root development of *CAB2p::NRT1.5* lines under K^+ deprivation.

Wild type Col-0, *nrt1.5-5* and three independent transgenic lines *CABp2::NRT1.5* (in *nrt1.5-5* background) which have increased *NRT1.5* transcripts in shoots were firstly germinated on 1/2 MS medium, then were transferred on plates containing 1 mM NO_3^- and 0 mM K^+ for growing 7 days.

The expression of *NRT1.5* under the control of the root specific *PHOSPHATE1* (*PHO1)* promoter in *nrt1.5-5* successfully complemented the K^+ deficiency phenotype in *nrt1.5-5* plants (Drechsler *et al.* 2015). To confirm the reduced LR density phenotype of *nrt1.5* mutants is indeed caused by loss-of-function mutation in *NRT1.5*, root growth of two independent *PHO1p::NRT1*.5 (*in nrt1.5-5*) complementation lines was examined on plates with 0 mM K^+ and 1.0 mM NO_3^- supply. Compared to the wild type, *nrt1.5-5* seedlings showed smaller rosettes and reduced LR numbers at 0 mM K^+ supply, whereas *PHO1p::NRT1*.5 #1 and #3 showed comparable rosette size and lateral root growth as that of wild type (Figure 9A). The LR density of both *PHO1p::NRT1.5* lines was nearly identical to that of wild-type seedlings (Figure 9B). These results demonstrate that the *NRT1.5* expression in roots is indeed required and important for the LR development under K^+ limiting conditions.

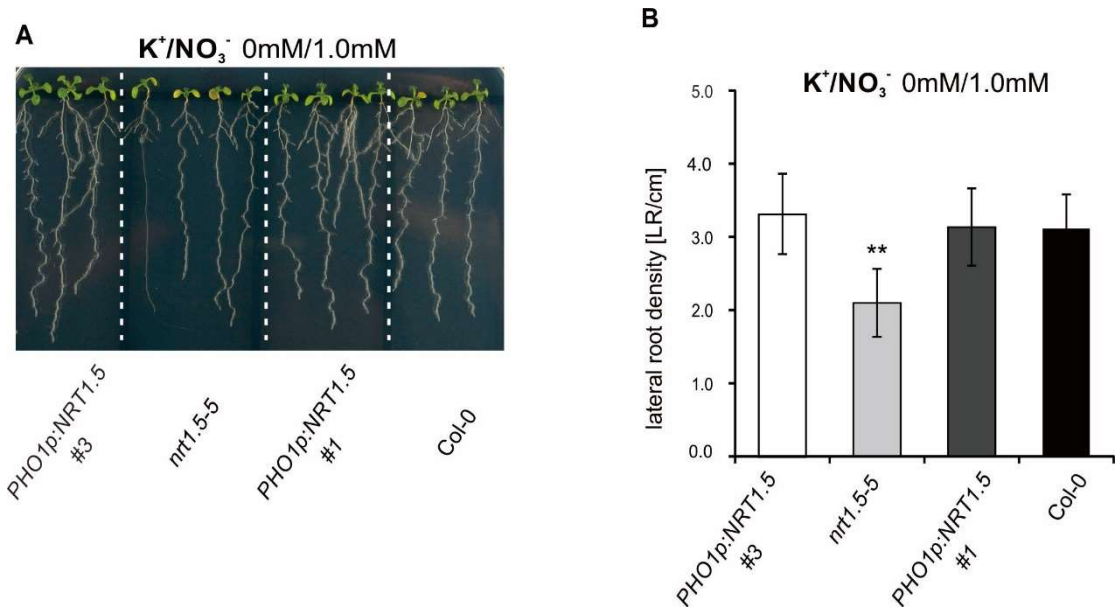

Figure 9. The K^+ deficiency dependent root phenotype of *nrt1.5-5* is complemented by root specific *NRT1.5* expression.

(A) Root morphology of wild type Col-0, *nrt1.5-5* and two independent *PHO1p::NRT1.5* lines (in *nrt1.5-5*) grown on medium containing 1 mM NO_3^- and 0 mM K^+. **(B)** Lateral root density of seedlings grown vertically on medium with 1 mM NO_3^- and 0 mM K^+ (means ± SD; n ≥ 25). ** indicates a statistically significant difference (Student's *t*-test) between *nrt1.5-5* and Col-0 with $P < 0.01$.

3.1.4 Auxin and cytokinin related genes were not deregulated in *nrt1.5-5* roots at limited K^+ supply

The reduced LR density phenotype of *nrt1.5* by K^+ deprivation resembles that of *myb77* mutant, which lacks the auxin signaling-modulating transcription factor *MYB77* whose expression is repressed by K^+ deprivation (Shin *et al.* 2007). Since it is well established that phytohormones like auxin and cytokinin play an important role in regulating LR development in *Arabidopsis*, it was intriguing to examine whether the auxin or cytokinin status in *nrt1.5* roots under K^+ limiting condition is changed or not in comparison to Col-0. In this study, expressions of auxin and cytokinin responsive and transporter genes were analyzed in roots of *nrt1.5-5* and Col-0 grown at 0 mM K^+ supply. *nrt1.5-5* had similar expression level of *MYB77* as Col-0, demonstrating that *nrt1.5-5* phenotype is not caused by the inhibition of *MYB77*. Genes encoding auxin-responsive proteins

IAA4, *Small Auxin-Upregulated RNA* (*SAUR*) and *SAUR41*, *Auxin Response Factors* (*ARF*) *ARF7*, *ARF9*, *ARF11*, *LATERAL ORGAN BOUNDARIES DOMAIN 29* (*LBD29*), as well as genes encoding auxin transporter *PIN-FORMED* (*PIN*) proteins *PIN1*, *PIN2*, *PIN5* and *NRT1.1* were not significantly deregulated in *nrt1.5-5* (Figure 9). These results indicate that auxin level in *nrt1.5-5* roots is not changed. In addition, cytokinin response genes *Arabidopsis thaliana Response Regulator* (*ARR*) *ARR5*, *ARR7* and *ARR10* were also stably expressed in *nrt1.5-5* (Figure 10). Consequently, it is unlikely that the reduced LR density phenotype of *nrt1.5-5* is due to the change of auxin and cytokinin level. However, it is also possible that those hormone related genes are only deregulated in specific root parts like LR, therefore, using the whole root material for expression study could not correctly reflect the real hormone status.

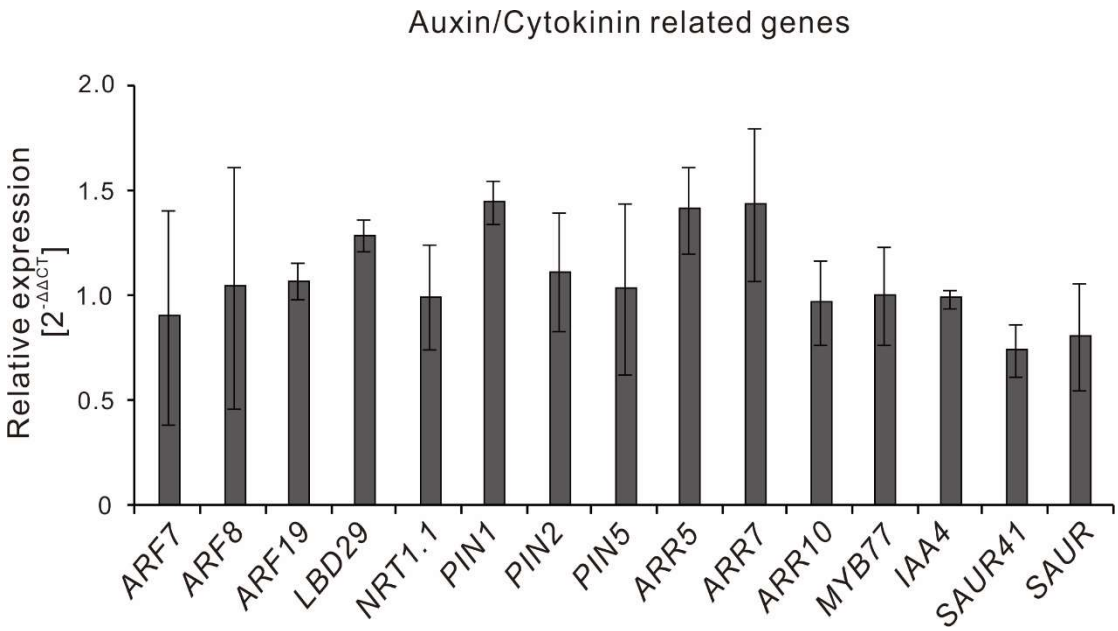

Figure 10. Expression level of auxin and cytokinin related genes in roots of *nrt1.5-5* at K^+ starvation condition by qRT-PCR.

The wild type Col-0 and *nrt1.5-5* seedlings were transferred on modified 1/2 MS medium with 1 mM NO_3^- and 0 mM K^+ after growing four days on 1/2 MS medium. Root materials of each line were harvested after growing 7 days. Roots from five seedlings were pooled as one biological replicate for qRT-PCR. Gene expression in *nrt1.5-5* samples was shown as the relative level ($2^{-\Delta\Delta CT}$) to that of Col-0 samples (means ± SD, n = 3). *UBQ10* was used for normalization.

3.1.5 *35Sp::NRT1.5* lines phenocopied *nrt1.5* at low K^+ availability

To better understand the role of NRT1.5 in root development under low K^+ conditions, besides *nrt1.5* knockout mutants, *35Sp::NRT1.5* overexpression lines (in Col-0 background) were generated under the control of the constitutive CaMV *35S* promoter. qRT-PCR was used to check the *NRT1.5* expression in *35Sp::NRT1.5* lines. Three independent homozygous T3 lines *35Sp::NRT1.5* #4-1, *35Sp::NRT1.5* #8-2 and *35Sp::NRT1.5* # 18-3 were shown to have enhanced *NRT1.5* level in both shoots and roots compared to wild type (Figure 11A), therefore these three lines were further used for root assays. The growth patterns of these three overexpression lines as well as Col-0 were examined under K^+ starvation conditions (0 µM and 10 µM K^+). Surprisingly, all three *35Sp::NRT1.5* lines demonstrated smaller rosettes and more severe leaf chlorosis than wild type under low K^+ concentrations. Moreover, three overexpression lines showed reduced LR numbers compared to wild type (Figure 11B). These growth patterns of *35Sp::NRT1.5* lines resemble *nrt1.5* mutants at K^+ deprivation (Figure 5A). It is interesting to note that complementation lines of *nrt1.5-5* (*PHO1p::NRT1.5*) which have the wild-type level *NRT1.5* expression restored the LR growth to the wild type (Figure 9), however, the overexpression of *NRT1.5* in three *35Sp::NRT1.5* lines led to the similar reduced LR phenotype as *nrt1.5* mutants.

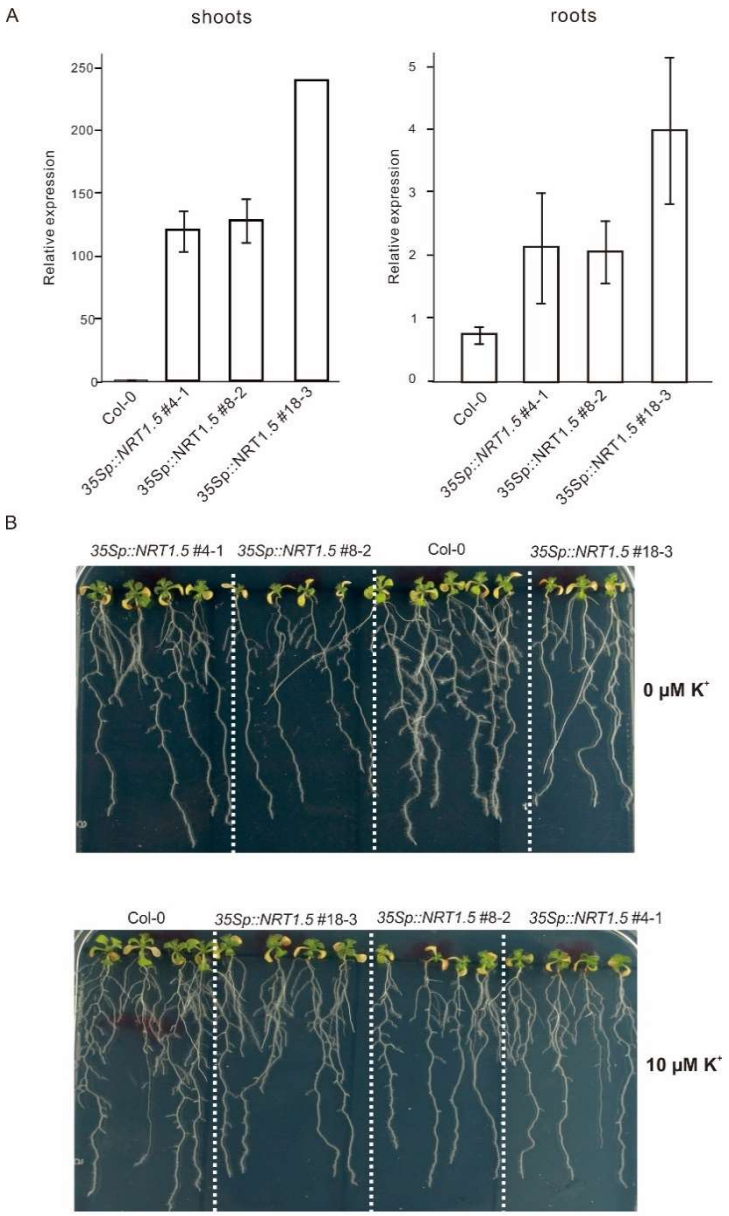

Figure 11. Expression of *NRT1.5* in Col-0 and *35Sp::NRT1.5* lines and their growth at K^+ deficiency conditions.

(A) The *NRT1.5* transcript level in shoots and roots of Col-0 and three T3 homozygous *35Sp::NRT1.5* line. Five days after germination (DAG) on 1/2 MS agar plates, seedlings were transferred to liquid 1/2 MS medium for cultivating further 10 days. Material from eight seedlings were pooled as one biological replicate. The relative transcript level [$2^{-\Delta\Delta CT}$] was measured by qRT-PCR (means ± SD, n ≥ 2). The *NRT1.5* level in Col-0 was set as 1.0. The gene *UBQ10* was used for normalization. **(B)** Morphology of three *35Sp::NRT1.5* lines and Col-0 at K^+ deficiency condition. Seeds of all lines were germinated at 1/2 MS agar plates, then 5 DAG seedlings were transferred on modified 1/2 MS agarose plates containing 1mM NO_3^- and either 0 µM K^+ or 10 µM K^+ for growing seven days vertically.

3.1.6 The *nrt1.5-5* and *35Sp*::*NRT1.5* lines had higher K accumulation in roots

Besides phytohormones, external and intrinsic nutrition amount could also affect the root morphology of *Arabidopsis*. To investigate whether alterations of macro or micro elements composition contribute to the reduced LR density phenotype in *nrt1.5* mutants and *35Sp::NRT1.5* lines, root and shoot material were separately harvested from seedlings growing vertically on modified 1/2 MS medium with 10 μM K^+ for elemental analysis by Inductively Coupled Plasma Optical Emission Spectrometry (ICP-OES). In agreement with the smaller rosettes and more severe leaf chlorosis (Figure 11B), K concentration in shoots of *nrt1.5-5* and all three *35Sp::NRT1.5* lines was reduced compared to that of Col-0, although the difference between *35Sp::NRT1.5 #4-1* and Col-0 was not statistically significant (Table 13). Besides K, shoot phosphorus (P) concentration in *nrt1.5-5* and *35Sp::NRT1.5* lines was also significantly lower than in Col-0. The higher accumulation of Calcium (Ca) was occurred in shoots of *nrt1.5-5*, but not in the overexpression lines. No higher accumulation of Magnesium (Mg) was observed in shoots of *nrt1.5-5* nor in the overexpression lines. Microelement manganese (Mn) was significantly decreased in shoots of *nrt1.5-5* and in overexpression lines. Surprisingly, unlike in shoots, except Ca, all other macroelements including K, Mg, P and S had a significantly higher accumulation in roots of *nrt1.5-5* and in three *35Sp::NRT1.5* lines in comparison with that of Col-0. Interestingly, root K concentration in three *35Sp::NRT1.5* lines was relatively lower than that in *nrt1.5-5*. Furthermore, root sodium (Na) concentration in *nrt1.5-5* and *35Sp::NRT1.5* lines was lower compared to Col-0. Except iron (Fe), all other microelements were accumulated more in roots of *nrt1.5-5* and three *35Sp::NRT1.5* lines compared to that in wild type, although the difference was not statically significant for some lines. These results lead to the speculation that under the low K^+ availability, the root-to-shoot transfer of various macroelements including K, as well as that of some microelements, is blocked in the roots of *nrt1.5-5* and

35Sp::NRT1.5 lines, and this block might account for the decreased LR density phenotype.

Table 13. Elemental analysis in Col-0, *nrt1.5-5* and three *35Sp::NRT1.5* lines growing vertically on plates with 10 µM K^+.

Five days after germination on 1/2 MS medium, seedlings were transferred on modified 1/2 MS medium with 10 µM K^+ and 1 mM NO_3^- and grew vertically for ten days. Roots and shoots from 40 seedlings were separated and were pooled as one biological replicate. Concentration of elements was analyzed by ICP-OE. Macroelements and microelements were shown as [mg/g DW] and [µg/g DW] (means ± SD, n = 8), respectively. The orange color indicates elements that were significantly deceased compared to wild-type level. The green color indicates elements that were significantly increased compared to wild-type level. * and ** indicates a statistically significant difference (Student's *t*-test) between *nrt1.5-5* (or *35Sp::NRT1.5* lines) and Col-0 with $P < 0.05$ and $P < 0.01$, respectively.

	Shoots				
	Col-0	***nrt1.5-5***	***35Sp::NRT1.5* #4-1**	***35Sp::NRT1.5* #8-2**	***35Sp::NRT1.5* #18-3**
Macroelements mg/g DW					
K	6.13 ± 0.31	**4.96 ± 0.29****	5.85 ± 0.27	**4.87 ± 0.32****	**5.34 ± 0.50***
Ca	25.00 ± 0.88	**26.06 ± 1.06***	26.00 ± 0.89	**22.57 ± 0.29****	25.82 ± 1.92
Mg	7.63 ± 0.32	7.72 ± 0.36	7.83 ± 0.20	**7.02 ± 0.10***	7.58 ± 0.62
P	11.07 ± 0.59	**10.29 ± 0.36****	9.71 ± 0.34	**8.96 ± 0.32****	**9.94 ± 0.07***
S	11.70 ± 0.52	12.12 ± 0.66	11.30 ± 0.31	11.03 ± 0.20	12.15 ± 0.77
Na	6.93 ± 0.53	6.50 ± 0.69	6.54 ± 0.35	**6.02 ± 0.25***	6.99 ± 0.46
Microelements µg/g DW					
Fe	66.98 ± 8.42	**85.99 ± 18.91***	71.17 ± 7.55	71.48 ± 2.38	**110.99 ± 43.87***
B	33.15 ± 1.47	30.72 ± 3.21	31.24 ± 2.10	**28.93 ± 1.29****	33.03 ± 2.83
Mn	520.19 ± 19.56	**617.62 ± 35.67****	**559.39 ± 28.55***	**544.73 ± 27.16****	**589.81 ± 46.03****
Zn	191.43 ± 15.14	197.12 ± 19.33	**171.12 ± 7.85***	198.31 ± 6.10	198.98 ± 14.99
	Roots				
	Col-0	***nrt1.5-5***	***35Sp::NRT1.5* #4-1**	***35Sp::NRT1.5* #8-2**	***35Sp::NRT1.5* #18-3**
Macroelements mg/g DW					
K	11.67 ± 0.39	**17.20 ± 1.21****	**14.91 ± 0.44****	**14.64 ± 0.66****	**14.67 ± 1.03****
Ca	9.12 ± 0.36	8.57 ± 0.73	9.18 ± 0.24	9.63 ± 0.43	**9.82 ± 0.21***
Mg	6.40 ± 0.62	**7.22 ± 0.61***	**7.34 ± 0.36****	**7.92 ± 0.24****	**7.73 ± 0.51****
P	4.87 ± 0.18	**5.29 ± 0.27****	**5.27 ± 0.15***	**5.79 ± 0.14****	**5.51 ± 0.05****
S	6.31 ± 0.14	**7.22 ± 0.49****	**6.67 ± 0.15****	**7.63 ± 0.21****	**7.17 ± 0.26****
Na	1.40 ± 0.10	**1.16 ± 0.14****	**1.17 ± 0.12****	**1.20 ± 0.05****	1.33 ± 0.09
Microelements µg/g DW					
Fe	306.64 ± 24.36	357.87 ± 78.96	**265.09 ± 22.41***	308.70 ± 49.51	**344.27 ± 23.76***
B	29.60 ± 0.96	30.64 ± 2.37	**31.24 ± 1.35***	**31.11 ± 0.39***	**32.29 ± 1.87****
Mn	302.87 ± 26.80	334.06 ± 105.07	318.63 ± 39.25	**392.61 ± 29.87****	**476.01 ± 65.65****
Zn	207.66 ± 20.81	243.02 ± 54.05	189.36 ± 15.09	**285.40 ± 59.68****	**266.51 ± 47.78***

3.1.7 Root growth retardation in *nrt1.5* mutants by brassinazole treatment

Expression data from Genevestigator (https://www.genevestigator.com/gv/index.jsp) (Zimmermann *et al.* 2004) show that *NRT1.5* is strongly upregulated in *BREVIS RADIX* (*brx*) knockout mutant which is defective in brassinosteroids (BRs) biosynthesis (Mouchel *et al.* 2006). This suggests *NRT1.5* might be regulated by BRs. It is well known that BRs play pivotal roles in many plant growth development processes including cell elongation and cell division (Wei and Li 2016). To explore the possible phenotype of *nrt1.5* knockout mutants when BRs synthesis is blocked, the BR synthesis inhibitor brassinazole (Asami *et al.* 2000) was utilized to treat Col-0 and *nrt1.5* seedlings. *nrt1.5* mutants showed the comparable growth like wild type Col-0 on 1/2 MS plates. Brassinazole (BZ) treatment inhibited the root growth of all lines. However, after growing vertically on 1/2 MS plates containing brassinazole for 6-7 days, both *nrt1.5-4* and *nrt1.5-5* demonstrated retarded root growth compared to Col-0 (Figure 12A). Moreover, *nrt1.5* mutants also showed mild gravitropic changes in response to brassinazole treatment. In agreement with the exhibited root morphology, the primary root length of both *nrt1.5* mutants was significantly reduced compared to wild type by 500 nM brassinazole treatment (Figure 12B). It is known that mutants impaired in BR biosynthesis or signaling transduction display a short-root phenotype (Li *et al.* 1996; Mussig *et al.* 2003). Therefore, the more sensitive response to brassinazole treatment of *nrt1.5* might indicate the lower BRs biosynthesis level in *nrt1.5* mutants.

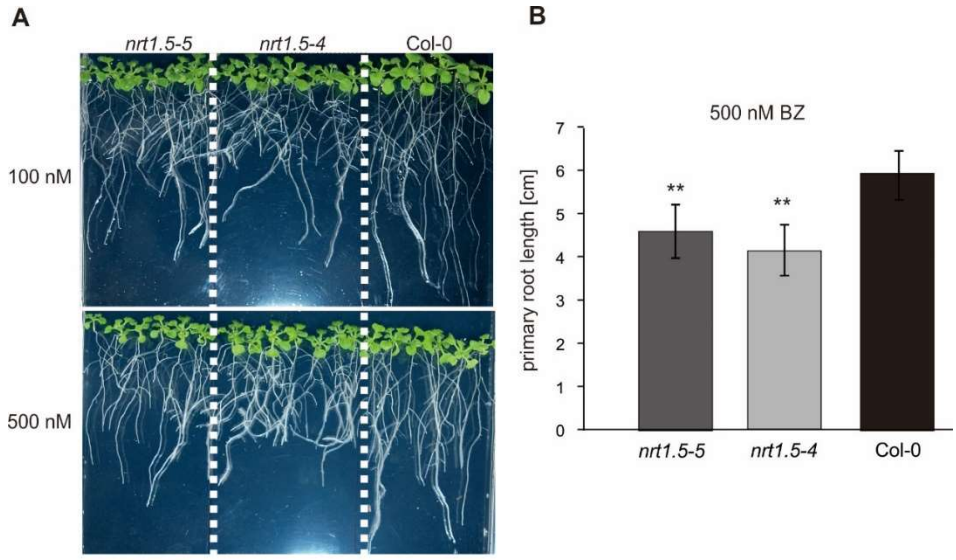

Figure 12. Brassinosteroid biosynthesis inhibitor brassinazole resulted in a stronger root retardation in *nrt1.5* seedlings.

(A) Root morphology of Col-0, *nrt1.5-4* and *nrt1.5-5* by 100 nM and 500 nM brassinazole treatment. **(B)** Primary root length of *nrt1.5* mutants was reduced by brassinazole (means ± SD; n = 18). Seedlings were grown on 1/2 MS medium supplemented with indicated concentrations of brassinazole for seven days. ** indicates a statistically significant difference (Student's *t*-test) between mutants and Col-0 with $P < 0.01$.

3.1.8 Smaller shoot size *of nrt1.5* mutants by Jasmonic acid treatment

To investigate whether phytohormone treatment can generate any different morphological responses in *nrt1.5* mutants, Indole-3-acetic acid (IAA), abscisic acid (ABA) and jasmonic acid (JA) were used to treat seedlings growing on 1/2 MS agar plates. No morphological changes of *nrt1.5* mutants compared to wild type were observed by IAA and ABA treatments (data not shown). Root length of all plant lines were comparable in response to JA treatment. However, shoots of *nrt1.5* mutants were apparently smaller than that of Col-0 by 10 µM JA treatment (Figure 13A). In comparison with Col-0, supplementation of 10 µM and 20 JA µM significantly reduced the shoot fresh weight gain of *nrt1.5-5* (Figure 13B). The similar trend was also shown for *nrt1.5-4* by 10 µM JA, though the difference was not statistically significant. The fresh weight differences between Col-0 and *nrt1.5* mutants was attenuated by the

increment of JA concentration to 30 µM JA, which might because this concentration is too high to generate the different responses. These results showed the stronger sensitivity of *nrt1.5* mutants to JA treatment, which might be caused by the higher JA production in *nrt1.5* mutants. This observation is supported with the finding that *nrt1.5-5* plants growing at soil produced more JA and jasmonoyl-isoleucine (JA-IIE) in rosettes compared to Col-0 (Drechsler, Dissertation 2016).

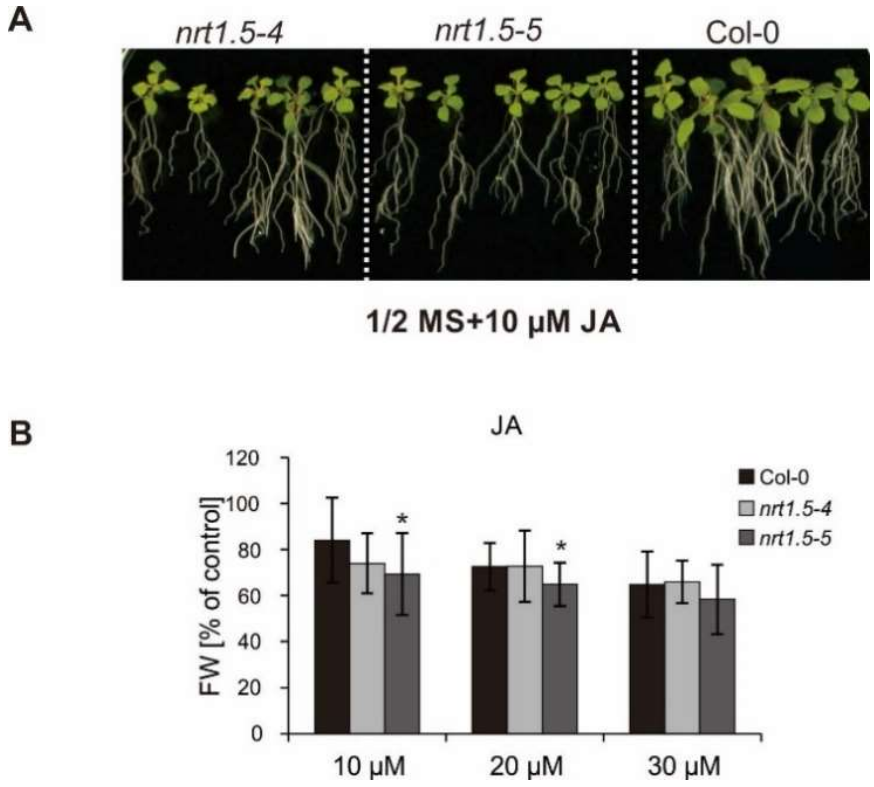

Figure 13. *Arabidopsis nrt1.5* mutant seedlings are more sensitive to jasmonic acid treatment. **(A)** Morphology of Col-0, *nrt1.5-4* and *nrt1.5-5* growing on 1/2 MS medium supplemented with 10 µM JA. **(B)** Rosette fresh weight (FW) of Col-0, *nrt1.5-4* and *nrt1.5-5* by JA treatment. Rosettes of three seedlings grown on 1/2 MS medium (untreated) or 1/2 MS medium containing JA (10, 20 or 30 µM) were pooled as one biological replicate for FW measurement. Results displayed here is the relative fresh weight ratio of JA treatment seedlings/untreated seedlings (means ± SD; n = 16). * indicates a statistically significant difference (Student's *t*-test) between mutants and Col-0 with $P < 0.05$.

3.2 Functional analysis of NRT1.5

The subsequent work presented in section 3.2.1, 3.2.3, Figure 17A and Figure 18A has been published as a part of the publication: Drechsler, N., Zheng, Y., Bohner, A.,

Nobmann, B., von Wirén, N., Kunze, R. and Rausch, C. (2015). Nitrate-dependent control of shoot K homeostasis by the Nitrate Transporter1/Peptide Transporter Family member NPF7.3/NRT1.5 and the stelar K^+ outward rectifier SKOR in *Arabidopsis*. Plant Physiology 169: 2832-2847.

3.2.1 Potassium import assay of NRT1.5 in *Saccharomyces cerevisiae*

To functionally test whether NRT1.5 itself can directly mediate K^+ uptake in the heterologous expression system, the coding sequence (CDS) of *NRT1.5* was cloned into yeast expression vector p426TEF and was subsequently introduced into *Saccharomyces cerevisiae* mutant BYT12 cells which lack two important potassium transporters Trk1 and Trk2. *Arabidopsis* inward rectifier K^+ channel *KAT1* was cloned into the same vector and was transformed into BYT12 cells as a positive control. BYT12 cells transformed with empty vector p426 showed normal growth like wild-type BY4741 cells transformed with empty vector p426 when 100 mM KCl was supplemented to Yeast nitrogen base (YNB) medium (Figure 14A, lower panel). However, without additional KCl supply, BYT12 cells with empty vector p426 cannot grow properly on YNB medium which contains only about 7 mM K^+ (Figure 14A, upper panel). Expression of *KAT1* greatly promoted the growth of BYT12 cells on YNB medium (Figure 14A, upper panel). However, two independent transformants with the expression of *NRT1.5* were not able to restore the growth retardation of BYT12 cells on YNB medium (Figure 14A, upper panel). Since the regular YNB medium contains 7 mM K^+, to determine whether NRT1.5 facilitates the uptake of potassium only in the high affinity range, another yeast performance test was conducted on modified K^+-free YNB medium supplemented with only 1 mM K^+. Yet, no complementation in growth of BYT12 cells by expression of *NRT1.5* was observed (Figure 14B, upper panel). These results suggested that NRT1.5 itself cannot directly mediate K^+ inward transport in the yeast system used in this study.

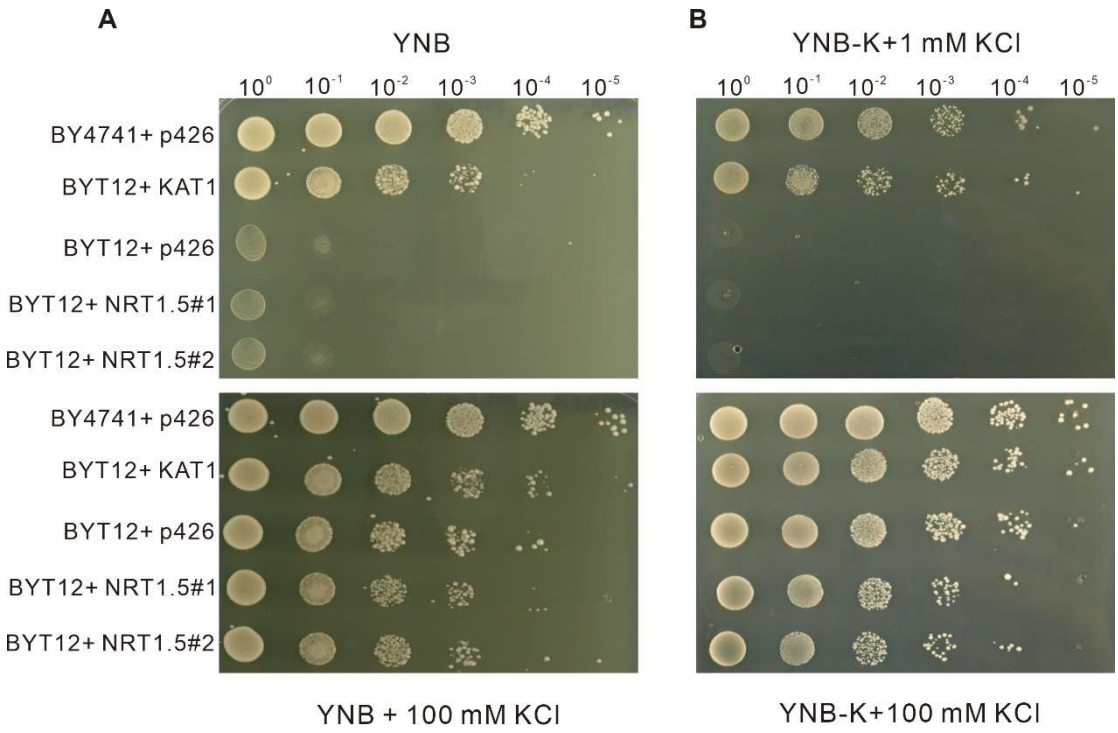

Figure 14. Potassium uptake capacity analysis of NRT1.5 in *Saccharomyces cerevisiae*.

(A) K^+ uptake capacity of NRT1.5 was analyzed in yeast mutant BYT12 (*trk1*Δ *trk2*Δ) cells grown on YNB medium. **(B)** K^+ uptake capacity of NRT1.5 was analyzed in yeast mutant BYT12 (*trk1*Δ *trk2*Δ) cells grown on K^+-free YNB medium. Yeast wild type strain BY4741 and mutant strain BYT12 were transformed with the expression constructs indicated on the left of the figure. Dilution series of 20 µl cell suspensions (OD_{600} from 1.0 to 10^{-5}) were dropped on YNB (-Ura) agar plates with (upper panel) or without (lower panel) 100 mM KCl. p426 is the empty vector control. *KAT1* and *NRT1.5* are coding sequences of the respective *Arabidopsis* genes cloned in p426 vector. 1 and 2 indicate two independent yeast transformants.

3.2.2 Ammonium uptake assay of NRT1.5 in *Saccharomyces cerevisiae*

It is known that ammonium (NH_4^+) inhibits potassium uptake systems (Coskun *et al.* 2015). In *S. cerevisiae* cells lacking *Trk* genes, K^+ might enter cells through the activity of Methylamine and ammonium permeases (Mep) unspecifically (Arino *et al.* 2010). In addition, because of the similarities between NH_4^+ and K^+ in terms of their hydrated diameters, charge and influence on membrane potentials, it is an obvious question to investigate whether NRT1.5 has NH_4^+ transport activity. To address this question, yeast expression vector p426TEF with *NRT1.5* CDS was introduced into yeast mutant

31019b which lacks the function of three methylamine and ammonium permeases Mep1, Mep2 and Mep3. *Arabidopsis* ammonium transporter AMT1.1 served as a positive control. Compared to wild type 233441c cells with the empty vector p426, the *Mep* mutant (31019b) cells with empty vector p426 showed the retarded growth even when external NH_4^+ concentration is 10 mM (Figure 15A). The stronger growth retardation of yeast mutant cells was observed on medium with 1 mM and 3 mM NH_4^+ supply. The Expression of *AMT1.1* restored the growth of *Mep* mutant to the performance level of wild type strain 233441c transformed with empty vector p426 (Figure 14A). However, three independent transformants of *Mep* mutant with the expression of *NRT1.5* failed to do so (Figure 15A). Yeast growth performance was tested with three different pH values 4.5, 5.0 and 6.0. However, at none of these pH conditions a different growth performance of *Mep* cells with the *NRT1.5* expression was generated. Even though yeast cannot directly use NO_3^- as N source, to exclude the possibility that the activity of NRT1.5 in yeast is dependent on the presence of NO_3^-, another yeast performance test was done on YNB medium with NH_4NO_3 as NH_4^+ source instead of NH_4Cl (Figure 15B). However, the different NH_4^+ source did not generate different results. These results show that NRT1.5 cannot mediate ammonium uptake in yeast system.

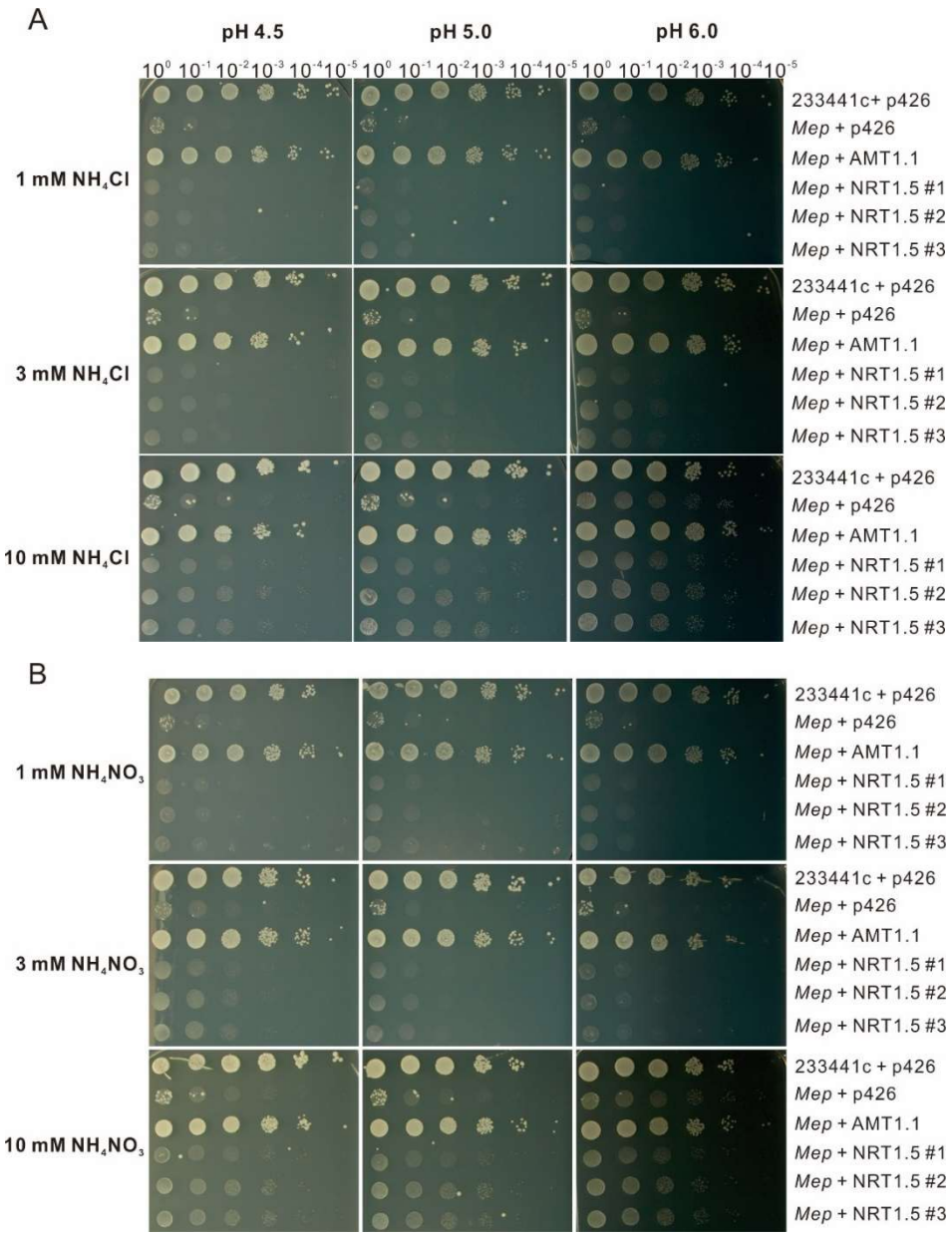

Figure 15. Ammonium uptake capacity analysis of NRT1.5 in *Saccharomyces cerevisiae*.

(A) NH_4^+ uptake capacity of NRT1.5 was analyzed in yeast *Mep* mutant 31019b (*mep1Δ mep2Δ mep3Δ*) cells grown on YNB medium with various NH_4Cl supply. **(B)** NH_4^+ uptake capacity of NRT1.5 was analyzed in yeast *Mep* mutant 31019b (*mep1Δ mep2Δ mep3Δ*) cells grown on YNB medium with various NH_4NO_3 supply. Yeast wild type 233441c and mutant *Mep* cells were transformed with expression constructs indicated on the right under various pH conditions (pH4.5, pH5.0 and pH6.0 from left to right). 20 µL cell suspensions (OD_{600} from 1.0 to 10^{-5}) were dropped on YNB (-Ura) agar plates with indicated amount of NH_4^+ (1mM, 3 mM and 10 mM, from upper to lower panel). p426 is the empty vector. *AMT1.1* and *NRT1.5* are coding sequences of the respective *Arabidopsis* genes cloned in p426 vector. 1, 2 and 3 indicate three independent yeast transformants.

3.2.3 Potassium export assay of NRT1.5 in *Saccharomyces cerevisiae*

Since NRT1.5 showed no K^+ inward transport function, it makes sense to test whether it can transport K^+ out of the yeast cells, either autonomously or by influencing the activity of SKOR, which is the well-known major potassium channel protein responsible for K^+ xylem loading in *Arabidopsis*. To answer this question, full length CDS of *NRT1.5* and *SKOR* were cloned into yeast expression vector p426TEF and p425TEF, respectively, followed by the introduction into yeast mutant BYT45 which lacks the activity of $Na^+(K^+)$-ATPase Ena1-5 and $H^+/Na^+(K^+)$ antiporter Nha1 (Borovikova *et al.* 2014). When additional 1 M KCl was supplemented in the YNB medium, BYT45 cells transformed with two empty vectors were not able to grow as vigorously as wild type BY4741 cells with empty vectors (Figure 16). Expression of *SKOR* in BYT45 cells restored the normal growth of transformed cells like BY4741, demonstrating the K^+ export capacity of SKOR. However, mutant cells with the expression of *NRT1.5* demonstrated the same growth retardation as mutant cells expressing empty vectors, suggesting that expression of *NRT1.5* failed to export K^+ in the yeast system used in this study. In addition, BYT45 transformants which co-expressed *SKOR* and *NRT1.5* just showed comparable growth like cells expressing *SKOR* alone, suggesting that the presence of NRT1.5 has no influence on the K^+ export activity of SKOR.

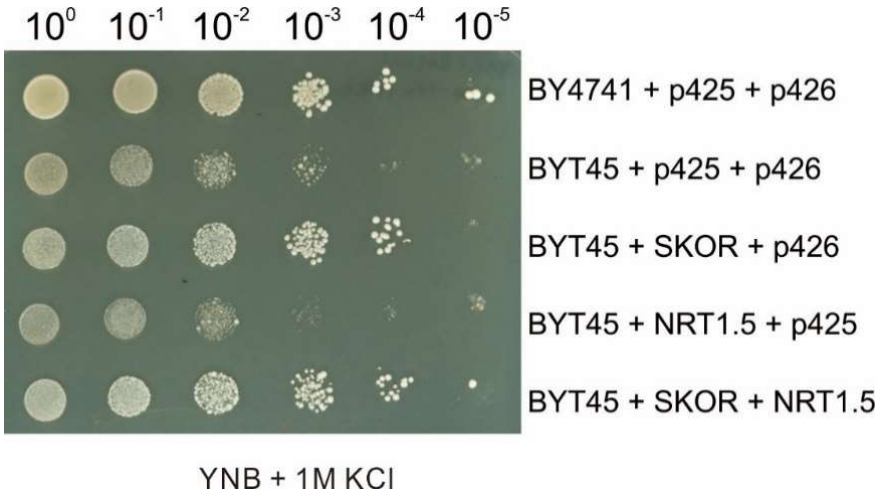

Figure 16. Potassium export capacity analysis of NRT1.5 in *Saccharomyces cerevisiae*.

K^+ export capacity was analyzed in yeast BY4741 and the mutant BYT45 (*ena1-5*Δ *nha1*Δ) cells transformed with the expression constructs indicated on the right. 20 µL cell suspensions (OD600 from 1.0 to 10^{-5}) were dropped on YNB (-Ura -Leu) agar plates with additional 1 M KCl supply (pH 5.9). p425 and p426 are the empty vectors. *SKOR* and *NRT1.5* are coding sequences of the respective *Arabidopsis* genes cloned in p425 or p426 vector.

3.2.4 The expression of *NRT1.5* renders *Saccharomyces cerevisiae* cells the susceptibility to toxic cationic compounds

In yeast, sensitivity to toxic cationic drugs like hygromycin B (HygB), tetramethylammonium (TMA), spermine and tetraethylammonium (TEA) is often linked to changes in the membrane potential which can be provoked by alterations in K^+ homeostasis (Barreto *et al.* 2011). Accordingly, BYT12 cells which lack *TRK1* and *TRK2* have a higher sensitivity to toxic cations even under nonlimiting K^+ concentrations, due to the hyperpolarization of the plasma membrane (Navarrete *et al.* 2010). To elucidate whether NRT1.5 has an influence on the membrane potential, p426 vector with *NRT1.5* CDS was transformed in wild type BY4741 and mutant BYT12 cells followed by growth tests on YNB plates contain concentration gradients of HygB, TMA or TEA. Compared to wild type BY4741 cells, mutant BYT12 cells expressing empty vector p426 did not grow properly on YNB medium with high concentrations of HygB (Figure 17A) or TMA (Figure 17B), which confirmed that membrane of BYT12 cells were more polarized. Expression of *NRT1.5* in BYT12 cells resulted in strongly increased HygB sensitivity compared to BYT12 cells with p426 empty vector (Figure 17A). A similar pattern was obtained in the TMA sensitivity test (Figure 17B). It is interesting to note that the expression of *NRT1.5* in wild type BY4741 cells did not cause the increased sensitivity to HygB or TMA (Figure 17A, 17B). It could be due to the concentration of HygB or TMA applied was not high enough to provoke the growth differences between BYT4741 cells with or without the *NRT1.5* expression. This explanation might be supported by the observation that on gradient plates containing another cationic drug TEA, the expression of *NRT1.5* in BY4741 cells caused the increased sensitivity of BY4741 cells compared to cells with empty vector p426 (Figure

17C). Altogether, the increased sensitivity of *NRT1.5*-expressing cells to toxic cationic compounds suggests that the expression of *NRT1.5* can provoke the hyperpolarization of yeast cell membrane.

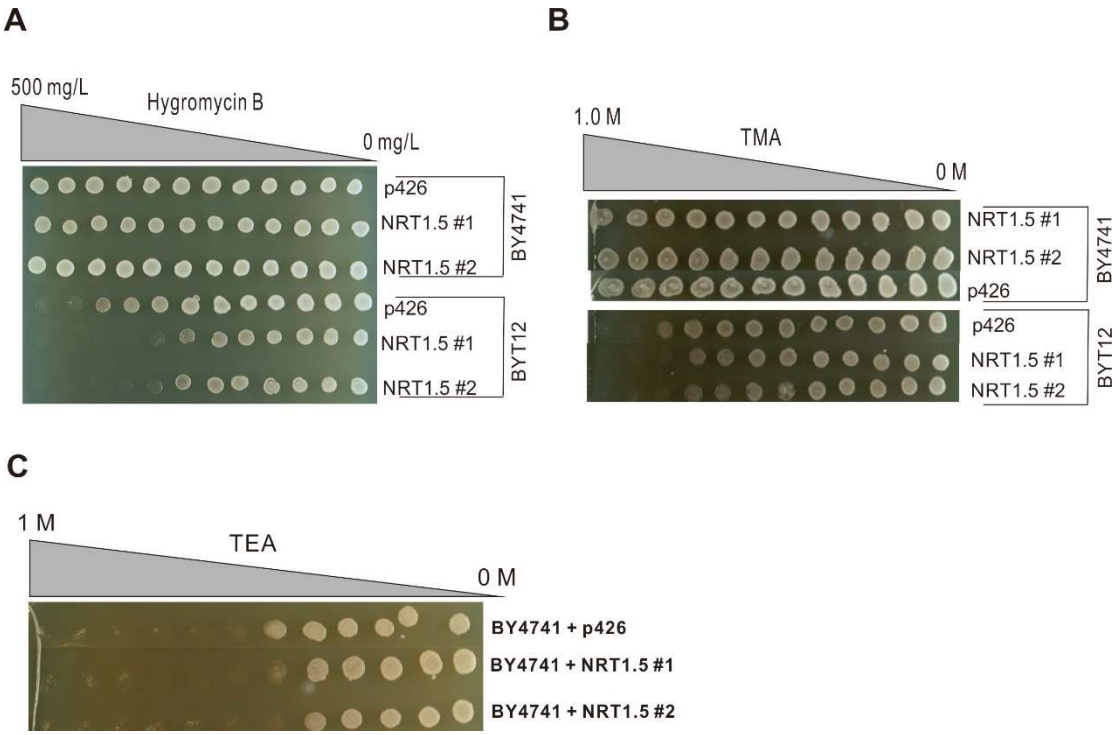

Figure 17. Cationic compound sensitivity test of *Saccharomyces cerevisiae* cells expressing *NRT1.5*.

(A) Yeast growth on YNB (-Ura) medium with increasing concentrations of hygromycin B from 0 to 0.5 g/l. **(B)** Yeast growth on YNB (-Ura) medium with increasing concentrations of tetramethylammonium from 0 to 1 M. **(C)** Yeast growth on YNB (-Ura) medium with increasing concentrations of tetraethylammonium from 0 to 1 M. BY4741 and BYT12 cells were transformed with the expression constructs indicated on the right. 100 mM KCl was supplemented to YNB medium to support the growth of BYT12 cells. Twelve 3 µl drops of each yeast cell suspension (OD600 = 1.0) were distributed on the plates. p426 is the empty vector and *NRT1.5* is the coding sequence of the *Arabidopsis* gene. 1 and 2 indicate two independent yeast transformants.

3.2.5 The *NRT1.5* level in *Arabidopsis* seedlings corelates with the sensitivity to hygromycin B

It has been reported that the T-DNA insertion mutant of *Arabidopsis* plasma membrane H^+-ATPase 2 (*AHA2*) was more resistant to toxic cations like HygB, cesium and lithium,

indicating that the protonmotive force in *aha2* mutant was impaired (Haruta *et al.* 2010). To assess whether the increased HygB sensitivity in yeast cells caused by the expression of *NRT1.5* also occurs in *Arabidopsis* plants, Col-0, *nrt1.5* mutants, *nrt1.5-5* complementation lines *PHO1p::NRT1.5* (in *nrt1.5-5* background) and overexpression lines *35Sp*::*NRT1.5* (in Col-0 background) were grown on 1/2 MS plates supplemented with either HygB or high amount of KCl which is known to cause the depolarization of the membrane. In comparison to Col-0, two *nrt1.5* mutants *nrt1.5-4* and *nrt1.5-5* were more resistant to 5 µg HygB treatment (Figure 18A), indicating the reduced plasma membrane potential of *nrt1.5* mutants. Two complementation lines *PHO1p::NRT1.5*#1 and *PHO1p::NRT1.5*#3, in which expression of *NRT1.5* was restored to wild type level in roots, exhibited the comparable response to HygB like Col-0 (Figure 18A). Compared to Col-0, three independent *35Sp::NRT1.5* overexpression lines were more sensitive to HygB (Figure 18B), which is consistent with the increased HygB sensitivity of yeast BYT12 cells expressing *NRT1.5*. Those results demonstrate the expression level of *NRT1.5* in *Arabidopsis* is in correlation with the plasma membrane potential: *nrt1.5* mutants are depolarized, while *35Sp::NRT1.5* overexpression lines are hyperpolarized in comparison to the wild type. It is known that high external K^+ concentration leads to a reduction in the membrane potential (Maathuis and Sanders 1993). In agreement with the response to HygB, *nrt1.5* mutants were more sensitive to the treatment with 50 mM KCl (Figure 18A) and *35Sp::NRT1.5* overexpression lines were more resistant to 100 mM KCl treatment (Figure 18B). All these observations strongly imply that *nrt1.5* mutants have depolarized plasma membrane, whereas plasma membrane of overexpression lines is hyperpolarized, in other words, the expression level of *NRT1.5* influences the plasma membrane potential of *Arabidopsis* plants.

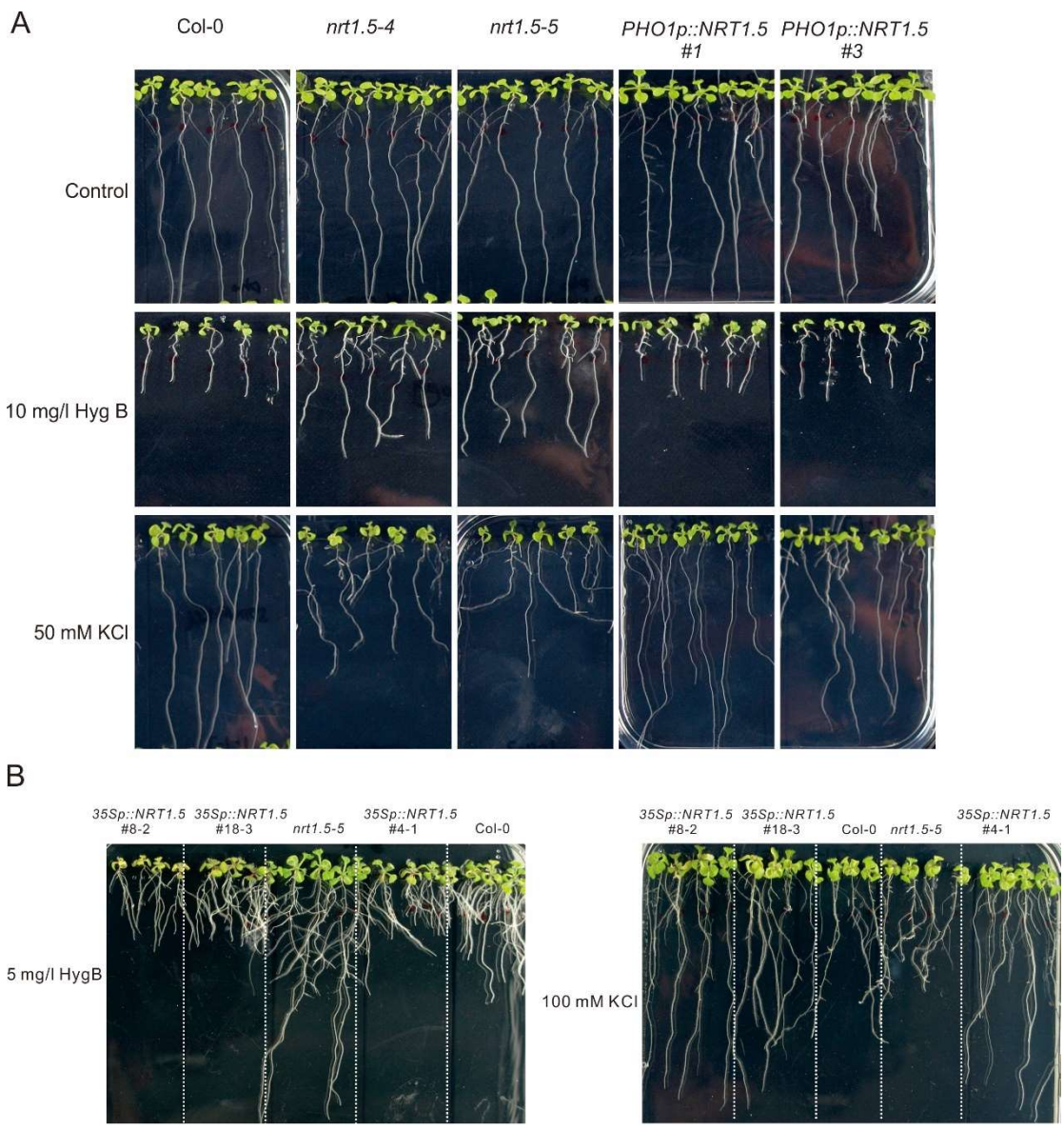

Figure 18. Growth of different plant lines in response to hygromycin B and high concentration of K^+ treatment.

(A) Morphology of Col-0, *nrt1.5* mutants and two *PHO1p::NRT1.5* complementation lines grown on 1/2 MS plates or 1/2 MS plates containing either 10 mg/l HygB or 50 mM KCl. **(B)** Morphology of Col-0, *nrt1.5-5* and three *35Sp::NRT1.5* overexpression lines grown on 1/2 MS plates containing either 5 mg/l HygB or 100 mM KCl. 5 DAG Seedlings germinated on 1/2 MS medium were transferred on 1/2 MS medium supplemented with HygB or with KCl and grew vertically for 6-7 more days.

3.3 Functional analysis of NRT1.8 in *Saccharomyces cerevisiae*

3.3.1 Potassium uptake and export assay of NRT1.8 in *Saccharomyces cerevisiae*

The function of *Arabidopsis* NRT1.8 is to remove NO_3^- from the xylem sap and transfer it into xylem parenchyma cells (Lin *et al.* 2008; Li *et al.* 2010; Chen *et al.* 2012). Among the 53 NRT1 members in *Arabidopsis*, NRT1.8 shares the highest sequence similarity with NRT1.5 (Li *et al.* 2010). The expression of both genes is oppositely regulated by various stress conditions (Li *et al.* 2010). In *nrt1.5* mutants roots, *NRT1.8* expression is strongly increased (Chen *et al.* 2012; Drechsler *et al.* 2015). Therefore, it is conceivable that the enhanced *NRT1.8* level in *nrt1.5* might contribute to the reduced K^+ root-to-shoot transfer in *nrt1.5* mutants. To test this hypothesis, the potassium transport assay of NRT1.8 was conducted in *S. cerevisiae* K^+ uptake mutant BYT12 and K^+ export mutant BYT45 cells. BYT12 cells with empty vector p426 did not grow on YNB medium, but the supplementation of 100 mM KCl restored the growth of BYT12 as that of *KAT1* transformed BYT12 cells and wild type BY4741 cells (Figure 19A). BYT45 cells grew normally on YNB medium, but their growth was nearly completely abolished by the addition of 1.2 M KCl (Figure 19B). Expression of *NRT1.8* in BYT12 cells was not able to complement the growth retardation of BYT12 cells on YNB medium without additional K^+ supply (Figure 19A), indicating that NRT1.8 cannot directly import K^+ into yeast cells. Interestingly, compared to BYT45 cells expressing empty vector p426, two independent BYT45 transformants with the expression of *NRT1.8* demonstrated the very weak growth at YNB medium with 1.2 M KCl (Figure 19B), implying that NRT1.8 might be able to export K^+ in yeast. However, due to the very weak growth of yeast cells, further analysis should be done to verify this observation.

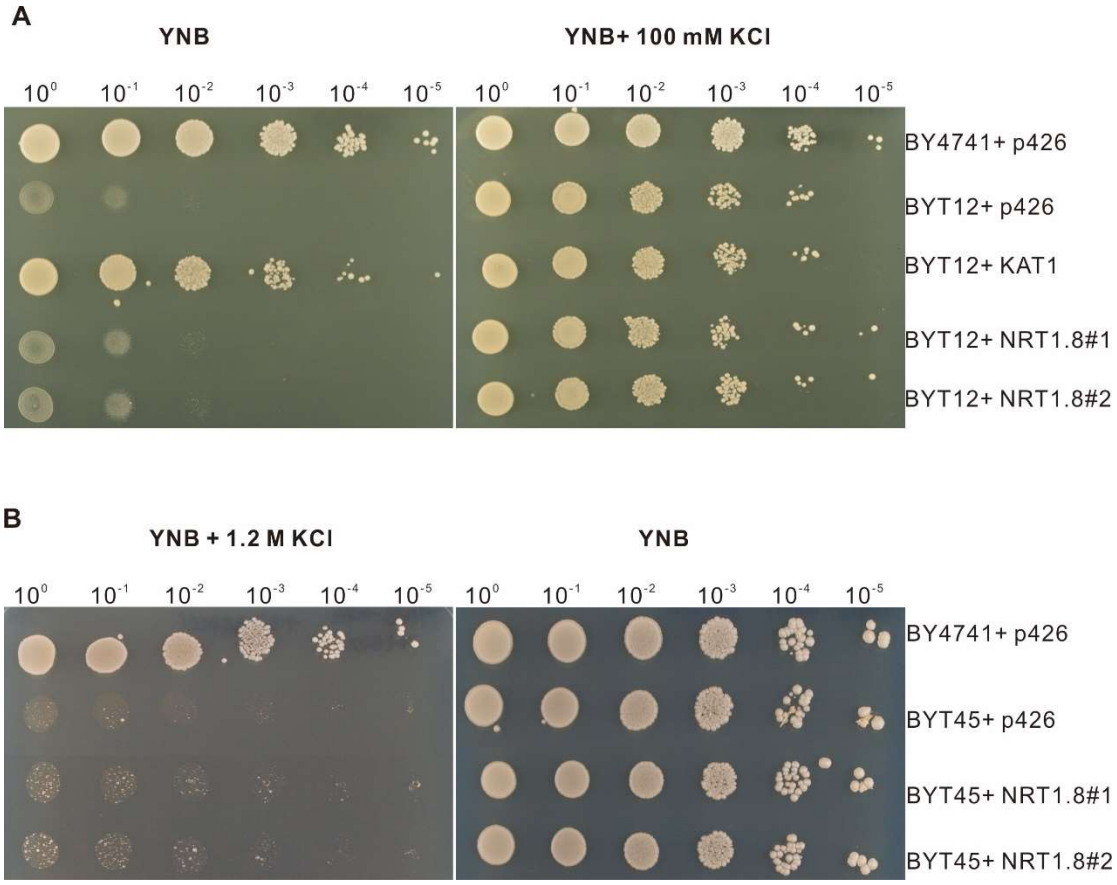

Figure 19. Potassium transport capacity analysis of NRT1.8 in *Saccharomyces cerevisiae*.

(A) Potassium uptake capacity of NRT1.8 was analyzed in yeast mutant BYT12 (*trk1*Δ *trk2*Δ) cells. **(B)** Potassium export capacity was analyzed in yeast mutant BYT45 (*ena1-5*Δ *nha1*Δ) cells. Wild type BY4741 and yeast mutant cells were transformed with the expression constructs indicated on the right. 20 µL cell suspensions (OD600 from 1.0 to 10^{-5}) were dropped on YNB (-Ura) agar plates or on YNB (-Ura) medium with 100 mM KCl or 1.2 M KCl as indicated on top of each figure. p426 is the empty vector. *NRT1.8* and *KAT1* are coding sequences of the respective *Arabidopsis* genes cloned in p426. 1 and 2 indicate two independent yeast transformants.

3.3.2 The expression of *NRT1.8* renders *Saccharomyces cerevisiae* cells more sensitive to cationic compounds

The high sequence similarity between NRT1.5 and NRT1.8, their opposite function in NO_3^- transport, as well as their opposite expression patterns under stress conditions make it interesting to test whether the expression of *NRT1.8* also affects the membrane potential like *NRT1.5* does in yeast cells. Compared to BYT12 cells with empty vector

p426, the expression of *NRT1.8* made BYT12 cells more sensitive to the cationic toxic compounds HygB (Figure 20A) and TEA (Figure 20B), indicating that the presence of *NRT1.8* increased the plasma membrane potential of yeast cells. Moreover, in comparison to BYT12 cells expressing *NRT1.5*, the expression of *NRT1.8* made BYT12 cells were more sensitive to HygB and TEA treatment (Figure 20A, 20B), which might indicate a stronger effect of NRT1.8 on the membrane potential of yeast cells.

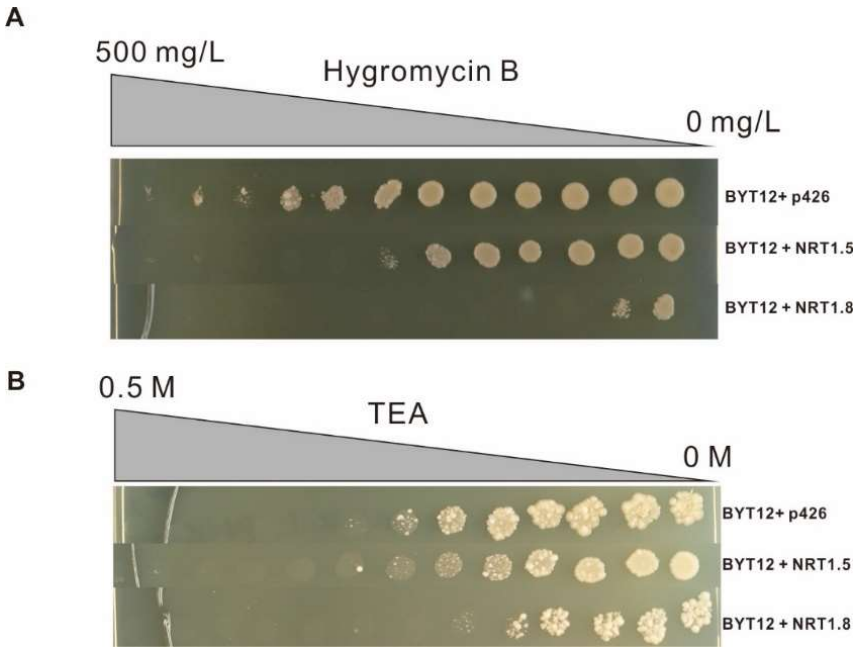

Figure 20. Cationic drug sensitivity test of *Saccharomyces cerevisiae* cells expressing *NRT1.8*. **(A)** Yeast growth test on YNB (-Ura) medium with increasing concentration of hygromycin B from 0 to 0.5 g/l. **(B)** Yeast growth test on YNB (-Ura) medium with increasing concentration of tetraethylammonium from 0 to 0.5 M. BY4741 and BYT12 cells were transformed with the expression constructs indicated on the right. Twelve 3 µL drops of each yeast cell suspension (OD_{600} = 1.0) were distributed on the plates. 100 mM KCl was supplemented to YNB medium to support the growth of BYT12 cells. p426 is the empty vector. *NRT1.5* and *NRT1.8* are coding sequences of the respective *Arabidopsis* genes cloned in p426.

3.4 The interplay of NRT1.5 and SKOR in potassium root-to-shoot transfer

The subsequent results presented in section 3.4.1, 3.4.2, 3.4.3, 3.4.4 and 3.4.5 have been published as part of the publication: Drechsler, N., Zheng, Y., Bohner, A., Nobmann, B., von Wirén, N., Kunze, R. and Rausch, C. (2015). Nitrate-dependent

control of shoot K homeostasis by the Nitrate Transporter1/Peptide Transporter Family Member NPF7.3/NRT1.5 and the stelar K^+ outward rectifier SKOR in *Arabidopsis*. Plant Physiology 169: 2832-2847.

3.4.1 Generation of the *nrt1.5-5/skor-2* double mutant

In *Arabidopsis*, SKOR is the most well-known protein responsible for K^+ translocation from root to shoot. At low NO_3^- supply, K concentration in shoots of hydroponically growing *nrt1.5* mutants was significantly reduced compared to that of wild type, indicating K^+ root-to-shoot transfer in *nrt1.5* was blocked (Drechsler *et al.* 2015). The reduction of K^+ in *nrt1.5* shoots resembles what has been observed for the *skor1* mutant (Gaymard *et al.* 1998). In this work, even though it was shown that NRT1.5 had no influence on the K^+ export activity of SKOR in yeast cells (Figure 16), this does not rigorously exclude such an activity in *planta*. To investigate the interplay between NRT1.5 and SKOR in root-to-shoot translocation of K^+ in *Arabidopsis*, two T-DNA insertion knockout mutants *skor-2* and s*kor-3* in the Col-0 background were isolated (Figure 21 A, 21B). Both *skor* mutants showed no morphological difference compared to Col-0 at low NO_3^- availability, however, they exhibited the leaf chlorosis phenotype at high NO_3^- supply (Figure 21C). *skor-2* knockout mutant plants, which carry the T-DNA insertion in the essential cyclic nucleotide binding domain (cNBD) (Dreyer *et al.* 2004) (Figure 21A), were crossed with *nrt1.5-5* plants to generate the double knockout mutant *skor-2/nrt1.5-5*. Absence of full-length transcripts of *NRT1.5* and *SKOR* in single and double mutant plants was verified by semi-quantitative RT-PCR (Figure 21B).

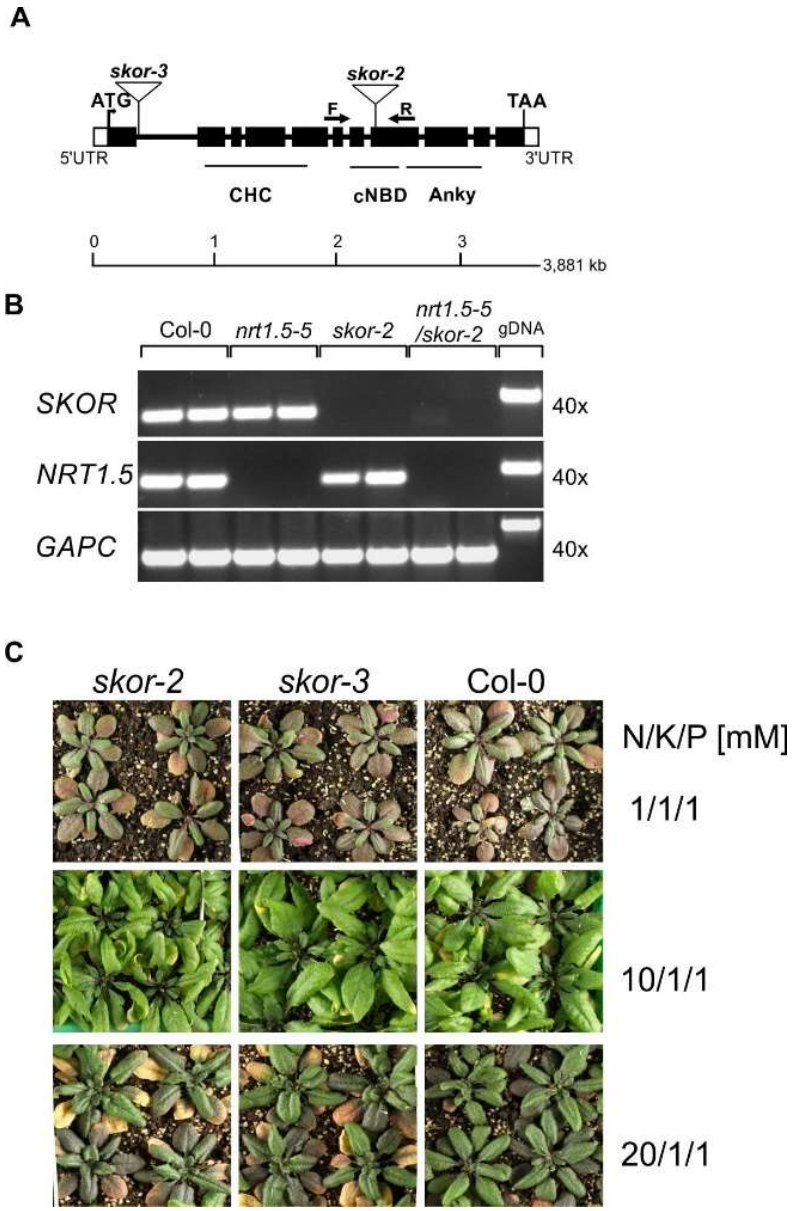

Figure 21. Identification and confirmation of the absence of full-length transcripts of *NRT1.5* and *SKOR* in the double mutant *nrt1.5-5/skor-2*.

(A) Scheme of T-DNA insertion sites in the *SKOR* genomic region of the *skor-2* and *skor-3*. The T-DNAs are inserted in the eighth and the second exon of the gene, respectively. CHC, channel hydrophobic core; cNBD, cyclic nucleotide-binding domain; Anky, ankyrin domain. Black and white boxes represent exons and untranslated regions (UTRs), respectively. The arrows indicate the annealing positions of the forward (F) and reverse (R) primers used for RT-PCR. **(B)** RT-PCR of single and the double mutant was performed with gene-specific primers for *SKOR* and *NRT1.5*. **(C)** Morphology of Col-0, *skor-2*, and *skor-3* grown on soil supplied with different NO_3^- regimes.

3.4.2 The leaf chlorosis phenotype of *nrt1.5* is caused by low potassium accumulation

To investigate how morphological changes of each plant line develop under various N/K regimes, Col-0, *nrt1.5-5*, *skor-2*, and *nrt1.5-5/skor-2* plants were cultivated on unfertilized soil supplemented with modified 1/2 MS solutions containing the macronutrients N/K/P in the concentrations 1/1/1, 1/1/10, 1/10/1, 10/1/1, 5/0/5 and 10/10/10 mM, respectively. N was supplied as NO_3^- and P was supplied in the form of Pi. When all plants were flowering, the inflorescence stems were removed and rosette FW, elemental composition and total N were determined (Figure 22).

In all plant lines including Col-0, early leaf chlorosis accompanied by yellow leaf tips and pale green inner rosettes occurred whenever the K concentration of plants dropped below 1% dry weight (DW) (Figure 22, red dotted line). Consequently, Ca and Mg in these rosettes were strongly accumulated probably to compensate the loss of K. When K concentration was higher than 1% DW, all plants were able to accumulate anthocyanins and developed a red-brown leaf pigmentation which presumably indicated N deficiency (Figure 22, treatments 1/1/1, 1/1/10, and 1/10/1 N/K/P [mM]). Under all tested nutrient regimes, compared to wild type plants, no significant reduction of total N in *nrt1.5-5* was detected. The results suggest that the observed leaf chlorosis phenotype of *nrt1.5-5* mutant was due to the low K concentration in shoots, which also corroborated our previous findings with hydroponically grown plants.

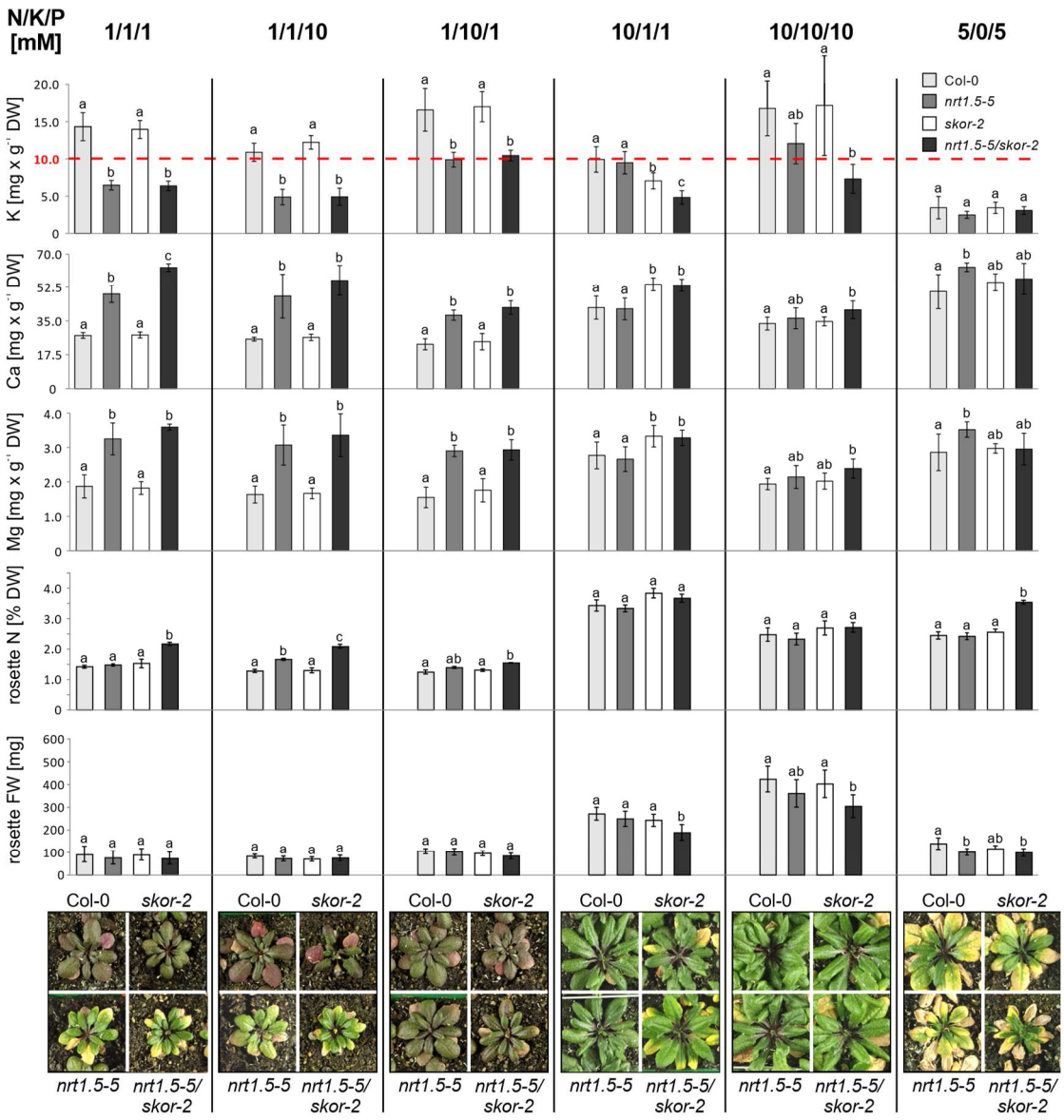

Figure 22. Correlation of the rosette phenotype with the K, Ca and Mg elemental composition in Col-0, *nrt1.5-5*, *skor-2* and *nrt1.5-5/skor-2* plants.

Each column shows on top the applied fertilization regime (N/K/P [mM]). The bar diagrams show the rosette K, Ca, Mg, total N and fresh weight gain, respectively. At the bottom the respective phenotypes of the plants are shown. The color codes of the bars are indicated in the top right corner. The dotted red line indicates a K concentration of 1% in the dry matter. The data were statistically analyzed by one-way ANOVA and subsequent multiple comparisons (Tukey's honestly significant difference mean-separation test). Means ($n \geq 4$) marked with different letters differ significantly at $P < 0.05$. Vertical bars denote standard deviations. The experiment was performed three times independently with similar phenotypic growth responses. The elemental analysis by ICP-OES was performed for two of the three independent experiments with similar results.

3.4.3 NRT1.5 affects shoot potassium accumulation at limited nitrate supply

At 1 mM NO_3^-, total N concentration in shoots of all plant lines was less than 2.5% (Figure 22), which reflected the low amount of NO_3^- supplied to the plants. Total N in *nrt1.5-5/skor-2* mutant plants was higher than that of the wild type and single mutants. FW analysis further reflected the importance of NO_3^- supply on plant growth, since the FW gain of all lines was below 110 mg under 1 mM NO_3^- supply, which was 2- to 3-fold less than plants growing with 10 mM NO_3^- supply (Figure 22).

The K concentration in *skor-2* was almost not altered compared to wild type at 1 mM NO_3^-, whereas, K concentrations in *nrt1.5-5* and the double mutant *nrt1.5-5/skor-2* plants were reduced to approximately 50% of wild-type level (Figure 22, treatments 1/1/1 and 1/1/10 N/K/P [mM]). Even the supply with high amount of K^+ (10 mM) could not revert the K concentration in *nrt1.5-5* and *nrt1.5-5/skor-2* plans back to wild-type level (Figure 22, treatment 1/10/1 N/K/P [mM]). Obviously, the results indicate that in comparison to SKOR, NRT1.5 made a more important contribution to the shoot K^+ concentration when NO_3^- supply is limited, regardless of the K^+ supply.

3.4.4 SKOR contributes to root-to-shoot transfer of potassium at high nitrate supply

At 10 mM NO_3^- fertilization (10/1/1 N/K/P [mM]), the *nrt1.5-5* mutant accumulated the comparable K concentration as wild-type plants (Figure 22), indicating that NRT1.5 was not primarily involved in establishing shoot K status under high NO_3^- conditions. However, at this condition, *skor-2* plants had a significantly lower K concentration compared with Col-0 and *nrt1.5-5*. Ca and Mg were not enriched, presumably because the K concentration had not dropped below 1% DW. Lack of both NRT1.5 and SKOR decreased K levels in *nrt1.5-5/skor-2* even further (Figure 22). These results were confirmed by a further experiment where a 20-fold excess of NO_3^- over K^+ (20/1/1 N/K/P [mM]) was supplied to plants. The *skor-2* and *nrt1.5-5/skor-2* plants

demonstrated the leaf chlorosis at this nutrient regime (Figure 23A). Correlatedly, the reduction in shoot K concentration was observed in *skor-2* and in *nrt1.5-5/skor-2* plants, but K concentration in *nrt1.5-5* was not affected (Figure 23A). Under a high equimolar N/K supply (10/10/10 and 10/10/1 N/K/P [mM]), K levels of both single mutants reached almost those of Col-0 (Figure 22, 23B). However, K concentrations in the *nrt1.5-5/skor-2* double mutant were still significantly reduced in comparison to Col-0 (Figure 22), which was probably attributed to the additive effect of loss of both genes.

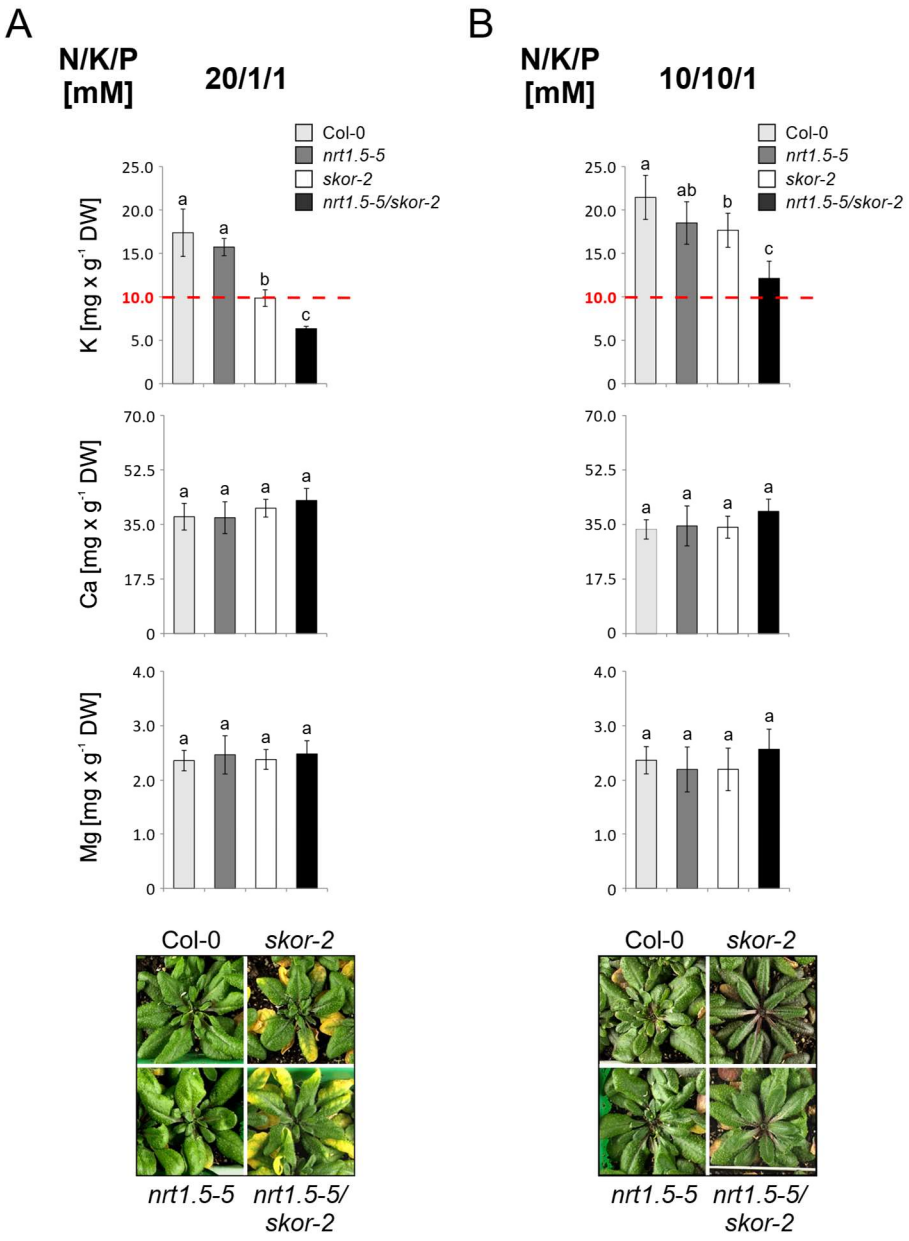

Figure 23. Rosette phenotype and K, Ca and Mg concentrations in Col-0, *nrt1.5-5*, *skor-2* and *nrt1.5-5/skor-2* plants at 20/1/1 and 10/10/1 N/K/P [mM] supply.

(A) K, Ca and Mg concentrations and morphology of Col-0, *nrt1.5-5*, *skor-2* and *nrt1.5-5/skor-2* rosettes at the fertilization with 20/1/1 N/K/P [mM]. **(B)** K, Ca and Mg concentrations and morphology of Col-0, *nrt1.5-5*, *skor-2* and *nrt1.5-5/skor-2* rosettes at the fertilization with 10/10/1 N/K/P [mM]. The color codes of the bars are indicated in the top right corner. The dotted red line indicates a K concentration of 1% in the dry matter. Statistical analysis of the data was performed by one-way ANOVA and subsequent multiple comparisons (Tukey's HSD test). Means ($n \geq 6$) marked with different letters differed significantly at $P < 0.05$. Vertical bars denote standard deviations.

In summary, this fertilization experiment highlighted the importance of both proteins for shoot K^+ homeostasis under defined nutritional supply: SKOR under high NO_3^- and low K^+ availability; and NRT1.5 under low NO_3^- availability irrespective of the K^+ supply. Enhancement of K deficiency in the double mutant under a high NO_3^- to K^+ ratio (10/1/1 and 20/1/1 N/K/P [mM]) and a high equimolar supply (10/10/10 N/K/P and 10/10/1 N/K/P [mM]) further suggests an interdependency of NRT1.5 and SKOR in K^+ root-to-shoot translocation under these conditions.

3.4.5 The induction of *SKOR* expression by high nitrate supply

To investigate whether the expression pattern of *SKOR* and *NRT1.5* is in accordance with the phenotype development of mutants, transcripts of *SKOR* and *NRT1.5* in roots of wild-type plants grown under various N/K regimes (1/1, 10/1, 1/10, and 10/10 N/K [mM], constant 1 mM Pi supply) were analysed by qRT-PCR. The expression of *NRT1.5* was relatively constant and was only slightly regulated by different N/K ratios (Figure 24). Relative to equimolar supply 1/1 N/K [mM], *NRT1.5* was 1.5-fold upregulated by high NO_3^- to K^+ ratio (10/1 N/K [mM]), and 1.5-fold down-regulated by low NO_3^- to K^+ ratio (1/10 N/K [mM]). In contrast to *NRT1.5*, *SKOR* was nearly not regulated by the NO_3^- to K^+ ratio, whereas it was strongly upregulated (about 5-fold) by high NO_3^- supply (10/1 and 10/10 N/K [mM]) compared to its level at 1/1 N/K [mM] (Figure 24).

The expression patterns of the two genes could partially explain the phenotypes of mutant plants. Under low NO_3^- supply (1 mM), the expression of *NRT1.5* was almost constant, whereas the expression of *SKOR* is 5-fold lower than under high NO_3^- supply.

Consistently, when grown with 1 mM NO_3^-, *nrt1.5-5* but not *skor-2* mutant plants had reduced K levels in the shoots (Figure 22). In contrast, under high NO_3^- supply (10 mM), *SKOR* is strongly expressed in roots. It is conceivable that, under high NO_3^- supply (10 mM), enhanced level SKOR can partially complement the lack of NRT1.5 in the *nrt1.5* mutants and facilitate root-to-shoot translocation of K^+, therefore, no significant K reduction occurred in *nrt1.5* shoots, but *skor-2* and *nrt1.5-5/skor-2* mutant had decreased K level (Figure 22, 23). However, the expression patterns of *NRT1.5* and *SKOR* by N/K regimes cannot explain all the physiological changes of mutants, thus it is possible that deregulation of other ion homeostasis-associated genes in *nrt1.5-5* roots (Drechsler *et al.* 2015) might also contribute to the K reduction phenotypes.

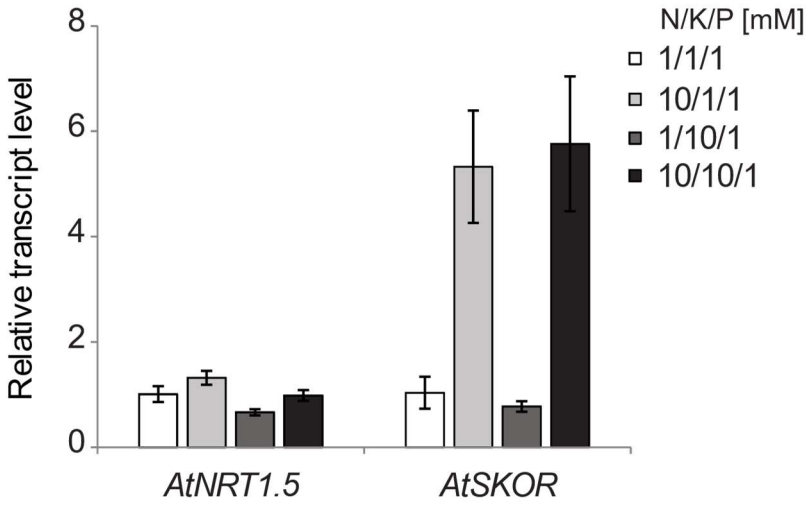

Figure 24. Expression of *NRT1.5* and *SKOR* under different fertilization regimes.

Relative transcript levels ($2^{-\Delta\Delta C_T}$) of *NRT1.5* and *SKOR* at various N/K regimes were measured in roots of Col-0 plants by qRT-PCR (means ± SD; n ≥ 4). *UBQ10* was used for normalization. Transcript levels of *NRT1.5* and *SKOR* in roots grown with 1/1/1 N/K/P [mM] were set to 1.0 as a control.

3.4.6 Ion homeostasis-associated genes deregulated in *nrt1.5-5* were not altered in *skor-2*

It has been shown that gene expression levels of several ion homeostasis-associated

genes including *SLAH1*, *SLAH3*, *NRT1.8*, *HAK5*, *CIPK9* and *SKOR* were altered in *nrt1.5-5* roots (Drechsler *et al.* 2015), which might contribute to the K deficiency in *nrt1.5-5* shoots. In this work, *skor-2* had reduced shoot K level at high NO_3^- supply (Figure 22, 23). Gaymard *et al.* (1998) also reported the reduction of shoot K in the *skor*-1 mutant which is in Wassilewskija background. To investigate whether the similar K reduction phenotype of *nrt1.5-5* and *skor-2* mutants is caused by the same molecular mechanism, expression patterns of those genes deregulated in *nrt1.5-5* were analyzed in roots of the single mutant *nrt1.5-5*, *skor-2* and in the double mutant *nrt1.5-5/skor-2* under various N/K regimes by qRT-PCR.

Anion transporter genes *SLAH1*, *SLAH3* and the potassium channel *SKOR* were upregulated in *nrt1.5-5* compared to Col-0 under low NO_3^- (1 mM) supply, which is consistent with earlier findings of our group which used hydroponically grown plant materials with 0.1 mM NO_3^- supply (Drechsler *et al.* 2015). Interestingly, when 10 mM NO_3^- was supplied, *SLAH1* and *SLAH3* expression in *nrt1.5-5* was indistinguishable to that of Col-0 (Figure 25A). This result indicates that *SLAH1* and *SLAH3* might contribute to the shoot K deficit phenotype of *nrt1.5-5* at low NO_3^- supply. Unlike the expression pattern in hydroponically grown plants with 0.1 mM NO_3^- supply, *CIPK9* was not downregulated in *nrt1.5-5* at all N/K regimes, and the downregulation of *HAK5* only occurred at 10/1 N/K [mM] supply (Figure 25A). Those discrepancies might be attributed to the differences in growth conditions and compositions of fertilization solution. In contrast to what was observed in *nrt1.5-5*, none of the tested ion homeostasis-associated genes were regulated in *skor-2* mutant plants, even at 10 mM NO_3^- supply when *skor-2* plants developed K deficit symptoms (Figure 25B). The differences of gene expression pattern in *nrt1.5-5* and *skor-2* suggest that the involvement of NRT1.5 in the K^+ root-to-shoot transfer process was independent of the function of SKOR, and the deregulation of those K^+ transporter or K^+ signaling related genes might contribute to the development of the K deficit phenotype in *nrt1.5* mutants.

Interestingly, the expression patterns of those ion homeostasis-associated genes in the *nrt1.5-5/skor-2* double mutant more resembled those in *nrt1.5-5* than in *skor-2*

(Figure 25C). However, compared to low NO_3^- supply, at high NO_3^- and low K^+ availability (10/1, N/K [mM]), *SLAH1* and *SLAH3* expression was induced around 5-fold in the double mutant (Figure 25C), which was neither observed in *nrt1.5-5* nor in *skor-2* mutant. At high NO_3^- and high K^+ supply (10/10, N/K [mM]), *HAK5* expression was strongly inhibited in the *nrt1.5-5/skor-2* double mutant. Based on the observed additive effect of K reduction in shoots of the double mutant at this nutrient condition (Figure 22, 23B), it could be speculated that the altered expression patterns of *SLAH1*, *SLAH3* and *HAK5* in the double mutant may contribute to the enhanced K deficit phenotype of the double mutant under high NO_3^- and high K^+ availability.

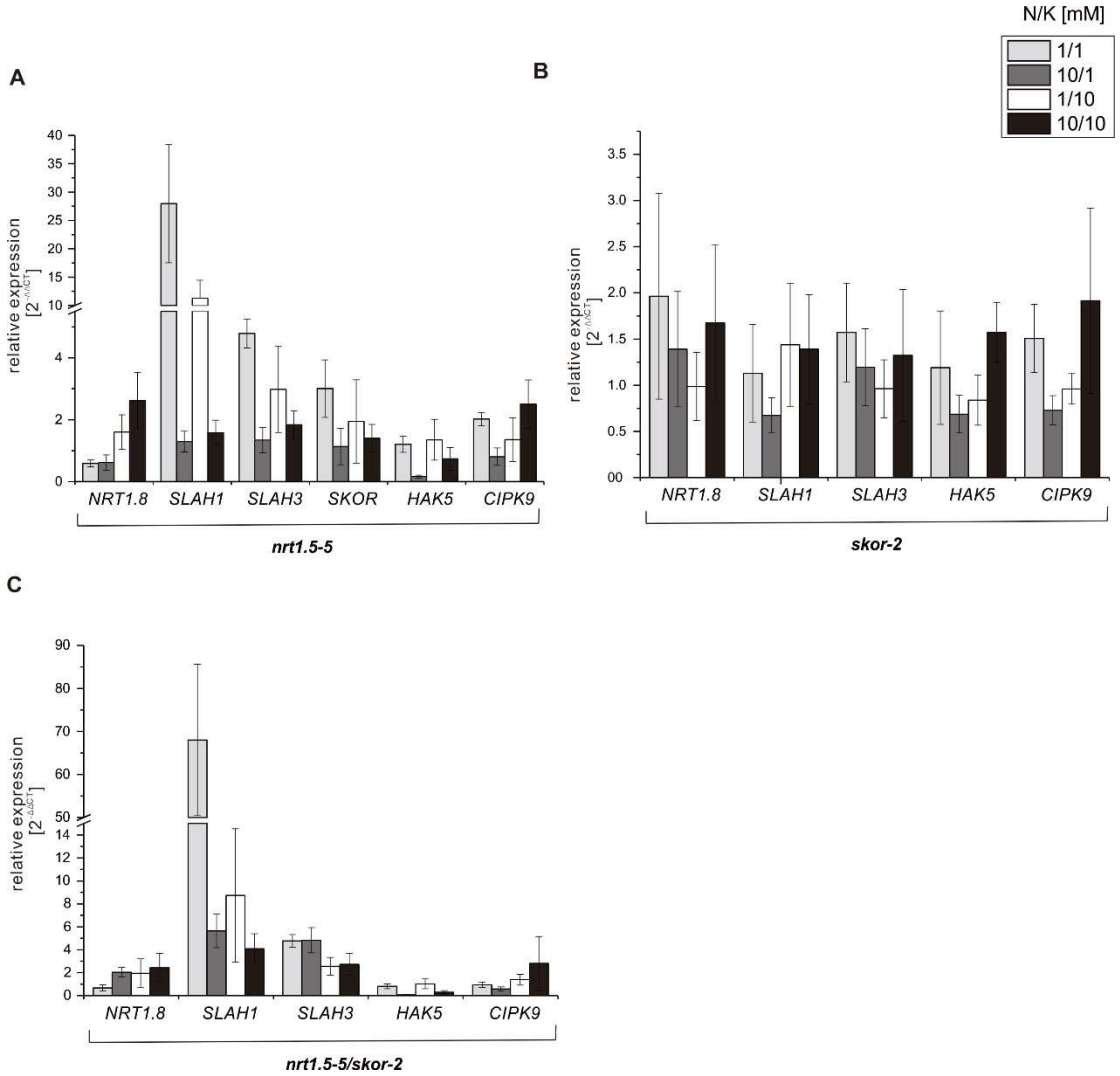

Figure 25. Expression of nitrate and potassium homeostasis-associated genes in roots of *nrt1.5-5*, *skor-2* and *nrt1.5-5/skor-2* under various fertilization regimes.

Relative transcript levels of six nitrate and potassium homeostasis-associated genes were

measured by qRT-PCR and normalized to *UBQ10* in roots of **(A)** *nrt1.5-5,* **(B)** *skor-2* and **(C)** *nrt1.5-5/skor-2* at indicated N/K regimes. Plants were grown on unfertilized soil supplied with modified 1/2 MS solution with 1/1, 10/1, 1/10 or 10/10 NO_3^-/K^+ [mM]. Plotted are the relative gene expression ($2^{-\Delta\Delta C_T}$) of each gene in mutant roots compared with Col-0 level (set as 1.0) at indicated fertilization regimes (means ± SD, n ≥ 4). Root materials from three plants were pooled as one biological replicate.

3.4.7 The *nrt1.5-5/skor-2* double mutant accumulated more sodium, sulfur and phosphorus at low nitrate supply

In addition to K, Ca and Mg concentration, sodium (Na) and macroelements sulfur (S), phosphorus (P) as well as microelements iron (Fe), boron (B), manganese (Mn), copper (Cu) and zinc (Zn) were also measured in Col-0, single mutants *nrt1.5-5* and *skor-2*, and the double mutant *nrt1.5-5/skor-2* by ICP-OES with the same shoot materials used for Figure 22. All four plant lines accumulated comparable concentration of microelements (data not shown). Mutation of *NRT1.5* did not significantly influence P and S accumulation in *nrt1.5-5* at all nutrient regimes (Figure 26). Under some conditions (1/10/1, 10/1/1 and 5/0/5 N/K/P [mM]), *nrt1.5-5* showed significantly higher concentration of Na compared to wild type (Figure 26). The *skor-2* mutant plants showed higher S concentration only at 10 mM NO_3^- supply. Interestingly, at most nutrient regimes, Na, P and S concentrations in the *nrt1.5-5/skor-2* double mutant plants were higher compared to other lines (Figure 26). These results suggested that a simultaneous defect in both *NRT1.5* and *SKOR* probably has a great influence on the specific or unspecific root-to-shoot transport of macroelements P and S as well as Na. In addition, the higher accumulation of Na could result in a high Na^+/K^+ ratio in the *nrt1.5-5/skor-2* double mutant, which may in turn cause the susceptibility to salinity stress of the double mutant.

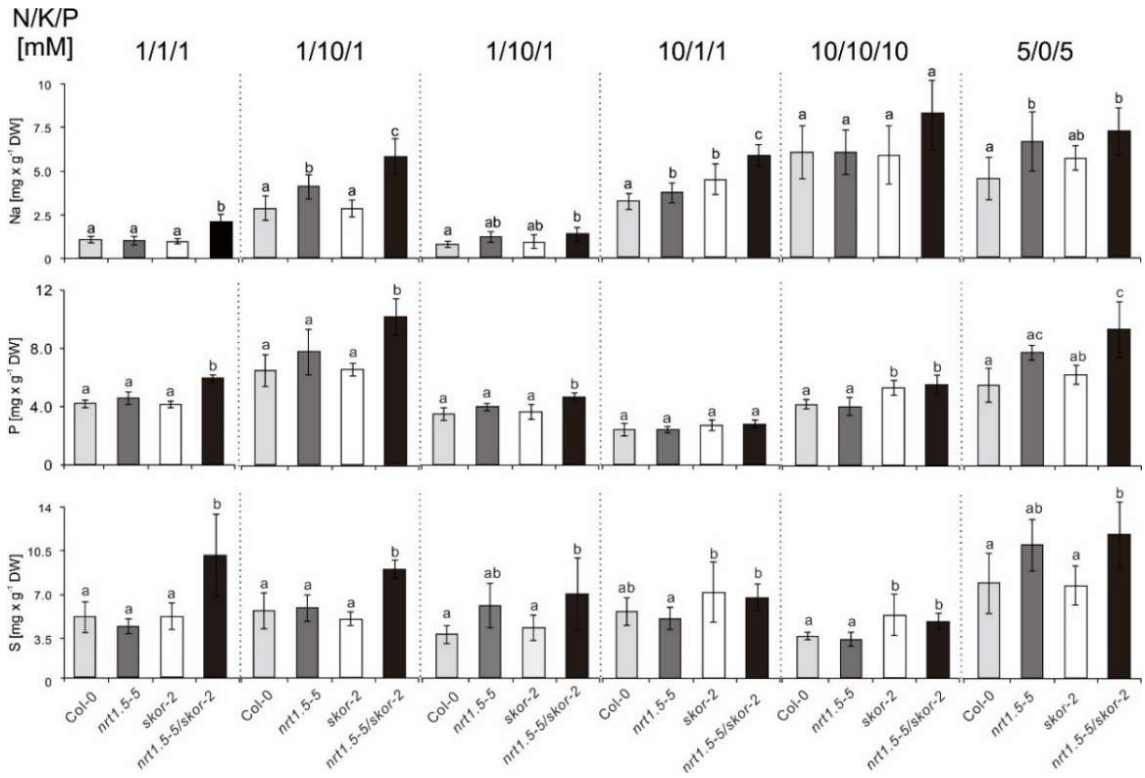

Figure 26. Concentration of sodium, phosphorus and sulfur in rosettes of Col-0, *skor-2*, *nrt1.5-5* and the double mutant.

Concentration [mg/g DW] of Na, P and S in the rosette were measured with the same material used in Figure 22. Data were shown as means ± SD (n ≥ 4). Different letters indicate significant difference at $P < 0.05$. The data were statistically analyzed by one-way ANOVA and subsequent multiple comparisons (Tukey's HSD test) for each fertilization treatment.

3.4.8 The *skor* mutants showed no root phenotype at K^+ deprivation

In the previous section (see 3.1.2), the reduced LR density phenotype of *nrt1.5* plants growing at K^+ deprivation conditions has been shown. In order to investigate whether this root phenotype of *nrt1.5* mutants is caused by the defect in K^+ xylem loading, *skor-2* and *skor-3* were also grown under various K^+ concentrations from 0 mM to 2 mM. Different from *nrt1.5* mutants, *skor-2* and *skor-3* mutant plants demonstrated comparable growth as wild-type plants at all tested K^+ concentrations. Even at 0 mM K^+ concentration, neither *skor-2* nor *skor-3* showed impaired shoot or root growth (Figure 27A), and the fresh weight gain of *skor-2* and *skor-3* was even higher than that of wild type (Figure 27B).

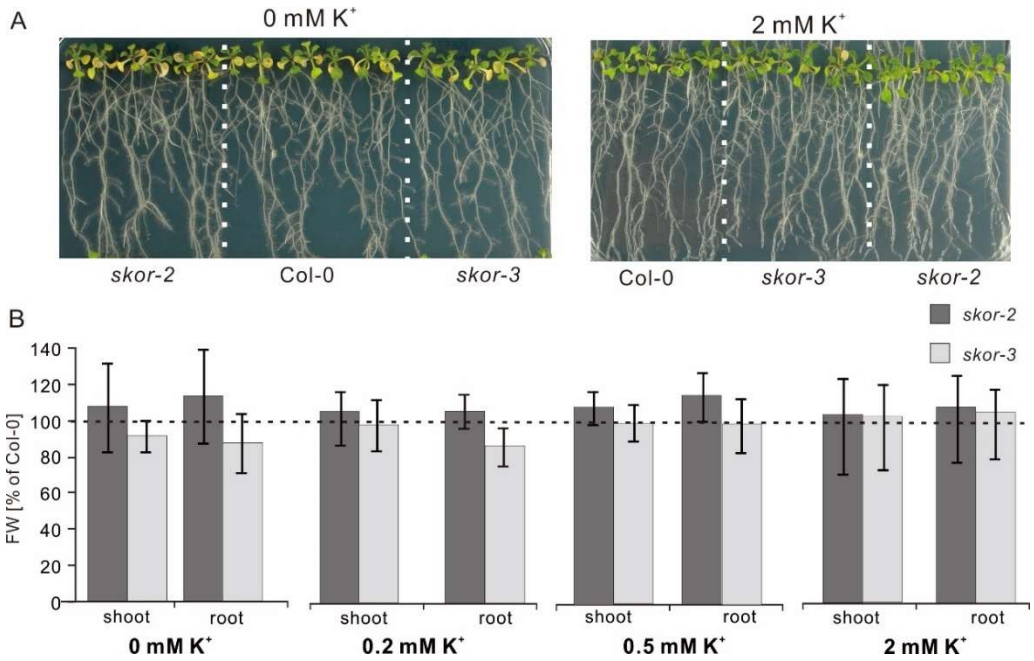

Figure 27. Potassium deficiency does not cause visible phenotype of *skor* mutants.

(A) Morphology of Col-0, *skor-2* and *skor-3* mutant seedlings growing on plates 0 mM or 2 mM K^+ (constant 1 mM NO_3^-). **(B)** Shoot and root fresh weight of *skor-2* and *skor-3* seedlings grown on plates containing increasing concentrations of K^+ from 0 to 2 mM (constant 1 mM NO_3^-). Four seedlings were pooled as one biological replicate. Results are displayed as relative to Col-0 FW (means ± SD; n = 12).

The *nrt1.5-5* and the double mutant *nrt1.5-5/skor-2* plants showed impaired LR growth (Figure 28A) and gained less fresh weight (Figure 28B) grown on plates with 0 mM K^+, in contrast, no visible morphological differences of *skor-2* compared to wild type were observed. These results demonstrated that the defect in SKOR function does not lead to the impairment of the root growth under K^+ deprivation conditions.

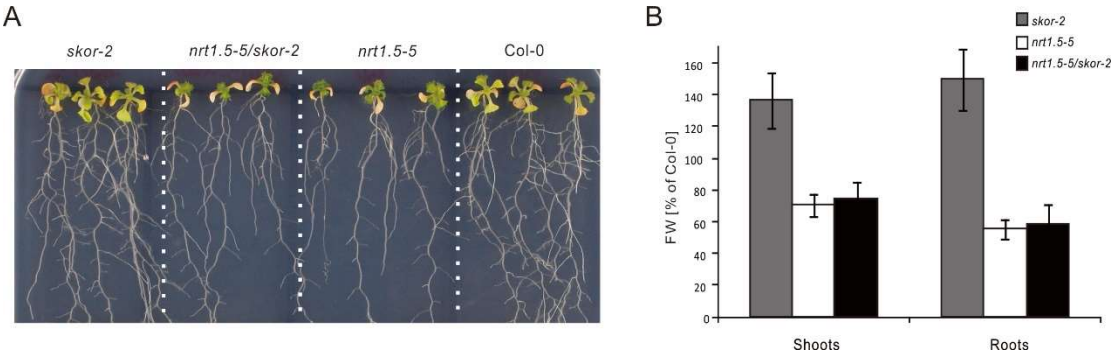

Figure 28. The root development of *skor-2* and *nrt1.5-5/skor-2* mutant under potassium deficiency.

(A) Morphology of Col-0, *skor-2, nrt1.5-5* and the double mutant *nrt1.5-5/skor-2* seedlings growing on plates 0 mM K^+ (1 mM NO_3^-). **(B)** Shoot and root fresh weight of Col-0, *skor-2* and *nrt1.5-5*/*skor-2* seedlings grown on plates containing 0 mM K^+ (constant 1 mM NO_3^-). Four seedlings were pooled as one biological replicates. Results were displayed as relative to the Col-0 FW (means ± SD; n = 12).

3.5 Identification of interacting partners of NRT1.5

3.5.1 Verification of NRT1.5-interacting partners by Bimolecular Fluorescence Complementation (BiFC)

In the previous study of our group, several interacting partners of NRT1.5 have been identified in *S. cerevisiae* by a split-ubiquitin assay (Drechsler, Dissertation 2016). To assess whether the protein-protein interaction observed in heterologous yeast cells also occur in living plant cells, the Bimolecular Fluorescence Complementation (BiFC) assay was applied in this study. NRT1.5 was fused to C-terminus of cYFP, and the potential NRT1.5-interacting partner SLAH1, SLAH3 or AHA2 was fused to the C-terminus of nYFP in the pBiFC-2in1 system (pBiFCt-2in1-NN) (Grefen and Blatt 2012) by Gateway® cloning, respectively (Figure 29E). Meanwhile, the pBiFCt-2in1-NN construct with unfused nYFP and NRT1.5-fused cYFP was also generated as a negative control. The generated pBiFCt-2in1-NN constructs were transformed into *A. tumefaciens* for transient verification expression in *Nicotiana benthamiana.* Three days post infection (dpi), fluorescence signals from lower leaf epidermal cells of transfected *N. benthamiana* were recorded by confocal fluorescence microscopy.

The RFP signal denotes the successful transformation and expression of the pBiFC-2in1 construct in tobacco leaves (Figure 29, the left panel). Without interacting partners, coexpression of cYFP-NRT1.5 with unfused nYFP did not lead to visible reconstituted YFP fluorescence signals (Figure 29A). By contrast, under the same setting of the microscope, coexpression of cYFP-NRT1.5 with its potential interacting partners nYFP-AHA2, nYFP-SLAH1 and nYFP-SLAH3 generated reconstituted YFP fluorescence signals which can be clearly attributed to localization in the plasma

membrane (Figure 29B, 29C, 29D). The localization of YFP signal matches the membrane localization of NRT1.5, SLAH1, SLAH3 and AHA2. These results demonstrate that NRT1.5 can interact with AHA2, SLAH1 and SLAH3 in tobacco leaves, which could further corroborate the assumption that NRT1.5 interacts with these three proteins in *Arabidopsis*.

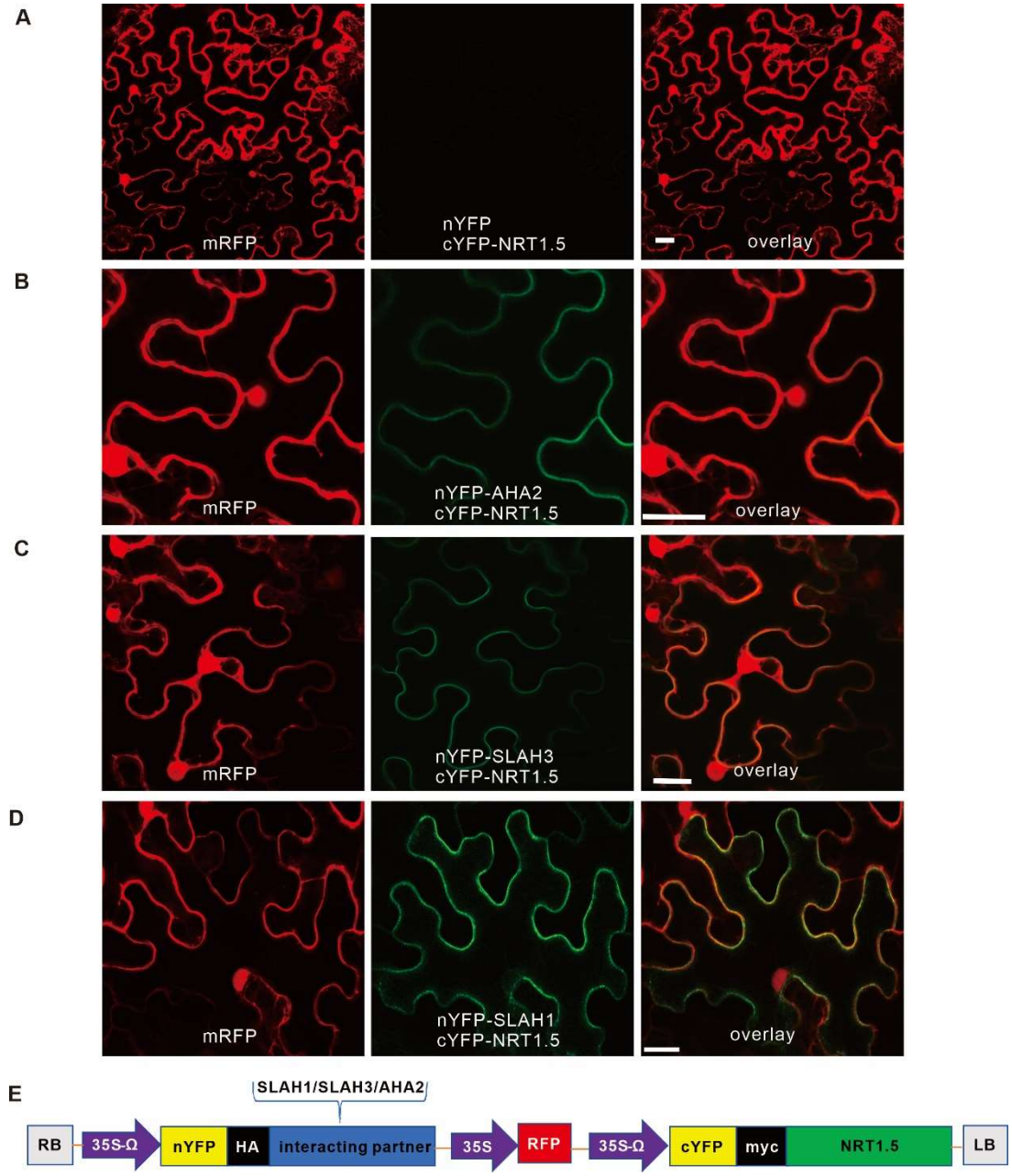

Figure 29. Verification of interacting partners of NRT1.5 by BiFC assay (pBiFC-2in1) in leaf epidermis cells of *Nicotiana benthamiana*.

Confocal microscope images of *N. benthamiana*. leaf epidermis cells expressing cYFP-NRT1.5 and **(A)** non-fused nYFP; **(B)** nYFP-AHA2; **(C)** nYFP-SLAH3; **(D)** nYFP-SLAH1 at 3 dpi. Left

panels: mRFP fluorescence signals visualizing the cytoplasm and the lumen of the nucleus. Center panels: YFP fluorescence signals of the indicated coexpressed fusion proteins containing the two YFP moieties (nYFP and cYFP). Right panels: superimposed YFP and mRFP signals. Scare bar = 25 µM. The two YFP moieties and mRFP for each assay were encoded on the same vector to ensure synchronized expression and equimolar protein levels. **(E)** Schematic depiction of the T-DNA of the pBiFCt-2in1-NN vector containing NRT1.5 and different interacting partners. RB/LB: right/left border of T-DNA. 35S-Ω: 35S promoter linked to an enhancer. RFP: mRFP marker. nYFP and cYFP are two YFP moieties.

However, even though BiFC has become a routine tool to identify interactions between proteins, it has been noticed that some available BiFC systems are still subject to problems like low signal-to-noise ratios (Lalonde *et al.* 2008; Kodama and Hu 2012). Therefore, to exclude possible false positive result generated by the pBiFC-2in1 system, a second BiFC system called pDOE (pDOE-08) was applied. Different from using YFP split at residue 155 in the pBiFC-2in1 system, the pDOE system uses monomeric Venus (mVenus) split at residue 210 to reduce the background signal from non-specific reassembly (Gookin and Assmann 2014). Interaction between NRT1.5 and SLAH1 was examined again by using construct pDOE-08. In addition, the glucosinolate transporter GTR2 (also known as NRT1.10, hereafter NRT1.10), which probably inhibits the nitrate transport activity of NRT1.5 in oocyte cells (Wang, Dissertation 2011), was shown to interact with NRT1.5 in yeast by the split-ubiquitin assay (Drechsler, Dissertation 2016). Therefore, NRT1.10 was also included in the BiFC study. NRT1.5 was fused to the C-terminus of NmVen210 (N-terminal moiety of mVen210), and potential interacting partner SLAH1 or NRT1.10 was fused to the C-terminus of CVen210 (C-terminal moiety of mVen210) by conventional cloning, respectively (Figure 30D). The pDOE-08 plasmid with NRT1.5-fused NmVen210 and unfused CVen210 was generated as a negative control.

The signal of the Golgi marker mTurquoise2 indicates the successful infiltration and expression of the constructs in tobacco leaves (Figure 30, left panels). Co-expression of NmVen210-NRT1.5 and unfused CVen210 lead to only background noise and no visible reconstituted YFP signal could be observed (Figure 30A). In contrast, coexpression of NmVen210-NRT1.5 with CVen210-SLAH1 led to clear YFP signals

localized on the plasma membrane (Figure 30B). Coexpression of NmVen210-NRT1.5 with CVen210-NRT1.10 generated even stronger YFP signals which can be clearly attributed to the localization on the plasma membrane (Figure 30C). The reconstituted YFP signals corroborated the interaction between NRT1.5 and SLAH1 *in planta* and suggests that NRT1.5 also interacts with NRT1.10 *in planta*.

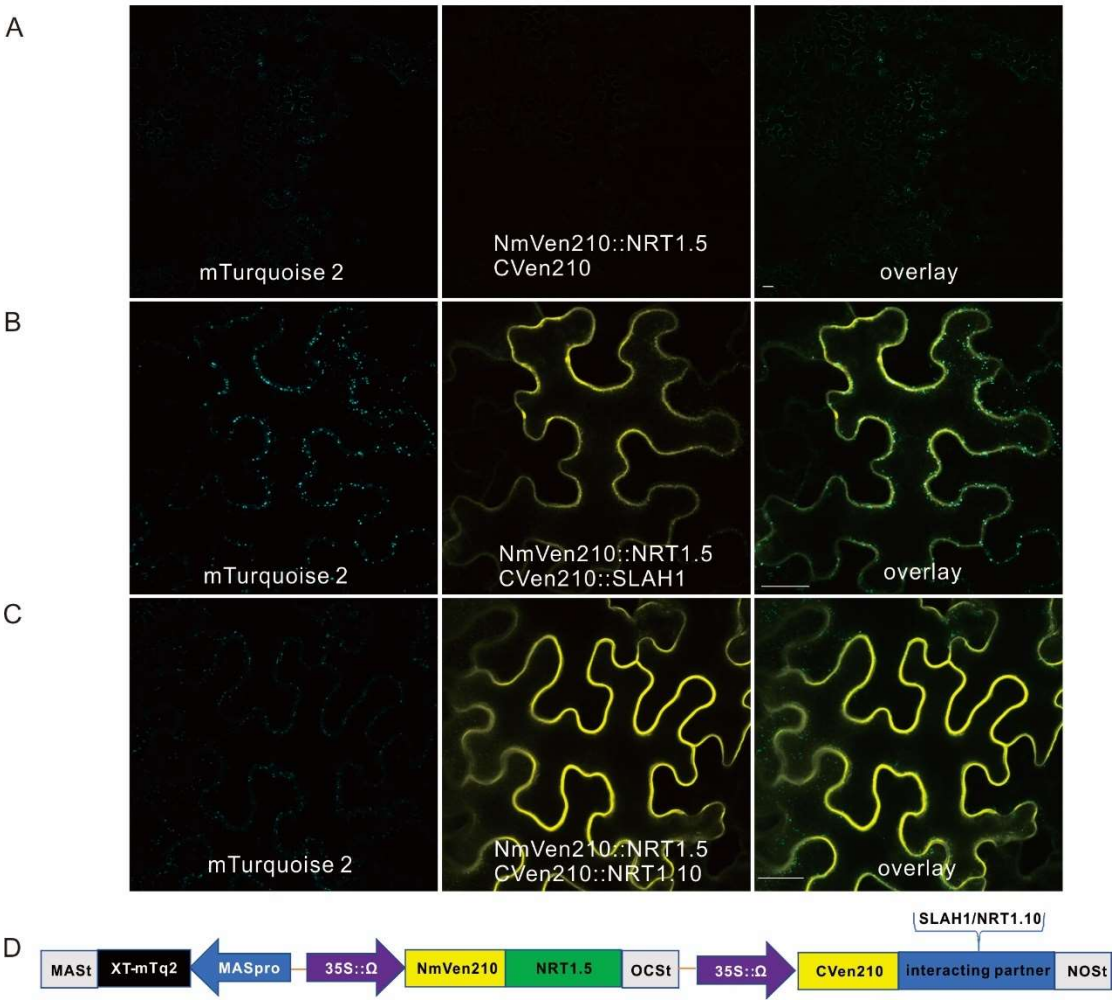

Figure 30. Verification of interacting partners by BiFC assay (pDOE-08) in leaf epidermis cells of *Nicotiana benthamiana*.

Confocal microscope images of *N. benthamiana*. leaf epidermis cells expressing NmVen210-NRT1.5 and **(A)** non-fused cVen210; **(B)** cVen210-SLAH1; **(C)** cVen210-NRT1.10 at 3 dpi. Left panels: mTurquoise2 fluorescence signals visualizing the Golgi. Center panels: fluorescence signals of the indicated coexpressed fusion proteins containing the two mVen210 moieties (NmVen210 and CVen210). Right panels: superimposed mTurquoise2 and mVen210 signals. Scare bar = 25 µM. **(D)** Schematic depiction of the construct pDOE-08 containing NRT1.5 and different interacting partners. MASp: MAS promoter. MASt: MAS terminator. NOSt: NOS

terminator. OCSt: OCS terminator. XT-mTq2: XT-Golgi-mTurquoise2 marker. 35S::Ω: 35S promoter linked to an enhancer. NmVen210 and cVen210 are two mVen210 moieties.

3.5.2 NRT1.5 interacts with CIPK23-CBL1/CBL9 complex in *Saccharomyces cerevisiae*

Recently, more and more studies indicate that CIPK23 may act as a common component controlling K^+ and NO_3^- transport through phosphorylating transporter proteins with the help of CBLs (Xu *et al.* 2006; Ho *et al.* 2009; Ragel *et al.* 2015). For example, CIPK23 has been shown to be able to activate nitrate transporter NRT1.1 and potassium transporter AKT1 and HAK5 (see introduction 1.6.2). Therefore, it is tempting to test whether NRT1.5 can also interact with CIPK23 directly or with the co-presence of CBLs by the split-ubiquitin assay in yeast. The full-length CDS of *CIPK23* was fused with the mutated N-terminal ubiquitin moiety Nub_G. The full-length CDS of *CBL1* and *CBL9* was cloned into yeast expression vector p14156. Subsequently, together with the construct NRT1.5-Cub (Drechsler, Dissertation 2016) in which NRT1.5 was fused to the C-terminal ubiquitin moiety Cub, the constructs were transformed in the auxotrophic (-Leu, -Trp, -His, -Ade, -Ura) *S. cerevisiae* strain THY.AP4 (Obrdlik *et al.* 2004). The N-terminal wild-type half of ubiquitin Nub_I, Nub_G-fused DUF679 Membrane Protein (DMP) Nub_G-DMP2 and Nub_G-DMP7 served as positive controls. Nub_G fused unrelated inward K^+ rectifying channel protein Nub_G-KAT1 and potato sucrose transporter Nub_G-StSUT1 served as negative controls. Yeast cells transformed with NRT1.5-Cub and positive control constructs showed growth on SD-deficient medium (-His, -Ade, -Leu, -Trp), whereas no growth of negative controls was detectable (Figure 31A). Coexpression of NRT1.5-Cub and Nub_G-CIPK23 led to the very weak yeast growth, which might indicate NRT1.5 could directly interact with CIPK23 (Figure 31A). The weak interaction could be explained by the fact that without CBLs, CIPKs *in vitro* have very little kinase activity (Li *et al.* 2009). In the presence of CBL9 or CBL1 especially, coexpression of NRT1.5-Cub and Nub_G-CIPK23 led to improved yeast growth compared to yeast cells without CBLs (Figure 31B). The results suggest that with the help of CBL1 and CBL9, NRT1.5 could interact with CIPK23 in

the yeast system.

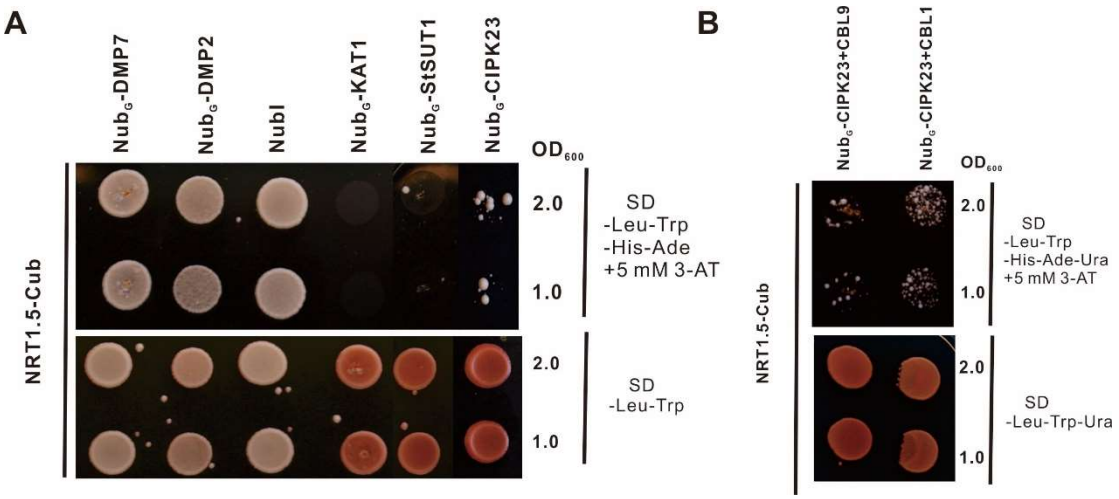

Figure 31. The interaction between NRT1.5 and CIPK23 with the help of CBLs in heterologous *Saccharomyces cerevisiae* system.

The interaction between NRT1.5 and CIPK23 were investigated either without **(A)** or with **(B)** the presence of CBL1 and CBL9. Nub_I, and Nub_G fused integral membrane proteins (DUF679 Membrane Protein) Nub_G-DMP2 and Nub_G-DMP7 were positive controls. Nub_G fused unrelated membrane proteins Nub_G-AtKAT1 (potassium transporter) and Nub_G-StSUT1 (potato sucrose transporter) were negative controls. For the selection of transformants, yeast cells were dropped on leucine- and tryptophan-deficient SD media (A, lower panel) or leucine-, tryptophan- and uracil-deficient SD media (B, lower panel). The detection of protein-protein interactions was carried out on SD-Leu-Trp media lacking histidine and adenine (A, upper panel) or SD-Leu-Trp-Ura media lacking histidine and adenine (B, upper panel). The addition of 5 mM 3-amino-1,2,4-triazole (3-AT) was used to reduce the nonspecific yeast growth not based on protein-protein interactions.

3.6 Phenotypical studies of double mutant lack NRT1.5 and its interacting partner

3.6.1 Identification of *slah3*, *nrt1.8* and *aha2* knockout mutants

In order to investigate the physiological meaning of the interaction between NRT1.5 and its interacting partners, single T-DNA insertion mutants *slah1* (SALK_039811), *slah3* (GK-317G03) and *aha2* (Gabi-219D04) were ordered from the *Arabidopsis* Biological Resource Center (ABRC). The *nrt1.8* (GK-756D01) mutant was also

included in this study because of its close functional correlation with NRT1.5. Genomic genotyping PCR was done to identify homozygotes of each single mutant (Figure 32). Semi-quantitative RT-PCR was carried out to verify the absence of full-length gene transcripts in homozygous mutants. *slah3* and *nrt1.8* are knockout mutants since no intact gene transcripts were detectable in single mutants (Figure 32). The *aha2* mutant is also a knockout mutant (RT-PCR for detecting *AHA2* in *aha2* was done by my colleague Florencia Sena). However, the transcript of *SLHA1* was still detectable in *slah1* mutant, which suggest that it was only the knockdown mutant and therefore it was not included in following experiments. The same RT-PCR result with *slah1* was also showed in a recent study of Zheng *et al*. (2015). Subsequently, homozygous single knockout mutants *slah3*, *nrt1.8* and *aha2* were crossed with *nrt1.5-5* to generate double mutants.

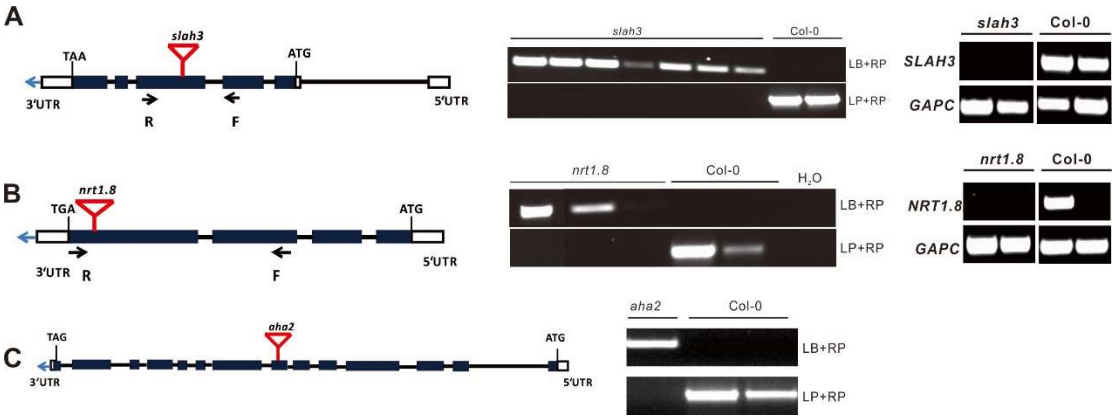

Figure 32. Scheme of T-DNA insertion lines and identification of homozygous knockout mutants. Left panels: map of the T-DNA insertion site in **(A)** *SLAH3*, **(B)** *NRT1.8*, **(C)** *AHA2*. Middle panels: genotyping PCR to identify homozygous single mutant **(A)** *slah3*, **(B)** *nrt1.8*, **(C)** *aha2.* Right panels: RT-PCR analysis to detect gene transcripts in single mutant **(A)** *slah3*, **(B)** *nrt1.8*, **(C)** *aha2.* Primers used for genomic PCR and RT-PCR are listed in Table 4.

3.6.2 Phenotypical analysis of the *nrt1.5-5/nrt1.8* double mutant

NRT1.5 and NRT1.8 share the highest sequence similarity among all NRT1 members, but their function was opposite in NO_3^- long-distance transport towards shoot, loading and unloading NO_3^- into xylem, respectively (Lin *et al.* 2008; Li *et al.* 2010). Consequently, it has been shown that NO_3^- concentration was decreased in *nrt1.5* mutant but increased in *nrt1.8* mutant (Li *et al.* 2010). In addition, *NRT1.8* expression was strongly upregulated in roots of *nrt1.5* mutant (Drechsler *et al.* 2015). It was thus interesting to test whether the reduced K^+ transport in *nrt1.5* shoots is due to the altered NO_3^- xylem loading, or whether the strong upregulation of *NRT1.8* in *nrt1.5* roots is necessary for the phenotype development in *nrt1.5* mutants. Single mutant *nrt1.5-5* and *nrt1.8*, wild type Col-0 and the *nrt1.5-5/nrt1.8* double mutant plants were grown on non-fertilized soil supplied with modified 1/2 MS solution with various N/K concentrations. Compared to Col-0, *nrt1.8* did not demonstrate any visible morphological changes under all tested fertilization regimes (Figure 33). This indicates that the increased NO_3^- concentration in xylem leads to no visible phenotypical changes. The double mutant *nrt1.5-5/nrt1.8* just showed the leaf chlorosis phenotype of *nrt1.5-5* under low NO_3^- supply, and no more distinction between the double mutant and *nrt1.5-5* could be observed (Figure 33). This observation indicates that the altered shoot K^+ homeostasis in *nrt1.5* might not be caused by the reduction in NO_3^- concentration in xylem, and the upregulation of *NRT1.8* in *nrt1.5-5* does not contribute to the phenotype development of *nrt1.5-5.*

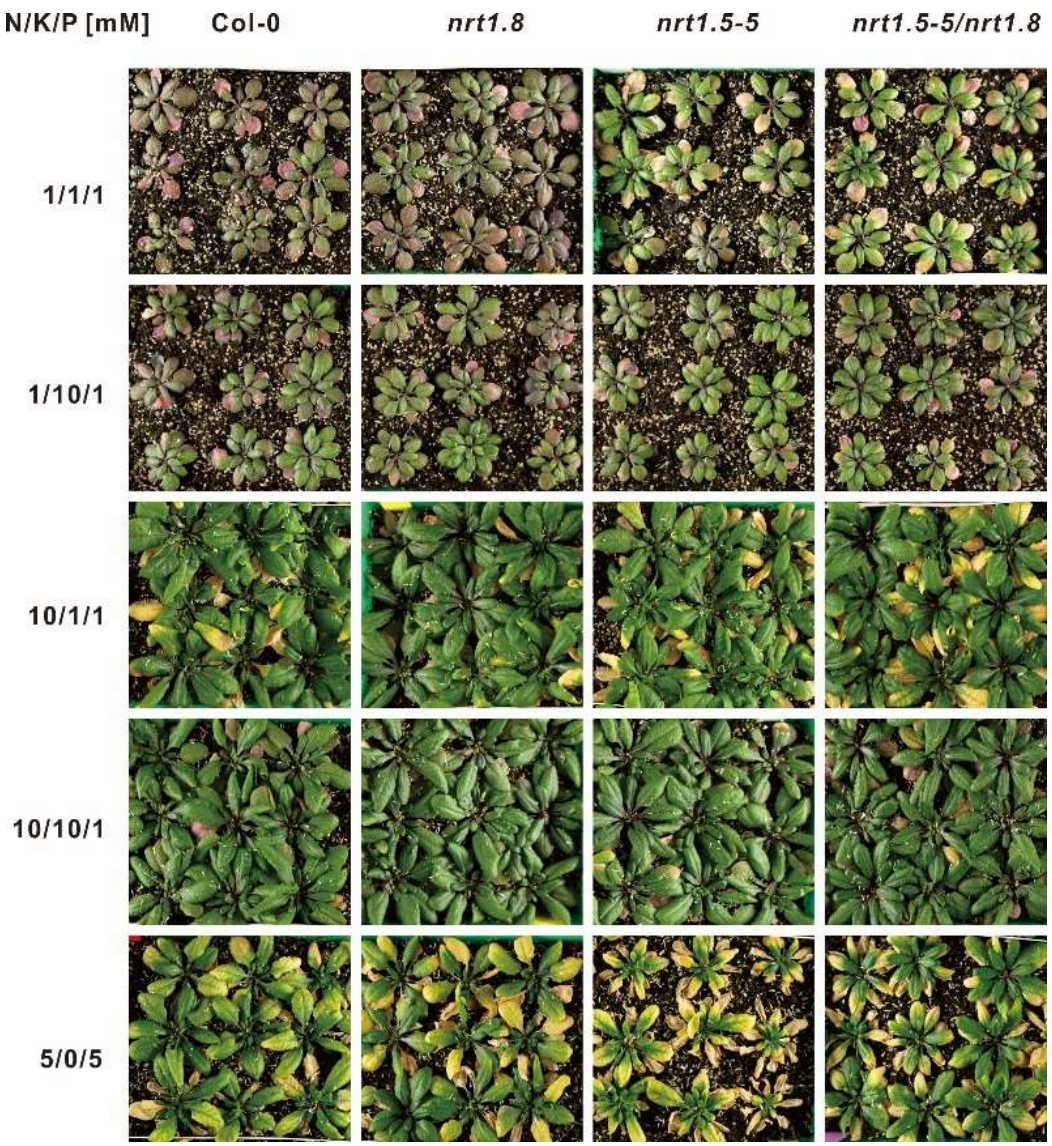

Figure 33. Rosette morphology of Col-0, *nrt1.5-5*, *nrt1.8* and *nrt1.5-5/nrt1.8* plants in response to varying N/K/P supply.

Plants were cultivated on unfertilized soil and were supplied with modified 1/2 MS nutrient solutions which contained indicated concentrations [mM] of the macronutrients N (NO_3^-), K and P (Pi). Each column shows on top the genotype and on left the applied fertilization regime (N/K/P [mM]).

3.6.3 Phenotypical analysis of the *nrt1.5-5/slah3* double mutant

To investigate the physiological meaning of the interaction between NRT1.5 and SLAH3, the phenotypical analysis of *slah3* single mutant and the *nrt1.5-5/slah3* double mutant was conducted under various nutrient concentrations on soil. Under all tested fertilization conditions, *slah3* single mutants showed comparable growth like Col-0 (Figure 34A). The *nrt1.5-5/slah3* double mutant developed a leaf chlorosis phenotype like *nrt1.5-5* at low NO_3^- supply. Interestingly, at low NO_3^- and high K^+ condition (1/10/1 N/K/P [mM]), the *nrt1.5-5/slah3* double mutant exhibited the stronger leaf chlorosis compared to *nrt1.5-5* (Figure 34A), indicating that the K concentration in the double mutant is lower than in *nrt1.5-5*. Since SLAH3 has been characterized to be strongly permeable to NO_3^-, the total N concentration in rosette leaves was measured to evaluate whether the interaction between NRT1.5 and SLAH3 affects N accumulation. At low NO_3^- supply (1/1/1, 1/10/1 N/K/P [mM]), the N concentration in shoots of *slah3* was higher than in Col-0, and the total N in the double mutant *nrt1.5-5/slah3* was higher than that of other three plant lines (Figure 34B). This high accumulation of N in the double mutant might be caused by the compensation of other proteins involved in NO_3^- root-to-shoot translocation. The similar N accumulation pattern has also been observed for the *nrt1.5-5/skor-2* double mutant (Figure 22), suggesting that the higher total N in double mutants might be an indirect and unspecific effect of the simultaneous mutation of two nitrate or potassium transporters located at root vascular.

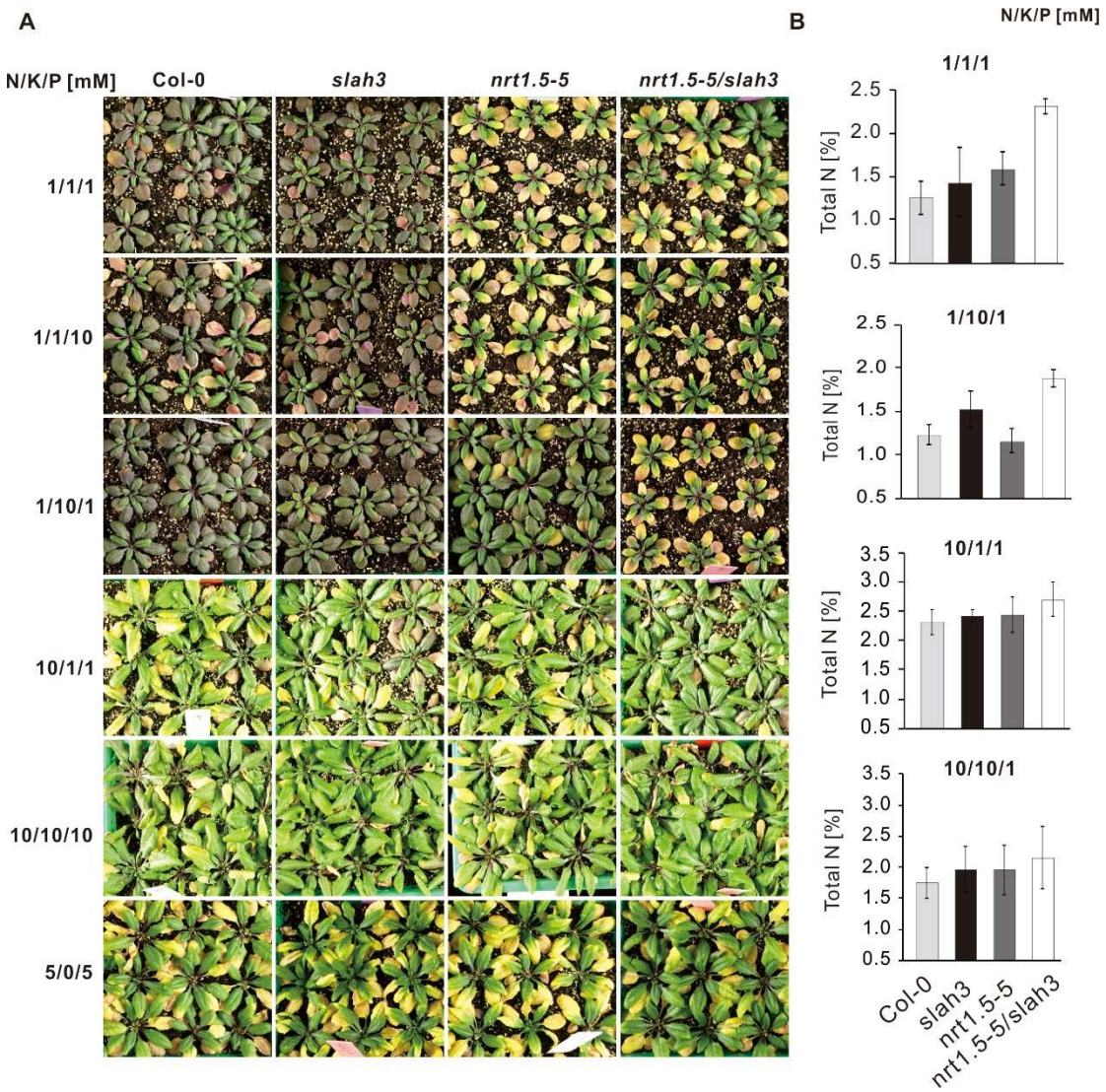

Figure 34. Rosette morphology and the total N concentration in Col-0, *nrt1.5-5*, *slah3* and *nrt1.5-5/slah3* plants in response to varying N/K/P supply.

(A) Rosette morphology of Col-0, *nrt1.5-5*, *slah3* and *nrt1.5-5/slah3* plants under varying N/K/P supply. Each column shows on top the genotype and on left the applied fertilization regime (N/K/P [mM]). Plants cultivated on unfertilized soil were fertilized with modified 1/2 MS nutrient solutions which contained indicated concentrations of N (NO_3^-), K and P (Pi). **(B)** Total N concentration in Col-0, *nrt1.5-5*, *slah3* and *nrt1.5-5/slah3* rosette leaves grown with indicated N/K/P supply. Results shown are the means ± SD (n=6).

To examine the concentration of macroelements, ICP-OES analysis was conducted with rosette leaves grown under four different N/K/P regimes (1/1/1, 1/10/1, 10/1/1 and 10/10/10 N/K/P [mM]). The K concentration in *nrt1.5* mutants was significantly lower than that of Col-0 under low NO_3^- (1 mM) condition, which was consistent with our previous findings (Figure 22). Concentrations of macroelements including K, Ca, Mg, S and P in *slah3* mutant were not significantly changed compared to Col-0 at all N/K/P regimes (Figure 35). At 1 mM NO_3^- and K^+ supply (1/1/1 N/K/P [mM]), the K concentration in the *nrt1.5/slah3* double mutant resembled that of *nrt1.5-5* mutant. However, it is noteworthy that unlike the other three fertilization conditions, at low NO_3^- and high K^+ supply (1/10/1 N/K/P [mM]), *slah3* mutant plants showed the slightly reduced K concentration compared to that of Col-0 (Figure 35), implying that SLAH3 might affect the K^+ transport at this condition. The K concentration in the double mutant *nrt1.5-5/slah3* plants was lower than that of *nrt1.5-5* plants, even though the difference was not statistically significant. The double mutant also accumulated significantly higher concentrations of Ca, Mg, S and P than all other lines at this condition (1/10/1 N/K/P [mM]), perhaps caused by the compensation effect of the reduced K content. The reduced K concentration in the double mutant was consistent with the observation that the double mutant showed a stronger leaf chlorosis phenotype compared with *nrt1.5-5* mutant (Figure 34A). These results suggest that at certain fertilization condition (low NO_3^- and high K^+), NRT1.5 and SLAH3 might work synergistically to maintain the homeostasis of K and a wide variety of other marcoelements in shoots.

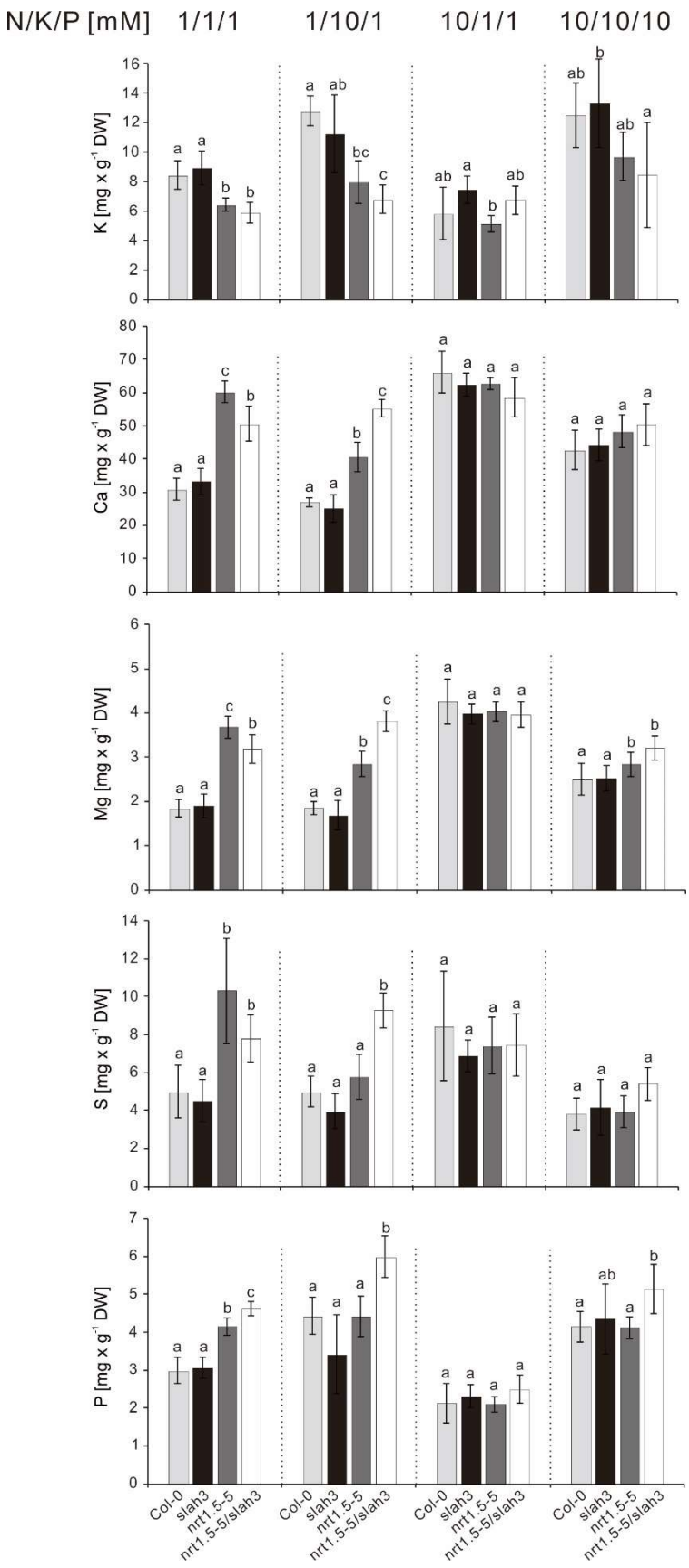

Figure 35. Elemental concentrations in the rosettes of Col-0, *nrt1.5-5*, *slah3* and *nrt1.5-5/slah3* plants.

Concentrations [mg/g DW] of the macroelements potassium, calcium, magnesium, sulphur and phosphorus in the rosettes of the Col-0, *nrt1.5-5*, *slah3* and *nrt1.5-5/slah3* plants. The applied fertilization regimes (N/K/P [mM]) were shown on top of the figure. Results shown are the means ± SD (n = 6). The data were statistically analysed by one-way ANOVA and subsequent multiple comparisons (Tukey's HSD test). Different letters represent significant differences at $P < 0.05$.

3.6.4 Phenotypical analysis of the *nrt1.5-5/aha2* double mutant

Among eleven *Arabidopsis* plasma membrane (PM) H^+-ATPases which have specific expression patterns, *AHA2* is the predominant root-expressed proton pump. *AHA2::GUS* construct revealed a strong signal in different cell layers including epidermis, cortex cells, phloem, xylem as well as root hairs (Fuglsang *et al.* 2007). The physical interaction between NRT1.5 and AHA2 has been demonstrated in heterologous yeast system (Drechsler, Dissertation 2016) and *in planta* in this study (Figure 29).

The *nrt1.5* mutants phenocopy *aha2* mutant in response to HygB treatment and the supply with high concentration K^+ (Figure 18). Based on these observations, it is tempting to speculate that the interaction between NRT1.5 and AHA2 is important for maintaining plasma membrane potential of root cells. The root-to-shoot transfer of K^+ might be subsequently influenced by the change in plasma membrane potential. Therefore, the HygB sensitivity test was carried out to examine the membrane potential of the *nrt1.5-5/aha2* double mutant plants. Consistent with the previous observation for *nrt1.5* mutants in this study (Figure 18) and what has been published for the *aha2* mutant (Haruta *et al.* 2010), *nrt1.5-5* and *aha2* were more tolerant to HygB treatment compared to wild-type plants (Figure 36), indicating the depolarization of the membrane potential in both mutants. Interestingly, compared to *aha2*, *nrt1.5-5* seedlings showed the stronger resistance to HygB. The *nrt1.5-5/aha2* double mutant showed the comparable root growth like *nrt1.5-5*, and no visible additive effect could be observed in the double mutant. These results indicate that NRT1.5 and AHA2 might share the same mechanism in influencing the plasma membrane potential.

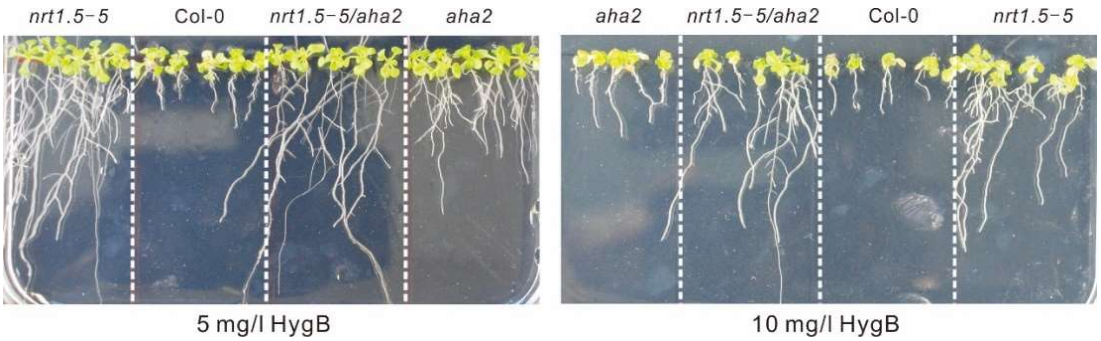

Figure 36. Root morphology of Col-0, *nrt1.5-5*, *aha2* and the *nrt1.5/aha2* double mutant in response to hygromycin B treatment.

4 DAG seedlings germinated on 1/2 MS medium were transferred on 1/2 MS medium supplemented with 5 mg/l or 10 mg/l HygB and continued to grow vertically for 6-7 more days.

To investigate whether the *aha2* single mutant and the *nrt1.5-5/aha2* double mutant develop any phenotype at certain nutrient conditions, seedlings of Col-0, *nrt1.5-5*, *aha2* and *nrt1.5-5/aha2* were grown on unfertilized soil supplied with four different N/K regimes. Under low NO_3^- supply (1/1/1 N/K/P [mM]), in comparison with Col-0 plants, *nrt1.5-5* and the *nrt1.5-5/aha2* plants showed the leaf chlorosis phenotype and reduced anthocyanin accumulation, indicating the K reduction in shoots. However, *aha2* mutant plants showed the similar morphology as Col-0 plants under all tested N/K regimes, and no visible differences of *aha2* plants were observed (Figure 37). Although showing no phenotype, *aha2* mutant plants yet gained significantly less fresh weight compared to Col-0 plants under 10/10/1 (N/K/P [mM]) supply. Similar trend was also observed at the other three N/K/P regimes except 1/1/1 (N/K/P [mM]) (Figure 38B). This result indicates the growth of *aha2* plants was inhibited at these conditions.

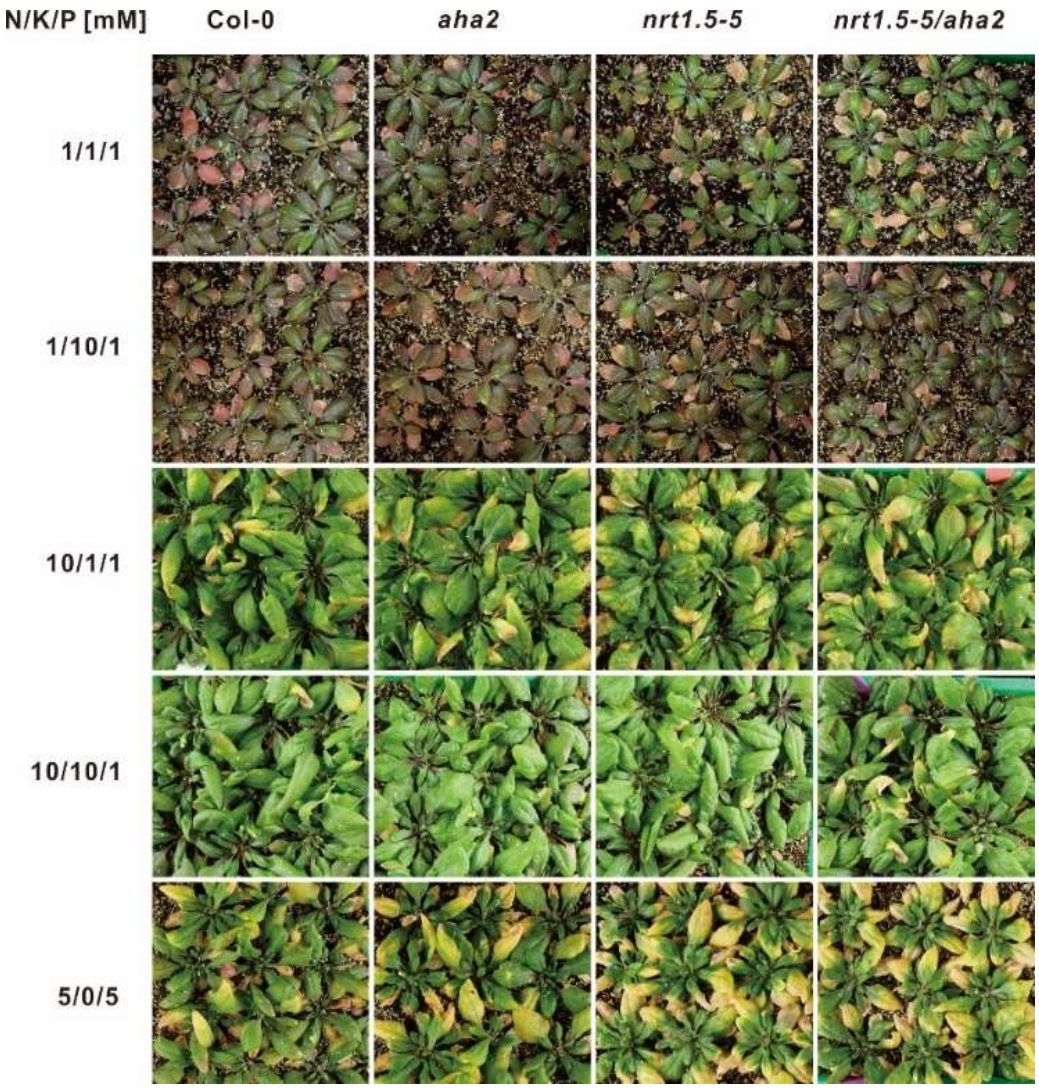

Figure 37. Rosette morphology of Col-0, *nrt1.5-5*, *aha2* and *nrt1.5-5/aha2* plants in response to varying N/K/P supply.

Each column shows on top the genotype and on left the applied fertilization regime (N/K/P [mM]). Plants cultivated on unfertilized soil were fertilized with modified 1/2 MS solutions which contained different concentrations [mM] of the macronutrients N (NO_3^-), K and P.

ICP-OES analysis was conducted to examine the K composition in rosettes of each line. Under low NO_3^- supply (1/1/1 N/K/P [mM]), *aha2* mutant plants accumulated the comparable K concentration as that of Col-0, whereas the K concentration in *nrt1.5-5* was significantly decreased (Figure 38A). The K concentration in the *nrt1.5-5/aha2* was slightly, but still significantly higher than that in *nrt1.5-5* at this condition. Interestingly, at high NO_3^- supply (10/1/1, 10/10/1 N/K/P [mM]), the *aha2* mutant showed the reduced K concentration compared with Col-0. This K reduction in *aha2* mutant was only statistically significant at high NO_3^- and low K^+ (10/1/1 N/K/P [mM])

supply (Figure 38A). However, the K concentration in *aha2* plants still approximately reached 1% DW at this condition, therefore, no visible leaf chlorosis phenotype in *aha2* was observed. The *nrt1.5-5/aha2* lines just demonstrated the leaf chlorosis phenotype and similar shoot K accumulation like *nrt1.5-5* at most circumstances. These results suggest that the mutation of *AHA2* did not greatly affect the K^+ root-to-shoot translocation. Haruta *et al.* (2010) also noticed that the impairment in *AHA2* had little consequence on *Arabidopsis* seedlings growing under ideal conditions, maybe due to the highly redundant function of AHAs.

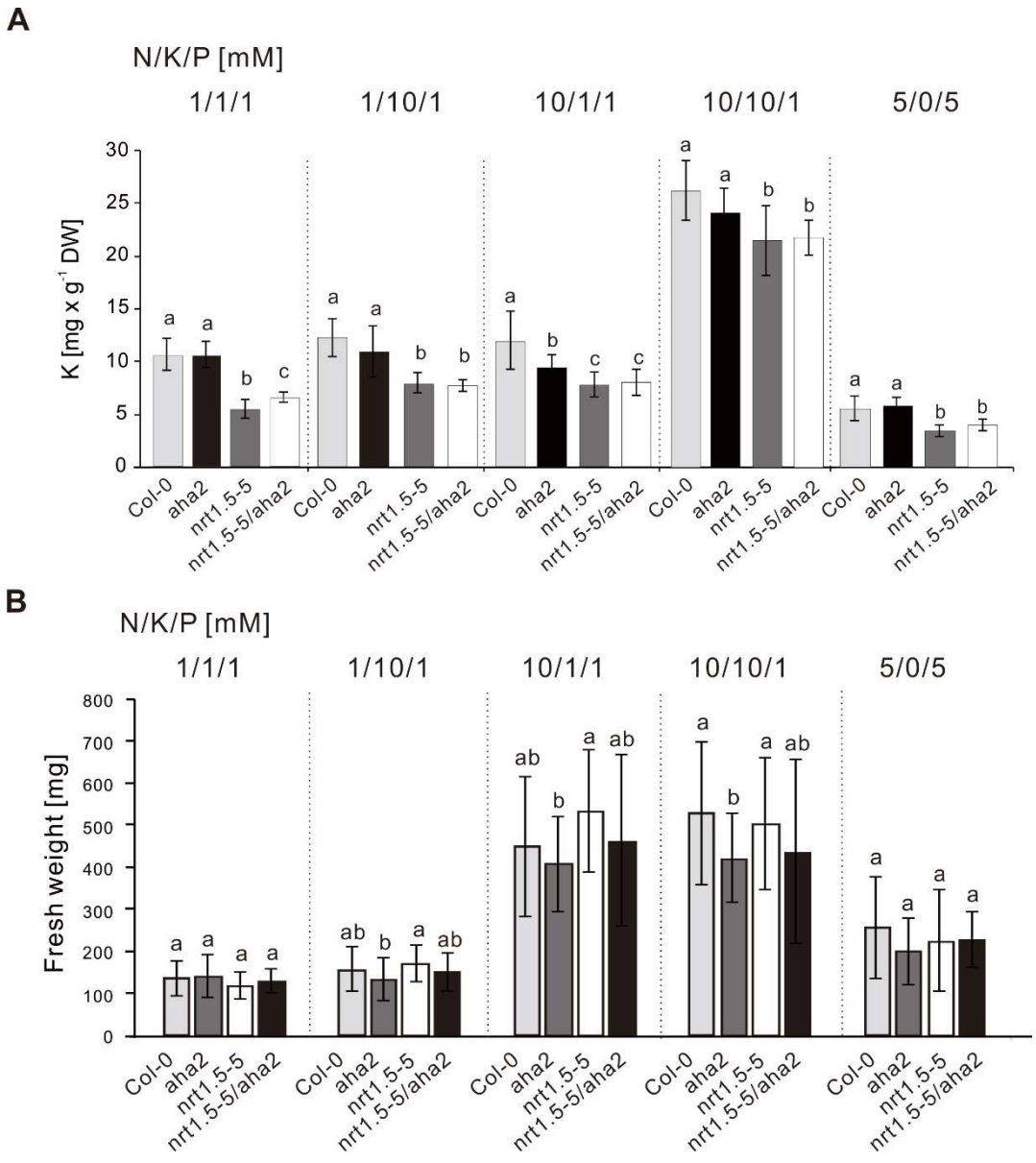

Figure 38. Potassium concentration and fresh weight of the rosettes of Col-0, *nrt1.5-5*, *aha2* and *nrt1.5-5/aha2* plants under various N/K regimes.

(A) K concentrations [mg/g DW] in the rosettes of the Col-0, *nrt1.5-5*, *aha2* and *nrt1.5-5/aha2* plants under various fertilization conditions as indicated on top of the columns. Data shown are means ± SD (n ≥ 7). **(B)** The fresh weight gain of rosettes of Col-0, *nrt1.5-5*, *aha2* and the double mutant *nrt1.5-5/aha2* under various fertilization regimes as indicated on top (means ± SD, n = 24). When all plant lines start flowering, florescence meristems were removed, then the fresh weight of each rosette was measured and followed by ICP-OES analysis. The data were statistically analyzed by one-way ANOVA and subsequent multiple comparisons (Tukey's HSD test) for each fertilization treatment. Different letters the indicate significant difference at $P < 0.05$.

To investigate whether *AHA2* transcript is regulated by *NRT1.5* level or by different N/K availabilities, qRT-PCR was applied to examine the expression of *AHA2* in roots of Col-0 and *nrt1.5-5* under four N/K regimes (Figure 39). Under all regimes, *AHA2* was nearly similarly expressed in Col-0 and in *nrt1.5-5*, indicating its expression was not affected by the *NRT1.5* level. Compared to 1/1/1 (N/K/P [mM]), elevated NO_3^- supply to 10 mM (10/1/1, N/K/P [mM]) did not change the expression of *AHA2* in Col-0, suggesting that external NO_3^- amount had no influence on *AHA2* transcript. However, an increment of K^+ concentration to 10 mM (1/10/1 and 10/10/1, N/K/P [mM]) enhanced *AHA2* level to 2-fold and 3.5-fold in Col-0, respectively. These results demonstrated that *AHA2* is stimulated by high K^+ supply at the transcriptional level.

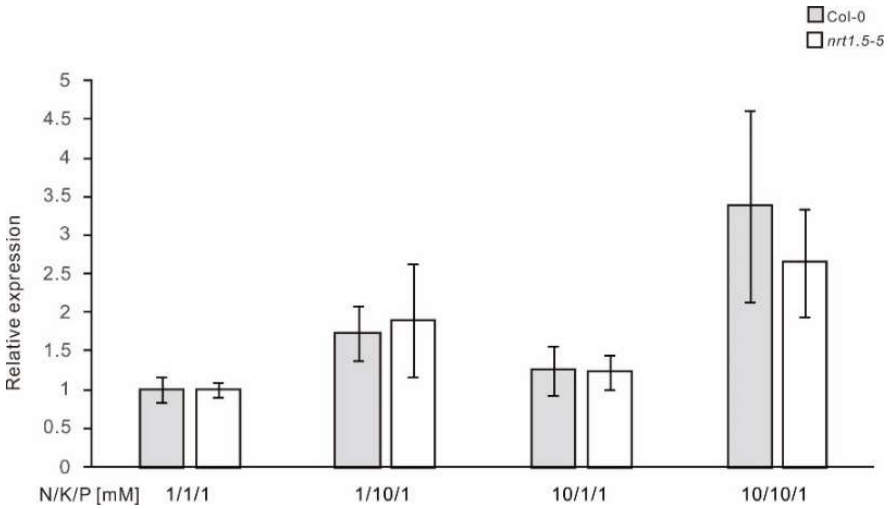

Figure 39. Expression of *AHA2* in roots of Col-0 and *nrt1.5-5* under various N/K regimes.

Relative transcriptional level ($2^{-\Delta\Delta C_T}$) of *AHA2* was measured by qRT-PCR and normalized to *UBQ10* in roots of Col-0 and *nrt1.5-5* plants grown on non-fertilized soil supplemented with various N/K regimes (means ± SD; n ≥ 4). Relative transcript level of *AHA2* in roots of Col-0 grown on unfertilized soil supplemented with 1/1/1 N/K/P [mM] was set to 1.0.

3.7 Potassium reduction in shoots of *35Sp::NRT1.5* at low nitrate supply

It has been shown that NRT1.5 function in roots rather than in shoots is responsible for the root-to-shoot K^+ transfer (Drechsler *et al.* 2015). Our group has successfully generated shoot specific *NRT1.5*-overexpression lines under the control of *CAB2* promoter (Drechsler, Dissertation 2016), however, the attempt to overexpress *NRT1.5* in roots under the control of its native promoter and the root specific *Pyk10* promoter failed (Drechsler *et al.* 2015 and unpublished data).

In this study, *NRT1.5* was overexpressed in *Arabidopsis* Col-0 plants under the control of the CaMV *35S* promoter. Enhanced expression of *NRT1.5* in transgenic lines was confirmed by qRT-PCR at the transcriptional level (Figure 11). To study the effect of overexpression of *NRT1.5* on K^+ transport, two independent homozygous *35Sp::NRT1.5* T3 lines, *nrt1.5-5* and Col-0 were grown on non-fertilized soil and supplied with modified 1/2 MS solution with various amounts of NO_3^- and K^+. As shown before, *nrt1.5-5* plants exhibited the early leaf chlorosis phenotype at low NO_3^- supply, which was an indication of the low K concentration in rosette leaves (Figure 40). However, two independent overexpression lines *35Sp::NRT1.5* #8-2 and #18-3 also developed the similar phenotype like *nrt1.5-5* mutant at the low NO_3^- conditions (1/1, 1/10 N/K [mM]) (Figure 40).

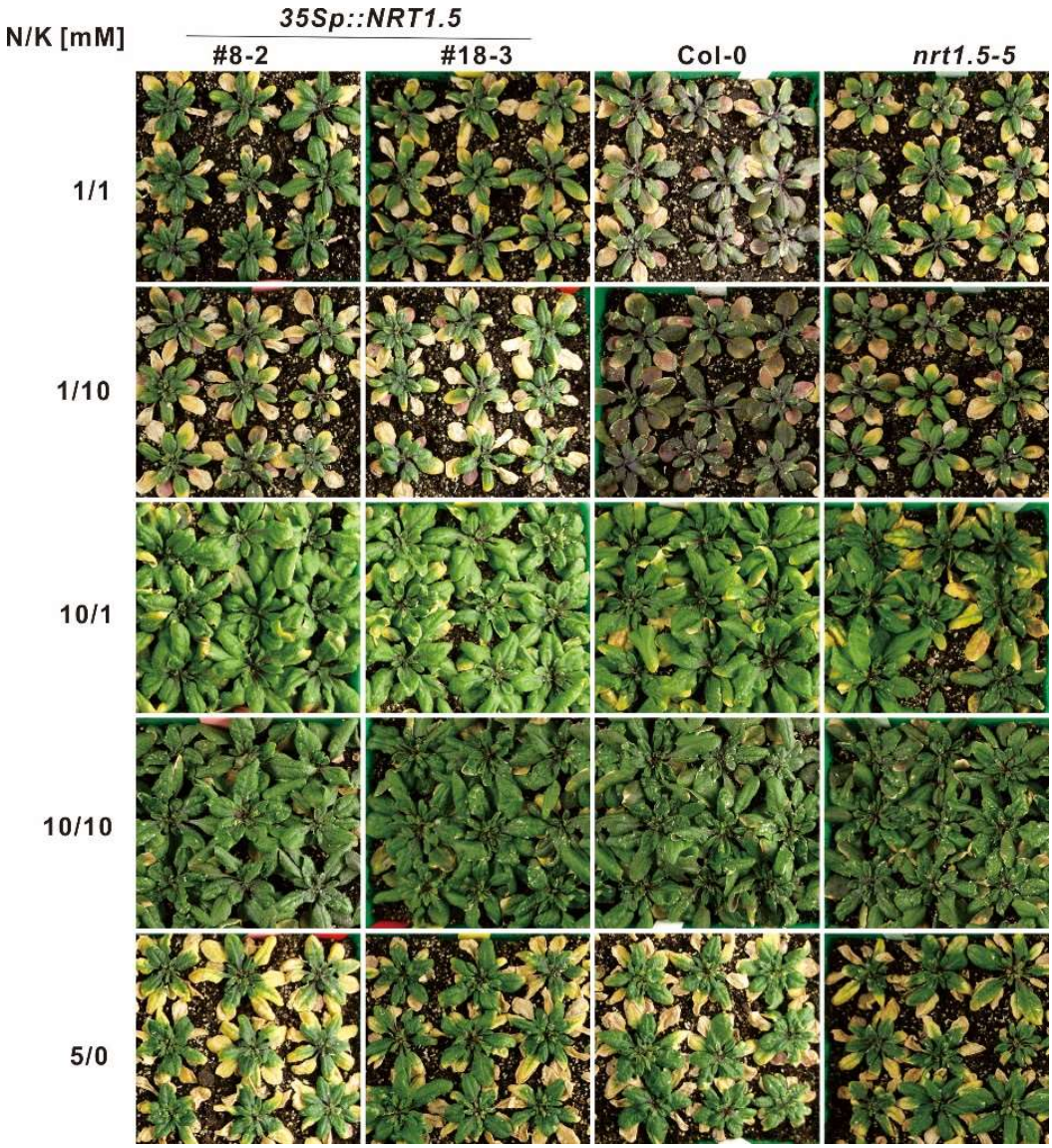

Figure 40. Rosette phenotype of Col-0, *nrt1.5-5* and *35Sp::NRT1.5* plants under varying N/K supply.

Each column shows on top the genotype and on left the applied fertilization regime (N/K [mM]). Phosphorus was always supplied as 1 mM at all conditions. Plants cultivated on unfertilized soil were additionally fertilized weekly with modified 1/2 MS nutrient solutions which contained different concentrations [mM] of the macronutrients N (NO_3^-) and K^+.

To figure out whether the leaf chlorosis phenotype of *35Sp::NRT1.5* lines was also attributed to the low shoot K concentration, the whole rosettes of all lines were harvested for elemental analysis by ICP-OES. Indeed, consistent with the phenotype, both *35Sp::NRT1.5* lines accumulated significantly reduced K concentration compared with Col-0 in rosettes (Figure 41). Accordingly, concentrations of Ca, Mg and Na were increased in rosettes of *35Sp::NRT1.5* possibly to compensate the charge balance

(Figure 41). This result confirmed that the leaf chlorosis phenotype of *35Sp::NRT1.5* lines was due to the K deficiency in shoots, like in *nrt1.5-5* plants.

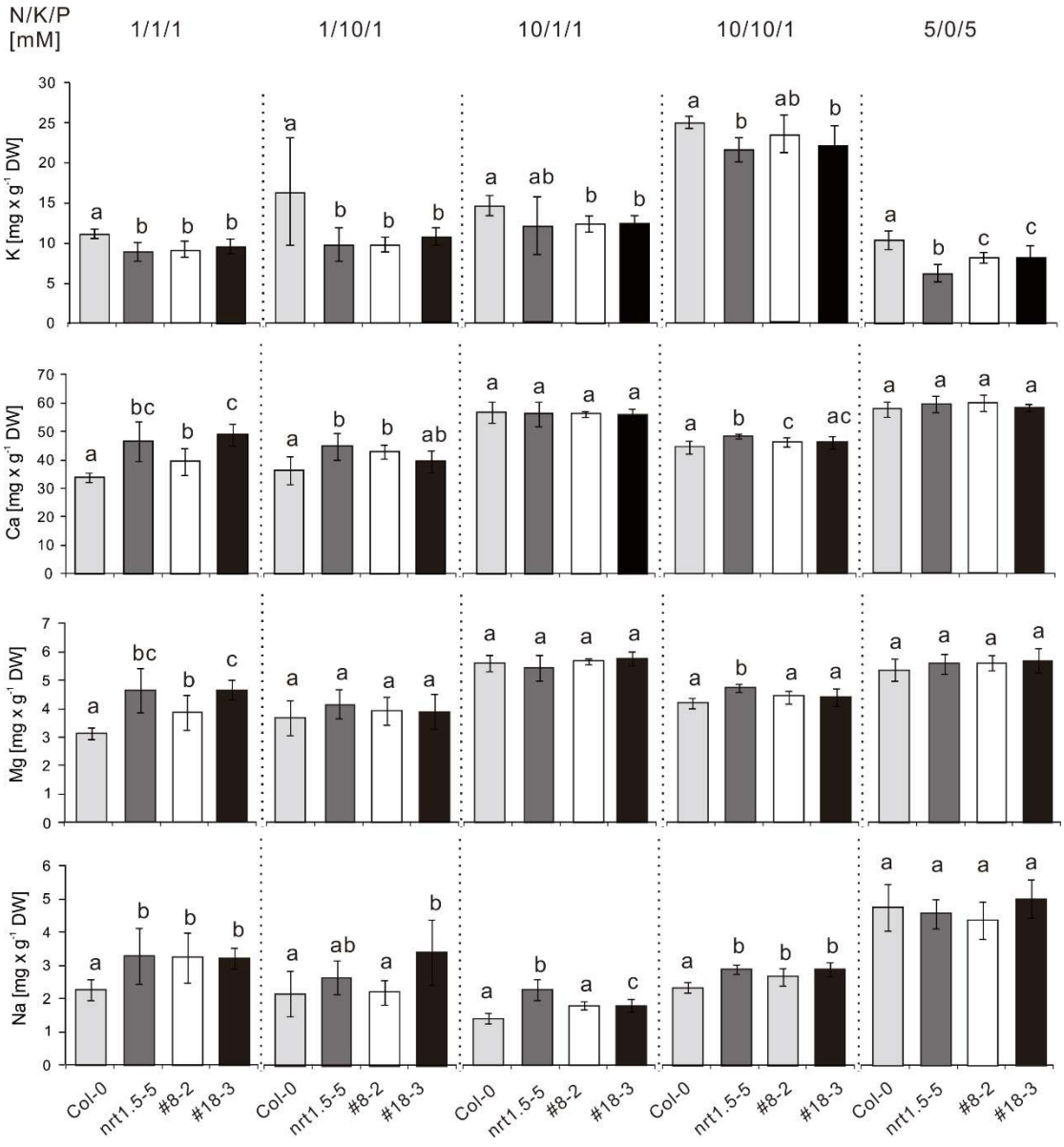

Figure 41. Potassium, calcium, magnesium and sodium concentration in the rosettes of Col-0, *nrt1.5-5* and *35Sp::NRT1.5* plants.

Concentrations [mg/g DW] of elements were examined by ICP-OES analysis with the rosettes of the Col-0, *nrt1.5-5* and two *35Sp::NRT1.5* overexpression lines #8-2 and #18-3 (means ± SD, n = 6). Various fertilization conditions were applied as indicated on top of the columns. The data were statistically analyzed by one-way ANOVA and subsequent multiple comparisons (Tukey's HSD test) for each fertilization treatment. Different letters the indicate significant difference at $P < 0.05$.

3.8 Expression profiles of nitrate- and potassium-transporters upon hormone treatment

Several studies have revealed the crosstalk between plant hormones and nutrients. For example, plant hormones including abscisic acid (ABA), auxin and cytokinins (CK) have been proposed to be involved in coordinating N acquisition and assimilation (Signora *et al.* 2001; Wilkinson and Davies 2002; Argueso *et al.* 2009). Besides N, the crosstalk between K^+ and hormones auxin and JA was also documented (Armengaud *et al.* 2004; Vicente-Agullo *et al.* 2004). To investigate how nitrate transporters and potassium transporters are regulated by phytohormones at the transcriptional level, various phytohormones were used to treat *Arabidopsis* seedlings for 24 h followed by qRT-PCR analysis with root materials. Eight transporters proposed to be involved in uptake and root-to-shoot transfer of NO_3^- and K^+ were investigated.

3.8.1 Genes involved in the uptake of nitrate and potassium

NRT1.1, responsible for nitrate uptake at both high and low affinities, and two potassium inward transporters *HAK5* and *AKT1* which work as high and low affinity transporters, respectively, were investigated in this study. The expression of *AKT1* is relatively stable by most of hormone treatments except JA and Methyl jasmonate (MeJA) which caused its dramatic downregulation (Figure 42). Unlike *AKT1*, *HAK5* expression is upregulated by a variety of hormones including ABA, salicylic acid (SA), indole-3-acetic acid (IAA), 6-Benzylaminopurine (BAP) and gibberellic acid (GA_3). Nitrate transporter *NRT1.1* was inhibited by most of hormones including JA, MeJA, SA, IAA, especially by BAP, whereas it was strongly induced by ABA and marginally enhanced by GA_3 and 24-epibrassinolide (EBR) (Figure 42). These results suggest ABA is in favour of the uptake of NO_3^- and K^+, while JA and MeJA inhibit this process.

3.8.2 Genes involved in root-to-shoot transfer of nitrate and potassium

Expression of *SKOR* and *NRT1.5* which are key proteins responsible for xylem loading of K^+ and NO_3^-, respectively, were investigated in this study. In addition, *NRT1.8* which is responsible for NO_3^- unloading from xylem, *SLAH1* and its analogue *SLAH3* which is highly permeable to NO_3^- and might contribute to root-to-shoot transfer of NO_3^- were also included in this study. *SKOR* was markedly inhibited by a variety of hormones including ABA, JA, MeJA, IAA and BAP, whereas it was slightly induced by GA_3, SA and EBR (Figure 42). *NRT1.5* was downregulated by nearly all the hormone treatments, except IAA and ABA which only marginally induced its expression. It is known that the expression of *NRT1.5* and *NRT1.8* was oppositely regulated by stress conditions (Li *et al.* 2010). This pattern was consistent with the observation that JA, MeJA and SA treatment upregulated *NRT1.8* while downregulated *NRT1.5* (Figure 42). Moreover, the *NRT1.8* expression was enhanced by ABA and IAA but reduced by BAP and GA_3.

SLAH1 was significantly upregulated by ABA, JA, MeJA, IAA and GA3, however, SA and BAP had a strong inhibition effect on its expression. *SLAH3* showed the similar expression pattern like *SLAH1* by ABA, SA, BAP treatment but with much attenuation. However, by JA, MeJA, IAA and GA_3 treatment, *SLAH3* showed the opposite regulation pattern compared to *SLAH1* (Figure 42), indicating different functions of these two proteins.

In conclusion, this study showed that the expression of nitrate and potassium transporters responsible for NO_3^- and K^+ uptake or xylem loading was influenced by most of the tested phytohormone treatments in roots, but in different patterns. Compared with ABA, JA, MeJA, SA and BAP treatment, IAA, EBR and GA_3 treatment had less impact on expression of these transporters. ABA treatment is probably in favor of the retention of nutrients in roots, since it upregulates transcripts of nitrate and potassium importers (*NRT1.1, HAK5*) while inhibited the expression of transporters for xylem loading (*SKOR*, *NRT1.5*). BAP inhibited all tested nitrate transporters, and it

might also support the retention of K^+ in roots through stimulating *HAK5* and inhibiting *SKOR*. The strong inhibition of *SLAH1* by SA might indicate its role in dealing with biotic or abiotic stress. This study will be helpful to understand more detail about the nutrient transport process controlled by phytohormone signals.

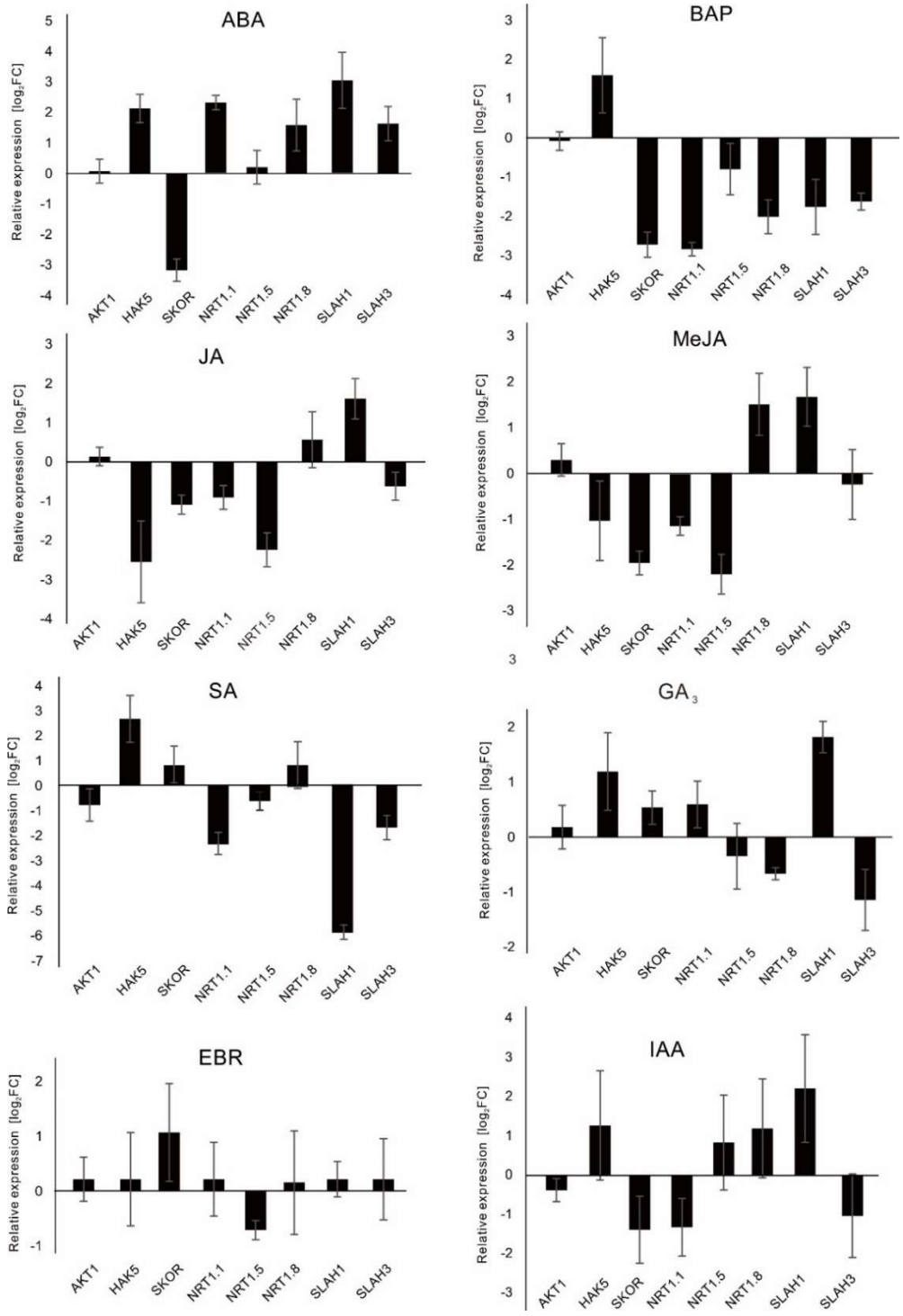

Figure 42. Expression profiles of nitrate and potassium transporters in roots by phytohormone treatment.

Relative expression level of eight nitrate and potassium transporter genes in phytomorne treated Col-0 roots were measured by qRT-PCR and normalized to *UBQ10* (means ± SD, n ≥ 3). Col-0 seedlings were grown in liquid 1/2 MS medium and were treated with phytomornes for 24 h. Root material from ten seedlings were pooled as one biological replicate. Plotted are log_2 fold expression changes (FCs) in hormone treated roots compared with untreated roots.

4 Discussion

4.1 Expression of *NRT1.5* in roots influences the lateral root growth at potassium deprivation

The *Arabidopsis* lateral root originates from pericycle founder cells adjacent to the two xylem poles (Dubrovsky *et al.* 2001). These cells undergo cell divisions and expansion to form a lateral root primordium. LR development can be divided into eight morphological events (Malamy and Benfey 1997). The importance of auxin and its transport in LR development has been well studied (Casimiro *et al.* 2001; Swarup *et al.* 2001; Marchant *et al.* 2002). For instance, auxin is required at several specific developmental stages to facilitate the LR formation (Dubrovsky *et al.* 2001; Stals and Inze 2001). Exogenous application of IAA stimulates LR development and elongation (Blakely *et al.* 1982; Muday and Haworth 1994). Contrary to the stimulation effect of auxin, many studies have reported the inhibitory effect of cytokinin on LR development (Torrey 1962; Bottger 1974; Li *et al.* 2006; Chang *et al.* 2013). Recently, it has been shown that nitrate transporter NRT1.1 is capable of exporting auxin out of LR primordia at low NO_3^- supply, consequently, *nrt1.1* mutant plants have more LRs compared to wild type plants (Krouk *et al.* 2010). *MYB77*, a R2R3-type MYB transcription factor, was downregulated by K^+ deprivation. MYB77 enhances auxin signal transduction through interacting with ARFs (Shin *et al.* 2007). Interestingly, *nrt1.5* mutants phenocopy the *myb77* mutant. Both mutants demonstrated the reduced LR density at K^+ deprivation, whereas no root phenotype was observed under nutrient sufficient conditions or under the N deprivation. This study shows that neither *NRT1.1* nor *MYB77* was transcriptionally significantly altered in roots of *nrt1.5-5* (Figure 9), indicating those two genes are not responsible for the root phenotype of *nrt1.5* mutants. Moreover, expression of several auxin or cytokinin related genes were also not deregulated in roots of *nrt1.5-5* compared to wild type (Figure 10), suggesting auxin and cytokinin status are not altered in *nrt1.5-5*. It is possible that those tested hormone

related genes are only expressed at specific root cells. For example, Genevestigator data showed that *MYB77* was mainly expressed in primary root and lateral root tips (Shin *et al.* 2007). Therefore, the expression changes of those genes might not be detected by using the whole root material in this study. Moreover, the low K^+-dependent LR phenotype of *nrt1.5* mutants makes it conceivable to speculate that NRT1.5 might be involved in K^+-dependent hormone homeostasis. Similar to the dual transport roles of NRT1.1 (NO_3^- and auxin), the KT/KUP/HAK family protein TRH1 (TINY ROOT HAIR 1) has been proposed to play a role in transport of both K^+ and auxin (Vicente-Agullo *et al.* 2004). TRH1 regulates auxin transport by influencing the localization of the auxin efflux protein PIN1 (Rigas *et al.* 2013). To answer the question whether NRT1.5 is directly or indirectly involved in the auxin transport process, experiments such as auxin immunolocalization or auxin transport assay in the heterologous systems are required to be included in following studies.

In addition to hormones, root growth can be determined by the availability of nutrients such as nitrogen (N), phosphorus (P), potassium (K), iron (Fe) and sulfur (S) (Gruber *et al.* 2013). Several studies have observed that K^+ availability influences the lateral root growth (Drew 1975; Armengaud *et al.* 2004; Shin and Schachtman 2004; Gruber *et al.* 2013). At very low external K^+ concentrations (<10 µM), the high-affinity K^+ transporter HAK5 is the only protein capable of taking up K^+ in *Arabidopsis* (Rubio *et al.* 2010). *HAK5* is transcriptionally upregulated in roots under K^+ deprivation (Gierth *et al.* 2005). The previous study in our group found that *HAK5* is approximately 3-fold downregulated in roots of *nrt1.5*-5 compared to Col-0 (Drechsler *et al.* 2015). It is therefore conceivable that at limited external K^+ supply, the reduced expression of *HAK5* leads to K^+ shortage, which could consequently result in the reduced LR density in *nrt1.5-5.* However, when growing on plates with only 10 µM K^+, root K^+ concentration in *nrt1.5-5* was dramatically increased rather than reduced, compared to that in Col-0 (Table 13). This observation is corroborated by a very recent study of Li *et al.* (2017) in which they also observed a significant increase of K content in the mutant of *LKS2* which turn out to encode *NRT1.5*. However, the former study of our group with

hydroponic growing plants (Drechsler *et al.* 2015), as well as the study by Meng *et al*. (2016) did not observe the significantly higher accumulation of K^+ in roots of *nrt1.5-5*. Notably, both two studies used hydroponic system and the K^+ supply was not limited in hydroponic solutions. The different cultivating systems and medium composition might be the reason for this discrepancy in K accumulation pattern in *nrt1.5-5* roots. SKOR is the main potassium channel protein responsible for K^+ transport from root to shoot through xylem loading (Gaymard *et al.* 1998), and it was 2-fold upregulated in *nrt1.5-5* roots (Drechsler *et al.* 2015). This study showed that *skor*-2 mutant plants did not exhibit morphological root growth differences compared to wild type under K^+ deprivation conditions (Figure 27), whereas the *nrt1.5-5/skor-2* double mutant plants just showed the *nrt1.5-5* root phenotype (Figure 28). The growth pattern of *skor-2* mutant observed here is consistent with the findings by Li *et al*. (2017). They investigated another T-DNA insertion knockout mutant of *SKOR* (SALK_132944) and did not observe the leaf chlorosis of *skor* mutant plants under K^+ deprivation (Li *et al.* 2017). These results suggest that the less LR phenotype of *nrt1.5* mutants is neither attributed to the reduced root K^+ concentration, nor dependent on the changed K^+ xylem loading activity of SKOR in *nrt1.5* mutants. However, it is noteworthy that 1 mM NO_3^- was supplied in the root assay of this work. At this amount of NO_3^- supply, NRT1.5 rather than SKOR is the main player for K^+ root-to-shoot translocation (see section 3.4). Therefore, the normal root growth of *skor-2* mutant does not exclude the possibility that the reduced LR growth of *nrt1.5* mutant may be caused by the disruption of rectifying K^+ out of pericycle cells. The higher accumulation of K^+ in pericycle cells where lateral roots originate may affect the turgor pressure or change the plasma membrane potential of pericycle cells, which in turn affect the LR development.

In addition to K, it is known that the deficiencies of P, Ca, Mn and B evoked an increase in the first-order (1°) LR density, whereas the limited supply of Mg and Fe led to decreased 1° LR density (Gruber *et al.* 2013). Besides K, the roots of *nrt1.5-5* accumulated more macroelements including P, S and Mg than in Col-0 roots (Table 13). Many studies have reported the relationship between nutrient deficiency and root

system architecture (RSA) (Armengaud *et al.* 2004; Gruber *et al.* 2013), however, little is known how do increased intrinsic marcoelement or microelement levels influence the RSA. It is tempting to speculated that the decreased LR density in *nrt1.5* mutants might be caused by the higher K, P, S and Mg concentrations at K^+ limitation condition.

4.2 NRT1.5 showed no potassium transport activity in yeast

There have been many successful examples of functional characterization of plant potassium channels in yeast mutant *trk1Δ trk2Δ* cells (Anderson *et al.* 1992; Sentenac *et al.* 1992; Obata *et al.* 2007). In this study, *nrt1.5-5* seedlings growing at low K^+ availability (10 µM) accumulated significantly higher amount of K in roots, whereas K in shoots was dramatically decreased compared to wild type (Table 13), implying again that K^+ xylem loading was defective in *nrt1.5-5*. The most plausible explanation would be that NRT1.5 directly transports K^+. However, this study detected no K^+ uptake activity of NRT1.5 in yeast experiments (Figure 14). There are some unsuccessful examples of functional expression of the plant transporter in heterologous expression systems (Dreyer *et al.* 1999). It might be because of the incompatibility of the heterologous expression system, for example, the functional expression of *AKT1* was failed in *Xenopus* oocytes but was successful in baculovirus/insect cell system (Gaymard *et al.* 1996). Alternatively, it might be due to the lack of a regulatory network involving protein-protein interactions and posttranslational modifications as described for potassium channel AKT1 and potassium transporter HAK5 (Honsbein *et al.* 2009; Ragel *et al.* 2015). The lack of such modifying activities or appropriate regulators in yeast might account for the negative K^+ uptake activity of NRT1.5.

However, more likely than K^+ uptake, a K^+ export function in roots would explain the *nrt1.5* leaf chlorosis phenotype which can be attributed to the block in exporting K^+ out of pericycle into xylem. This study demonstrated the K^+ export activity of SKOR in yeast system for the first time, however, it was failed to detect K^+ export activity of NRT1.5 in the same experiment (Figure 16). In this study, NRT1.5 was not fused to a tag, which

makes it difficult to directly detect the NRT1.5 protein level in yeast. Therefore, it is possible that the negative transport activity might be caused by misexpression or incorrect folding of the NRT1.5 protein in yeast cells. Moreover, it is worth noting that the NO_3^- efflux activity of NRT1.5 is regulated by external pH, as the NO_3^- export activity increases with an increase in pH (Lin *et al.* 2008). Therefore, it is conceivable that the lack of K^+ export activity in this study is resulted from an inappropriate pH value (pH 6.0) of the YNB medium. Very recently, Li *et al.* (2017) reported the K^+ export function of NRT1.5. In addition to using electrophysiological assay to show K^+ export activity of NRT1.5 in *Xenopus* oocyte cells, the K^+ export function of NRT1.5 was also demonstrated in yeast cells. Different from our approach to score the growth of yeast cells on agar plates, they cultured yeast cells in K^+-free buffer and measured the K accumulation in buffer after several hours. By this means, a higher accumulation of K in buffer for growing *NRT1.5*-transformed yeast cells was observed, which supports the K^+ export function of NRT1.5. Moreover, Li *et al*. (2017) also showed that the K^+ release function of NRT1.5 relied on the external acidic pH value. With the increase in pH from 5.5 to 7.4, the K^+ export activity of NRT1.5 was greatly reduced. This observation supports the argument that the failure to detect K^+ export activity of NRT1.5 in the present study might be caused by the inappropriate pH value of medium.

4.3 Expression of *NRT1.5* increases the plasma membrane polarization

Membrane potential is the difference in electrical potential between intracellular and extracellular fluids of a living cell. The interior of the cell is electrically negative to the exterior, which results a transmembrane voltage usually ranging from -10 mV to -100 mV (Gutknecht 1970). The more negative cell membrane potential is called hyperpolarization, whereas the less negative charge inside the cell is defined as depolarization. It is known that the activity of ion channels can be influenced by membrane polarization. In *Arabidopsis*, six and two members of the Shaker K^+ channel family can be activated by hyperpolarization and depolarization, respectively (Lebaudy

et al. 2007). Therefore, it is tempting to hypothesize that other than transporting K^+ itself, NRT1.5 might be capable of modulating the activity of potassium transporters or channel proteins through regulating plasma membrane potential. The aminoglycoside antibiotic hygromycin B (HygB) has been used as an indicator for the membrane potential, because of its penetration into yeast cells and thus its toxic effect is dependent on the membrane potential (Barreto *et al.* 2011). In this study, yeast BYT12 cells were more sensitive to increased concentrations of HygB (Figure 16), indicating the hyperpolarized plasma membrane of BYT12 caused by the defective K^+ uptake function. This observation is consistent with what has been demonstrated in a previous study (Navarrete *et al.* 2010). In addition to HygB, TMA and TEA have been also used to indicate yeast cell membrane potential (Barreto *et al.* 2011). Compared to BYT12 with empty vector, BYT12 cells with *NRT1.5* expression were more sensitive to high concentrations of HygB, TMA and TEA, suggesting the expression of *NRT1.5* additionally resulted in the increased membrane hyperpolarization (Figure 16A). Li *et al.* (2017) has reported the amino acid residue Gly209 of NRT1.5 is indispensable for its K^+ export function. The mutation of Gly209 to Glu209 abolished the K^+ transport activity of NRT1.5. In following studies, it would be interesting to investigate whether the mutated NRT1.5 (G209E) can change the membrane potential of yeast cells or not. It will be helpful to answer the question whether the change of membrane potential observed in this study relies on the K^+ export function of NRT1.5 or not.

Consistent with the observation in yeast system, compared to Col-0 plants, *Arabidopsis NRT1.5* overexpression plants *35Sp::NRT1.5* showed more susceptibility, whereas *nrt1.5* mutant plants showed the enhanced tolerance to high concentrations of HygB (Figure 18). Moreover, it is reported that the binding of BRs (brassinosteroids) to the BR receptor BRI1 (brassinosteroid insensitive 1) induces membrane hyperpolarization (Caesar *et al.* 2011). It is conceivable to expect that the application of BR inhibitor brassinazole to plants could decrease the membrane potential. Consistent with this notion, in this study, *nrt1.5* mutant plants were more sensitive to brassinazole treatment compared to wild-type plants (Figure 12). In addition, the

inhibition of plasma membrane H^+-ATPase induces plasma membrane depolarization (Sze *et al.* 1999) and the decrease in plasma membrane potential renders plants the resistance to draught stress. For instance, transgenic plants overexpressing *VAMP711*, the negative regulator of AHA1 (*Arabidopsis* plasma membrane H^+-ATPase 1), were resistance to drought stress (Xu *et al*., 2018). Plants with the mutated hyperactive AHA1 were hypersensitive to drought stress (Merlot *et al.* 2007). Intriguingly, Chen *et al*. (2010) have also reported that *nrt1.5* mutants had enhanced tolerance to drought stress. These observations are further support the notion that the plasma membrane of *nrt1.5* plants is depolarized.

This study suggests that the *NRT1.5* expression level in roots is critical for regulating the plasma membrane potential. Membrane potential can be both the cause and the result of ionic transport processes (Gutknecht 1970). Therefore, it is tempting to speculate that plasma membrane potential changes in pericycle and xylem parenchyma cells may modulate K^+ translocation by indirectly regulating the activity of voltage-dependent potassium channel proteins, which in turn results in the interruption of K^+ root to-shoot transport in *nrt1.5* plants. Alternatively, Li *et al.* (2017) has demonstrated NRT1.5 works as an H^+/K^+ antiporter, it is thus also possible that the membrane polarization change resulted from the *NRT1.5* expression could be the outcome of the altered K^+ transport activity. However, study of Li *et al.* (2017) suggests that NRT1.5 may mediate electroneutral transport of H^+ and K^+. This finding does not explain the membrane potential changes by *NRT1.5* expression observed in the present study. It is noteworthy that in addition to the inhibition of proton pump, the activation of anion currents also induces the depolarizing processes (Brault *et al.* 2004). As a nitrate transporter, it is conceivable that through nitrate transport activity mediated by itself or through its interaction with other anion transporters/channels that membrane potential is influence by the expression of *NRT1.5*.

4.4 Job Sharing between NRT1.5 and SKOR in nitrate-dependent potassium translocation

When the present study was carrying on, SKOR was known as the main player for root-to-shoot translocation of K^+ through xylem loading (Sharma *et al.* 2013), which was based on the observation that its disruption strongly reduced the K content in the shoot, whereas the K content in the roots remained unaffected. However, the K^+ root-to-shoot translocation in *skor* mutant was not completely abolished, suggesting that more proteins are involved in this process (Gaymard *et al.* 1998). The previous study in our group found that the *nrt1.5-5* mutant growing in hydroponic solutions with limited NO_3^- supply accumulated less K in shoots, although the expression of *SKOR* was increased in the roots of *nrt1.5-5* (Drechsler *et al.* 2015). Therefore, a NO_3^- dependent job sharing between SKOR and NRT1.5 in the root-to-shoot translocation of K^+ is conceivable.

This study showed that under low NO_3^- (1 mM) conditions, *skor-2* accumulated comparable K content as its wild-type level (Figure 22). This observation with *skor-2* mutant is consistent with the study of Li *et al*. (2017), as neither leaf chlorosis phenotype nor the reduction of K content were observed in *skor* mutant under K^+ limitation. However, it has been shown that K content in *skor-1* mutant, which is in the Wassilewskija background, was dramatically decreased (Gaymard *et al.* 1998). This discrepancy might be attributed to the different growth conditions. Since *skor-1* plants were grown on substrate with unknown NO_3^- to K^+ ratio, therefore, no direct comparison of phenotypes of *skor* mutants could be made.

In contrast with *skor-2*, the K concentration in *nrt1.5-5* mutants was always lower than in the wild type, even at a 10-fold excess of K^+ over NO_3^- (1/10/1, N/K/P [mM], Figure 22), indicating that, irrespective of the K^+ supply, primarily NRT1.5 but not SKOR is involved in root-to-shoot translocation of K^+ under low NO_3^- concentrations. Notably, when K^+ supply was sufficient (10 mM), although the K concentration in *nrt1.5* shoots was significantly lowered than in wild type, no leaf chlorosis phenotype of *nrt1.5* was

shown, which is probably due to the higher than 1% of DW K concentration in shoots of *nrt1.5* mutant. This could also explain why no leaf chlorosis phenotype of *nrt1.5* mutant was observed by Li *et al.* (2017) when growing on plates with high K^+ concentration.

The reduction of shoot K concentrations in *skor-2* occurred at high NO_3^-/K^+ ratio (10/1 and 20/1) conditions (Figure 22, 23A). It thus seems that SKOR is most important for the root-to-shoot translocation of K^+ when the transport of NO_3^- toward the xylem is not restricted while the supply with the counterion K^+ is limited, which suggests that the abundance or activity of SKOR might be regulated by availability of NO_3^- and K^+. By contrast, when the NO_3^-/K^+ ratio is high, NRT1.5 is not mainly involved in root-to-shoot transport of K^+, because no significant reduction of shoot K was observed in *nrt1.5* mutants (Figure 22, 23). Similar observations were also shown by Li *et al.* (2017) and Meng *et al.* (2016) that along with the increment in NO_3^- supply, K concentration in *nrt1.5* plants restored to the wild-type level. Interestingly, inconsistent with the observations with *Arabidopsis* plants, Li *et al.* (2017) showed that the external NO_3^- concentration did not affect the K^+ transport function of NRT1.5 in *Xenopus* oocyte. Therefore, it is tempting to argue that high NO_3^- availability may affect the activity of NRT1.5 through regulating its interaction with other proteins, alternatively, high NO_3^- concentration may regulate the activity of other potassium transporters or channels such as SKOR, which were missing in the oocyte system. It has been known that SKOR activity is influenced by a variety of triggers, including membrane depolarization (Gaymard *et al.* 1998), pH (Lacombe *et al.* 2000), intracellular and external K^+ status (Johansson *et al.* 2006; Liu *et al.* 2006), as well as reactive oxygen species in the form of hydrogen peroxide (Garcia-Mata *et al.* 2010). This study showed that *SKOR* was strongly induced by high concentration of NO_3^- (10 mM), whereas it was not altered by K^+ availability (Figure 24). The strong upregulation of *SKOR* by NO_3^- is consistent with the observation by Xu *et al*. (2016), moreover, it is also in accordance with the observation that K accumulation in *skor-2* was significantly lower than that in wild type at high NO_3^- supply (Figure 22). Unlike *SKOR*, *NRT1.5* transcript was relatively

constant under various N/K supply in this study (Figure 24). However, Lin *et al.* (2008) showed that *NRT1.5* was downregulated by K^+ limitation and was induced by the presence of NO_3^-. It is noteworthy that in their study, plant age, medium composition and growth conditions were different from this study, therefore, their findings do not contradict with results presented in this study. It is conceivable that at high NO_3^- supply (10/1/1, 20/1/1 and 10/10/1, N/K/P [mM]), K reduction in *nrt1.5* mutant may be compensated by the enhanced SKOR activity, therefore, *nrt1.5-5* and Col-0 plants accumulated comparable shoot K amount (Figure 22, 23). The study of expression pattern of *NRT1.5* and *SKOR* under different N/K supply will be helpful to understand how they work synergistically on root-to-shoot translocation of K^+ under certain nutrient conditions.

The importance of both proteins for root-to-shoot translocation of K^+ is illustrated by the observation that, under high equimolar NO_3^- and K^+ supplies (10/10/10 and 10/10/1, N/K/P [mM]), both single mutants reached K concentrations close to that of wild-type plants, whereas the *nrt1.5-5/skor-2* double mutant failed to do so (Figure 22).

To sum it up, this study demonstrated a nitrate-dependent interplay of NRT1.5 and SKOR on K^+ root-to-shoot translocation, which is important for K^+ homeostasis in shoots. However, root-to-shoot translocation of K^+ was not completely blocked in the *nrt1.5-5/skor-2* double mutant, indicating the activity of additional K^+ transport systems in the root vasculature. Fox example, a recent study showed that KUP7 may also contribute to K^+ xylem loading under low K^+ avaliablility conditions (Han *et al.* 2016). In addition to *NRT1.5*, the knockout mutant of *NPF2.3*, a recently characterized nitrate excretion transporter, also exhibited the decreased K^+ translocation to shoots (Taochy *et al.* 2015), supporting the presence of a regulatory loop of NO_3^- and K^+ xylem transport. The job sharing of NRT1.5 and SKOR examined in this study may be of great importance for plants to regulate the K^+ root-to-shoot translocation under fluctating nutritional conditions.

4.5 NRT1.5 affects potassium root-to-shoot transfer independent on SKOR

The indistinguishable growth performances between yeast cells expressing *SKOR* alone and cells expressing both *SKOR* and *NRT1.5* indicates that NRT1.5 does not functionally interact with SKOR (Figure 16). Moreover, it has been shown that several ion-homeostasis related genes were deregulated in *nrt1.5-5* roots (Drechsler *et al.* 2015), however, these genes were not regulated in *skor-2* mutant under all tested N/K regimes (Figure 25). These results indicate that the K^+ root-to-shoot transfer controlled by NRT1.5 and SKOR are two different mechanisms. This speculation could be corroborated by the findings that: 1) the split-ubiquitin assay showed no protein-protein interaction between NRT1.5 and SKOR in yeast (Drechsler, Dissertation 2016); 2) unlike *nrt1.5* mutant which showed inhibited LR development by K^+ deprivation, *skor-2* mutant gained normal root growth like wild-type plants (Figure 27); 3) Li *et al*. (2017) showed that *skor* mutant did not exhibit a K^+-deficiency phenotype. Even though Li *et al.* (2017) successfully demonstrated the K^+ export function of NRT1.5 in heterologous systems *Xenopus* oocyte and in yeast, it is not yet clear why *nrt1.5* mutant and *skor* mutant have different phenotypes at K^+ deprivation. Interestingly, the high upregulation of *SLAH1* and *SLAH3* in roots of *nrt1.5-5* only occurs at low NO_3^- supply (1 mM). In contrast, these two genes were only marginally upregulated in roots of *nrt1.5-5* at high NO_3^- supply (10 mM) (Figure 25A), implying that the strong upregulation of these two *SLAH* genes may contribute to the K reduction in the *nrt1.5-5* shoots at low NO_3^- availabilities.

4.6 Interaction complex NRT1.5-SLAH1-SLAH3?

By using the split-ubiquitin method, eight NRT1.5-interacting partners were identified in the heterologous yeast system (Drechsler, Dissertation 2016). In this study, BiFC assay was further applied to confirm four of the NRT1.5-interacting partners SLAH1, SLAH3, AHA2 and NRT1.10 *in planta*. All four potential candidates demonstrated clear

reconstituted fluorescence signal at the plasma membrane of tobacco epidermal cells (Figure 29, 30).

SLAH3 itself is a NO_3^- and Cl^- efflux channel (Geiger *et al.* 2011) and it can inhibit the inward K^+ conduct through direct protein-protein interaction with KAT1, and therefore influences the stomata closure (Zhang *et al.* 2016). SLAH1 modifies Cl^- transport through activating SLAH3 (Cubero-Font *et al.* 2016). Based on the reported transport function of NRT1.5 and SLAH1/SLAH3, it is likely that the interaction between NRT1.5, SLAH1 and SLAH3 could influence the anion (NO_3^- and Cl^-) transport activities of plants. However, no reduction in total N concentration was detected in rosettes of *slah3* mutant or in the double mutant *nrt1.5-5/slah3* compared to wild type (Figure 34B). This observation is consistent with the recent finding of Cubero-Font *et al.* (2016) that no reduction of NO_3^- was observed in xylem sap of *slah3* mutant. The unchanged N concentration in mutant plants may reflect the high redundancy of nitrate transporters. Based on the reported interaction between SLAH3 and KAT1, the formation of an interacting complex NRT1.5-SLAH3-KAT1 is conceived. Therefore, the potassium transport may be affected by NRT1.5-SLAH3 interaction through modulating KAT1 activity. In addition, the AP2/ERF transcription factor *RAP2.11* is induced by K^+ deficiency and regulates the expression of numerous genes involved in the K^+ deficient signaling cascade including *HAK5* (Kim *et al.* 2012). Both *SLAH3* and *NRT1.5* were moderately induced by the *RAP2.11* overexpression in roots (Kim *et al.* 2012), which further supports that the NRT1.5-SLAH3 complex might regulate K^+ homeostasis. Soil grown *slah3* mutant plants demonstrated no shoot morphological changes compared to Col-0 under various N/K regimes (Figure 34A). No significant K reduction in shoots of *slah3* was detected, although at low NO_3^- and high K^+ supply (1/10 N/K [mM]), K in *slah3* shoots was slightly deceased compared to Col-0 (Figure 35). These results suggest that the disruption of *SLAH3* itself does not apparently affect K^+ root-to-shoot transfer. However, interestingly, under low NO_3^- and high K^+ supply (1/10 N/K [mM]), an additive effect of K reduction was observed in shoots of the double mutant *nrt1.5-5/slah3* in comparison with that of *nrt1.5-5* and *slah3* mutant, although the difference

was not statistically significant (Figure 35). Consistent with the reduced K concentration, the double mutant *nrt1.5-5/slah3* developed a more severe leaf chlorosis phenotype than *nrt1.5-5* at this condition (Figure 34A). These observations indicate that, when NO_3^- supply is limited but K^+ supply is ample, SLAH3 might be regulated in the *nrt1.5* mutant, either transcriptionally or post-transcriptionally, and therefore indirectly influence the K^+ transport. The statistical insignificance of K concentration between *nrt1.5-5* and the *nrt1.5/slah3* double mutant might be caused by the late timepoint for harvesting material, at which the K concentration in all plant lines has become too low to be distinguishable. To verify this presumption, several earlier timepoints should be adopted to harvest plant material for detecting K concentration.

Besides the interaction with SLAH3, NRT1.5 could also interact with SLAH1 *in planta* (Figure 29D). The heteromerization of SLAH1/SLAH3 has been demonstrated recently (Cubero-Font *et al.* 2016). Moreover, *NRT1.5*, *SLAH1* and *SLAH3* are co-expressed in root pericycle cells (Lin *et al.* 2008; Cubero-Font *et al.* 2016), therefore, it is conceivable to speculate the formation of the NRT1.5-SLAH1-SLAH3 complex. The generation of the *nrt1.5/slah1/slah3* triple mutant will be helpful to interpret the physiological meaning of their physical interactions. Up to now, no *slah1* knockout mutant (in Col-0 background) is available. In future experiments, the CRISPR-Cas9 systems should be applied to generate a *slah1* mutant as well as the double or triple mutants.

4.7 Could AHA2 and NRT1.5 activate each other?

Another potential NRT1.5-interacting partner verified by both split-ubiquitin and BiFC is the plasma membrane H^+-ATPase AHA2. Through generating a chemical proton gradient, the plasma membrane H^+-ATPase is supposed to play a role in phloem loading (Blatt 2004), regulating the stomatal aperture (Zeiger 1983; Merlot *et al.* 2007), energizing nutrient uptake in the roots (Michelet and Boutry 1995) as well as regulating the growth of root hairs (Zhu *et al.* 2015) and pollen tubes (Pertl-Obermeyer *et al.*

2014). It was also suggested that the loading of root xylem with inorganic nutrients is dependent on the active transport process driven by the H^+-ATPase (Paretssoler *et al.* 1990). Among eleven AHA members in *Arabidopsis*, *AHA2* is the predominant proton pump expressed in the roots (Haruta *et al.* 2010). It is expressed in roots in epidermis, cortex, phloem, root hair and xylem (Fuglsang *et al.* 2007), indicating a role in the xylem loading of the nutrients. In addition, the plasma membrane H^+-ATPase is also critical for maintaining the membrane potential (Falhof *et al.* 2016). Consistent with its function in extruding proton out of cytoplasm, it was suggested that *aha2* mutant has a more depolarized membrane potential based on its susceptibility to high external K^+ concentration and resistance to HygB (Haruta *et al.* 2010).

In this work, *aha2* mutant grew indistinguishable from the wild type under all N/K regimes on soil (Figure 37), which is in accordance with the previous report that *aha2* mutant grew normally under standard conditions on plates (Haruta *et al.* 2010). However, the fresh weight gain of *aha2* mutant was significantly lower compared to that of Col-0 under several nutrient conditions (Figure 38B), indicating the importance of AHA2 for increasing plant biomass. This observation is consistent with the previous report that the overexpression of *AHA2* in guard cells promoted stomatal opening and enhanced plant growth (Wang *et al.* 2014). This study showed that the transcript of *AHA2* in Col-0 roots was enhanced by high K^+ availability but not regulated by NO_3^- supply (Figure 39). The constant expression of *AHA2* at different NO_3^- concentrations is consistent with the previous study of Maathuis *et al*. (2003). However, a recent study reported that *AHA2* expression was induced at both transcriptional and protein level by low NO_3^- availability (Mlodzinska *et al.* 2015). This discrepancy may be attributed to the different growth conditions and the age of plants.

The structure and the post-translational modification of AHA2 has been intensively investigated in the past (Morth *et al.* 2011). The C-terminal cytoplasmic domain of AHA2 serves as an autoinhibitory domain (Palmgren 2001), which is important for the phosphorylation and the binding of 14-3-3 proteins (Falhof *et al.* 2016). For instance, the phosphorylation of the penultimate residue Thr-947 creates a binding site for 14-

3-3 proteins and release the autoinhibition of AHA2. In addition to 14-3-3 proteins, the C-terminal of AHA2 also interacts directly with PSY1R, a leucine-rich-repeat receptor kinase, and PP2C-D phosphatases. The BiFC experiment in this study confirmed the protein-protein interaction between NRT1.5 and AHA2 *in planta* (Figure 29B), however, it is not clear yet that whether NRT1.5 also interacts with AHA2 in the C-terminal region.

The *nrt1.5* plants phenocopied *aha2* mutants with respect to the resistance to HygB treatment (Figure 18, 36) and susceptibility to high external K^+ treatment (Figure 18) (Haruta and Sussman, 2012), indicating that the membrane potential in both mutants appears to be altered in a similar way. Interestingly, *nrt1.5-5* mutant was more resistant to HygB treatment compared to *aha2* mutant, indicating the more depolarized plasma membrane of *nrt1.5-5* (Figure 36). Since the expression level of *AHA2* was indistinguishable in roots of *nrt1.5-5* and in Col-0 (Figure 37), thus the increased depolarization in *nrt1.5-5* is probably not caused by the alteration in *AHA2* transcript. Based on the BiFC result, it is tempting to hypothesize that NRT1.5 could activate AHA2 through their protein-protein interaction. Because of the high redundancy of AHAs, other AHAs might be post-transcriptionally modulated in *aha2* mutant to compensate the loss-function of AHA2. Whereas in *nrt1.5-5*, compensation of other AHAs does not occur because of the presence of the AHA2, although in the nonactivated form. This hypothesis could explain the stronger resistance of *nrt1.5-5* to HygB treatment than *aha2* mutant. However, this does not explain the indistinguishable growth pattern between *nrt1.5-5* and the *nrt1.5-5/aha2* double mutant (Figure 36). One reason might be the concentration of HygB in this experiment is not high enough to provoke the growth differences between *nrt1.5-5* and the double mutant. To verify whether NRT1.5 indeed affects the AHA2 activity, in future experiments, it is worth examining the H^+-ATPase activity in *nrt1.5-5*, *35Sp::NRT1.5* overexpression lines as well as in the *nrt1.5-5/aha2* double mutant. Alternatively, electrophysiology techniques like patch clamp could be used to record the membrane potential differences between *Xenopus* oocytes expressing *NRT1.5*, *AHA2* and both of them. Moreover, it would be interesting to investigate whether the expression of mutated *NRT1.5* which lost K^+

export function could change the membrane potential of yeast cells or not.

It has been shown that the expression of potassium transporter *HAK5* and cation/H^+ antiporter 17 (*CHX17*) in the *aha2* mutant is enhanced by more than 2-fold (Haruta and Sussman 2012), supporting the speculation that AHA2 is important for K^+ transport through regulating plasma membrane potential. K^+ outward rectifier SKOR and GORK are well known to be activated by plasma membrane depolarization, which is the expected situation for *aha2* mutant and *nrt1.5* mutant. However, the supposedly activated SKOR by depolarization did not promote the K^+ root-to-shoot transfer in *aha2* mutant in any utilized fertilization regime (Figure 39A). Interestingly, under high NO_3^- and low K^+ supply (10/1 N/K [mM]), the K amount in *aha2* shoots was significantly reduced compared to that of Col-0, though it was not as low as that in *nrt1.5-5*. The similar trend was also observed under high NO_3^- and high K^+ (10/10 N/K [mM]) condition, although the K concentration difference between *aha2* and Col-0 was not statistically significant (Figure 39A). These findings imply that, under certain circumstances, for example, at high NO_3^- supply (10 mM), AHA2 might regulate the activity of NRT1.5 through their physical interaction, therefore, K amount was reduced in *aha2* shoots due to the inhibition of the NRT1.5 activity. The observation that no additive K reduction was observed in the *nrt1.5-5/aha2* double mutant is in agreement with this assumption.

Results obtained in this work hint that NRT1.5 and AHA2 might activate each other through their interaction, by this means that the membrane potential and K^+ transport are affected in their single mutants. Since the K reduction in *aha2* shoots only occurs at certain high NO_3^- supply, it is possible that the interaction between NRT1.5 and AHA2 might be regulated by NO_3^- availability. There are some questions remain to be solved in the future study. First, it is worth finding out the protein domain responsible for the interaction between NRT1.5 and AHA2. In addition, it would be interesting to investigate whether their interaction is dependent on the nitrate/potassium transport of NRT1.5 or not. These answers will be helpful to interpret the biological meaning of their interaction.

4.8 NRT1.5 is regulated by CIPK23-CBL1/CBL9 complex

The CBL-CIPK signaling modules have been shown to be able to interact with a number of transporting proteins involved in nutrient translocation and homeostasis (Li *et al.* 2009). CIPK23 is the most well-known CIPK mainly involved in regulating the transport of K^+ and NO_3^-. Recent studies showed that with the help of CBLs, CIPK23 interacts with nitrate transporter NRT1.1 and nitrate-specific anion channel SLAH2 (Ho *et al.* 2009; Maierhofer *et al.* 2014). Moreover, CIPK23 is strongly upregulated by K^+ deprivation (Cheong *et al.* 2007) and it also interacts with AKT1 and HAK5 which are two most important transporters responsible for K^+ uptake (Li *et al.* 2006; Ragel *et al.* 2015). The split-ubiquitin study of this work demonstrated that CIPK23-CBLs complex can also interact with NRT1.5 in yeast (Figure 31). The *Arabidopsis cipk23* mutant and the *cbl1/cbl9* double mutant demonstrated the sensitivity to low K^+ (Cheong *et al.* 2007), which is similar to the phenotype of *nrt1.5* mutants observed in this study (Figure 5). This similarity may indicate that CIPK23-CBL1/CBL9 complex may regulate the K^+ root-to-shoot translocation assumed by NRT1.5. In addition, *cipk23* mutant showed the stronger resistance to drought stress than wild type (Cheong *et al.* 2007), which is similar to the behavior of *nrt1.5* mutant observed by Chen *et al.* (2012). These findings support the speculation that NRT1.5 activity may be regulated by CIPK23-CBL1/CBL9 complex. The interaction between NRT1.5 and CIPK23-CBL1/CBL9 complex indicates that CIPK23 may act as a common component modulating the uptake and translocation of NO_3^- and K^+. In future studies it would be interesting to investigate whether the NO_3^-/K^+ transport activity or selectivity of NRT1.5 could be regulated by CIPK23-CBL1/CBL9 complex under different NO_3^- and K^+ availabilities.

4.9 Overexpression studies of *NRT1.5* in *Arabidopsis*

Overexpressing a transporter driven by a constitutive promoter sometimes failed, for example, the attempt to overexpress *PHO1* driven by CaMV *35S* promoter failed to

increase the *PHO1* expression in wild type (Stefanovic *et al.* 2011). In this study, *35S* promoter was used to overexpress *NRT1.5* in wild type Col-0. The *NRT1.5* expression was indeed increased in both shoots and roots of three independent transgenic lines (Figure 11A). Since *NRT1.5* was not fused to a tag in the *35Sp::NRT1.5* construct, therefore, it is difficult to detect the NRT1.5 protein in overexpression lines. However, *35Sp::NRT1.5* overexpression lines were more sensitive to HygB treatment, which was the opposite response of *nrt1.5* mutants (Figure 18B). This response indirectly proved the NRT1.5 protein was indeed increased. Interestingly, these overexpressing lines showed reduced LR density at K^+ deprivation (Figure 11B), and reduced K^+ concentrations in shoots at low NO_3^- supply (Table 13, Figure 41), which are the same phenotypes of *nrt1.5* mutants. One plausible explanation would be the misexpression of *NRT1.5* in cell layers where it was not supposed to express in wild-type plants. Alternatively, these similar phenotypes may reflect the tight regulation of K^+ root-to-shoot translocation. Similar phenomenon has also been observed for the study of SLAC1. K_{in}^+-channel currents were reduced in a similar way in *slac1* mutant and in *SLAC1* or *SLAH3* overexpression lines (Laanemets *et al.* 2013; Zhang *et al.* 2016). Another speculation is that the increased NRT1.5 protein presumably interferes at some level with its interaction complex, acting as an antimorph (Prelich 2012). As has been observed for histone pair SPT5, SPT6 and SPT16, which function as part of multiprotein complexes. Overexpression of each of them causes the loss-of-function mutant phenotypes, whereas co-overexpressing the other histone pair restored the wild-type phenotype (Clarkadams and Winston 1987; Malone *et al.* 1991; Swanson *et al.* 1991). Since several proteins have been identified as interacting partners of NRT1.5 in yeast and *in planta*, it is conceivable that the *nrt1.5* mutant phenotypes observed in *35Sp::NRT1.5* overexpression lines are due to disrupting stoichiometry or disruption of the complexes.

4.10 Phytohormones regulate nitrate and potassium transporters

A close relationship between phytohormones and environmental signals such as nutrient availability has been demonstrated. For instance, it has been proposed that ABA, auxin and cytokinin (CK) are involved in the acquisition of N. Moreover, there may exist a tight link between phytohormones and K^+ signaling pathway (Pilot *et al.* 2003). Low K^+ availability leads to increases in JA and ABA, and decrease in CK and auxin (Schachtman 2015). Many genes related to hormone JA metabolism and signaling were also regulated by K^+ availability (Armengaud *et al.* 2004)

Arabidopsis seedlings grown on high concentration of NO_3^- generated more CK than those grown on low NO_3^- condition, suggesting the role of CK as a N status signal (Sakakibara *et al.* 2006). Moreover, it has been observed that CK treatment downregulated a lot of root-type NRTs, therefore, it was indicated that CK function as a root-to-shoot long distance signal of N supplement. The strong downregulation of *NRT1.1* and *NRT1.8* observed in this study is consistent with the previous observation (Kiba *et al.* 2011). *SLAH1* and *SLAH3* which is a potential contributor to NO_3^- root-to-shoot translocation, were also inhibited by 6-Benzylaminopurine (BAP). Since CK was thought as a repressor of genes responsive to many nutrient starvations (Rubio *et al.* 2009), the results suggest that *SLAH1* and *SLAH3* might be involved in NO_3^- starvation responses. The inhibition of *SKOR* was consistent with the previous finding (Pilot *et al.* 2003). Unlike *SKOR*, *HAK5* was induced by BAP. The response of *SKOR* and *HAK5* to BAP treatment is very similar to their response to ABA treatment (Figure 42). These results suggest that retaining more K^+ in roots through decreasing K^+ secretion into xylem by inhibiting *SKOR and* promoting K^+ uptake by inducing *HAK5* may be under the tight control.by various hormones.

Although ABA content is not affected by N amount, increasing evidences showed that ABA is involved in N signaling (Zhang *et al.* 2007). For example, ABA deficient and insensitive mutants lost the sensitivity to inhibitory effect on LRs growth by HN (Signora

et al. 2001). This study showed that *NRT1.1* was induced by ABA. The similar result was observed by Kita *et al.* (2011) under low NO_3^- (LN, 0.1 mM) supply. Together with the strong inhibition of *NRT1.5* (Figure 42), ABA might be in favor of the retention of NO_3^- in roots. In guard cells, ABA activates anion channel SLAC1 and subsequent anion efflux (Yamamoto *et al.* 2016). In accordance with this, we showed that the transcript of *SLAH1*, the homologue of *SLAC1*, was dramatically induced by ABA treatment. However, other two studies by Qiu *et al.* (2016) and Cubero-Font *et al.* (2016) observed the strong inhibition of *SLAH1* transcript by ABA treatment. It seems likely that this discrepancy results from different nutrient supplies, growth conditions, the age of plants and the treatment duration. It has been suggested that through modulating K^+ channel activity, application of ABA was in favor of reducing K^+ transport to xylem vessel and enhancing K^+ accumulation in the root (Roberts and Snowman, 2000). Consistent with this notion, our results showed that *SKOR* was strongly inhibited by ABA, which has been also observed in other studies (Gaymard *et al.* 1998; Tester 1999). Interestingly, potassium importer *AKT1* was not regulated at all, whereas *HAK5* was strongly induced by ABA treatment (Figure 42). It was observed that ABA had no effect on K^+ uptake by the epidermis (Roberts and Snowman 2000), therefore, the upregulation of *HAK5* might indicate a link between ABA and K^+ deprivation adaption.

JA and MeJA inhibited expression of *NRT1.5* whereas upregulated expression of *NRT1.8*, which is consistent with the earlier finding (Chen *et al.* 2012). It has been shown that this regulation pattern of *NRT1.5* and *NRT1.8* was controlled via the ethylene/JA-NRT module, and it helps plants to keep NO_3^- in root under adverse growth conditions, in a nitrate reductase-dependent manner (Zhang *et al.* 2014). JA was also suggested to be involved in nutrient recycling under K^+ deprivation stress (Rubio *et al.* 2009). The downregulation of *HAK5* and *SKOR* indicates that JA and MeJA treatments lead to the reduction of K in shoots under K^+ deprivation.

To date, no experimental evidences support the connection between GA or SA signalling and N/K homeostasis. Under both high NO_3^- (HN, 10 mM) and LN conditions, GA and SA hardly affected the expression of both root-and shoot-type NRTs (Kiba *et*

al. 2011). Similar results were observed for expression pattern of *NRT1.1*, *NRT1.5* and *NRT1.8* by GA_3 treatment in this study (Figure 42). *SLAH1* and *SLAH3* were strongly induced and inhibited by GA_3, respectively, indicating different roles of two proteins in GA_3 signalling responses. In addition to acting an important component in biotic stress tolerance mechanism, SA is also supposed to be involved in plant abiotic responses like salinity tolerance (Ashraf *et al.* 2010). Shoot Cl^- content is related to salinity sensitivity (Teakle and Tyerman 2010). Therefore, the dramatic downregulation of *SLAH1* by SA supports the potential role of SLAH1 in the salinity stress adaption.

It has been demonstrated that LN availability increases IAA content in *Arabidopsis* roots (Walch-Liu *et al.* 2006). However, the application of auxins had no influence on the lateral root growth of plants growing under HN supply, suggesting auxin might not be directly involved in NO_3^- signaling (Zhang *et al.* 2007). In this study, due to the big standard deviation, no obvious regulation of nitrate and potassium transporters could be concluded by IAA treatment (Figure 42).

It is worth noting that, in this study, 1/2 MS medium was used to support the growth of plants. It has been observed that under nutrient starvation conditions, responses of ion transporters to hormone treatment were even contrary to that under nutrient sufficient conditions. For example, Kiba *et al.* (2011) showed that the NO_3^- availability influenced the expression of nitrate transporter in response to CK treatment. At LN supply, the root-predominant expression of *NRT1.1* as well as the inhibition effect of *NRT1.1* by CK was abolished. Moreover, it has been noticed that the effects of ABA treatment on ion transport is sensitive to nutrient status of roots (Roberts and Snowman, 2000). Therefore, to better understand the connection between phytohormone and nutrient transport, in future studies, gene expression analysis with plants growing under NO_3^- and K^+ starvation should be included to compare the difference of these datasets.

5 Summary

Potassium (K) and nitrogen (N) are two of the most important macroelements needed by plants. After the absorption through roots, nitrate (NO_3^-) and K^+ undergo the long-distance root-to-shoot transport. Xylem loading is a critical step for the root-to-shoot translocation of nutrients. In *Arabidopsis thaliana*, NPF7.3/NRT1.5 and SKOR are responsible for the xylem loading of NO_3^- and K^+, respectively. Our group has demonstrated the K concentration in shoots of *nrt1.5* knockout mutants was dramatically decreased compared to wild type at low NO_3^- supply, suggesting NRT1.5 is involved in K^+ transport in a NO_3^--dependent manner. The aim of this work is to investigate the role of NRT1.5 in the root-to-shoot translocation of K^+ in *Arabidopsis.*

In this work, we show that NRT1.5 is important for the lateral root development of *Arabidopsis* at K^+ deprivation conditions. Lateral root density of *nrt1.5* knockout mutants was significantly reduced by K^+ limitation compared to wild type. No K^+ transport activity of NRT1.5 was not observed in *Saccharomyces cerevisiae*. However, yeast BYT12 cells expressing *NRT1.5* were more sensitive to hygromycin B. Similar and the opposite responses to HygB were also observed for *Arabidopsis 35Sp::NRT1.5* overexpression lines and *nrt1.5* mutant plants, respectively. These results indicate that expression of *NRT1.5* results in the hyperpolarization of the plasma membrane in yeast and in *Arabidopsis*.

Phenotypical and the elemental analysis with single and the double mutant plants suggest a NO_3^--dependent job-sharing of NRT1.5 and SKOR in K^+ root-to-shoot translocation: NRT1.5 is important when external NO_3^- amount is limited, whereas SKOR is predominant at high NO_3^- concentrations. The protein-protein interaction between NRT1.5 and SLAH1, SLAH3 and AHA2 were verified in *Nicotiana benthamiana* by BiFC. Moreover, the split-ubiquitin assay showed the interaction between NRT1.5 and the CIPK23-CBL1/CBL9 complex in yeast. To investigate the physiological meanings of the interaction, double mutants *nrt1.5/slah3* and *nrt1.5/aha2* were generated and grown under various NO_3^- and K^+ supply conditions for

phenotypical and physiological studies.

At last, the expression profiles of several nitrate and potassium transporters in response to various phytohormone treatments were studied. ABA is probably in favor of the retention of nutrients in roots through upregulating nitrate and potassium importers (*NRT1.1, HAK5*) and inhibiting the expression of transporters for xylem loading (*SKOR*, *NRT1.5*). Cytokinin BAP inhibited expression of all tested nitrate transporters and *SKOR* but stimulated *HAK5*. *SLAH1* expression was strongly impaired by SA treatment. These observations will be helpful to understand the NO_3^- and K^+ transport mediated by phytohormone signals.

6 Zusammenfassung

Kalium (K) und Stickstoff (N) sind zwei der wichtigsten Makroelemente, die Pflanzen benötigen. Nach der Aufnahme in die Wurzeln durchlaufen Nitrat (NO_3^-) und K^+ den Ferntransport von den Wurzeln zu den oberirdischen Sprossorganen. Die Beladung des Xylems ist ein kritischer Schritt bei der Translokation von Nährstoffen von der Wurzel in den Spross. In *Arabidopsis thaliana* sind NPF7.3/NRT1.5 und SKOR für die Beladung des Xylemsmit NO_3^- und K^+ verantwortlich. Unsere Gruppe hat nachgewiesen, dass *nrt1.5* Knockout Mutanten bei niedriger NO_3^- Versorgung im Vergleich zum Wildtyp signifikant geringere Kaliumkonzentrationen im Spross aufweisen. Dies deutet darauf hin, dass NRT1.5 in einer NO_3^--abhängigen Weise am K^+ Transport beteiligt ist. Das Ziel dieser Arbeit war es, die Rolle des NRT1.5 Proteins bei der Translokation von K^+ in *Arabidopsis* zu untersuchen.

In dieser Arbeit zeigten wir, dass NRT1.5 für die laterale Wurzelentwicklung von *Arabidopsis* unter K^+ Mangelbedingungen wichtig ist. So war die Anzahl der Lateralwurzeln bei den *nrt1.5* Knockout Mutanten unter Kaliummangel im Vergleich zum Wildtyp signifikant reduziert. In *Saccharomyces cerevisiae* wurde keine K^+ Transportaktivität von NRT1.5 beobachtet. Hefe BYT12 Zellen, die NRT1.5 exprimieren, waren jedoch gegenüber hygromycin B empfindlicher. Ähnliche und entgegengesetzte Reaktionen auf HygB wurden auch für *Arabidopsis 35Sp::NRT1.5*-Überexpressionslinien bzw. *nrt1.5* Knockout Pflanzen beobachtet. Diese Ergebnisse zeigen, dass die Expression von NRT1.5 zu einer Hyperpolarisierung der Plasmamembran in Hefe und in *Arabidopsis* führt.

Die phänotypischen Untersuchungen und Elementanalysen der Einzel- und Doppelmutanten weisen auf eine Nitrat-abhängige Arbeitsteilung von NRT1.5 und SKOR bei der K^+ Translokation zwischen Wurzel und Sprosshin: die NRT1.5 Funktion ist essentiell, wenn die externe NO_3^- Menge limitiert ist, während die SKOR Funktion bei hohen NO_3^- Konzentrationen dominiert. Die Protein-Protein-Interaktion zwischen NRT1.5 und SLAH1, SLAH3 und AHA2 wurde in *Nicotiana benthamiana* durch BiFC

verifiziert. Darüber hinaus dokumentierte der Split-Ubiquitin Assay die Interaktion zwischen NRT1.5 und dem CIPK23-CBL1/CBL9-Komplex in Hefe. Um die physiologische Bedeutung der Interaktionen zu untersuchen, wurden die Doppelmutanten *nrt1.5/slah3* und *nrt1.5/aha2* generiert und mit verschiedenen NO_3^-- und K^+- Gaben für phänotypische und physiologische Studien kultiviert.

Zuletzt wurden die Expressionsprofile verschiedener Nitrat- und Kaliumtransporter als Antwort auf verschiedene Phytohormonbehandlungen untersucht. ABA fördert vermutlich die Nährstoffspeicherung in den Wurzeln durch eine Heraufregulierung der Nitrat- und Kaliumimporteure (*NRT1.1*, *HAK5*) und die Hemmung der Expression von Transportern für die Xylembeladung (*SKOR*, *NRT1.5*). BAP inhibierte die Expression von allen getesteten Nitrattransportern und SKOR, stimulierte jedoch die *HAK5* Expression. Die *SLAH1* Expression wurde durch SA-Behandlung stark inhibiert. Diese Beobachtungen werden hilfreich sein, um die NO_3^-- und K^+ Transport, die durch Phytohormonsignale vermittelt werden, zu verstehen.

7 References

Achard, P., Vriezen, W. H., Van Der Straeten, D. and Harberd, N. P. (2003). Ethylene regulates *Arabidopsis* development via the modulation of DELLA protein growth repressor function. Plant Cell 15(12): 2816-2825.

Alboresi, A., Gestin, C., Leydecker, M. T., Bedu, M., Meyer, C. and Truong, H. N. (2005). Nitrate, a signal relieving seed dormancy in *Arabidopsis*. Plant, Cell & Environment 28(4): 500-512.

Almagro, A., Lin, S. H. and Tsay, Y. F. (2008). Characterization of the *Arabidopsis* nitrate transporter NRT1.6 reveals a role of nitrate in early embryo development. Plant Cell 20(12): 3289-3299.

Andersen, T. G., Nour-Eldin, H. H., Fuller, V. L., Olsen, C. E., Burow, M. and Halkier, B. A. (2013). Integration of biosynthesis and long-distance transport establish organ-specific glucosinolate profiles in vegetative *Arabidopsis*. Plant Cell 25(8): 3133-3145.

Anderson, J. A., Huprikar, S. S., Kochian, L. V., Lucas, W. J. and Gaber, R. F. (1992). Functional expression of a probable *Arabidopsis thaliana* potassium channel in *Saccharomyces cerevisiae*. Proceedings of the National Academy of Sciences of the United States of America 89(9): 3736-3740.

Argueso, C. T., Ferreira, F. J. and Kieber, J. J. (2009). Environmental perception avenues: the interaction of cytokinin and environmental response pathways. Plant, Cell & Environment 32(9): 1147-1160.

Arino, J., Ramos, J. and Sychrova, H. (2010). Alkali metal cation transport and homeostasis in yeasts. Microbiology and Molecular Biology Reviews 74(1): 95-120.

Armengaud, P., Breitling, R. and Amtmann, A. (2004). The potassium-dependent transcriptome of *Arabidopsis* reveals a prominent role of jasmonic acid in nutrient signaling. Plant Physiology 136(1): 2556-2576.

Arvidsson, S., Kwasniewski, M., Riano-Pachon, D. M. and Mueller-Roeber, B. (2008). QuantPrime - a flexible tool for reliable high-throughput primer design for quantitative PCR. Bmc Bioinformatics 9.

Asami, T., Min, Y. K., Nagata, N., Yamagishi, K., Takatsuto, S., Fujioka, S., Murofushi, N., Yamaguchi, I. and Yoshida, S. (2000). Characterization of brassinazole, a triazole-type brassinosteroid biosynthesis inhibitor. Plant Physiology 123(1): 93-99.

Ashraf, M., Akram, N. A., Arteca, R. N. and Foolad, M. R. (2010). The physiological, biochemical and molecular roles of brassinosteroids and salicylic acid in plant processes and salt tolerance. Critical Reviews in Plant Sciences 29(3): 162-190.

Balkos, K. D., Britto, D. T. and Kronzucker, H. J. (2010). Optimization of ammonium acquisition and metabolism by potassium in rice (*Oryza sativa* L. cv. IR-72). Plant, Cell & Environment 33(1): 23-34.

Barbier-Brygoo, H., De Angeli, A., Filleur, S., Frachisse, J. M., Gambale, F., Thomine, S. and Wege, S. (2011). Anion channels/transporters in plants: from molecular bases to regulatory networks. Annual Review of Plant Biology, 64(62): 25-51.

Barreto, L., Canadell, D., Petrezselyova, S., Navarrete, C., Maresova, L., Perez-Valle, J., Herrera, R., Olier, I., Giraldo, J., Sychrova, H., Yenush, L., Ramos, J. and Arino, J. (2011).

A genomewide screen for tolerance to cationic drugs reveals genes important for potassium homeostasis in *Saccharomyces cerevisiae*. Eukaryotic Cell 10(9): 1241-1250.

Baxter, I., Hosmani, P. S., Rus, A., Lahner, B., Borevitz, J. O., Muthukumar, B., Mickelbart, M. V., Schreiber, L., Franke, R. B. and Salt, D. E. (2009). Root suberin forms an extracellular barrier that affects water relations and mineral nutrition in *Arabidopsis*. Plos Genetics 5(5).

Blakely, L. M., Durham, M., Evans, T. A. and Blakely, R. M. (1982). Experimental studies on lateral root-formation in Radish seedling roots .I. general-methods, developmental stages, and spontaneous formation of laterals. Botanical Gazette 143(3): 341-352.

Blatt, M. R. (2004). Membrane transport in plants. First edition. CRC press.

Borovikova, D., Herynkova, P., Rapoport, A. and Sychrova, H. (2014). Potassium uptake system Trk2 is crucial for yeast cell viability during anhydrobiosis. Fems Microbiology Letters 350(1): 28-33.

Bottger, M. (1974). Apical Dominance in Roots of *Pisum sativum* L. Planta 121(3): 253-261.

Brault, M., Amiar, Z., Pennarun, A. M., Monestiez, M., Zhang, Z. S., Cornel, D., Dellis, O., Knight, H., Bouteau, F. O. and Rona, J. P. (2004). Plasma membrane depolarization induced by abscisic acid in *Arabidopsis* suspension cells involves reduction of proton pumping in addition to anion channel activation, which are both Ca^{2+} dependent. Plant Physiology 135(1): 231-243.

Caesar, K., Elgass, K., Chen, Z. H., Huppenberger, P., Witthoft, J., Schleifenbaum, F., Blatt, M. R., Oecking, C. and Harter, K. (2011). A fast brassinolide-regulated response pathway in the plasma membrane of *Arabidopsis thaliana*. Plant Journal 66(3): 528-540.

Casimiro, I., Marchant, A., Bhalerao, R. P., Beeckman, T., Dhooge, S., Swarup, R., Graham, N., Inze, D., Sandberg, G., Casero, P. J. and Bennett, M. (2001). Auxin transport promotes *Arabidopsis* lateral root initiation. Plant Cell 13(4): 843-852.

Cerezo, M., Tillard, P., Filleur, S., Munos, S., Daniel-Vedele, F. and Gojon, A. (2001). Major alterations of the regulation of root NO_3^- uptake are associated with the mutation of *Nrt2.1* and *Nrt2.2* genes in *Arabidopsis*. Plant Physiology 127(1): 262-271.

Chang, L., Ramireddy, E. and Schmulling, T. (2013). Lateral root formation and growth of *Arabidopsis* is redundantly regulated by cytokinin metabolism and signalling genes. Journal of Experimental Botany 64(16): 5021-5032.

Chen, C. Z., Lv, X. F., Li, J. Y., Yi, H. Y. and Gong, J. M. (2012). *Arabidopsis* NRT1.5 is another essential component in the regulation of nitrate reallocation and stress tolerance. Plant Physiology 159(4): 1582-1590.

Cheong, Y. H., Pandey, G. K., Grant, J. J., Batistic, O., Li, L., Kim, B. G., Lee, S. C., Kudla, J. and Luan, S. (2007). Two calcineurin B-like calcium sensors, interacting with protein kinase CIPK23, regulate leaf transpiration and root potassium uptake in *Arabidopsis*. Plant Journal 52(2): 223-239.

Chiba, Y., Shimizu, T., Miyakawa, S., Kanno, Y., Koshiba, T., Kamiya, Y. and Seo, M. (2015). Identification of *Arabidopsis thaliana* NRT1/PTR FAMILY (NPF) proteins capable of transporting plant hormones. Journal of Plant Research 128(4): 679-686.

Chiu, C. C., Lin, C. S., Hsia, A. P., Su, R. C., Lin, H. L. and Tsay, Y. F. (2004). Mutation of a nitrate transporter, AtNRT1:4, results in a reduced petiole nitrate content and altered leaf development. Plant & Cell Physiology 45(9): 1139-1148.

Chopin, F., Orsel, M., Dorbe, M. F., Chardon, F., Truong, H. N., Miller, A. J., Krapp, A. and

Daniel-Vedele, F. (2007). The *Arabidopsis* ATNRT2.7 nitrate transporter controls nitrate content in seeds. Plant Cell 19(5): 1590-1602.

Clarkadams, C. D. and Winston, F. (1987). The *SPT6* gene is essential for growth and is required for delta-mediated transcription in *Saccharomyces cerevisiae*. Molecular and Cellular Biology 7(2): 679-686.

Clough, S. J. and Bent, A. F. (1998). Floral dip: a simplified method for *Agrobacterium*-mediated transformation of *Arabidopsis thaliana*. Plant Journal 16(6): 735-743.

Colmenero-Flores, J. M., Martinez, G., Gamba, G., Vazquez, N., Iglesias, D. J., Brumos, J. and Talon, M. (2007). Identification and functional characterization of cation-chloride cotransporters in plants. Plant Journal 50(2): 278-292.

Corratge-Faillie, C. and Lacombe, B. (2017). Substrate (un)specificity of *Arabidopsis* NRT1/PTR FAMILY (NPF) proteins. Journal of Experimental Botany 68(12): 3107-3113.

Coskun, D., Britto, D. T. and Kronzucker, H. J. (2015). The nitrogen-potassium intersection: Membranes, metabolism, and mechanism. Plant, Cell & Environment 40: 2029-2041.

Crawford, N. M. and Glass, A. D. M. (1998). Molecular and physiological aspects of nitrate uptake in plants. Trends in Plant Science 3(10): 389-395.

Cubero-Font, P., Maierhofer, T., Jaslan, J., Rosales, M. A., Espartero, J., Diaz-Rueda, P., Muller, H. M., Hurter, A. L., Al-Rasheid, K. A., Marten, I., Hedrich, R., Colmenero-Flores, J. M. and Geiger, D. (2016). Silent S-type anion channel subunit SLAH1 gates SLAH3 open for chloride root-to-shoot translocation. Current Biology 26(16): 2213-2220.

David, L. C., Berquin, P., Kanno, Y., Seo, M., Daniel-Vedele, F. and Ferrario-Mery, S. (2016). N availability modulates the role of NPF3.1, a gibberellin transporter, in GA-mediated phenotypes in *Arabidopsis*. Planta 244(6): 1315-1328.

Dechorgnat, J., Nguyen, C. T., Armengaud, P., Jossier, M., Diatloff, E., Filleur, S. and Daniel-Vedele, F. (2011). From the soil to the seeds: the long journey of nitrate in plants. Journal of Experimental Botany 62(4): 1349-1359.

Desai, U. J. and Pfaffle, P. K. (1995). Single-step purification of a thermostable DNA-polymerase expressed in *Escherichia coli*. Biotechniques 19(5): 780-782, 784.

Dolan, L., Janmaat, K., Willemsen, V., Linstead, P., Poethig, S., Roberts, K. and Scheres, B. (1993). Cellular-organization of the *Arabidopsis thaliana* root. Development 119(1): 71-84.

Drechsler, N. (2016). Der Nitrattransporter AtNRT1.5/AtNPF7.3-Ein Schlüsselprotein in der Regulierung des pflanzlichen Kaliumhaushaltes. Doctoral Dissertation; Institute of Biology/Applied Genetics, Freie Universität Berlin.

Drechsler, N., Zheng, Y., Bohner, A., Nobmann, B., von Wiren, N., Kunze, R. and Rausch, C. (2015). Nitrate-dependent control of shoot K homeostasis by the Nitrate Transporter1/Peptide transporter family member NPF7.3/NRT1.5 and the stelar K^+ outward rectifier SKOR in *Arabidopsis*. Plant Physiology 169(4): 2832-2847.

Drew, M. C. (1975). Comparison of the effects of a localized supply of phosphate, nitrate, ammonium and potassium on the growth of the seminal root system and the shoot in barley. New Phytologist 75: 479-490.

Drew, M. C., Saker, L. R. and Ashley, T. W. (1973). Nutrient supply and the growth of the seminal root system in Barley. Journal of Experimental Botany 24: 1189-1202.

Dreyer, I., Horeau, C., Lemaillet, G., Zimmermann, S., Bush, D. R., Rodriguez-Navarro, A.,

Schachtman, D. P., Spalding, E. P., Sentenac, H. and Gaber, R. F. (1999). Identification and characterization of plant transporters using heterologous expression systems. Journal of Experimental Botany 50: 1073-1087.

Dreyer, I., Poree, F., Schneider, A., Mittelstadt, J., Bertl, A., Sentenac, H., Thibaud, J. B. and Mueller-Roeber, B. (2004). Assembly of plant *Shaker*-like K_{out} channels requires two distinct sites of the channel alpha-subunit. Biophysical Journal 87(2): 858-872.

Dubrovsky, J. G., Rost, T. L., Colon-Carmona, A. and Doerner, P. (2001). Early primordium morphogenesis during lateral root initiation in *Arabidopsis thaliana*. Planta 214(1): 30-36.

Falhof, J., Pedersen, J. T., Fuglsang, A. T. and Palmgren, M. (2016). Plasma membrane H^+-ATPase regulation in the center of plant physiology. Molecular Plant 9(3): 323-337.

Falkengren-Grerup, U., Mansson, K. F. and Olsson, M. O. (2000). Uptake capacity of amino acids by ten grasses and forbs in relation to soil acidity and nitrogen availability. Environmental and Experimental Botany 44(3): 207-219.

Fan, S. C., Lin, C. S., Hsu, P. K., Lin, S. H. and Tsay, Y. F. (2009). The *Arabidopsis* nitrate transporter NRT1.7, expressed in phloem, is responsible for source-to-sink remobilization of nitrate. Plant Cell 21(9): 2750-2761.

Filleur, S., Dorbe, M. F., Cerezo, M., Orsel, M., Granier, F., Gojon, A. and Daniel-Vedele, F. (2001). An *Arabidopsis* T-DNA mutant affected in *Nrt2* genes is impaired in nitrate uptake. FEBS Letters 489(2-3): 220-224.

Forster, J. C. and Jeschke, W. D. (1993). Effects of potassium withdrawal on nitrate transport and on the contribution of the root to nitrate reduction in the whole plant. Journal of Plant Physiology 141(3): 322-328.

Frink, C. R., Waggoner, P. E. and Ausubel, J. H. (1999). Nitrogen fertilizer: retrospect and prospect. Proceedings of the National Academy of Sciences of the United States of America 96(4): 1175-1180.

Fuglsang, A. T., Guo, Y., Cuin, T. A., Qiu, Q. S., Song, C. P., Kristiansen, K. A., Bych, K., Schulz, A., Shabala, S., Schumaker, K. S., Palmgren, M. G. and Zhu, J. K. (2007). *Arabidopsis* protein kinase PKS5 inhibits the plasma membrane H^+-ATPase by preventing interaction with 14-3-3 protein. Plant Cell 19(5): 1617-1634.

Garcia-Mata, C., Wang, J., Gajdanowicz, P., Gonzalez, W., Hills, A., Donald, N., Riedelsberger, J., Amtmann, A., Dreyer, I. and Blatt, M. R. (2010). A minimal cysteine motif required to activate the SKOR K^+ channel of *Arabidopsis* by the reactive oxygen species H_2O_2. Journal of Biological Chemistry 285(38): 29286-29294.

Gaymard, F., Cerutti, M., Horeau, C., Lemaillet, G., Urbach, S., Ravallec, M., Devauchelle, G., Sentenac, H. and Thibaud, J. B. (1996). The baculovirus/insect cell system as an alternative to *Xenopus oocytes* - first characterization of the AKT1 K^+ channel from *Arabidopsis thaliana*. Journal of Biological Chemistry 271(37): 22863-22870.

Gaymard, F., Pilot, G., Lacombe, B., Bouchez, D., Bruneau, D., Boucherez, J., Michaux-Ferriere, N., Thibaud, J. B. and Sentenac, H. (1998). Identification and disruption of a plant shaker-like outward channel involved in K^+ release into the xylem sap. Cell 94(5): 647-655.

Geiger, D., Maierhofer, T., AL-Rasheid, K. A. S., Scherzer, S., Mumm, P., Liese, A., Ache, P., Wellmann, C., Marten, I., Grill, E., Romeis, T. and Hedrich, R. (2011). Stomatal closure by fast abscisic acid signaling is mediated by the guard cell anion channel SLAH3 and

the receptor RCAR1. Science Signaling 4(173).

Gierth, M., Maser, P. and Schroeder, J. I. (2005). The potassium transporter *AtHAK5* functions in K^+ deprivation-induced high-affinity K^+ uptake and *AKT1* K^+ channel contribution to K^+ uptake kinetics in *Arabidopsis* roots. Plant Physiology 137(3): 1105-1114.

Glass, A. D. M., Britto, D. T., Kaiser, B. N., Kronzucker, H. J., Kumar, A., Okamoto, M., Rawat, S. R., Siddiqi, M. Y., Silim, S. M., Vidmar, J. J. and Zhuo, D. (2001). Nitrogen transport in plants, with an emphasis on the regulation of fluxes to match plant demand. Journal of Plant Nutrition and Soil Science 164(2): 199-207.

Gojon, A. and Gaymard, F. (2010). Keeping Nitrate in the Roots: An unexpected requirement for cadmium tolerance in plants. Journal of Molecular Cell Biology 2(6): 299-301.

Gookin, T. E. and Assmann, S. M. (2014). Significant reduction of BiFC non-specific assembly facilitates *in planta* assessment of heterotrimeric G-protein interactors. Plant Journal 80(3): 553-567.

Granato, T. C. and Raper, C. D. (1989). Proliferation of maize (*Zea mays* L) roots in response to localized supply of nitrate. Journal of Experimental Botany 40(211): 263-275.

Grefen, C. and Blatt, M. R. (2012). A 2in1 cloning system enables ratiometric bimolecular fluorescence complementation (rBiFC). Biotechniques 53(5): 311-314.

Gruber, B. D., Giehl, R. F. H., Friedel, S. and von Wiren, N. (2013). Plasticity of the *Arabidopsis* root system under nutrient deficiencies. Plant Physiology 163(1): 161-179.

Gupta, N., Gupta, A. K., Gaur, V. S. and Kumar, A. (2012). Relationship of nitrogen use efficiency with the activities of enzymes involved in nitrogen uptake and assimilation of finger millet genotypes grown under different nitrogen inputs. The Scientific World Journal 2012.

Gutknecht, J. (1970). The origin of bioelectrical potentials in plant and animal cells. Am Zool 10(3): 347-354.

Han, M., Wu, W., Wu, W. H. and Wang, Y. (2016). Potassium transporter KUP7 is involved in K^+ acquisition and translocation in *Arabidopsis* toot under K^+-limited conditions. Molecular Plant 9(3): 437-446.

Haruta, M., Burch, H. L., Nelson, R. B., Barrett-Wilt, G., Kline, K. G., Mohsin, S. B., Young, J. C., Otegui, M. S. and Sussman, M. R. (2010). Molecular characterization of mutant *Arabidopsis* plants with reduced plasma membrane proton pump activity. Journal of Biological Chemistry 285(23): 17918-17929.

Haruta, M. and Sussman, M. R. (2012). The effect of a genetically reduced plasma membrane protonmotive force on vegetative growth of *Arabidopsis*. Plant Physiology 158(3): 1158-1171.

Hedrich, R. and Geiger, D. (2017). Biology of SLAC1-type anion channels - from nutrient uptake to stomatal closure. New Phytologist 216(1): 46-61.

Herdel, K., Schmidt, P., Feil, R., Mohr, A. and Schurr, U. (2001). Dynamics of concentrations and nutrient fluxes in the xylem of *Ricinus* communis - diurnal course, impact of nutrient availability and nutrient uptake. Plant, Cell & Environment 24(1): 41-52.

Hirsch, R. E., Lewis, B. D., Spalding, E. P. and Sussman, M. R. (1998). A role for the AKT1 potassium channel in plant nutrition. Science 280(5365): 918-921.

Ho, C. H., Lin, S. H., Hu, H. C. and Tsay, Y. F. (2009). CHL1 Functions as a Nitrate Sensor in Plants. Cell 138(6): 1184-1194.

Hong, J. P., Takeshi, Y., Kondou, Y., Schachtman, D. P., Matsui, M. and Shin, R. (2013). Identification and characterization of transcription factors regulating *Arabidopsis HAK5*. Plant and Cell Physiology 54(9): 1478-1490.

Honsbein, A., Sokolovski, S., Grefen, C., Campanoni, P., Pratelli, R., Paneque, M., Chen, Z., Johansson, I. and Blatt, M. R. (2009). A tripartite SNARE-K^+ channel complex mediates in channel-dependent K^+ nutrition in *Arabidopsis*. Plant Cell 21(9): 2859-2877.

Hsu, P. K. and Tsay, Y. F. (2013). Two phloem nitrate transporters, NRT1.11 and NRT1.12, are important for redistributing xylem-borne nitrate to enhance plant growth. Plant Physiology 163(2): 844-856.

Hu, H. C., Wang, Y. Y. and Tsay, Y. F. (2009). AtCIPK8, a CBL-interacting protein kinase, regulates the low-affinity phase of the primary nitrate response. Plant Journal 57(2): 264-278.

Huang, N. C., Chiang, C. S., Crawford, N. M. and Tsay, Y. F. (1996). *CHL1* encodes a component of the low-affinity nitrate uptake system in Arabidopsis and shows cell type-specific expression in roots. Plant Cell 8(12): 2183-2191.

Huang, N. C., Liu, K. H., Lo, H. J. and Tsay, Y. F. (1999). Cloning and functional characterization of an *Arabidopsis* nitrate transporter gene that encodes a constitutive component of low-affinity uptake. Plant Cell 11(8): 1381-1392.

Jamtgard, S., Nasholm, T. and Huss-Danell, K. (2008). Characteristics of amino acid uptake in barley. Plant and Soil 302(1-2): 221-231.

Johansson, I., Wulfetange, K., Poree, F., Michard, E., Gajdanowicz, P., Lacombe, B., Sentenac, H., Thibaud, J. B., Mueller-Roeber, B., Blatt, M. R. and Dreyer, I. (2006). External K^+ modulates the activity of the *Arabidopsis* potassium channel SKOR via an unusual mechanism. Plant Journal 46(2): 269-281.

Jung, J. Y., Shin, R. and Schachtman, D. P. (2009). Ethylene mediates response and tolerance to potassium deprivation in *Arabidopsis*. Plant Cell 21(2): 607-621.

Kanno, Y., Hanada, A., Chiba, Y., Ichikawa, T., Nakazawa, M., Matsui, M., Koshiba, T., Kamiya, Y. and Seo, M. (2012). Identification of an abscisic acid transporter by functional screening using the receptor complex as a sensor. Proceedings of the National Academy of Sciences of the United States of America 109(24): 9653-9658.

Kanno, Y., Kamiya, Y. and Seo, M. (2013). Nitrate does not compete with abscisic acid as a substrate of AtNPF4.6/NRT1.2/AIT1 in *Arabidopsis*. Plant Signaling & Behavior 8(12): e26624.

Kanno, Y., Oikawa, T., Chiba, Y., Ishimaru, Y., Shimizu, T., Sano, N., Koshiba, T., Kamiya, Y., Ueda, M. and Seo, M. (2016). AtSWEET13 and AtSWEET14 regulate gibberellin-mediated physiological processes. Nature Communications 7.

Kasaras, A. (2012). Characterization of the senescence-associated membrane protein DMP1 and the DMP family in *Arabidopsis thaliana*. Doctoral Dissertation; Institute of Biology/Applied Genetics, Freie Universität Berlin.

Kiba, T., Feria-Bourrellier, A. B., Lafouge, F., Lezhneva, L., Boutet-Mercey, S., Orsel, M., Brehaut, V., Miller, A., Daniel-Vedele, F., Sakakibara, H. and Krapp, A. (2012). The *Arabidopsis* nitrate transporter NRT2.4 plays a double role in roots and shoots of nitrogen-straved plants. Plant Cell 24(1): 245-258.

Kiba, T., Kudo, T., Kojima, M. and Sakakibara, H. (2011). Hormonal control of nitrogen

acquisition: roles of auxin, abscisic acid, and cytokinin. Journal of Experimental Botany 62(4): 1399-1409.

Kim, M. J., Ciani, S. and Schachtman, D. P. (2010). A peroxidase contributes to ROS production during *Arabidopsis* root response to potassium deficiency. Molecular Plant 3(2): 420-427.

Kim, M. J., Ruzicka, D., Shin, R. and Schachtman, D. P. (2012). The *Arabidopsis AP2/ERF* transcription factor RAP2.11 modulates plant response to low-potassium conditions. Molecular Plant 5(5): 1042-1057.

Kodama, Y. and Hu, C. D. (2012). Bimolecular fluorescence complementation (BiFC): A 5-year update and future perspectives. Biotechniques 53(5): 285-298.

Koncz, C. and Schell, J. (1986). The promoter of T_L-DNA Gene 5 controls the tissue-specific expression of chimeric genes carried by a novel type of *Agrobacterium* binary vector. Molecular & General Genetics 204(3): 383-396.

Kotur, Z., Mackenzie, N., Ramesh, S., Tyerman, S. D., Kaiser, B. N. and Glass, A. D. (2012). Nitrate transport capacity of the *Arabidopsis thaliana* NRT2 family members and their interactions with AtNAR2.1. New Phytologist 194(3): 724-731.

Krapp, A., David, L. C., Chardin, C., Girin, T., Marmagne, A., Leprince, A. S., Chaillou, S., Ferrario-Mery, S., Meyer, C. and Daniel-Vedele, F. (2014). Nitrate transport and signalling in *Arabidopsis*. Journal of Experimental Botany 65(3): 789-798.

Krouk, G., Lacombe, B., Bielach, A., Perrine-Walker, F., Malinska, K., Mounier, E., Hoyerova, K., Tillard, P., Leon, S., Ljung, K., Zazimalova, E., Benkova, E., Nacry, P. and Gojon, A. (2010). Nitrate-regulated auxin transport by NRT1.1 defines a mechanism for nutrient sensing in plants. Developmental Cell 18(6): 927-937.

Laanemets, K., Wang, Y. F., Lindgren, O., Wu, J. Y., Nishimura, N., Lee, S., Caddell, D., Merilo, E., Brosche, M., Kilk, K., Soomets, U., Kangasjarvi, J., Schroeder, J. I. and Kollist, H. (2013). Mutations in the SLAC1 anion channel slow stomatal opening and severely reduce K^+ uptake channel activity via enhanced cytosolic [Ca^{2+}] and increased Ca^{2+} sensitivity of K^+ uptake channels. New Phytologist 197(1): 88-98.

Lacombe, B., Pilot, G., Gaymard, F., Sentenac, H. and Thibaud, J. B. (2000). pH control of the plant outwardly-rectifying potassium channel SKOR. FEBS Letters 466(2-3): 351-354.

Lagarde, D., Basset, M., Lepetit, M., Conejero, G., Gaymard, F., Astruc, S. and Grignon, C. (1996). Tissue-specific expression of *Arabidopsis AKT1* gene is consistent with a role in K^+ nutrition. Plant Journal 9(2): 195-203.

Lalonde, S., Ehrhardt, D. W., Loque, D., Chen, J., Rhee, S. Y. and Frommer, W. B. (2008). Molecular and cellular approaches for the detection of protein-protein interactions: latest techniques and current limitations. Plant Journal 53(4): 610-635.

Lebaudy, A., Very, A. A. and Sentenac, H. (2007). K^+ channel activity in plants: genes, regulations and functions. FEBS Letters 581(12): 2357-2366.

Lee, S. C., Lan, W. Z., Kim, B. G., Li, L., Cheong, Y. H., Pandey, G. K., Lu, G., Buchanan, B. B. and Luan, S. (2007). A protein phosphorylation/dephosphorylation network regulates a plant potassium channel. Proceedings of the National Academy of Sciences of the United States of America 104(40): 15959-15964.

Leigh, R. A. and Jones, R. G. W. (1984). A hypothesis relating critical potassium concentrations for growth to the distribution and functions of this ion in the plant-cell. New Phytologist 97(1): 1-13.

Leran, S., Garg, B., Boursiac, Y., Corratge-Faillie, C., Brachet, C., Tillard, P., Gojon, A. and Lacombe, B. (2015). AtNPF5.5, a nitrate transporter affecting nitrogen accumulation in *Arabidopsis* embryo. Scientific Reports 5: 7962.

Leran, S., Munos, S., Brachet, C., Tillard, P., Gojon, A. and Lacombe, B. (2013). *Arabidopsis* NRT1.1 is a bidirectional transporter involved in root-to-shoot nitrate translocation. Molecular Plant 6(6): 1984-1987.

Leran, S., Varala, K., Boyer, J. C., Chiurazzi, M., Crawford, N., Daniel-Vedele, F., David, L., Dickstein, R., Fernandez, E., Forde, B., Gassmann, W., Geiger, D., Gojon, A., Gong, J. M., Halkier, B. A., Harris, J. M., Hedrich, R., Limami, A. M., Rentsch, D., Seo, M., Tsay, Y. F., Zhang, M., Coruzzi, G. and Lacombe, B. (2014). A unified nomenclature of NITRATE TRANSPORTER 1/PEPTIDE TRANSPORTER family members in plants. Trends in Plant Science 19(1): 5-9.

Lezhneva, L., Kiba, T., Feria-Bourrellier, A. B., Lafouge, F., Boutet-Mercey, S., Zoufan, P., Sakakibara, H., Daniel-Vedele, F. and Krapp, A. (2014). The *Arabidopsis* nitrate transporter NRT2.5 plays a role in nitrate acquisition and remobilization in nitrogen-starved plants. Plant Journal 80(2): 230-241.

Li, H., Yu, M., Du, X. Q., Wang, Z. F., Wu, W. H., Quintero, F. J., Jin, X. H., Li, H. D. and Wang, Y. (2017). NRT1.5/NPF7.3 Functions as a Proton-Coupled H^+/K^+ Antiporter for K^+ Loading into the Xylem in *Arabidopsis.* Plant Cell 29(8): 2016-2026.

Li, J. M., Nagpal, P., Vitart, V., McMorris, T. C. and Chory, J. (1996). A role for brassinosteroids in light-dependent development of *Arabidopsis*. Science 272(5260): 398-401.

Li, J. Y., Fu, Y. L., Pike, S. M., Bao, J., Tian, W., Zhang, Y., Chen, C. Z., Zhang, Y., Li, H. M., Huang, J., Li, L. G., Schroeder, J. I., Gassmann, W. and Gonga, J. M. (2010). The *Arabidopsis* nitrate transporter NRT1.8 functions in nitrate removal from the xylem sap and mediates cadmium tolerance. Plant Cell 22(5): 1633-1646.

Li, L., Kim, B. G., Cheong, Y. H., Pandey, G. K. and Luan, S. (2006). A Ca^{2+} signaling pathway regulates a K^+ channel for low-K response in *Arabidopsis*. Proceedings of the National Academy of Sciences of the United States of America 103(33): 12625-12630.

Li, R. F., Zhang, J. W., Wei, J. H., Wang, H. Z., Wang, Y. Z. and Ma, R. C. (2009). Functions and mechanisms of the CBL-CIPK signaling system in plant response to abiotic stress. Progress in Natural Science 19(6): 667-676.

Li, X., Mo, X. R., Shou, H. X. and Wu, P. (2006). Cytokinin-mediated cell cycling arrest of pericycle founder cells in lateral root initiation of *Arabidopsis*. Plant and Cell Physiology 47(8): 1112-1123.

Lin, S. H., Kuo, H. F., Canivenc, G., Lin, C. S., Lepetit, M., Hsu, P. K., Tillard, P., Lin, H. L., Wang, Y. Y., Tsai, C. B., Gojon, A. and Tsay, Y. F. (2008). Mutation of the *Arabidopsis* NRT1.5 nitrate transporter causes defective root-to-shoot nitrate transport. Plant Cell 20(9): 2514-2528.

Linkohr, B. I., Williamson, L. C., Fitter, A. H. and Leyser, H. M. O. (2002). Nitrate and phosphate availability and distribution have different effects on root system architecture of *Arabidopsis*. Plant Journal 29(6): 751-760.

Liu, K., Li, L. and Luan, S. (2006). Intracellular K^+ sensing of SKOR, a Shaker-type K^+ channel from *Arabidopsis*. Plant Journal 46(2): 260-268.

Liu, K. H. and Tsay, Y. F. (2003). Switching between the two action modes of the dual-affinity

nitrate transporter CHL1 by phosphorylation. Embo Journal 22(5): 1005-1013.

Ma, Q., Longnecker, N. and Dracup, M. (1997). Nitrogen deficiency slows leaf development and delays flowering in narrow-leafed Lupin. Annals of Botany 79(4): 403-409.

Maathuis, F. J. M. (2009). Physiological functions of mineral macronutrients. Current Opinion in Plant Biology 12(3): 250-258.

Maathuis, F. J. M., Filatov, V., Herzyk, P., Krijger, G. C., Axelsen, K. B., Chen, S. X., Green, B. J., Li, Y., Madagan, K. L., Sanchez-Fernandez, R., Forde, B. G., Palmgren, M. G., Rea, P. A., Williams, L. E., Sanders, D. and Amtmann, A. (2003). Transcriptome analysis of root transporters reveals participation of multiple gene families in the response to cation stress. Plant Journal 35(6): 675-692.

Maathuis, F. J. M. and Sanders, D. (1993). Energization of potassium uptake in *Arabidopsis thaliana*. Planta 191(3): 302-307.

Maierhofer, T., Lind, C., Huttl, S., Scherzer, S., Papenfuss, M., Simon, J., Al-Rasheid, K. A. S., Ache, P., Rennenberg, H., Hedrich, R., Muller, T. D. and Geiger, D. (2014). A Single-pore residue renders the *Arabidopsis* root anion channel SLAH2 highly nitrate selective. Plant Cell 26(6): 2554-2567.

Malamy, J. E. (2005). Intrinsic and environmental response pathways that regulate root system architecture. Plant, Cell & Environment 28(1): 67-77.

Malamy, J. E. and Benfey, P. N. (1997). Organization and cell differentiation in lateral roots of *Arabidopsis thaliana*. Development 124(1): 33-44.

Malone, E. A., Clark, C. D., Chiang, A. and Winston, F. (1991). Mutations in *SPT16/CDC68* suppress *cis* and *trans*-Acting mutations that affect promoter function in *Saccharomyces cerevisiae*. Molecular and Cellular Biology 11(11): 5710-5717.

Marchant, A., Bhalerao, R., Casimiro, I., Eklof, J., Casero, P. J., Bennett, M. and Sandberg, G. (2002). AUX1 promotes lateral root formation by facilitating indole-3-acetic acid distribution between sink and source tissues in the *Arabidopsis* seedling. Plant Cell 14(3): 589-597.

Marchive, C., Roudier, F., Castaings, L., Brehaut, V., Blondet, E., Colot, V., Meyer, C. and Krapp, A. (2013). Nuclear retention of the transcription factor NLP7 orchestrates the early response to nitrate in plants. Nature Communications 4.

Marini, A. M., Soussi-Boudekou, S., Vissers, S. and Andre, B. (1997). A family of ammonium transporters in *Saccharomyces cerevisiae.* Molecular and Cellular Biology 17(8): 4282-4293.

Marschner, P. (2012). Marschner's Mineral Nutrition of Higher Plants. Third edition, Academic Press.

Meng, S., Peng, J. S., He, Y. N., Zhang, G. B., Yi, H. Y., Fu, Y. L. and Gong, J. M. (2016). *Arabidopsis* NRT1.5 mediates the suppression of nitrate starvation-induced leaf senescence by modulating foliar potassium level. Molecular Plant 9(3): 461-470.

Menz, J., Li, Z., Schulze, W. X. and Ludewig, U. (2016). Early nitrogen-deprivation responses in *Arabidopsis* roots reveal distinct differences on transcriptome and (phospho-) proteome levels between nitrate and ammonium nutrition. Plant Journal 88(5): 717-734.

Merlot, S., Leonhardt, N., Fenzi, F., Valon, C., Costa, M., Piette, L., Vavasseur, A., Genty, B., Boivin, K., Muller, A., Giraudat, M. and Leung, J. (2007). Constitutive activation of a plasma membrane H^+-ATPase prevents abscisic acid-mediated stomatal closure. Embo

Journal 26(13): 3216-3226.

Michelet, B. and Boutry, M. (1995). The plasma-membrane H^+-ATPase - a highly regulated enzyme with multiple physiological functions. Plant Physiology 108(1): 1-6.

Miller, A. J. and Cramer, M. D. (2005). Root nitrogen acquisition and assimilation. Plant and Soil 274(1-2): 1-36.

Mlodzinska, E., Klobus, G., Christensen, M. D. and Fuglsang, A. T. (2015). The plasma membrane H^+-ATPase AHA2 contributes to the root architecture in response to different nitrogen supply. Physiologia Plantarum 154(2): 270-282.

Monachello, D., Allot, M., Oliva, S., Krapp, A., Daniel-Vedele, F., Barbier-Brygoo, H. and Ephritikhine, G. (2009). Two anion transporters AtClCa and AtClCe fulfil interconnecting but not redundant roles in nitrate assimilation pathways. New Phytologist 183(1): 88-94.

Morth, J. P., Pedersen, B. P., Buch-Pedersen, M. J., Andersen, J. P., Vilsen, B., Palmgren, M. G. and Nissen, P. (2011). A structural overview of the plasma membrane Na^+,K^+-ATPase and H^+-ATPase ion pumps. Nature Reviews Molecular Cell Biology 12(1): 60-70.

Mouchel, C. F., Osmont, K. S. and Hardtke, C. S. (2006). BRX mediates feedback between brassinosteroid levels and auxin signalling in root growth. Nature 443(7110): 458-461.

Muday, G. K. and Haworth, P. (1994). Tomato root-growth, gravitropism, and lateral development - correlation with auxin transport. Plant Physiology and Biochemistry 32(2): 193-203.

Murray, M. G. and Thompson, W. F. (1980). Rapid isolation of high molecular-weight plant DNA. Nucleic Acids Research 8(19): 4321-4325.

Mussig, C., Shin, G. H. and Altmann, T. (2003). Brassinosteroids promote root growth in *Arabidopsis*. Plant Physiology 133(3): 1261-1271.

Navarrete, C., Petrezselyova, S., Barreto, L., Martinez, J. L., Zahradka, J., Arino, J., Sychrova, H. and Ramos, J. (2010). Lack of main K^+ uptake systems in *Saccharomyces cerevisiae* cells affects yeast performance in both potassium-sufficient and potassium-limiting conditions. Fems Yeast Research 10(5): 508-517.

Nazoa, P., Vidmar, J. J., Tranbarger, T. J., Mouline, K., Damiani, I., Tillard, P., Zhuo, D. G., Glass, A. D. M. and Touraine, B. (2003). Regulation of the nitrate transporter gene *AtNRT2.1* in *Arabidopsis thaliana*: responses to nitrate, amino acids and developmental stage. Plant Molecular Biology 52(3): 689-703.

Negi, J., Matsuda, O., Nagasawa, T., Oba, Y., Takahashi, H., Kawai-Yamada, M., Uchimiya, H., Hashimoto, M. and Iba, K. (2008). CO_2 regulator SLAC1 and its homologues are essential for anion homeostasis in plant cells. Nature 452(7186): 483-486.

Nieves-Cordones, M., Aleman, F., Martinez, V. and Rubio, F. (2010). The *Arabidopsis thaliana* HAK5 K^+ transporter is required for plant growth and K^+ acquisition from low K^+ solutions under saline conditions. Molecular Plant 3(2): 326-333.

Nieves-Cordones, M., Aleman, F., Martinez, V. and Rubio, F. (2014). K^+ uptake in plant roots. The systems involved, their regulation and parallels in other organisms. Journal of Plant Physiology 171(9): 688-695.

Nieves-Cordones, M., Miller, A. J., Aleman, F., Martinez, V. and Rubio, F. (2008). A putative role for the plasma membrane potential in the control of the expression of the gene encoding the tomato high-affinity potassium transporter HAK5. Plant Molecular Biology 68(6): 521-532.

Nour-Eldin, H. H., Andersen, T. G., Burow, M., Madsen, S. R., Jorgensen, M. E., Olsen, C. E., Dreyer, I., Hedrich, R., Geiger, D. and Halkier, B. A. (2012). NRT/PTR transporters are essential for translocation of glucosinolate defence compounds to seeds. Nature 488(7412): 531-534.

O'Brien, J. A., Vega, A., Bouguyon, E., Krouk, G., Gojon, A., Coruzzi, G. and Gutierrez, R. A. (2016). Nitrate transport, sensing, and responses in plants. Molecular Plant 9(6): 837-856.

Obata, T., Kitamoto, H. K., Nakamura, A., Fukuda, A. and Tanaka, Y. (2007). Rice Shaker potassium channel OsKAT1 confers tolerance to salinity stress on yeast and rice cells. Plant Physiology 144(4): 1978-1985.

Obrdlik, P., El-Bakkoury, M., Hamacher, T., Cappellaro, C., Vilarino, C., Fleischer, C., Ellerbrok, H., Kamuzinzi, R., Ledent, V., Blaudez, D., Sanders, D., Revuelta, J. L., Boles, E., Andre, B. and Frommer, W. B. (2004). K^+ channel interactions detected by a genetic system optimized for systematic studies of membrane protein interactions. Proceedings of the National Academy of Sciences of the United States of America 101(33): 12242-12247.

Okamoto, M., Kumar, A., Li, W., Wang, Y., Siddiqi, M. Y., Crawford, N. M. and Glass, A. D. (2006). High-affinity nitrate transport in roots of *Arabidopsis* depends on expression of the *NAR2*-like gene *AtNRT3.1*. Plant Physiology 140(3): 1036-1046.

Okamoto, M., Vidmar, J. J. and Glass, A. D. M. (2003). Regulation of *NRT1* and *NRT2* gene families of *Arabidopsis thaliana*: responses to nitrate provision. Plant and Cell Physiology 44(3): 304-317.

Orsel, M., Eulenburg, K., Krapp, A. and Daniel-Vedele, F. (2004). Disruption of the nitrate transporter genes *AtNRT2.1* and *AtNRT2.2* restricts growth at low external nitrate concentration. Planta 219(4): 714-721.

Orsel, M., Krapp, A. and Daniel-Vedele, F. (2002). Analysis of the NRT2 nitrate transporter family in *Arabidopsis*. Structure and gene expression. Plant Physiology 129(2): 886-896.

Owen, A. G. and Jones, D. L. (2001). Competition for amino acids between wheat roots and rhizosphere microorganisms and the role of amino acids in plant N acquisition. Soil Biology & Biochemistry 33(4-5): 651-657.

Palmgren, M. G. (2001). Plant plasma membrane H^+-ATPases: Powerhouses for nutrient uptake. Annual Review of Plant Physiology and Plant Molecular Biology 52: 817-845.

Paretssoler, A., Pardo, J. M. and Serrano, R. (1990). Immunocytolocalization of plasma-membrane H^+-ATPase. Plant Physiology 93(4): 1654-1658.

Parker, J. L. and Newstead, S. (2014). Molecular basis of nitrate uptake by the plant nitrate transporter NRT1.1. Nature 507(7490): 68-72.

Pertl-Obermeyer, H., Schuze, W. X. and Obermeyer, G. (2014). *In vivo* cross-linking combined with mass spectrometry analysis reveals receptor-like kinases and Ca^{2+} signalling proteins as putative interaction partners of pollen plasma membrane H^+ ATPases. Journal of Proteomics 108: 17-29.

Petrezselyova, S., Zahradka, J. and Sychrova, H. (2010). *Saccharomyces cerevisiae* BY4741 and W303-1A laboratory strains differ in salt tolerance. Fungal Biology 114(2-3): 144-150.

Pike, S., Gao, F., Kim, M. J., Kim, S. H., Schachtman, D. P. and Gassmann, W. (2014). Members of the NPF3 transporter subfamily encode pathogen-inducible nitrate/nitrite transporters in Grapevine and *Arabidopsis*. Plant and Cell Physiology 55(1): 162-170.

Pilot, G., Gaymard, F., Mouline, K., Cherel, I. and Sentenac, H. (2003). Regulated expression

of *Arabidopsis* Shaker K^+ channel genes involved in K^+ uptake and distribution in the plant. Plant Molecular Biology 51(5): 773-787.

Prelich, G. (2012). Gene Overexpression: Uses, Mechanisms, and Interpretation. Genetics 190(3): 841-854.

Qi, Z., Hampton, C. R., Shin, R., Barkla, B. J., White, P. J. and Schachtman, D. P. (2008). The high affinity K^+ transporter AtHAK5 plays a physiological role *in planta* at very low K^+ concentrations and provides a caesium uptake pathway in *Arabidopsis*. Journal of Experimental Botany 59(3): 595-607.

Qiu, J., Henderson, S. W., Tester, M., Roy, S. J. and Gilliham, M. (2016). SLAH1, a homologue of the slow type anion channel SLAC1, modulates shoot Cl^- accumulation and salt tolerance in *Arabidopsis thaliana*. Journal of Experimental Botany 67(15): 4495-4505.

Ragel, P., Rodenas, R., Garcia-Martin, E., Andres, Z., Villalta, I., Nieves-Cordones, M., Rivero, R. M., Martinez, V., Pardo, J. M., Quintero, F. J. and Rubio, F. (2015). The CBL-interacting protein kinase CIPK23 tegulates HAK5-mediated high-affinity K^+ uptake in *Arabidopsis* roots. Plant Physiology 169(4): 2863-2873.

Rahayu, Y. S., Walch-Liu, P., Neumann, G., Romheld, V., von Wiren, N. and Bangerth, F. (2005). Root-derived cytokinins as long-distance signals for NO_3^--induced stimulation of leaf growth. Journal of Experimental Botany 56(414): 1143-1152.

Remans, T., Nacry, P., Pervent, M., Filleur, S., Diatloff, E., Mounier, E., Tillard, P., Forde, B. G. and Gojon, A. (2006). The *Arabidopsis* NRT1.1 transporter participates in the signaling pathway triggering root colonization of nitrate-rich patches. Proceedings of the National Academy of Sciences of the United States of America 103(50): 19206-19211.

Ren, X. L., Qi, G. N., Feng, H. Q., Zhao, S., Zhao, S. S., Wang, Y. and Wu, W. H. (2013). Calcineurin B-like protein CBL10 directly interacts with AKT1 and modulates K^+ homeostasis in *Arabidopsis*. Plant Journal 74(2): 258-266.

Rigas, S., Ditengou, F. A., Ljung, K., Daras, G., Tietz, O., Palme, K. and Hatzopoulos, P. (2013). Root gravitropism and root hair development constitute coupled developmental responses regulated by auxin homeostasis in the *Arabidopsis* root apex. New Phytologist 197(4): 1130-1141.

Riveras, E., Alvarez, J. M., Vidal, E. A., Oses, C., Vega, A. and Gutierrez, R. A. (2015). The calcium ion Is a second messenger in the nitrate signaling pathway of *Arabidopsis*. Plant Physiology 169(2): 1397-1404.

Roberts, S. K. and Snowman, B. N. (2000). The effects of ABA on channel-mediated K^+ transport across higher plant roots. Journal of Experimental Botany 51(350): 1585-1594.

Robinson, D., Linehan, D. J. and Gordon, D. C. (1994). Capture of nitrate from soil by wheat in relation to root length, nitrogen inflow and availability. New Phytologist 128(2): 297-305.

Rubio, F., Aleman, F., Nieves-Cordones, M. and Martinez, V. (2010). Studies on *Arabidopsis athak5, atakt1* double mutants disclose the range of concentrations at which AtHAK5, AtAKT1 and unknown systems mediate K^+ uptake. Physiologia Plantarum 139(2): 220-228.

Rubio, V., Bustos, R., Irigoyen, M. L., Cardona-Lopez, X., Rojas-Triana, M. and Paz-Ares, J. (2009). Plant hormones and nutrient signaling. Plant Molecular Biology 69(4): 361-373.

Rufty, T. W., Jackson, W. A. and Raper, C. D. (1981). Nitrate reduction in roots as affected by the presence of potassium and by flux of nitrate through the roots. Plant Physiology 68(3):

605-609.

Saito, H., Oikawa, T., Hamamoto, S., Ishimaru, Y., Kanamori-Sato, M., Sasaki-Sekimoto, Y., Utsumi, T., Chen, J., Kanno, Y., Masuda, S., Kamiya, Y., Seo, M., Uozumi, N., Ueda, M. and Ohta, H. (2015). The jasmonate-responsive GTR1 transporter is required for gibberellin-mediated stamen development in *Arabidopsis*. Nature Communications 6.

Sakakibara, H., Takei, K. and Hirose, N. (2006). Interactions between nitrogen and cytokinin in the regulation of metabolism and development. Trends in Plant Science 11(9): 440-448.

Sambrook, J. F. and Russell, D. W. (2001). Molecular Cloning: A Laboratory Manual, 3rd edition., Cold Spring Harbor Laboratory Press.

Sattelmacher, B., Gerendas, J., Thoms, K., Bruck, H. and Bagdady, N. H. (1993). Interaction between root-growth and mineral-nutrition. Environmental and Experimental Botany 33(1): 63-73.

Schachtman, D. P. (2015). The role of ethylene in plant responses to K^+ deficiency. Frontiers in Plant Science 6.

Scheible, W. R., Lauerer, M., Schulze, E. D., Caboche, M. and Stitt, M. (1997). Accumulation of nitrate in the shoot acts as a signal to regulate shoot-root allocation in tobacco. Plant Journal 11(4): 671-691.

Segonzac, C., Boyer, J. C., Ipotesi, E., Szponarski, W., Tillard, P., Touraine, B., Sommerer, N., Rossignol, M. and Gibrat, R. (2007). Nitrate efflux at the root plasma membrane: Identification of an *Arabidopsis* excretion transporter. Plant Cell 19(11): 3760-3777.

Sentenac, H., Bonneaud, N., Minet, M., Lacroute, F., Salmon, J. M., Gaymard, F. and Grignon, C. (1992). Cloning and expression in yeast of a plant potassium-ion transport-system. Science 256(5057): 663-665.

Sharma, T., Dreyer, I. and Riedelsberger, J. (2013). The role of K^+ channels in uptake and redistribution of potassium in the model plant *Arabidopsis thaliana*. Frontiers in Plant Science 4.

Shin, R., Berg, R. H. and Schachtman, D. P. (2005). Reactive oxygen species and root hairs in *Arabidopsis* root response to nitrogen, phosphorus and potassium deficiency. Plant and Cell Physiology 46(8): 1350-1357.

Shin, R., Burch, A. Y., Huppert, K. A., Tiwari, S. B., Murphy, A. S., Guilfoyle, T. J. and Schachtman, D. P. (2007). The *Arabidopsis* transcription factor MYB77 modulates auxin signal transduction. Plant Cell 19(8): 2440-2453.

Shin, R. and Schachtman, D. P. (2004). Hydrogen peroxide mediates plant root cell response to nutrient deprivation. Proceedings of the National Academy of Sciences of the United States of America 101(23): 8827-8832.

Siebrecht, S. and Tischner, R. (1999). Changes in the xylem exudate composition of poplar (*Populus tremula x P. alba*) - dependent on the nitrogen and potassium supply. Journal of Experimental Botany 50(341): 1797-1806.

Signora, L., De Smet, I., Foyer, C. H. and Zhang, H. (2001). ABA plays a central role in mediating the regulatory effects of nitrate on root branching in *Arabidopsis*. Plant Journal 28(6): 655-662.

Stals, H. and Inze, D. (2001). When plant cells decide to divide. Trends in Plant Science 6(8): 359-364.

Stefanovic, A., Arpat, A. B., Bligny, R., Gout, E., Vidoudez, C., Bensimon, M. and Poirier, Y.

(2011). Over-expression of *PHO1* in *Arabidopsis* leaves reveals its role in mediating phosphate efflux. Plant Journal 66(4): 689-699.

Sun, J., Bankston, J. R., Payandeh, J., Hinds, T. R., Zagotta, W. N. and Zheng, N. (2014). Crystal structure of the plant dual-affinity nitrate transporter NRT1.1. Nature 507: 73-77.

Swanson, M. S., Malone, E. A. and Winston, F. (1991). *SPT5*, an essential gene important for normal transcription in *Saccharomyces cerevisiae*, encodes an acidic nuclear-protein with a carboxy terminal repeat. Molecular and Cellular Biology 11(6): 3009-3019.

Swarup, R., Friml, J., Marchant, A., Ljung, K., Sandberg, G., Palme, K. and Bennett, M. (2001). Localization of the auxin permease AUX1 suggests two functionally distinct hormone transport pathways operate in the *Arabidopsis* root apex. Genes & Development 15(20): 2648-2653.

Sze, H., Li, X. H. and Palmgren, M. G. (1999). Energization of plant cell membranes by H^+-pumping ATPases: regulation and biosynthesis. Plant Cell 11(4): 677-689.

Tal, I., Zhang, Y., Jorgensen, M. E., Pisanty, O., Barbosa, I. C. R., Zourelidou, M., Regnault, T., Crocoll, C., Olsen, C. E., Weinstain, R., Schwechheimer, C., Halkier, B. A., Nour-Eldin, H. H., Estelle, M. and Shani, E. (2016). The *Arabidopsis* NPF3 protein is a GA transporter. Nature Communications 7.

Taochy, C., Gaillard, I., Ipotesi, E., Oomen, R., Leonhardt, N., Zimmermann, S., Peltier, J. B., Szponarski, W., Simonneau, T., Sentenac, H., Gibrat, R. and Boyer, J. C. (2015). The *Arabidopsis* root stele transporter NPF2.3 contributes to nitrate translocation to shoots under salt stress. Plant Journal 83(3): 466-479.

Teakle, N. L. and Tyerman, S. D. (2010). Mechanisms of Cl^- transport contributing to salt tolerance. Plant, Cell & Environment 33(4): 566-589.

Tester, M. (1999). The control of long-distance K^+ transport by ABA. Trends in Plant Science 4(1): 5-6.

Thornton, B. and Robinson, D. (2005). Uptake and assimilation of nitrogen from solutions containing multiple N sources. Plant, Cell & Environment 28(6): 813-821.

Torrey, J. G. (1962). Auxin and purine interactions in lateral root initiation in isolated pea root segments. Physiologia Plantarum 15(1): 177-185.

Tsay, Y. F., Schroeder, J. I., Feldmann, K. A. and Crawford, N. M. (1993). The herbicide sensitivity gene *CHL1* of *Arabidopsis* encodes a nitrate-inducible nitrate transporter. Cell 72(5): 705-713.

van der Graaff, E., Schwacke, R., Schneider, A., Desimone, M., Flugge, U. I. and Kunze, R. (2006). Transcription analysis of *Arabidopsis* membrane transporters and hormone pathways during developmental and induced leaf senescence. Plant Physiology 141(2): 776-792.

Varshney, R. K. and Koebner, R. M. D. (2006). Model plants and crop improvement. Boca Raton, FL: CRC Press, Taylor & Francis.

Verwoerd, T. C., Dekker, B. M. M. and Hoekema, A. (1989). A small-scale procedure for the rapid isolation of plant RNAs. Nucleic Acids Research 17(6): 2362-2362.

Vicente-Agullo, F., Rigas, S., Desbrosses, G., Dolan, L., Hatzopoulos, P. and Grabov, A. (2004). Potassium carrier TRH1 is required for auxin transport in *Arabidopsis* roots. Plant Journal 40(4): 523-535.

Voinnet, O., Rivas, S., Mestre, P. and Baulcombe, D. (2003). An enhanced transient expression

system in plants based on suppression of gene silencing by the p19 protein of tomato bushy stunt virus (Retracted article. See vol. 84, pg. 846, 2015). Plant Journal 33(5): 949-956.

von der Fecht-Bartenbach, J., Bogner, M., Dynowski, M. and Ludewig, U. (2010). CLC-b-mediated NO_3^-/H^+ exchange across the tonoplast of *Arabidopsis* vacuoles. Plant and Cell Physiology 51(6): 960-968.

Vos, J., van der Putten, P. E. L. and Birch, C. J. (2005). Effect of nitrogen supply on leaf appearance, leaf growth, leaf nitrogen economy and photosynthetic capacity in maize (*Zea mays* L.). Field Crops Research 93(1): 64-73.

Walch-Liu, P., Ivanov, II, Filleur, S., Gan, Y., Remans, T. and Forde, B. G. (2006). Nitrogen regulation of root branching. Annals of Botany 97(5): 875-881.

Wang, R. C., Guegler, K., LaBrie, S. T. and Crawford, N. M. (2000). Genomic analysis of a nutrient response in *Arabidopsis* reveals diverse expression patterns and novel metabolic and potential regulatory genes induced by nitrate. Plant Cell 12(8): 1491-1509.

Wang, Y., He, L., Li, H. D., Xu, J. and Wu, W. H. (2010). Potassium channel alpha-subunit AtKC1 negatively regulates AKT1-mediated K^+ uptake in *Arabidopsis* roots under low-K^+ stress. Cell Res 20(7): 826-837.

Wang, Y., Noguchi, K., Ono, N., Inoue, S., Terashima, I. and Kinoshita, T. (2014). Overexpression of plasma membrane H^+-ATPase in guard cells promotes light-induced stomatal opening and enhances plant growth. Proceedings of the National Academy of Sciences of the United States of America 111(1): 533-538.

Wang, Y. and Wu, W. H. (2013). Potassium transport and signaling in higher plants. Annual Review of Plant Biology, 64: 451-476.

Wang, Y. H., Garvin, D. F. and Kochian, L. V. (2001). Nitrate-induced genes in tomato roots. Array analysis reveals novel genes that may play a role in nitrogen nutrition. Plant Physiology 127(1): 345-359.

Wang, Y.Y. (2011). Functional analyses of two nitrate transporters, NRT1.9 and NRT1.10, in *Arabidopsis thaliana*. Doctoral Dissertation; Department of Life Sciences and Institute of Genome Sciences, National Yang-Ming University

Wang, Y. Y. and Tsay, Y. F. (2011). *Arabidopsis* Nitrate Transporter NRT1.9 Is Important in Phloem Nitrate Transport. Plant Cell 23(5): 1945-1957.

Wei, Z. Y. and Li, J. (2016). Brassinosteroids regulate root growth, development, and symbiosis. Molecular Plant 9(1): 86-100.

Weigel, D. and Glazebrook, J. (2002). Arabidopsis: A Laboratory Manual.

Wetherell, D. F. and Dougall, D. K. (1976). Sources of nitrogen supporting growth and embryogenesis in cultured wild carrot tissue. Physiologia Plantarum 37(2): 97-103.

Wilkinson, S. and Davies, W. J. (2002). ABA-based chemical signalling: the co-ordination of responses to stress in plants. Plant, Cell & Environment 25(2): 195-210.

Xu, J., Li, H. D., Chen, L. Q., Wang, Y., Liu, L. L., He, L. and Wu, W. H. (2006). A protein kinase, interacting with two calcineurin B-like proteins, regulates K^+ transporter AKT1 in *Arabidopsis*. Cell 125(7): 1347-1360.

Xu, N., Wang, R. C., Zhao, L. F., Zhang, C. F., Li, Z. H., Lei, Z., Liu, F., Guan, P. Z., Chu, Z. H., Crawford, N. M. and Wang, Y. (2016). The *Arabidopsis* NRG2 protein mediates nitrate signaling and interacts with and regulates key nitrate regulators. Plant Cell 28(2): 485-

504.

Yamamoto, Y., Negi, J., Wang, C., Isogai, Y., Schroeder, J. I. and Iba, K. (2016). The transmembrane region of guard cell SLAC1 channels perceives CO_2 signals via an ABA-independent pathway in *Arabidopsis*. Plant Cell 28(2): 557-567.

Yang, D. L., Yao, J., Mei, C. S., Tong, X. H., Zeng, L. J., Li, Q., Xiao, L. T., Sun, T. P., Li, J. G., Deng, X. W., Lee, C. M., Thomashow, M. F., Yang, Y. N., He, Z. H. and He, S. Y. (2012). Plant hormone jasmonate prioritizes defense over growth by interfering with gibberellin signaling cascade. Proceedings of the National Academy of Sciences of the United States of America 109(19): E1192-E1200.

Yao, F. Y., Qi, G. N., Ren, H. M., Zhang, A., Hussain, J. and Wang, Y. F. (2017). S-type anion channel SLAC1's homologues inhibit inward potassium channels AKT2 and KAT2 in *Arabidopsis*. Science Bulletin 62(7): 464-466.

Yong, Z. H., Kotur, Z. and Glass, A. D. M. (2010). Characterization of an intact two-component high-affinity nitrate transporter from *Arabidopsis* roots. Plant Journal 63(5): 739-748.

Zeiger, E. (1983). The giology of stomatal guard-cells. Annual Review of Plant Physiology and Plant Molecular Biology 34: 441-475.

Zepeda-Jazo, I., Shabala, S., Chen, Z. and Pottosin, II (2008). Na-K transport in roots under salt stress. Plant Signaling & Behavavior 3(6): 401-403.

Zhang, A., Ren, H. M., Tan, Y. Q., Qi, G. N., Yao, F. Y., Wu, G. L., Yang, L. W., Hussain, J., Sun, S. J. and Wang, Y. F. (2016). S-type anion channels SLAC1 and SLAH3 function as essential negative regulators of inward K^+ channels and stomatal opening in *Arabidopsis*. Plant Cell 28(4): 949-965.

Zhang, F., Niu, J. F., Zhang, W. F., Chen, X. P., Li, C. J., Yuan, L. X. and Xie, J. C. (2010). Potassium nutrition of crops under varied regimes of nitrogen supply. Plant and Soil 335(1-2): 21-34.

Zhang, G. B., Yi, H. Y. and Gong, J. M. (2014). The Arabidopsis ethylene/jasmonic acid-NRT signaling module coordinates nitrate reallocation and the trade-off between growth and environmental adaptation. Plant Cell 26(10): 3984-3998.

Zhang, H. M. and Forde, B. G. (1998). An *Arabidopsis* MADS box gene that controls nutrient-induced changes in root architecture. Science 279(5349): 407-409.

Zhang, H. M. and Forde, B. G. (2000). Regulation of Arabidopsis root development by nitrate availability. Journal of Experimental Botany 51(342): 51-59.

Zhang, H. M., Jennings, A., Barlow, P. W. and Forde, B. G. (1999). Dual pathways for regulation of root branching by nitrate. Proceedings of the National Academy of Sciences of the United States of America 96(11): 6529-6534.

Zhang, H. M., Rong, H. L. and Pilbeam, D. (2007). Signalling mechanisms underlying the morphological responses of the root system to nitrogen in *Arabidopsis thaliana*. Journal of Experimental Botany 58(9): 2329-2338.

Zheng, X., He, K., Kleist, T., Chen, F. and Luan, S. (2015). Anion channel SLAH3 functions in nitrate-dependent alleviation of ammonium toxicity in *Arabidopsis*. Plant, Cell & Environment 38(3): 474-486.

Zheng, Y., Drechsler, N., Rausch, C. and Kunze, R. (2016). The *Arabidopsis* nitrate transporter NPF7.3/NRT1.5 is involved in lateral root development under potassium deprivation. Plant Signaling & Behavior 11(5). e1176819

Zhu, C. H., Yang, N., Ma, X. L., Li, G. J., Qian, M., Ng, D., Xia, K. and Gan, L. J. (2015). Plasma membrane H^+-ATPase is involved in methyl jasmonate-induced root hair formation in lettuce (*Lactuca sativa* L.) seedlings. Plant Cell Reports 34(6): 1025-1036.

Zhuo, D., Okamoto, M., Vidmar, J. J. and Glass, A. D. (1999). Regulation of a putative high-affinity nitrate transporter (*Nrt2;1At*) in roots of *Arabidopsis thaliana*. Plant Journal 17(5): 563-568.

Zimmermann, P., Hirsch-Hoffmann, M., Hennig, L. and Gruissem, W. (2004). GENEVESTIGATOR. *Arabidopsis* microarray database and analysis toolbox. Plant Physiology 136(1): 2621-2632.

8 Publications

Some of the results presented in this dissertation have been published in following two publications in 2015 and 2016, respectively. The relevant publications are attached separately to the dissertation.

- Zheng, Y., Drechsler, N., Rausch, C., Kunze, R. (2016). The *Arabidopsis* nitrate trans-porter NPF7.3/NRT1.5 is involved in lateral root development under potassium deprivation. Plant Signaling & Behavior 11 (5): e1176819.
- Drechsler, N., Zheng, Y., Bohner, A., Nobmann, B., von Wirén, N., Kunze, R., Rausch, C. (2015). Nitrate-dependent control of shoot K homeostasis by the Nitrate Trans-porter1/Peptide Transporter Family member NPF7.3/NRT1.5 and the Stelar K^+ Outward Rectifier SKOR in *Arabidopsis*. Plant Physiology 169: 283-2847.

9 Acknowledgements

Foremost, I would like to express my sincerest gratitude to my supervisor Prof. Dr. Reinhard Kunze for giving me this great chance to doing my doctoral study in his group. His patience, encouragement, support and immense knowledge helped me overcome various difficulties before finishing this work. I am also very grateful to Dr. Christine Rausch for her inspiration, skill-training and guidance during my study.

I express my sincere gratitude to Prof. Dr. Thomas Schmülling for being the second reviewer of my dissertation.

I would like to thank all the colleagues who worked with me in AG Kunze and Institute of Applied Genetics. Many thanks to Kevin Mielich, Dr. Zhenxing Wang, Dr. Alexis Kasaras, Jana Oberländer, Dr. Vajiheh Safavi-Rizi, Florencia Sena and Charlotte Thomas for their help and meaningful discussions. Special thanks to Dr. Navina Drechsler, who worked together with me on the NRT1.5 topic, for her enormous discussions, suggestions and corrections to my dissertation.

I am grateful to Prof. Dr. Nicolaus von Wirén for discussions and suggestions to our project, and the support with the ICP-OES analysis. Thanks to Sabine Artelt and Gabriele Erzigkeit (Ecology of Plants, FU) for their help with the N/C analysis.

I would like to thank China Scholarship Council for the financial support for four years.

I give my thanks to all my friends for their companionship and help.

Finally, I would like to express my gratitude to my family. Thanks to my parents and parents-in-law for their unlimited support. Special thanks to my husband Hao and my son Hexuan for their companionship, support and encouragement.

10 Appendix

Table S1. The detail description of existing plasmids.

Plasmid name	Description
pPTKan3	binary T-DNA vector with *35S* promoter
p425	yeast expression vector with *TEF* promoter
p426	yeast expression vector with *TEF* promoter
pDONR^{TM}222	Gateway® donor vector
pDONR221_p3-p2	Gateway® donor vector
pDONR221_p3-p2_SLAH1 mit Stopp	Gateway® donor vector with *AtSLAH1* full length coding sequence
pDONR221_p3-p2_SLAHA3 mit Stopp	Gateway® donor vector with *AtSLAH3* full length coding sequence
pDONR221_p3-p2_CBL3 mit Stopp	Gateway® donor vector with *AtCBL3* full length coding sequence
pDONR221_p1-p4_NRT1.5 mit Stopp	Gateway® donor vector with AtNRT1.5 full length coding sequence
pBiFC-2in1-NN	pBiFC-2in1 destination vector with split nYFP and cYFP
pDOE-08	BiFC vector with split NmVen210 and cVen210
pBT3-N_AtNRT1.5	yeast expression vector with Cub-NRT1.5 fusion construct
pNubI-X-HA	Gateway® expression destination vector for expression of NubI-X-HA
pNubG-X-HA	Gateway® expression destination vector for expression of NubG-X-HA
pNubG-AtDMP2	Gateway® expression destination vector for expression of NubG-DMP2
pNubG-AtDMP7	Gateway® expression destination vector for expression of NubG-DMP7
pNubG-KAT1	Gateway® expression destination vector for expression of NubG-KAT1
pAG426GPD-ccdb/p14156	Gateway® compatible mbSUS vector with URA3 marker

Table S2. Nutrient composition of the soil used in this study.

For the propagation of *Arabidopsis*, we used a 1:1 [v/v] mixture of the two commercially available soil types: 'P' and '0' (unfertilized) from the company Einheitserde, Sinntal-Altengronau, Germany. Soil composition analysis was performed for type 'P', '0' and the resulting low fertilized soil mixture which was used in fertilization experiments by Institut Koldingen GmbH, Sarstedt, Germany.

		Soil type		
Parameter	**Unit**	**P-type**	**P/0 mixture**	**unfertilized soil (0-type)**
salt content (soluble)	mg/l	1518	1062	890
soluble N	mg/l	83	43	23
nitrate N	mg/l	75	36	14
ammonium N	mg/l	8	7	9
phosphate	mg/l	82	44	15
potassium	mg/l	211	100	10
conductivity	µS/cm	439	310	253
pH		5.2	5.1	5.2

Table S3. The composition of various N/K/P fertilization solutions.

Fertilization solutions are based on the composition of 1/2 Murashige-Skoog medium, with the exception of the NO_3^-, K and Pi concentrations.

	N/K/P [mM]	**1/1/1**	**1/1/10**	**1/10/1**	**10/1/1**	**10/10/10**	**5/0/5**	**20/1/1**	**10/10/1**
Macro-elements	KNO_3	1 mM	1 mM	1 mM	1 mM	10 mM	0 mM	1 mM	10 mM
	KCl	0 mM	0 mM	9 mM	0 mM	0 mM	0 mM	0 mM	0 mM
	$Ca(NO_3)_2$	0 mM	0 mM	0 mM	4.5 mM	0 mM	2.5 mM	9.5 mM	0 mM
	NaH_2PO_4	1 mM	10 mM	1 mM	1 mM	10 mM	5 mM	1 mM	1 mM
	$MgSO_4$	1 mM	1 mM	1 mM	1 mM	1 mM	1 mM	1 mM	1 mM
	$CaCl_2$	1.5 mM	1.5 mM	1.5 mM	0 mM	1.5 mM	0 mM	0 mM	1.5 mM
Micro-elements	H_3BO_4	50 µM							
	$MnSO_4$	50 µM							
	$ZnSO_4$	15 µM							
	KI	2.5 µM							
	Na_2MoO_4	0.5 µM							
	$CuSO_4$	0.05 µM							
	$CoCl_2$	0.05 µM							
	Fe-EDTA	50 µM							
	MES	0.5 g/l							
	pH	5							